Microbial nitrification in urban streams: from single cell activity to ecosystem processes

Stephanie Nikola Merbt

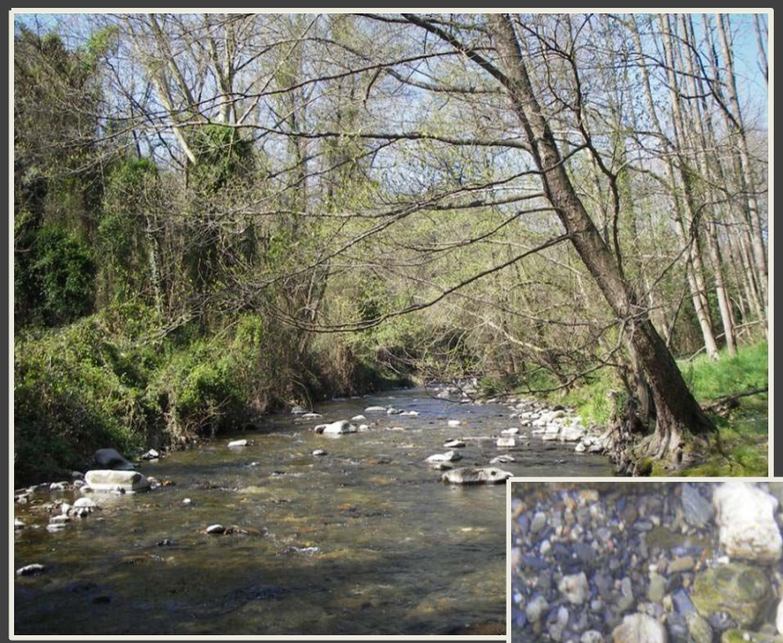

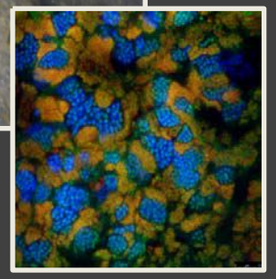

Microbial nitrification in urban streams:
from single cell activity to ecosystem processes

Stephanie N. Merbt
PhD thesis 2014

Microbial nitrification in urban streams:
from single cell activity to ecosystem processes

Stephanie N. Merbt
PhD thesis -University of Barcelona

Tesis doctoral

Universitat de Barcelona
Facultat de Biologia – Departament d'Ecologia
Programa de doctorat en Ecologia Fonamental i Aplicada

Microbial nitrification in urban streams: *from single cell activity to ecosystem processes*

Memoria presentada por Stephanie Nikola Merbt para optar al título de Doctor por la Universitat de Barcelona.

Centro de Estudios Avanzados de Blanes (CEAB)
Consejo Superior de Investigaciones Científicas (CSIC)
Barcelona, Octubre de 2014

Stephanie Nikola Merbt

La directora de la tesis	El director de la tesis	El tutor de la tesis
Dra. Eugènia Martí i Roca	**Dr. Emilio Ortega Casamayor**	**Dr. Francesc Sabater**
Científica Titular	Investigador Cientifico	Profesor titular
CEAB-CSIC	CEAB-CSIC	Universitat de Barcelona

Cover: Riverbed of La Tordera river, Santa Fe. Photograph by Dr. Daniel von Schiller.

Merbt, S.N. (2015) Microbial nitrification in urban streams: from single activity to ecosystem processes. PhD Thesis, Universitat de Barcelona

231 pages

Für meine Familie

Acknowledgements

I studied Biology emphasizing biochemistry and cell biology aiming to come back to work at the pharmaceutical industry where I worked before and where I was guaranteed a well paid and opened – end contract. However, this was before I came to Catalonia as an ERASMUS student, before I got to know stream and molecular ecology, before I was aware of the importance of streams and rivers, and before I knew about the gaps of knowledge that needed to be filled. That was before I got to know Eugènia and *los del río*, a bunch of wonderful people who crushed into my life with such a power that everything I knew before just was washed away – like a huge flood….;)

Well, apparently I was really trapped when Eugènia offered me to realize my Diploma work in her group and we started the collaboration with Emilio and Jean-Christophe. This work was the cornerstone for my fascination for stream and molecular ecology, for this dissertation and will be for all what comes next. I am really grateful you gave me this opportunity and trust to try something new….

> **Eugènia y Emili**, tuve mucha suerte de tener dos "jefes" como vosotros. Aunque en muchos aspectos sois como el *Jing-Jang*, lo más importante para los dos siempre han sido los estudiantes y nuestra educación. Me siento muy afortunada de haber tenido la posibilidad de aprender de los dos, me habéis guiado, escuchado y aconsejado en momentos de duda. Gracias por vuestras confianza, el espacio que me disteis para desarrollar mis ideas y seguir mis sueños, y por las puertas abiertas en cada momento.

But, this thesis would not have been possible if I would not have been supported (in life and work) by the most wonderful team the world has ever seen before, *los del río.* All of them know how to transmit fascination, fun and motivation – even after night time experiments in stinky, scary places!

> **Miquel, Clara, Edu, Sandrix, Marc, Susana, Elliot, Dani, Alba A., Lorenzo** - la secta de *los del río* – sin vosotros esto no hubiera sido posible, ni hubiera disfrutado tanto estos años en Blanes. Me faltan palabras para agradeceros que siempre estuvierais dispuestos a ayudarme en el trabajo y

en la vida. Gracias por intentar ensenarme el "espanish", salvarme de mala gente de Barna, las discusiones sobre el río, y la vida, los cálculos eternos bajo la lluvia y los abrazos calmantes. Gracias por pillar el teléfono y explicarme por quinta vez el uptake velocity, llevarme a esquiar cuando más lo necesitaba, y por todas las birras en la playa, en la roca, en la nieve, en el río. Podría llenar un libro entero describiendo todos los momentos chulos que compartimos y que nunca olvidaré – pero diría que no hace falta de decir más – sois los mejores y nunca os dejare escapar…prost!

My second home at the CEAB was the office of the alpine lakes group. They always had a solution to whatever problem I had…

Jean-Christophe, que lástima que te fuiste a Pau, te eché mucho de menos por aquí estos últimos años! Gracias por tus intentos de enseñarme la bioinformática…. y por los años mano a mano en el lab. y esquiando. **Albert**, gracias por los buenos tiempos que pasamos juntos. **Antoni, Carmen, Xevi, Tomas, Natalia** – gracias por enseñarme estadística, el p…cloning, rallarnos sobre los cálculos de las Q y que fuisteis mi segunda casa en el CEAB.

CEAB is a highly interdisciplinary and international institute where one can learn a lot about small freshwater "bichos", Cystoseira, GIS, the movements of worms at one lunch table with some "patatas bravas" at Leopodo. In the last years, I was lucky to be part of this very special community, which developed on the top of the little mountain. Thank you all for always being there for me!

Maria y Carlos, gracias por la compañía tan divertida en el despacho durante tantos anyos. Había una vez una italiana, una portuguesa, una suiza, una española y una alemana en un bar..…**Mariaelena, Lili, Willi, Kathrin, Aitana, Roser, Simone, Guillem, Gemma** vosotros fuisteis mis columnas de Blanes, convertisteis Blanes en un sitio "caloroso" y me hicisteis sentir en casa durante muchos años. A vuestro lado me siento rica, y aquí os quiero dar las gracias porque siempre compartisteis vuestra sabiduría conmigo y estuvisteis preparados para cualquier tontería. Os llevaré en mi corazón a donde sea – y para siempre.

Thanks also to my friends from home, for drawings, photoshop work and coming to visit each year.

Vroni vielen dank für die schönen Bilder und dafür, dass Du mich immer überall besuchen kommst, egal wo ich wohn´. Und die Tübinger Bande, danke, dass ihr mich nicht vergessen habt im fernen Spanien!

But I can't miss the most important people who made this work smooth and fluent.

Gemma, Carmela gracias por los ratos que nos reímos en el *magazem* y que todo de repente parecía fácil con vuestra ayuda! **Ángel** gracias a tu ingenio, una gran parte de mi tesis salió bien! A ver si algún día esquiamos juntos.

This part would not be completed without mentioning my experience abroad. I had the great chance to spend three months in Aberdeen and Vienna; two so different places where I found nice people who shared not only science, but also friendship with me.

Jim, thank you for accepting me in your lab, teaching me Student T-tests, growth rates, giving me good food and, sharing your thoughts with me. During my stay in your lab I started to really understand. I hope very much we can share soon some work again. In your **Cecil** and **Graeme** I found new friends and I will always remember the good time we had in the lab and Fridays in St Marchers.

Holger, auch Dir vielen Dank dafür, dass ich für leider nur eine sehr kurze Zeit Teil Deines Labors sein durfte und an all die Master Studenten, die nicht müde wurden mir das Labor zu erklären und obendrain immer einen Witz auf den Lippen liegen hatten. **Faris**, danke für deine unglaubliche Gedult und für die Dope, Click, Card- FISH, und was sonst noch versuche meine Archaen zum Leuchten zu bringen. Und **Mischa**, vielen Dank für die ungewöhnlichsten Stadführungen, den Wein am Yppen-Platz, die Pilzgerichte und das viele Lachen. Dich vermiss ich sehr-du alter Kautz.

I spent the last year in the Vall de Boí writing up. I also want to mention all these very nice and fun people who managed to trick me to go skiing or climbing – and could not be bothered by my urge to come back to work. This was the best you could have done for me!

A todos los que viven en el Paraiso - **Laura, María, Javi, Ana, Dani, Faina, Mariana, Iván, Sergi, todos los Jordis, Hania**,… gracias por acogerme y por los días de aventura que pasamos juntos! Sois los mejores y uno puede aprender mucho de vosotros.

And finally, I want to thank my family for their support and trust ever since.

Mama, nur dank Deiner Unterstützung hab ich, wider aller Erwartungen, doch noch schreiben gelernt und sieh was dabei rausgekommen ist. Danke, dass du immer für mich da bist. **Papa, Famor, Uli, Philipp, Hans, Tristan, Vicky**, auch wenn ich standing weit weg bin und nicht wirklich aktiv an Eurem Leben teilhaben kann, ohne euch würde es nicht gehen. Wo ihr seid, bin ich daheim! Y a **Unai**, gracias por sacarme de la cueva para poder ver lejos, por enseñarme a vivir la vida sin miedo. A tu lado yo soy yo.

I was founded by the JAE – pre-doctoral scholarship of the Spanish Research Council, Consejo Superior de Investigacion Científica (2010 – 2014). Furthermore I want to thank Ignasi Rodriguez-Roda for contracting me during the last phase of the thesis at ICRA.

Taüll, 20 November 2014,

Stephanie Nikola Merbt

Informe de los directores

La Dra. Eugènia Martí Roca i el Dr. Emilio Ortega Casamayor, del Centre d'Estudis Avançats de Blanes (CEAB-CSIC), directors de la Tesi Doctoral elaborada per Stephanie Nikola Merbt i que porta per títol "Microbial nitrification in urban streams: *from single activity to ecosystems processes*".

INFORMEN

Que els treballs de recerca portats a terme per Stephanie Nikola Merbt com a part de la seva formació pre-doctoral i inclosos a la seva Tesi Doctoral han donat lloc a tres articles publicats, i tres manuscrits adicionals a punt de ser enviats a revistes científiques d'àmbit internacional. A continuació es detalla la llista d'articles publicats, així com els índexs d'impacte (segons el SCI de la ISI Web of Knowledge) de les revistes on han estat publicats els treballs i les cites que han tingut a la data de presentació de la tesi (novembre 2014).

1. **Merbt, S.N., Jean-Christophe Auguet, Emilio O. Casamayor, and Martí, E.** 2011. Biofilm recovery in a wastewater treatment plant-influenced stream and spatial segregation of ammonia-oxidizing microbial populations. *Limnol Oceanogr* **56**: 1054–1064

L'índex d'impacte de la revista *Limnology and Oceanography* al 2011 va ser de 3.416. Aquesta revista està inclosa a la categoria "Limnology". Aquesta categoria té una mediana d'índex d'impacte de 1.425 i inclou un total de 20 revistes. Tenint en compte l'índex d'impacte de *Limnology and Oceanography,* aquesta ocupa el 1er lloc de la seva categoria, quedant inclosa en les revistes del1er quartil. Les cites que ha tingut aquest article fins al moment són 19 (google acadèmic).

2. **Merbt, S.N., Stahl, D.A., Casamayor, E.O., Martí, E., Nicol, G.W., and Prosser, J.I.** 2012. Differential photoinhibition of bacterial and archaeal ammonia oxidation. *FEMS Microbiology Letters* **327**: 41-46.

L'índex d'impacte del *FEMS Microbiology Letters* al 2012 va ser de 2.046. Aquesta revista està inclosa a la categoria "Microbiology". Aquesta categoria té una mediana d'índex d'impacte de 2.424 i inclou un total de 109 revistes. Aquest article ha rebut un elevat nombre de cites, tot i la seva breu trajectòria. Les cites que ha tingut aquest article fins al moment són 39 (google acadèmic).

3. **Merbt, S.N., Auguet, J.-C., Blesa, A., Martí, E., and Casamayor, E.** 2014. Wastewater Treatment Plant Effluents Change Abundance and Composition of Ammonia-Oxidizing Microorganisms in Mediterranean Urban Stream Biofilms. *Microbial Ecology*: 1-9

L'índex d'impacte de la revista *Microbial Ecology* al 2013 va ser de 3.118. Tenint en compte aquest índex d'impacte, la revista ocupa el 9è lloc de la categoria "Marine and Freshwater Biology", quedant inclosa en les revistes del 1er quartil. Aquesta categoria té una mediana d'índex d'impacte de 2.424 i inclou un total de 103 revistes. Donada la seva recent publicació, l'article encara no té cap cita

Alhora, els directors CERTIFIQUEN

Que el Sra. Stephanie Nikola Merbt ha participat activament en el desenvolupament del treball de recerca associat a cadascun d'aquests articles, així com en la seva elaboració. En concret, la seva participació en cadascun dels articles ha estat la següent:

- Participació en el plantejament inicial dels objectius de cadascun dels treballs, els quals estaven emmarcats en dos projectes del Plan Nacional del Ministerio de Ciencia e Innovación (DARKNESS i MED_FORESTREAM) i en dos projectes, un dins del marc de la ESF (COMIX), i l'altre finançat per la Comissió Europea (REFRESH).
- Plantejament i realització de la part experimental de cada estudi, i posada a punt de les metodologies de camp i de laboratori associades a cadascun dels experiments.
- Processat i anàlisi de totes les mostres obtingudes. Càlcul de resultats i anàlisi estadístic de les dades.
- Redacció dels articles i seguiment del procés de revisió dels mateixos

Finalment, els directors CERTIFIQUEN que cap dels co-autors dels articles abans esmentats ha utilitzat o bé té present utilitzar implícita o explícitament aquests treballs per a l'elaboració d'una altra Tesi Doctoral.

Atentament, Blanes, 20. Novembre 2014

Eugènia Martí i Roca Emilio Ortega Casamayor

Table of Contents

Resumen

El objetivo de esta tesis ha sido el estudio de los mecanismos y factores reguladores del proceso microbiano de oxidación del amonio (NH4) en ríos urbanos afectados por vertidos de depuradoras. Arqueas (AOA) y bacterias (AOB) oxidadoras de amonio (OA) fueron detectadas en comunidades microbianas (biofilms) desarrolladas sobre los cantos rodados del río. Su abundancia, composición, distribución y actividad fueron examinadas, con técnicas de ecología microbiana molecular y de biogeoquímica fluvial, en estudios realizados con cultivos, microcosmos e *in situ*. Tanto la concentración natural de amonio (NH_4) como la radiación solar fueron factores clave en la regulación de dichos parámetros de los AO. En condiciones ambientales de baja concentración de NH_4, las AOA (cluster *Nitrososophaera*) dominaron la comunidad de OA, mostrando una baja actividad nitifricante. Bajo altas concentraciones de NH_4, las AOB eran dominantes (clusters *Nitrosospira* y *N. oligotropha*) y mostraban una alta actividad. En cultivos monoespecíficos, el crecimiento de AOA y AOB fue inmediatamente inhibido por luz. Las AOA mostraron una mayor fotosensibilidad y una menor capacidad de recuperación que las AOB. Estos hallazgos sugerían que la luz podría ser un factor determinante en la distribución y actividad de OA en ecosistemas naturales.

En concordancia, en biofilms naturales incipientes se observó mayor preferencia de las OA para colonizar las superficies orientadas hacia el sedimento que para colonizar superficies orientadas hacia la luz solar. Esta segregación espacial no se observó en biofilms maduros. Además, se observó una relación significativa entre biomasa total y abundancia de OA para los biofilms del lado luminoso pero no para los del lado oscuro. Este hecho sugiere la existencia de un efecto fotoprotector *in situ* (efecto "sombra"). Este efecto podría explicar porque la nitrificación medida a nivel de tramo fluvial fue independiente de la intensidad de la luz y del ciclo solar diario. Las poblaciones de OA fueron también

abundantes en el sedimento. Sin embargo, la partición de la contribución de sedimento y biofilms a la nitrificación de un tramo fluvial desveló un papel proporcional preponderante de las poblaciones de OA que se desarrollan en biofilms protegidos de la luz.

Abstract

The main goal of this PhD thesis was the study of the ammonium oxidation process in high nutrient loaded urban streams. We aimed to unveil regulating factors and driving mechanisms from the organisms to the ecosystem scales using a combined biogeochemistry-microbial ecology approach.

Ammonia oxidization is the first and rate-limiting step of nitrification. Nitrification is the key process linking nitrogen (N) inputs (fixation, mineralization) and losses (denitrification, anamox) in the aquatic ecosystem. Ammonia oxidizing archaea (AOA) and bacteria (AOB) drive this process through the enzyme ammonia monooxygenase. Although sharing a common function, AOB and AOA are phylogenetically distinct, suggesting different evolution and phenotypic characteristics.

AOA and AOB were detected in the stream biofilms. The abundance, community composition and distribution of these microbial components were driven by environmental physical and chemical conditions, mainly ammonia (NH_4) concentrations and sun irradiance.

Ammonia oxidizing activity in biofilms under low NH_4 availability was low and only 2 % of the inorganic NH_4 was nitrified. Under these conditions AOA dominated ammonia oxidizing community and were key players of the observed ammonia oxidation (*Nitrososophaera* cluster). Conversely, under high NH_4 load in the stream up to 100 % of the inorganic NH_4 was oxidized to nitrate (NO_3). Such high ammonia oxidizing activity was mostly driven by AOB (*Nitrosospira* and *N. oligotropha* clusters). Under these conditions AOB outnumbered AOA by orders of magnitude. AOA in contrast were poorly active under high NH_4 concentrations and a consistent community composition shift was observed between high and low NH_4 conditions.

In laboratory cultures the growth of AOA and AOB was immediately inhibited by light. In particular, at lower light intensities, archaeal growth was much more photosensitive than bacterial growth and unlike AOB, AOA showed no evidence of recovery during dark phases. These findings provide evidence for niche differentiation in aquatic environments and suggested light as a main driving factor for the distribution and activity of ammonia oxidizers in the aquatic environment. Accordingly, in early stage biofilms developing on streams cobbles the percentage of ammonia oxidizers was higher in darkness (i.e., sediment facing side or dark-side biofilms) than in biofilms grown on the upper, light exposed side of the cobbles (light-side biofilm). However, this spatial segregation was missed in mature biofilms suggesting that the complex microbial structure present in light-side biofilms may protect both AOA and AOB against photoinhibition. This finding was further confirmed by a significant relationship found between light-side biofilm biomass and the abundance of ammonia oxidizers *in situ*. In contrast, for dark-side biofilms the relationship was missed. Therefore, irradiance was not an inhibitory factor for AOA and AOB in mature light-side biofilms probably due to an "umbrella effect". The umbrella effect and the fact that AOA and AOB were highly abundant in the sediment (light avoiding strategy) are probably the reasons why nitrification at the ecosystem scale was independent from both light intensity and dial light cycling. Altogether these results highly contributed to improve the current knowledge on nitrification in urban streams and provided insights on niche differentiation between AOA and AOB.

Key words: nitrification, biofilm, urban stream, ammonia oxidizers, archaea, bacteria

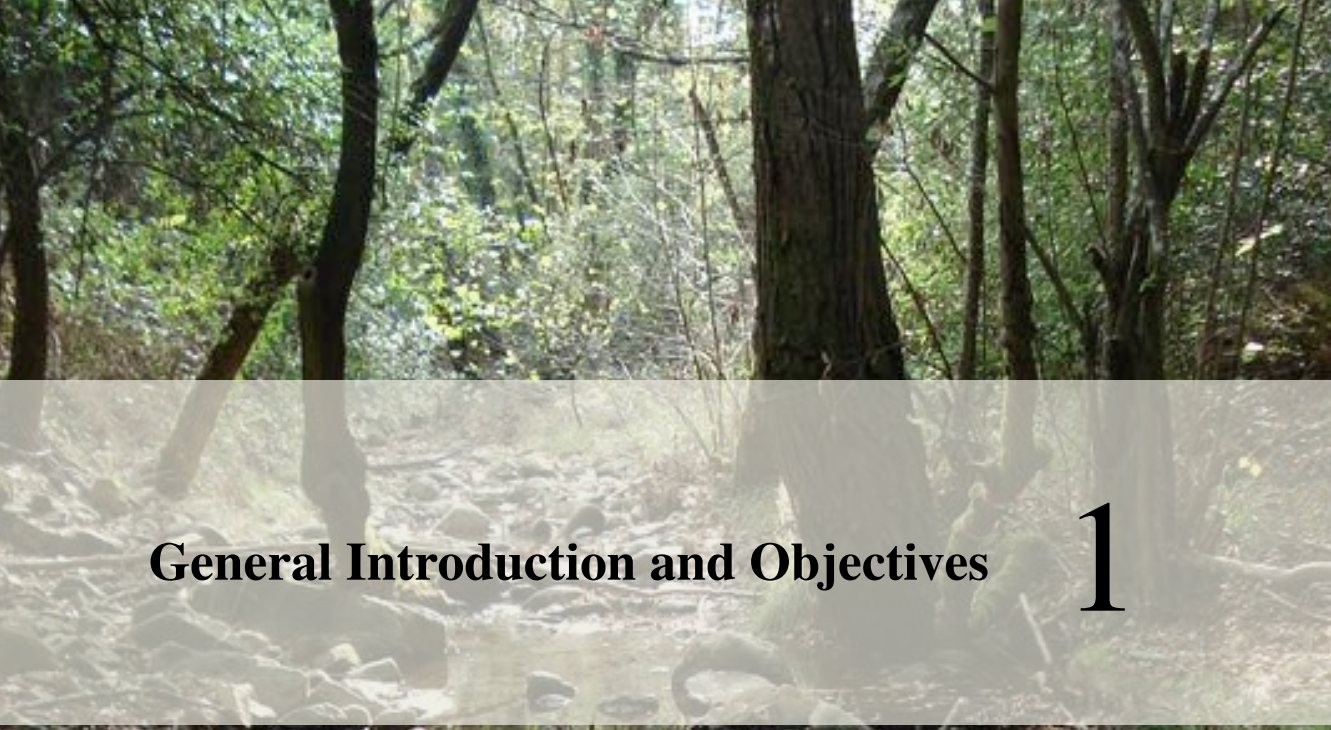

General Introduction and Objectives 1

Cover: Fuirosos river, tributary of the Tordera river (NE Spain). Photograph by Daniel von Schiller

1.1 European River status

Streams and rivers draining urban areas are of key importance for society because they provide water for municipal, industrial and agricultural uses as well as esthetic and recreational values for citizens (Palmer et al., 2004). However, more than half of the European freshwater bodies are currently allocated below the threshold of what is considered a good ecological status, being rivers in a worse ecological status than lakes (Kristensen, 2012). This is related to the fact that streams and rivers are, in general, more directly exposed to anthropogenic pressures than lakes. For instance, diffuse nutrient sources, such as agricultural runoff, cause nutrient enrichment in about 40 % of European rivers (Kristensen, 2012). In addition, in urban areas the discharge from wastewater treatment plants (WWTP) – as point sources - cause an increase in nutrient concentrations and changes in flow regime in 22 % of European rivers (Figure 1.1).

Nowadays in Europe, most of the wastewater produced by human population is connected to WWTP systems. The introduction of secondary and tertiary treatment steps in the WWTPs over the last 30 years has significantly improved the chemical quality of the WWTP effluents (Kristensen, 2012). Nonetheless, WWTP effluents still represent a physical and chemical discontinuity along the receiving streams and rivers. WWTP effluents significantly alter water temperature, discharge, and conductivity; and still are one of the major nitrogen (N) inputs to streams and rivers, which increase ammonium (NH_4^+) and nitrate (NO_3^-) concentrations (Martí et al., 2010).

N is an essential nutrient and is key compound in many biochemical processes critical for life; however, at high concentrations it can be harmful. While NO_3^- is more stable and basically nontoxic in the aquatic environment, the most reduced form of N is present in two forms: the ionized form NH_4^+, which is harmless, and the un-ionized form ammonia (NH_3), which is highly toxic to aquatic life.

NH_3 can passively diffuse through cell membranes and trigger a series of harmful effects on microbiota, invertebrates and fish, leading to a decrease of both phylogenetic richness and population density (Camargo and Alonso, 2006; United States Environmental Protection Agency, 2013). The proportion of NH_3 in water tends to increase with higher pH and higher temperature, and with lower dissolved oxygen concentration. Unfortunately, these are the conditions that frequently prevail during the low flow summer conditions, especially in Mediterranean streams.

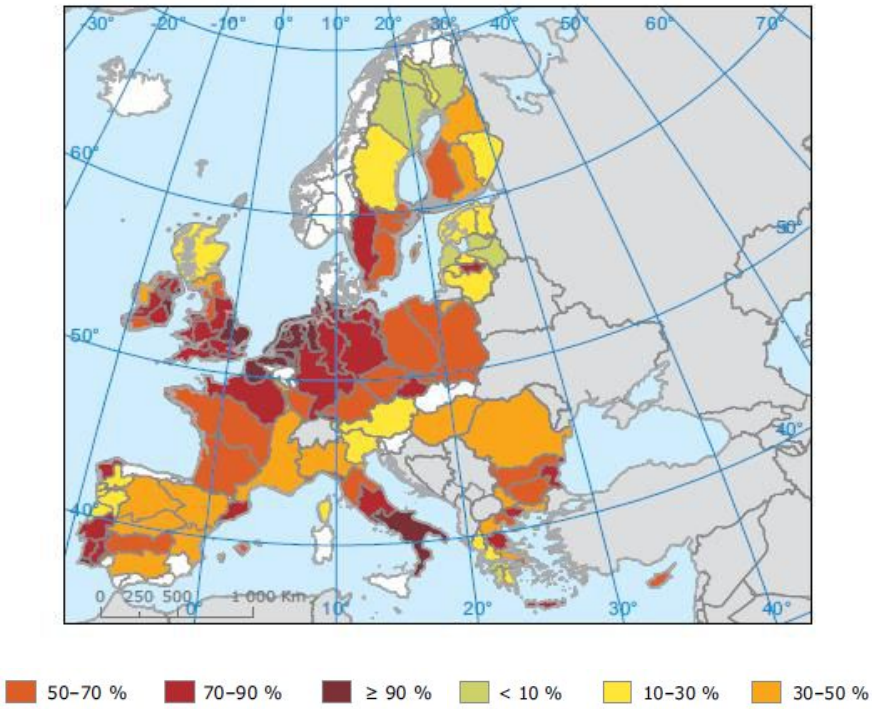

Figure 1.1: Proportion (%) of classified water bodies (rivers and lakes) in different River Basin Districts affected by point and diffuse nutrient sources. Adapted from Kristensen, 2012 -European Environment Agency (EEA).

1.2 Nitrogen cycling in streams

We currently know that in-stream biogeochemical processes can retain more than 50 % of such N inputs and hence influence the N export to downstream ecosystems (Peterson et al., 2001). This has been mostly attributed to the high surface-to-volume ratio in these streams, which enhances their bioreactive capacity (Peterson et al., 2001). However, N uptake efficiency saturates above a certain N concentration, which finally leads to higher downstream N loads and favors eutrophication in downstream waters (Martí et al., 2004; Camargo and Alonso, 2006; O'Brien and Dodds, 2008).

Dissolved inorganic N (i.e., NH_4^+ and NO_3^-) in the water column is quickly incorporated and retained in the biofilm biomass, both through autotrophic and heterotrophic assimilation (Peterson et al., 2001; Hall and Tank, 2003; Arango et al., 2008). However, this N uptake is transitory because the organic N may again be mineralized and released as NH_4^+ to the water column. NH_4^+ can also be oxidized to NO_3^- via NO_2^- by the nitrification process. This is a crucial pathway paving the way for net N losses from the system via denitrification and anaerobic ammonium oxidation (anammox, Figure 1.2). Furthermore, dissimilatory nitrate reduction to ammonium (DNRA) may also play an important role in in-stream N regulation providing NH_4^+ to be further nitrified (Burgin and Hamilton, 2007).

This thesis particularly focuses on nitrification linking reduced and oxidized N forms. Nitrification at whole-reach scale has been assessed in pristine streams, showing high variability among streams representing 3-to 60 % of total NH_4^+ uptake (Peterson et al. 2001). These investigations unveiled NH_4^+ availability and discharge as the most important regulating factor at whole reach scale (Peterson et al., 2001; Strauss et al., 2002; Levi et al., 2013). But also low C:N ratio, neutral pH, higher temperature and aerobic conditions are key factors for whole reach nitrification (Strauss and Lamberti, 2000; Bernhardt et al., 2002;

Strauss et al., 2002; Strauss et al., 2004) resulting in spatial and seasonal patterns of nitrification (Strauss et al., 2004). In streams in urban areas, such as those receiving inputs from WWTP effluents nitrification has consistently shown to be an important biogeochemical process (Groffman et al., 2005; Haggard et al., 2005; Merseburger et al., 2005; Merseburger, 2006; Ribot et al., 2012). This can be favoured by high NH_4^+ concentration delivered by the WWTP. However, experimental evidences on the environmental and biological controlling factors are still scarce in these high N loaded streams.

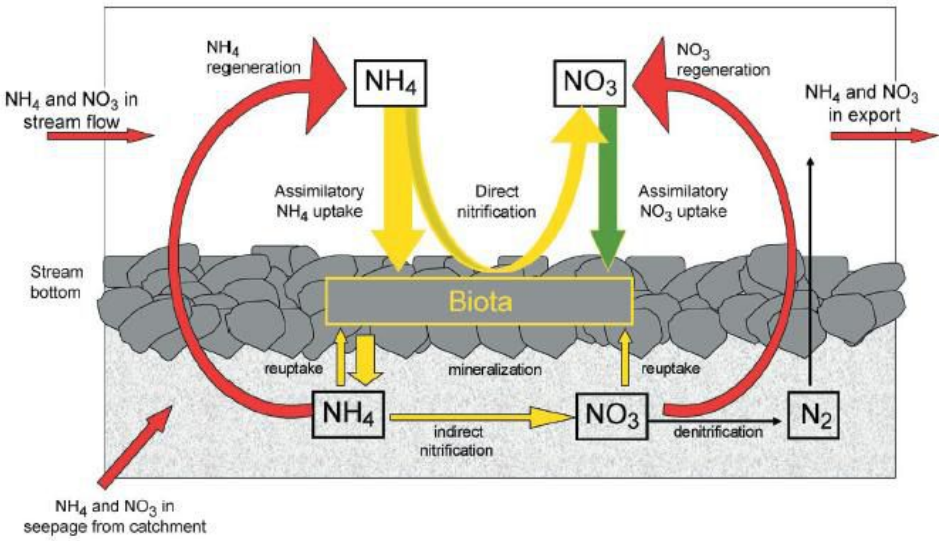

Figure 1.2: Conceptual model of biogeochemical processes driving dissolved inorganic N cycling in headwater stream ecosystems. NH_4^+ and NO_3^- enter the stream reach via stream flow and lateral seepage. NH_4^+ removal from the water column occurs through assimilation by primary producers, bacteria, and fungi plus direct nitrification. Indirect nitrification is the conversion of NH_4^+ from organic matter mineralization to NO_3^-. NO_3^- removal from the water column occurs primarily via assimilation by biota and denitrification on the channel bottom. Regeneration is the release of NH_4^+ and NO_3^- from the stream bottom to the water column and is the net result of several interacting processes, including mineralization, indirect nitrification, denitrification, and re-uptake by organisms. NO_3^- and NH_4 in the water column is also subjected to downstream export. Adapted from Peterson et al. (2001).

1.3 Benthic biofilms in streams

In streams and rivers, microbial assemblages (i.e., biofilms) coat the streambed substrata. Biofilms play a key role in stream ecosystem functioning because they drive the different processes involved in N cycling; and thus, they act as natural bioreactors within the stream ecosystems (Peterson et al., 2001; Battin et al., 2003a; Findlay, 2010; Ribot et al., 2012). However, microbial composition and activity of biofilms are prone to environmental conditions, which may ultimately influence ecosystem function (Singer et al., 2010; Cardinale et al., 2012; Besemer et al., 2013; Widder et al., 2014).

Biofilms form complex three-dimensional structures kept together by a polysaccharide matrix (Lock et al., 1984). These structures include voids, which turn biofilms into living zones of transient storage (Battin et al., 2003a) retarding the downstream transport of water and providing microenvironments as niches for microbial specialists (Stoodley et al., 2002). Physical and chemical factors such as flow velocity, temperature, light, and nutrient availability determine the biofilm structure as well as biomass accrual and compositional heterogeneity (Battin et al., 2003b; Besemer et al., 2007; Schiller v. et al., 2007; Singer et al., 2010; Romaní et al., 2014). Therefore, these factors can be drivers for the development of distinct biofilm types within the same fluvial system contributing differently to the N cycle at whole reach scale. For example, biofilms growing in darkness on the sediment facing side of a cobble (*dark-side biofilm*) are exposed to different flow regime than biofilms that grow under full sun irradiance on the upper side of the cobble (*light-side* biofilm). A picture of the natural biofilms growing on both faces is shown in Figure 1.3, where the light-side biofilm appears as a thick, deep green layer that is dominated by photoautotrophic organisms, whereas the dark-side biofilm is brown, more encrusted and with less conspicuous presence of photoautotrophs.

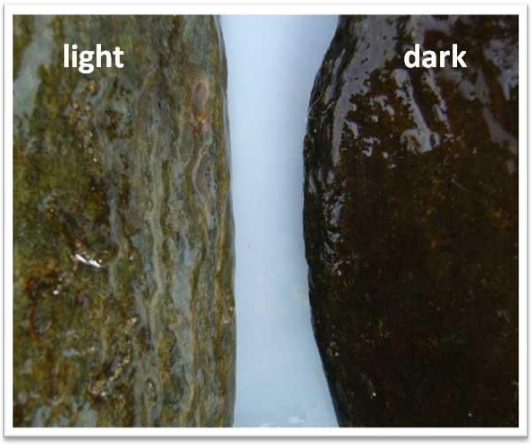

Figure 1.3: Biofilms growing on upper (light) and sediment facing (dark) sides of a cobble collected in La Tordera in Santa Maria Palautordera, Barcelona, NE Spain.

1.4 Main microbial players of nitrification

Nitrification is an aerobic two-step process carried out by chemoautotrophic ammonia and nitrite oxidizing organism (Figure 1.4). The ammonia oxidation is the rate limiting step of nitrification, and historically it was thought to be restricted to the kingdom of Bacteria (AOB) with the first successful isolation of an *Nitrosomonas europaea* in 1890 (Winogradsky, 1890). Despite this initial assumption, at the beginning of the XXI century, the ammonia oxidizing gene for archaea was found in widespread environmental surveys, and the first chemoautotrophic archaeal ammonia oxidizer (AOA), *Nitrosopumilus maritimus,* was cultured in the laboratory just a few years ago (Venter et al., 2004; Könneke et al., 2005; Treusch et al., 2005). Since then, much effort has been spent in understanding the cellular physiology, ecology, biogeochemistry, ecophysiology, and genomics of AOA, and in assessing the driving factors for the niche separation between AOA and AOB (Nicol et al., 2008; Tourna et al., 2008; Martens-Habbena et al., 2009).

Culture-independent molecular approaches, such as the survey of functional genes as molecular markers, have been used to characterize both AOA and

AOB in environmental samples and have permitted to establish linkages between microbes and biogeochemical transformations. The most common molecular marker used is the gene encoding for the subunit A of the ammonia monooxygenase (*amoA*), a transmembrane enzyme catalyzing the conversion of ammonia to hydroxylamine (Hyman and Arp, 1992; Vajrala et al., 2013), which is present in both AOA and AOB (Figure 1.4).

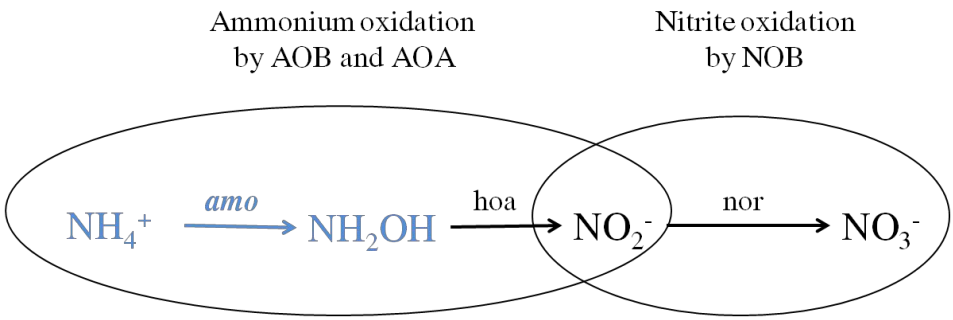

Figure 1.4: Nitrification decrypted. Archaea and bacteria ammonia oxidizing organism (AOA and AOB, respectively) convert ammonia to nitrite through hydroxylamine using ammonia monooxygenase (*amo*) and hydroxylamine oxidoreductase (*hoa*). Autotrophic nitrite oxidizers subsequently use the enzyme nitrite oxidoreductase (*nor*) to convert nitrite to nitrate.

Despite the closely related *amoA* genes sequence, AOA and AOB are metabolically different. AOB oxidize ammonia to hydroxylamine (NH_2OH) by the ammonium monooxigenase (*amo*) enzyme, and re-oxidize it to NO_2^- by the hydroxylamine oxidoreductase (*hao*) enzyme. However, there is no evidence of genes encoding the latter enzyme (*hao*) in archaeal ammonia oxidation. Furthermore, AOB are obligate chemoautotrophs exclusively using CO_2 as carbon source. Conversely, AOA can also have a heterotrophic or mixotrophic metabolism; and thus, can use organic substances as carbon sources (e.g., *N. viennensis* can grow on pyruvate) (Walker et al., 2010; Mußmann et al., 2011; Tourna et al., 2011).

Recent studies have shown that AOA are highly abundant in many ecosystems. For instance, they account for 20-30 % of the microbial plankton in the global oceans (Martens-Habbena and Stahl, 2010). In fact, AOA frequently outnumber AOB by orders of magnitude in soils (Leininger et al., 2006; Nicol et al., 2008), oceans (Wuchter et al., 2006), and oligotrophic lakes (Auguet et al., 2012). Nevertheless, other studies have shown opposite patterns, with a dominance of AOB over AOA, for instance in agricultural soils and in both coastal and estuarine sediments (Santoro et al., 2008; Di et al., 2009; Magalhães et al., 2009; Zhang et al., 2009). The aforementioned studies together with results from culture studies indicate that AOA and AOB respond differently to specific environmental factors, which dictate their population dynamics and evolutionary history (Fernàndez-Guerra and Casamayor, 2012). Among other factors, low NH_4^+ availability and acidic pH have been shown to select for AOA (Nicol et al., 2008; Martens-Habbena et al., 2009). In streams and rivers, scarce information is available so far on the presence, abundance, activity and characteristics of the ammonia oxidizing assemblages (Cebron et al., 2003; Herrmann et al., 2011; Sonthiphand et al., 2013).

1.5 Linking ecosystem biogeochemistry and molecular ecology

We need to elucidate the mechanisms underlying the observed ecological patterns to confidentially predict and understand processes (Levin, 1992).

Two separated scientific disciplines have traditionally focused on describing N cycling in aquatic systems, i.e., biogeochemistry and microbial ecology. Biogeochemistry deals with physical, chemical, geological and biological processes but allows only deduction of intrinsic causes for observed patterns. Its advantage is that it takes into account abiotic factors, like sorption of N to the sediment and detects fluxes between compartments within the ecosystem. The use of stable isotopes is a highly powerful tool in biogeochemistry, which allow understanding different processes involved in nutrient fluxes within the stream

and quantify the relative contribution of different biotic compartments to the nutrient fluxes (Peipoch et al., 2012; Pastor et al., 2014; Peipoch et al., 2014). Biogeochemical methods can be used to characterize processes at different scales of organization, from microcosms to whole ecosystem. However, it is very challenging to correctly interpret spatial and temporal patterns of different biogeochemical processes especially if there is no causal evidence of the factors and mechanisms that drive them.

In contrast, microbial molecular ecology describes function and composition of the microorganisms mediating biogeochemical processes through the use of particular enzymes encoded by functional genes (Zak et al., 2006; Falkowski et al., 2008; Findlay, 2010). Applying molecular techniques on an environmental sample is like opening a black-box. These techniques allow identifying the community composition and quantifying the abundance and expression of particular genes. This information can reveal firstly, how molecular mechanisms regulate biogeochemical dynamics and, secondly, explain why biogeochemical patterns occur (Figure 1.5). Nonetheless, molecular techniques can also hold many uncertainties due to methodological biases, like unspecific primers and low sample replication due to high costs and high background noise that deserve careful interpretations (e.g. Prosser, 2010).

Despite the weakness of each particular discipline when used complimentary, they have shown great potential (see for example Beman and Francis, 2006). Therefore, the design of this thesis takes advantage of a combined approach using both, biogeochemistry and molecular ecology aiming to overcome some of the limitations and consistently strengthen our current understanding on in-stream nitrification.

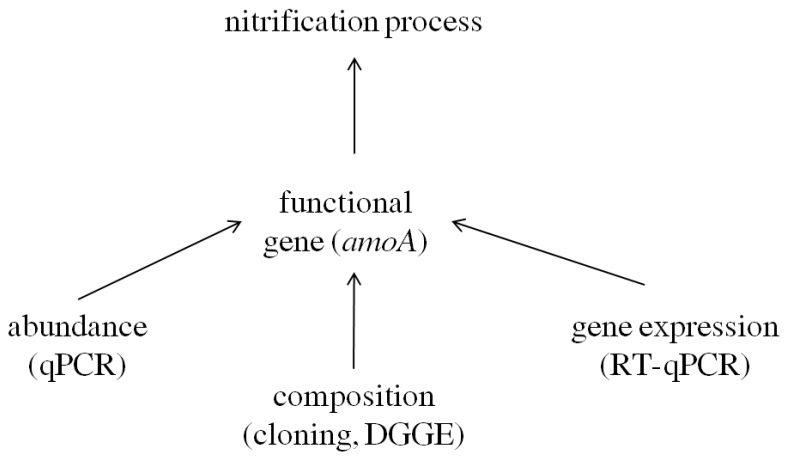

Figure 1.5: conceptual model linking biogeochemical processes to functional genes via the intensive characterization of the mediating key enzyme ammonium monooxygenase. Molecular techniques that provide insight into the abundance (quantitative polymerase chain reaction; qPCR), composition (cloning and denaturing gradient gel electrophoresis DGGE) and gene expression (reverse transcriptase-qPCR) are listed. Figure modified from Zak et al. (2006)

1.6 Objectives

The main goal of this dissertation was to study the ammonium oxidation process (i.e., nitrification) in streams, especially those receiving high nutrient loads from WWTPs. In particular, this dissertation aimed to unveil regulating factors and driving mechanisms of in-stream nitrification from the single cell activity to the ecosystem processes. We used an approach based on the combination of concepts and techniques from biogeochemistry and microbial ecology. This combined view required the use of diverse and interdisciplinary set of methods and approaches. The different chapters included in this thesis have been divided into two parts based on the study approach used. Part I includes two chapters based on explorative studies. Part II includes three chapters based on experimental studies.

Specific objectives of the different chapters are:

Part I (chapters 3 and 4)

The specific objective of Part I was to describe the abundance, distribution, and identity of AOA and AOB in a set of different stream biofilms receiving inputs from WWTP effluents. The main aim was to infer the intrinsic and extrinsic biofilm properties driving the distribution and segregation of AOA and AOB. One of the main findings of Part I suggested irradiance as one of the driving factors for AOA and AOB community dynamics, which was fundamental for the focus of the experiments included in Part II.

Part II (chapters 5, 6 and 7)

The specific objective of Part II was to experimentally assess the effect of light on AOA and AOB at different scales of organization (chapter 5: monoespecific cultures; chapter 6: biofilm matrix bound, and chapter 7: at whole-reach scale) and how this effect imprints on whole reach organization of nitrification.

1.7 Contribution and novelty of the thesis

Only very recently, AOA and AOB have been shown to be key components of stream biofilms (Merbt et al 2011, Herrmann et al., 2011), although since decades it is known that biofilms exhibit nitrification activity (Tanaka and Dunn, 1982; Daims et al., 2001; Wagner et al., 2002; Lydmark et al., 2006). However, little is known on the specific *in situ* distribution of AOA and AOB and whether or not both groups have an equivalent contribution to whole stream nitrification. There is also a lack of information on niche separation between AOA and AOB in stream ecosystems and what factors may control it. This is of particular interest because only through mechanistic insights causalities and implications concerning whole reach N cycle can be fully assessed and predicted.

A more interdisciplinary approach, like combining two disciplines with complementary views such as biogeochemistry and molecular microbial ecology, may improve our understanding on the nitrification process across different spatial and temporal scales giving valuable insights on the environmental factors controlling the N cycle in urban streams.

1.8 References

Arango, C., Tank, J., Johnson, L., and Hamilton, S. (2008) Assimilatory uptake rather than nitrification and denitrification determines nitrogen removal patterns in streams of varying land use. *Limnology and Oceanography* **53**: 2558–2572.

Auguet, J.-C., Triadó-Margarit, X., Nomokonova, N., Camarero, L., and Casamayor, E.O. (2012) Vertical segregation and phylogenetic characterization of ammonia-oxidizing Archaea in a deep oligotrophic lake. *The ISME Journal* **6**: 1786-1797.

Battin, T.J., Kaplan, L.A., Denis Newbold, J., and Hansen, C.M.E. (2003a) Contributions of microbial biofilms to ecosystem processes in stream mesocosms. *Nature* **426**: 439-442.

Battin, T.J., Kaplan, L.A., Newbold, J.D., Cheng, X., and Hansen, C. (2003b) Effects of Current Velocity on the Nascent Architecture of Stream Microbial Biofilms. *Applied and Environmental Microbiology* **69**: 5443-5452.

Beman, J.M., and Francis, C.A. (2006) Diversity of Ammonia-Oxidizing Archaea and Bacteria in the Sediments of a Hypernutrified Subtropical Estuary: Bahía del Tóbari, Mexico. *Applied and Environmental Microbiology* **72**: 7767-7777.

Bernhardt, E.S., Hall Jr, R.O., and Likens, G.E. (2002) Whole-system estimates of nitrification and nitrate uptake in streams of the Hubbard Brook Experimental Forest. *Ecosystems* **5**: 419-430.

Besemer, K., Singer, G., Quince, C., Bertuzzo, E., Sloan, W., and Battin, T.J. (2013) Headwaters are critical reservoirs of microbial diversity for fluvial networks. *Proceedings of the Royal Society B: Biological Sciences* **280**. doi**:** 10.1098/rspb.2013.1760

Besemer, K., Singer, G., Limberger, R., Chlup, A.-K., Hochedlinger, G., Hodl, I. et al. (2007) Biophysical Controls on Community Succession in Stream Biofilms. *Appl Environ Microbiol* **73**: 4966-4974.

Burgin, A.J., and Hamilton, S.K. (2007) Have we overemphasized the role of denitrification in aquatic ecosystems? A review of nitrate removal pathways. *Frontiers in Ecology and the Environment* **5**: 89-96.

Camargo, J.A., and Alonso, Á. (2006) Ecological and toxicological effects of inorganic nitrogen pollution in aquatic ecosystems: A global assessment. *Environment International* **32**: 831-849.

Cardinale, B.J., Duffy, J.E., Gonzalez, A., Hooper, D.U., Perrings, C., Venail, P. et al. (2012) Biodiversity loss and its impact on humanity. *Nature* **486**: 59-67.

Cebron, A., Berthe, T., and Garnier, J. (2003) Nitrification and Nitrifying Bacteria in the Lower Seine River and Estuary (France). *Appl Environ Microbiol* **69**: 7091-7100.

Daims, H., Nielsen, J.L., Nielsen, P.H., Schleifer, K.-H., and Wagner, M. (2001) In Situ Characterization ofNitrospira-Like Nitrite-Oxidizing Bacteria Active in Wastewater Treatment Plants. *Applied and Environmental Microbiology* **67**: 5273-5284.

Di, H., Cameron, K., Shen, J.P., Winefield, C., O'Callaghan, M., Bowatte, S., and He, J. (2009) Nitrification driven by bacteria and not archaea in nitrogen-rich grassland soils. *Nature Geoscience* **2**: 621-624.

Falkowski, P.G., Fenchel, T., and Delong, E.F. (2008) The Microbial Engines That Drive Earth's Biogeochemical Cycles. *Science* **320**: 1034-1039.

Fernàndez-Guerra, A., and Casamayor, E.O. (2012) Habitat-Associated Phylogenetic Community Patterns of Microbial Ammonia Oxidizers. *PLoS ONE* **7**: e47330.

Findlay, S. (2010) Stream microbial ecology. *Journal of the North American Benthological Society* **29**: 170-181.

Groffman, P.M., Dorsey, A.M., and Mayer, P.M. (2005) N processing within geomorphic structures in urban streams. *Journal of the North American Benthological Society* **24**: 613-625.

Haggard, B.E., Stanley Emily H., and E., S.D. (2005) Nutrient retention in a point-source-enriched stream. *Journal of the North American Benthological Society* **24**: 29-47.

Hall, R.O., Jr., and Tank, J.L. (2003) Ecosystem Metabolism Controls Nitrogen Uptake in Streams in Grand Teton National Park, Wyoming. *Limnology and Oceanography* **48**: 1120-1128.

Herrmann, M., Scheibe, A., Avrahami, S., and Küsel, K. (2011) Ammonium Availability Affects the Ratio of Ammonia-Oxidizing Bacteria to Ammonia-Oxidizing Archaea in Simulated Creek Ecosystems. *Applied and Environmental Microbiology* **77**: 1896-1899.

Hyman, M.R., and Arp, D.J. (1992) 14C2H2- and 14CO2-labeling studies of the de novo synthesis of polypeptides by Nitrosomonas europaea during recovery from acetylene and light inactivation of ammonia monooxygenase. *Journal of Biological Chemistry* **267**: 1534-1545.

Könneke, M., Bernhard, A.E., de la Torre, J.R., Walker, J.B., Waterbury, C.B., and Stahl, D.A. (2005) Isolation of an autotrophic ammonia-oxidizing marine archaeon *nature* **437**: 543-546.

Kristensen, P. (2012) European waters: assessment of status and pressures. Luxembourg : Publications Office of the European Union.

Leininger, S., Urich, T., Schloter, M., Schwark, L., Qi, J., Nicol, G.W. et al. (2006) Archaea predominate among ammonia-oxidizing prokaryotes in soils. *Nature* **442**: 806-809.

Levi, P.S., Tank, J.L., Tiegs, S.D., Chaloner, D.T., and Lamberti, G.A. (2013) Biogeochemical transformation of a nutrient subsidy: salmon, streams, and nitrification. *Biogeochemistry* **113**: 643-655.

Levin, S. (1992) The problem of pattern and scale in ecology. *Ecology* **73**: 1943-1967.

Lock, M., Wallace, R., Costerton, J., Ventullo, R., and Charlton, S. (1984) River epilithon: toward a structural-functional model. *Oikos*: 10-22.

Lydmark, P., Lind, M., Sörensson, F., and Hermansson, M. (2006) Vertical distribution of nitrifying populations in bacterial biofilms from a full-scale nitrifying trickling filter. *Environmental Microbiology* **8**: 2036-2049.

Magalhães, C.M., Machado, A., and Bordalo, A.A. (2009) Temporal variability in the abundance of ammonia-oxidizing bacteria vs. archaea in sandy sediments of the Douro River estuary, Portugal. *Aquatic Microbial Ecology* **56**: 13.

Martens-Habbena, W., Berube, P.M., Urakawa, H., de la Torre, J.R., and Stahl, D.A. (2009) Ammonia oxidation kinetics determine niche separation of nitrifying Archaea and Bacteria. *Nature* **461**: 976-979.

Martí, E., Aumatell, J., Gode, L., Poch, M., and Sabater, F. (2004) Nutrient retention efficiency in streams receiving inputs from wastewater treatment plants. *J Environ Qual* **33**: 285-293.

Martí, E., Riera, J., and Sabater, F. (2010) Effects of Wastewater Treatment Plants on Stream Nutrient Dynamics Under Water Scarcity Conditions. In *Water Scarcity in the Mediterranean*. Sabater, S., and Barceló, D. (eds): Springer Berlin Heidelberg, pp. 173-195.

Merbt, S.N., Jean-Christophe Auguet, Emilio O. Casamayor, and Martı, E. (2011) Biofilm recovery in a wastewater treatment plant-influenced stream and spatial segregation of ammonia-oxidizing microbial populations. *Limnol Oceanogr* **56**: 1054–1064

Merseburger, G. (2006) Nutrient dynamics and metamolism in Mediterranean streams affected by nutrient inputs from human activities. *PhD Thesis, Department d`Ecologia, Universitat de Barcelona*: 26.

Merseburger, G., Martí, E., and Sabater, F. (2005) Net changes in nutrient concentrations below a point source input in two streams draining catchments with contrasting land uses. *Science of the total environment* **347**: 217-229.

Mußmann, M., Brito, I., Pitcher, A., Sinninghe Damsté, J.S., Hatzenpichler, R., Richter, A. et al. (2011) Thaumarchaeotes abundant in refinery nitrifying sludges express amoA but are not obligate autotrophic ammonia oxidizers. *Proceedings of the National Academy of Sciences* **108**: 16771-16776.

Nicol, G.W., Sven, L., Christa, S., and James, I.P. (2008) The influence of soil pH on the diversity, abundance and transcriptional activity of ammonia oxidizing archaea and bacteria. *Environmental Microbiology* **10**: 2966-2978.

O'BRIEN, J.M., and Dodds, W.K. (2008) Ammonium uptake and mineralization in prairie streams: chamber incubation and short-term nutrient addition experiments. *Freshwater Biology* **53**: 102-112.

Palmer, M., Bernhardt, E., Chornesky, E., Collins, S., Dobson, A., Duke, C. et al. (2004) Ecology for a Crowded Planet. *Science* **304**: 1251-1252.

Pastor, A., Riera, J.L., Peipoch, M., Cañas, L., Ribot, M., Gacia, E. et al. (2014) Temporal variability of nitrogen stable isotopes in primary uptake compartments in four streams differing in human impacts. *Environmental Science & Technology*.

Peipoch, M., Martí, E., and Gacia, E. (2012) Variability in δ15N natural abundance of basal resources in fluvial ecosystems: a meta-analysis. *Freshwater Science* **31**: 1003-1015.

Peipoch, M., Gacia, E., Blesa, A., Ribot, M., Riera, J.L., and Martí, E. (2014) Contrasts among macrophyte riparian species in their use of stream water nitrate and

ammonium: insights from 15N natural abundance. *Aquatic Sciences* **76**: 203-215.

Peterson, B.J., Wollheim, W.M., Mulholland, P.J., Webster, J.R., Meyer, J.L., Tank, J.L. et al. (2001) Control of nitrogen export from watersheds by headwater streams. *Science* **292**: 86-90.

Prosser, J.I. (2010) Replicate or lie. *Environmental Microbiology* **12**: 1806-1810.

Ribot, M., Martí, E., von Schiller, D., Sabater, F., Daims, H., and Battin, T.J. (2012) Nitrogen processing and the role of epilithic biofilms downstream of a wastewater treatment plant. *Freshwater Science* **31**: 1057-1069.

Romaní, A.M., Borrego, C.M., Díaz-Villanueva, V., Freixa, A., Gich, F., and Ylla, I. (2014) Shifts in microbial community structure and function in light-and dark-grown biofilms driven by warming. *Environmental Microbiology*.

Santoro, A.E., Christopher, A.F., Nicholas, R.d.S., and Alexandria, B.B. (2008) Shifts in the relative abundance of ammonia-oxidizing bacteria and archaea across physicochemical gradients in a subterranean estuary. *Environmental Microbiology* **10**: 1068-1079.

Schiller v., D., MartÍ, E., Lluis Riera, J., and Sabater, F. (2007) Effects of nutrients and light on periphyton biomass and nitrogen uptake in Mediterranean streams with contrasting land uses. *Freshwater Biology* **52**: 891-906.

Singer, G., Besemer, K., Schmitt-Kopplin, P., Hödl, I., and Battin, T.J. (2010) Physical Heterogeneity Increases Biofilm Resource Use and Its Molecular Diversity in Stream Mesocosms. *PLoS ONE* **5**: e9988.

Sonthiphand, P., Cejudo, E., Schiff, S.L., and Neufeld, J.D. (2013) Wastewater Effluent Impacts Ammonia-Oxidizing Prokaryotes of the Grand River, Canada. *Applied and Environmental Microbiology* **79**: 7454-7465.

Stoodley, P., Sauer, K., Davies, D.G., and Costerton, J.W. (2002) BIOFILMS AS COMPLEX DIFFERENTIATED COMMUNITIES. *Annual Review of Microbiology* **56**: 187-209.

Strauss, E.A., and Lamberti, G.A. (2000) Regulation of nitrification in aquatic sediments by organic carbon. *Limnol Oceanogr* **45**: 1854-1859.

Strauss, E.A., Mitchell, N.L., and Lamberti, G.A. (2002) Factors regulating nitrification in aquatic sediments: effects of organic carbon, nitrogen availability, and pH. *Canadian Journal of Fisheries and Aquatic Sciences* **59**: 554-563.

Strauss, E.A., Richardson, W.B., Bartsch, L.A., Cavanaugh, J.C., Bruesewitz, D.A., Imker, H. et al. (2004) Nitrification in the Upper Mississippi River: patterns, controls, and contribution to the NO3-budget. *Journal of the North American Benthological Society* **23**: 1-14.

Tanaka, H., and Dunn, I. (1982) Kinetics of biofilm nitrification. *Biotechnology and Bioengineering* **24**: 669-689.

Tourna, M., Freitag, T.E., Nicol, G.W., and Prosser, J.I. (2008) Growth, activity and temperature responses of ammonia-oxidizing archaea and bacteria in soil microcosms. *Environmental Microbiology* **10**: 1357-1364.

Tourna, M., Stieglmeier, M., Spang, A., Könneke, M., Schintlmeister, A., Urich, T. et al. (2011) Nitrososphaera viennensis, an ammonia oxidizing archaeon from soil. *Proceedings of the National Academy of Sciences* **108**: 8420-8425.

Treusch, A.H., Leininger, S., Kletzin, A., Schuster, S.C., Klenk, H.P., and Schleper, C. (2005) Novel genes for nitrite reductase and Amo-related proteins indicate a

role of uncultivated mesophilic crenarchaeota in nitrogen cycling. *Environmental Microbiology* **7**: 1985-1995.

United States Environmental Protection Agency, E. (2013) Aquatic life criteria: Final Ammonia Criteria. Office of Water, EPA 822-R-13-001

Vajrala, N., Martens-Habbena, W., Sayavedra-Soto, L.A., Schauer, A., Bottomley, P.J., Stahl, D.A., and Arp, D.J. (2013) Hydroxylamine as an intermediate in ammonia oxidation by globally abundant marine archaea. *Proceedings of the National Academy of Sciences* **110**: 1006-1011.

Venter, J.C., Remington, K., Heidelberg, J.F., Halpern, A.L., Rusch, D., Eisen, J.A. et al. (2004) Environmental genome shotgun sequencing of the Sargasso Sea. *Science* **304**: 66-74.

Wagner, M., Loy, A., Nogueira, R., Purkhold, U., Lee, N., and Daims, H. (2002) Microbial community composition and function in wastewater treatment plants. *Antonie Van Leeuwenhoek* **81**: 665-680.

Walker, C., De La Torre, J., Klotz, M., Urakawa, H., Pinel, N., Arp, D. et al. (2010) Nitrosopumilus maritimus genome reveals unique mechanisms for nitrification and autotrophy in globally distributed marine crenarchaea. *Proceedings of the National Academy of Sciences* **107**: 8818-8823.

Widder, S., Besemer, K., Singer, G.A., Ceola, S., Bertuzzo, E., Quince, C. et al. (2014) Fluvial network organization imprints on microbial co-occurrence networks. *Proceedings of the National Academy of Sciences*.

Winogradsky, S. (1890) Recherches sur les organismes de la nitrification. *Ann Inst Pasteur* **4**: 213–331.

Wuchter, C., Abbas, B., Coolen, M.J.L., Herfort, L., van Bleijswijk, J., Timmers, P. et al. (2006) Archaeal nitrification in the ocean. *Proceedings of the National Academy of Sciences* **103**: 12317-12322.

Zak, D.R., Blackwood, C.B., and Waldrop, M.P. (2006) A molecular dawn for biogeochemistry. *Trends in ecology & evolution* **21**: 288-295.

Zhang, T., Jin, T., Yan, Q., Shao, M., Wells, G., Criddle, C., and Fang, H.H.P. (2009) Occurrence of ammonia-oxidizing Archaea in activated sludges of a laboratory scale reactor and two wastewater treatment plants. *Journal of Applied Microbiology* **107**: 970-977.

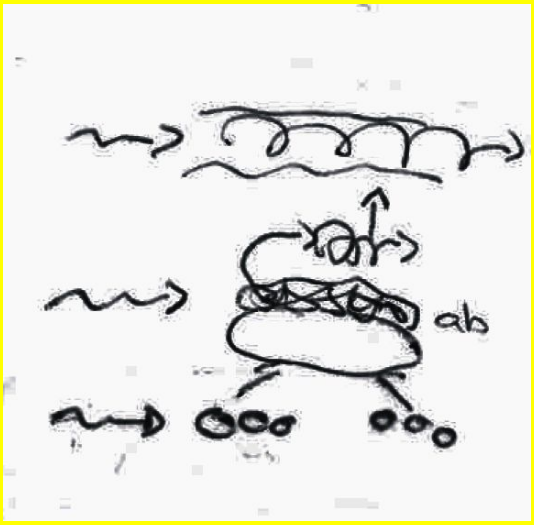

2

Study design

Cover: Conceptual illustration of the study approach by Dr Eugènia Martí

2.1. Study design

Fieldwork was carried out in La Tordera catchment (Catalonia, NE Spain), in stream reaches subjected to the continuous input of WWTP effluents. Previous studies in this catchment had shown that WWTP inputs significantly change physical and chemical conditions of receiving streams, which result in a predominantly high load of $N\text{-}NH_4^+$. These studies also showed that receiving streams can be hotspots of nitrification (Merseburger et al., 2005; Martí et al., 2010). Taking advantage of this model system, with an exacerbated N cycling promoted by nutrient inputs from human activity, we used an exploratory approach to examine the driving intrinsic and extrinsic factors for AOA and AOB abundance, spatial distribution, and community composition based on two different sampling strategies. The sampling strategy in **Chapter 3** followed the temporal patterns of biofilm development from early succession stage to mature status after a remarkable flood. The particular abundance pattern found for AOA and AOB suggested that $N\text{-}NH_4^+$ concentration, microbial inoculation from the WWTP, and sun irradiance as the main driving factors influencing the ammonia oxidizing community. In **Chapter 4** we carried out a spatial survey in five different streams affected by the inputs from WWTP effluents. This survey aimed to test the consistency of findings in Chapter 3 among streams and among seasons in a particular stream.

Clear differences in the abundance and composition of ammonia oxidizers in biofilms exposed to light and permanently shaded conditions from the exploratory studies lead us to experimentally characterize and evaluate the effect of light on in-stream nitrification. For this, a bottom up experimental strategy was designed to approach this question at different scales of organization (Figure 2.1).

First, AOA and AOB pure monospecific cultures were exposed to continuous light and light:dark cycles in the laboratory (Figure 2.2 A) to asses how light

affected their nitrification activity. This experiment revealed that the nitrification activity of both AOA and AOB was highly photoinhibited and barely recovered during the dark phase (**Chapter 5**). Second, we tested the effect of light on nitrification capacity of stream biofilm assemblages. For this, we set a microcosm experiment, using recirculating chambers in the laboratory, in which stream biofilms from a reach upstream and a reach downstream of a WWTP input were exposed to light, darkness and different light regime treatments (Figure 2.2 B).

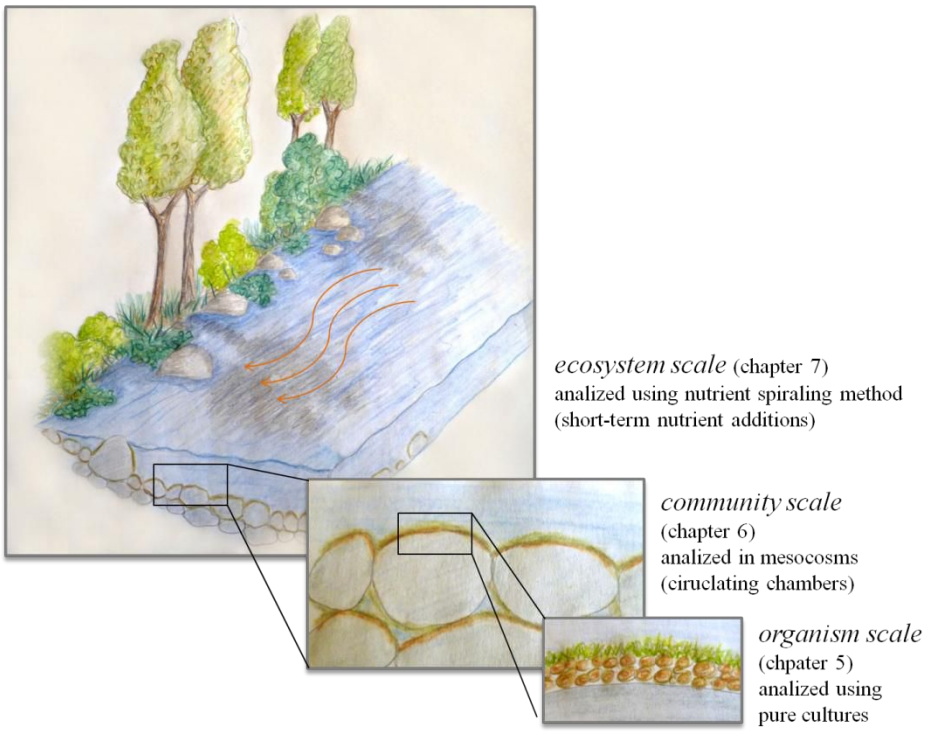

Figure 2.1: conceptual setting of the experimental study design of the part II of the thesis. The effect of light on nitrification was tested at three organizational scales. First the effect of light was tested on cultures of single species of AOA and AOB; second on AOA and AOB embedded in the matrix of benthic stream biofilms; and third on whole-reach nitrification rates. Illustrated by Veronika Rubner.

The microcosm experiment showed that mature biofilms naturally developed under light conditions were less susceptible to the light treatment than biofilms naturally developed under dark conditions in terms of nitrification capacity. These findings suggested that AOA and AOB in biofilms developed under light conditions were protected from photoinhibition possibly due to the biofilm matrix; and thus, an *umbrella effect* by the biofilm matrix was proposed to sustain nitrification in the light-exposed biofilms (**Chapter 6**). Finally, to evaluate the effect of light on in-stream nitrification at the ecosystem level, a whole-reach experiment was carried, where nitrification was measured in two stream reaches differing significantly in canopy cover; and thus in light availability (Figure 2.2 C; **Chapter 7**). In addition, to further asses the effect of dial variation in light, at each reach nitrification was measured at daytime and nighttime. This study revealed that nitrification at whole-reach scale was not subjected to diurnal variation and was independent of light availability in stream reaches. Lack of photoinhibition effect on nitrification at reach scale could be explained by results from previous studies in the mesocosms, which showed several light avoiding strategies for AOA and AOB to develop in natural stream environments regardless of the light availability.

To further understand the mechanistic explanation of nitrification patterns at whole-reach scale, in the general discussion we provide a back-to-the-envelope exercise where biofilm-scale nitrification rates from Chapter 6 were scaled to whole-reach rates aiming to evaluate the particular contribution of biofilms developed in different streambed habitats (i.e., cobbles and sediment).

Figure 2.2: A- Stock of pure cultures of ammonia oxidizing organism used in Chapter 5; B- Recirculating chambers with oxygen probe in the water bath used in the experiments of Chapter 6; C- Experimental setting of the constant rate addition of NH_4^+ in a stream reach to measure whole-reach nitrification used in the study of chapter 7.

2.2 References

Martí, E., Riera, J., and Sabater, F. (2010) Effects of Wastewater Treatment Plants on Stream Nutrient Dynamics Under Water Scarcity Conditions. In *Water Scarcity in the Mediterranean*. Sabater, S., and Barceló, D. (eds): Springer Berlin Heidelberg, pp. 173-195.

Merseburger, G., Martí, E., and Sabater, F. (2005) Net changes in nutrient concentrations below a point source input in two streams draining catchments with contrasting land uses. *Science of the total environment* **347**: 217-229.

PART I

Biofilm recovery in a wastewater treatment plant influenced stream andspatial segregation of ammonia-oxidizing microbial populations

3

Reproduction with permission of Stephanie N. Merbt, Jean-Christophe Auguet, Emilio O. Casamayor, Eugènia Martí (2011) Biofilm recovery in a wastewater treatment plant-influenced stream and spatial segregation of ammonia-oxidizing microbial populations. Limnology and Oceanography 56(3), 2011, 1054–1064 doi: 10.4319/lo.2011.56.3.1054

Cover: Effluent of the waste water treatment plant of Santa Maria Palautordera (NE Spain). Photograph by SN Merbt.

3.1 Abstract

We monitored the effects of a wastewater treatment plant (WWTP) inputs on the recovery of stream biofilms after a large flood event that eroded most of the former biofilm communities. We monitored biomass recovery, chlorophyll *a*, nitrogen content, and stable isotope natural abundance (^{15}N) over eight weeks in light- and dark-exposed biofilms upstream and downstream from WWTP inputs, respectively, as well as the abundance of ammonia oxidizers by quantitative polymerase chain reaction (qPCR). Biomass and chlorophyll *a* recovered quickly (< 2 weeks), and were significantly higher for light- than for dark-exposed biofilms. There was no consistent effect of WWTP inputs on these parameters, except for the biomass on dark-exposed biofilm that was higher at the WWTP-influenced sites. The influence of the WWTP inputs on stream-water ammonium concentration and its isotopic ^{15}N signature increased as the flood receded. Biofilm ^{15}N downstream of WWTP increased over time tracking the increase in ^{15}N-ammonium from the WWTP waters. Bacterial and archaeal ammonia oxidizers were present within the biofilm assemblages from early stages of post-flood recovery. However, spatial distribution of these two clades was clearly segregated among sites and between light and dark-exposed biofilms, probably related to ammonium availability and the development of photoautotrophic organisms.

3.2 Introduction

Streams transport dissolved and particulate materials from adjacent terrestrial ecosystems to larger rivers and coastal zones. Human activity alters stream nutrient concentrations through nutrient-rich sources through point (e.g., effluents from wastewater treatment plants-WWTP) or diffuse (e.g., from agricultural activities) inputs. In urban areas, nutrient point sources can be a significant cause of the urban stream syndrome (Walsh et al. 2005). High nutrient concentrations in WWTP-influenced streams lead to decreasing nutrient retention efficiency and loss of species diversity, which ultimately results in eutrophication of downstream ecosystems (Martí et al. 2004; Camargo and Alonso 2006; Sánchez-Pérez et al. 2009). However, these streams have also been reported as hot spots for microbial nitrification, when they are subjected to large inputs of ammonium (NH_4^+) from the WWTPs (Merseburger et al. 2005). In the Mediterranean region, both water scarcity, a common feature that drives the hydrological regime of these streams, and relatively constant anthropogenic inputs from WWTPs, have a very pronounced effect on stream ecology and biogeochemistry because of the reduced diluting capacity (Martí et al. 2010). Moreover, the Intergovernmental Panel to Climate Change (IPCC) has predicted for the Mediterranean region consistent decreases in precipitation and annual runoff (Bates et al. 2008), which will further exacerbate the local effects of anthropogenic inputs.

Increases in nitrogen (N) concentration (mainly NH_4^+) are commonly observed in streams loaded with inputs from urban WWTP effluents (Martí et al. 2010). NH_4^+ is the preferential N source for primary uptake and a potential limiting nutrient for stream communities (Borchardt 1996; Hall and Tank 2003). However, even at relatively low concentrations, NH_4^+ can be highly toxic to aquatic organisms, whereas at high concentrations it may promote eutrophication (Camargo and Alonso 2006). Stream microbial communities

(biofilms) can play a key role controlling bioreactive N loads since microbes mostly mediate the processes of N transformation and retention (Peterson et al. 2001; Falkowski et al. 2008; Mulholland et al. 2008). In benthic ecosystems, biofilms are a substrata-attached, matrix embedded, complex mixture of algae, bacteria, fungi, and microzoans (Lock et al. 1984; Battin et al. 2003). Their three dimensional layer structure, compositional heterogeneity and biomass accrual depend on flow velocity, light and nutrients availability (Bersemer et al. 2007; von Schiller et al. 2007; Singer et al. 2010). Microbial diversity and identity in biofilms determine the efficiency at which N is uptaken and transformed; and thus, it may influence N biogeochemistry at the whole-reach scale (Loreau et al. 2001; Prosser et al. 2007).

Understanding both the structure of the biofilm and how it processes N inputs can provide insights on the mechanisms driving global stream N cycling. In particular, excess of NH_4^+ inputs can be biologically modulated by both assimilation and microbial nitrification associated to biofilms (Merseburger et al. 2005). Nitrification is a key process in highly N-loaded streams since the end product (i.e., nitrate; NO_3^-) can be further transformed under anaerobic conditions into N_2 gas through denitrification, which finally results in a net loss of N to the atmosphere. Microbial nitrification is a two-step oxidation process of NH_4^+ to NO_3^- via nitrite (NO_2^-). Ammonia oxidation is the rate-limiting step of nitrification. This step is carried out by two phylogenetically distant groups, which include three genera of the Bacteria domain (*Nitrosomonas, Nitrosococcus,* and *Nitrosospira;* Koops and Pommerening-Röser 2001) and a few recently described members of the domain Archaea, apparently restricted to the highly diverse *Thaumarchaeota* phylum (Spang et al. 2010). Both, bacterial and archaeal ammonia oxidizers encode for the alpha subunit of the enzyme ammonium monooxygenase (*AMO*); however, the gene sequence is different enough to easily distinguish ammonia oxidizing archaea (AOA) from bacteria (AOB).

In the present study, we examined the patterns of biofilm development from emerging to mature communities in a WWTP-influenced stream after an unusually high flood disturbance. Development of the biofilm was separately examined for communities coating the light- and dark-exposed sides of cobbles since we expected they would differently respond to the influence of WWTP inputs. For this study we followed a multiparametric approach considering several structural and biogeochemical parameters. To the best of our knowledge, there is a lack of combined stream ecology and microbial ecology studies addressing the development, structure and function of biofilm communities in high N-loaded streams. The information provided here is relevant for understanding the fate of external N inputs, especially in WWTP-influenced streams.

3.3 Methods

Study site. The study was conducted in La Tordera river catchment (41°41'3.47"N; 2°27'33.19"W; NE Spain) from January to March 2009. We selected a 850 m reach along the mainstream located near the village of Santa Maria de Palautordera which receives the inputs from the local WWTP effluent (population 8235 inhabitants). The WWTP was not submitted to tertiary treatment and had a partial nitrifying capacity. Over the study period, average concentrations of NO_3^- and NH_4^+ in the WWTP effluent were 4.9±2.6 mg N L^{-1} and 5.7±1.7 mg N L^{-1}, respectively; and average effluent outflow was 32.6±5.5 L s^{-1} (data provided by the Santa Maria de Palautordera WWTP management agency). A previous study indicated that the selected reach was a hot spot for chemotrophic activity (i.e., nitrification; Merseburger et al. 2005). The reach had a channel with low sinuosity and a slope close to 1%. The streambed substrate was dominated by cobbles (34%), pebbles (22%), and boulders (22%). Three sampling sites were defined along the reach based on the distance to the WWTP. The first sampling site was located 75 m upstream of the point source

(hereafter referred to as UP) and was used as the reference site. The other two sampling sites were located 150 m and 850 m downstream from the WWTP input, respectively (hereafter referred to as DW1 and DW2, respectively). These two sites were selected to represent different availabilities of NO_3^--N and NH_4^+-N due to the high rates of nitrification previously observed along this reach (Merseburger et al. 2005). Thus, dominance of NH_4^+-N was expected at DW1, whereas dominance of NO_3^--N was expected at DW2.

Early in January 2009, a large storm event lasting for two weeks caused an abrupt and remarkable increase in stream discharge, which completely eroded the biofilm from the surface of cobbles. The sampling sites were sampled weekly from 23 January to 23 March (a total of 8 sampling dates). During this period, stream flow gradually decreased, except from the occurrence of another rainfall event between the 3rd (30 January 2009) and 4th (09 February 2009) sampling week, which resulted in another flood of minor intensity.

Field measurements and sample collection: On each sampling date, discharge was estimated at sites UP and DW2 by measuring both water depth and velocity at 50 cm intervals, respectively, using a tape and a velocity meter (Schiltknecht Messtechnik) in a selected channel transect. Water temperature and conductivity were measured at all sites using a portable conductivity meter (WTW Weilheim).

At each site we collected 5 L water samples for the analysis of NO_3^--N and NH_4^+-N, and their respective ^{15}N isotope signatures. The samples were stored on ice for less than 2 h and once in the laboratory were immediately filtered through ignited glass fiber filters (FVF; 0.7 μm pore size, Albet). Biofilm samples from riffle areas were collected from the surface of 6 randomly selected, fist sized, submerged cobbles not embedded into the sediment. Biofilm samples from the light-exposed side of the cobble (hereafter referred to as light

side) and from the reverse side of the cobble facing the sediment (hereafter referred to as dark side) were separately treated.

For the measurement of biofilm biomass (expressed as ash free dry mass – AFDM), chlorophyll *a* (Chl *a*), N content, and ^{15}N isotopic signature, biofilm was sampled from 3 cobbles by scraping their surface and filtering the sludge onto ignited, pre-weighted glass fiber filters (FVF). The total surface scraped was estimated after covering cobbles with aluminum foil and following a weight-to-area relationship. Filters for Chl *a* analysis were stored at -20°C, whereas the remaining filters were dried (60 °C) until constant weight (ca. 0.1 mg, Sartorius analytical balance, model MC1). For the quantification of the ammonia oxidizers, the biofilm of 3 additional cobbles was washed with MilliQ-water, scratched, and pooled together in a single 250 mL plastic beaker. All samples were transported to the laboratory on ice within two hours after sampling.

Laboratory methods. NH^+_4-N concentration was analyzed with a Nova 60 Spectroquant (Merk) with the photometric ammonium test (Merck, 1.14752.0001). This method was sensitive enough for this analysis considering the high *in situ* concentrations. The concentration of NO_3^--N was analyzed using a Bran+Lubbe Aace 5.23 Technicon Autoanalyzer (Scientific-Technical Services). The two analyses were carried out following standard colorimetric methods (APHA 1995). The ^{15}N natural abundance of NH_4^+ and NO_3^- in the water was determined following the ammonia diffusion protocol by Holmes et al. (1998) and the sequential reduction and diffusion method by Sigman et al. (1997), respectively, as described in von Schiller et al. (2009). Briefly, a certain volume of filtered water sample containing ca. 100 μg NH^+_4-N, was poured into a high density polyethylene bottle, and further amended with 3.0 g L^{-1} of MgO, 50 g L^{-1} of NaCl, and a Teflon filter packet, which contained a 1 cm diameter ashed glass fibre filter (GF/D grade, Whatman, Kent), acidified with 25 μL of

2.5 m $KHSO_4$. Water bottles were tightly capped and incubated in a shaker at 40 ºC for four weeks to allow the diffusion of volatilized NH_3 onto the acidified filter. To analyze ^{15}N natural abundance of NO_3^-, a volume of water sample containing ca. 100 μg NO_3^--N was poured into a beaker; and it was amended with 3.0 g of MgO and 5.0 g of NaCl and boiled to remove the NH_4^+ and to concentrate the sample. The sample was then transferred into a HDPE bottle to which 0.5 g of MgO, 0.5 g of Devarda's alloy, and a Teflon filter packet were added. Bottles were tightly capped and incubated at 60 ºC for 48 h to reduce NO_3^- to NH_4^+, and then they were placed on a shaker for 7 d to allow for diffusion of NH_3 onto the acidified filter. Once the incubations were completed, filters were removed from the bottles, placed in scintillation vials, dried in a desiccator for 4 d, encapsulated in tins, and stored until ^{15}N analysis. A set of blanks and standards of known concentration for ^{15}N-NH_4^+ and ^{15}N-NO_3^- were processed along with the water samples.

To estimate AFDM (in g m^{-2}), biofilm samples collected on glass fiber filters were combusted at 500 °C for 5 h and weighted as indicated above. The AFDM was estimated as the mass difference between dry and combusted filters and was reported per unit of surface area. Chl *a* (in μg cm^{-2}) was determined in acetone extracts by spectrophotometry (UV-2401PC, ultraviolet-visible Spectrometer, Shimadzu) following Steinman and Lamberti (1996), and correcting for phaeopigments by further acidification. A sub-sample of the glass fiber filters (i.e., 1 cm diameter) was placed in scintillation vials, dried in a desiccator for 4 d, weighted, encapsulated in tins, and stored until ^{15}N analysis. The filters for ^{15}N and N content analysis of NH_4^+, NO_3^- and biofilm were sent to the University of California Stable Isotope Facility (Davis). The analysis was done by continuous flow isotope ratio mass spectrometry (20–20 mass spectrometer; PDZ Europa) after sample combustion in an on-line elemental analyzer (PDZ Europa, ANCA-GSL). The ^{15}N content of the samples is reported as the ^{15}N:^{14}N

ratio of the sample relative to the ^{15}N:^{14}N ratio of the standard (N_2 from the atmosphere) using the notation $\delta^{15}N$ (in ‰).

Deoxyribonucleic acid (DNA) extraction and quantification of ammonia-oxidizing microorganisms. A sub-set of selected biofilm samples from light- and dark-sides of sites UP, DW1, and DW2, and sampling weeks 1, 6, and 8 was processed. Microorganisms were detached from particles by incubation with Tween 20 detergent (10^{-6} % w v^{-1}) for 5 min followed by soft sonication (Sonopuls ultrasonic homogenizer HD 2070) with 20 s pulses at 10% power (Epstein and Rossel 1995). Supernatant was filtered through a 0.2 μm pore size policarbonate membrane (Millipore). Filters were incubated with lysozyme, Proteinase K, and sodium dodecyl sulfate in lysis buffer (40 mmol L^{-1} ethylenediaminetetraacetic acid, 50 mmol L^{-1} Tris, pH 8.3, and 0.75 mol L^{-1} sucrose), and phenol-extracted as previously described (Dumestre et al. 2002). Presence and quantification of AOB and AOA was based on *amoA* gene copy numbers estimated by quantitative real-time polymerase chain reaction (qPCR) amplification. The qPCR assays were run on 96 well transparent plates with adhesive seals (Bio-Rad) in a DNA Engine thermal cycler (Bio-Rad, Hercules) equipped with a Chromo 4 Real-Time Detector (Bio-Rad). The AOB primers amoA-1F (5_-GGGTTTCTACTGGTGGT-3_) and amoA-2R (5_-CCCCTCKGSAAAGCCTTCTTC-3_) generated a 491base pairs (bp) fragment (Rotthauwe et al. 1997). The AOA primer sets CrenamoA23f (5_-ATGGTCTGGCTWAGACG-3_) and CrenamoA616r (5_-GCCATCCATCTGTATGTCCA-3_) amplified a 628 bp fragment (Tourna et al. 2008). The selected primer sets had been previously tested in the qPCR approach (Wessén et al. 2009). The quantification was run in a final volume of 20 μL containing 10 μL solution of SsoFast EvaGreen supermix (BioRad), 20 ng of template genomic DNA, 10μmol L^{-1} of each corresponding primer, and molecular biology grade water (Sigma). The reaction started with an initial denaturation step of 2 min at 98°C, followed by 45 cycles of denaturation at 98

°C for 5 s annealing at 58°C for *amoA* of AOB, and 57 °C for *amoA* of AOA, respectively for 20 s, and elongation at 72 °C for 15 s. Fluorescence signal was read after each elongation step. Finally, a denaturation step was done for 1 min at 98 °C followed by 1 min at 65 °C to ensure stringent coupled DNA fragments. All reactions were finished with a melting curve starting at 55 °C and increasing by 0.5 °C until 95 °C to verify amplicon specificity. Each approach was run in triplicate with standard curves spanning from 10^2 to 10^8 copies of DNA *amoA* genes. Standards were obtained after conventional PCR amplification of available environmental clones. The standard was purified (QIAquick, QIAGEN), quantified (Qubit flourometer, Invitrogen), and serial diluted for standard curves (r^2=0.99 for both standard curves). Overall, average efficiencies of all quantification reactions ranged from 74 % to 99 %. Controls without templates resulted in undetectable values in all samples. Specificity of the PCR reactions was confirmed by agarose gel electrophoresis (data not shown). No unspecific PCR products such as primer dimers or gene fragments of unexpected length were observed. The results of the qPCR analysis are expressed in copies of *amoA* per g AFDM (i.e., organic matter) of the biofilm to allow comparison of results among sampling sites, cobble sides, and sampling dates.

Statistical analysis. The effect of the WWTP inputs on stream N concentration was assessed by comparing NH_4^+-N and NO_3^--N concentrations and their ^{15}N signatures among sites over the study period, using a Kruskal-Wallis analysis of variance (ANOVA) non parametric test (site as a factor). This test was also used to compare AOA and AOB *amoA* gene copy numbers on light and dark side biofilms between the sampling sites (side as a factor). Spearman rank R non parametric correlations were used to examine relationships among hydrology, N concentrations, and ^{15}N signatures of dissolved inorganic N (DIN) forms. Comparison of AFDM, chlorophyll *a* content, N content and ^{15}N natural abundance among sites and between samples from light- and dark-sides was

done using two-way ANOVA tests (site and cobble side as factors) with repeated measures (sampling week as the within-effect). This allowed testing the WWTP effect on the biofilms of both sides of cobbles considering the patterns of temporal variation of the dependent variables after the flood disturbance. The test was done on Ln-transformed values to fit statistical requirements of normality. ^{15}N signatures of DIN forms and those of biofilms at each site were compared using a Wilcoxon matched pair test on data from light- and dark-side biofilm samples separately. Finally, relationships between temporal variation of ^{15}N signatures of DIN forms and those of biofilm were examined using Spearman rank R non parametric correlations. For these last two tests we used average ^{15}N biofilm values from the 3 replicates collected on each date at each site and from each cobble side. Results were considered significant for $p < 0.05$. All statistical analyses were done using Statistica 6.0 (Statsoft).

3.3 Results

Physical and chemical parameters. Water discharge consistently decreased over time after the intense rainfalls of early January (Figure 3.1). During the third sampling week, another storm event increased stream discharge again up to ~ 1.4 $m^3 s^{-1}$. By the end of the sampling period, despite we observed a significant decrease in discharge, it was still relatively high compared to typical base flow levels (c.a. <0.1 $m^3 s^{-1}$). Conversely, the WWTP effluent discharge was relatively constant over the study period (data from the WWTP management agency) and its contribution to downstream discharge ranged from 2.3 % at the beginning to 11.5 % at the end of the study. As a result of this variation, discharge at UP and DW2 sites was similar at the beginning of the study, but it tended to be higher below the WWTP by the end of the study. At the UP site, water temperature decreased from 8.5 °C to 6.2 ºC over the first sampling weeks

with a minimum value on the 3rd sampling week, after the second flood. After this event, temperature gradually increased up to 9 ºC by the end of the study (data not shown). The pattern of temporal variation in water temperature was similar for all sites, but values were on average (±1SEM) 1.1±0.4 °C higher at the DW1 and DW2 sites than at the UP site. Conductivity ranged between 88.5 and 132.7 μS cm^{-1} and had no clear temporal pattern at any site, although at the UP site it tended to decrease by the end of the study period. On average, conductivity was 1.4 times lower at the UP site than at the DW1 and DW2 sites (Kruskal-Wallis ANOVA, $p<0.001$).

NO_3^--N concentration was already high at the UP site (i.e., ~ 2 mg N L^{-1}, Figure 3.1) and no significant differences were found among the three sites (Kruskal-Wallis ANOVA, $p>0.05$). Temporal variation of NO_3^--N concentration was similar among sites and it was positively related with discharge (Spearman correlation, $n=24$, $r=0.65$, $p<0.001$). Conversely, NH_4^+-N concentration was clearly affected by the WWTP input. At the UP site, NH_4^+-N concentration was consistently below detection limit (i.e., <0.01 mg N L^{-1}). Downstream of the WWTP, NH_4^+-N concentration was significantly higher (Figure 3.1), ranging from 0.2 to 1.4 mg N L^{-1} over the entire study period with no significant differences between DW1 and DW2 (Kruskal-Wallis ANOVA, $p>0.05$).

The N input from the WWTP represented an average increase in DIN concentration below the WWTP of 1.4 times the upstream concentration. It also represented a shift in the relative proportion of DIN as NO_3^--N from 99.9% at the UP site to 79.5% at the downstream sites. At these sites, temporal variation in NH_4^+-N concentration was negatively related with NO_3^--N concentration (Spearman correlation, $n=14$, $r=-0.67$, p=0.008) and with discharge (Spearman correlation, $n=14$, $r=-0.63$, $p=0.016$).

The δ^{15}N values of NO_3^--N in the water column had no significant variation both among sites (Kruskal-Wallis, $p>0.05$) and over time (Figure 3.2). Taking all

sites and dates together, the average (±1SEM) of δ^{15}N-NO_3^- was 5.75±0.17‰. The δ^{15}N values of NH_4^+-N in the water column were significantly lower at the UP site than at the two downstream sites (Kruskal-Wallis, p=0.004). No significant difference in δ^{15}N-NH_4^+ was found between DW1 and DW2. At the UP site, the δ^{15}N-NH_4^+ was relatively constant over time and averaged -4.92±0.61‰ (Figure 3.2). At the downstream sites, the δ^{15}N-NH_4^+ increased over time from 14.1‰ to 29.5‰ at DW1 and from 10.7‰ to 32.0‰ at DW2. The δ^{15}N-NH_4^+ at these two sites was negatively related with stream discharge (Spearman correlation, n= 16, r=-0.60, p=0.013).

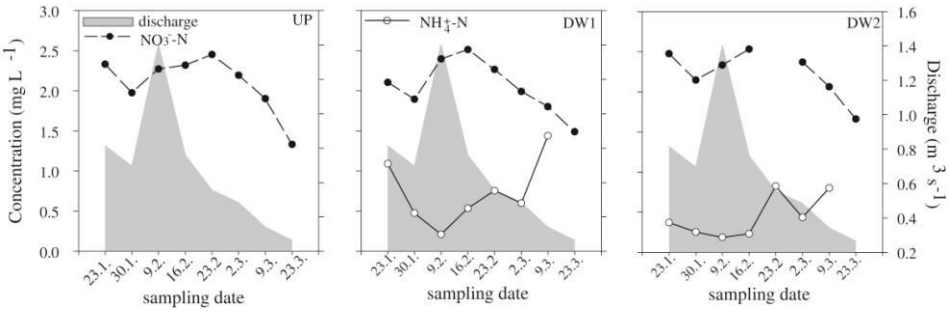

Figure 3.1: Temporal variation in discharge (shaded area), and NH_4^+-N (white dots) and NO_3^--N (black dots) concentrations during the study period at UP, DW1, and DW2. Missing data are lost samples. NH_4^+-N concentration at UP site was below detection limits.

Biofilm characterization. Biofilm biomass (expressed as AFDM) increased over time at all sites (Figure 3.3). However, the increases in AFDM were more evident for biofilms on the light-side, which showed a faster recovery after the flood, than on the dark-side. For instance, one week after the flood, biofilm AFDM on the light-side had increased by 75% at the UP site. After the 4th sampling week, AFDM accrual on the light side stabilized reaching similar values at all sites. However, at the DW2 site, light-side AFDM decreased tremendously on the last two sampling weeks. Significant differences (two-way ANOVA) in AFDM accrual were found between light- and dark-side biofilms,

but not among sites (Table 3.1). However, when sites were compared, we found that dark-side, but not light-side, biofilms had significantly higher AFDM at the downstream sites than at the UP site (one-way ANOVA, p=0.011).

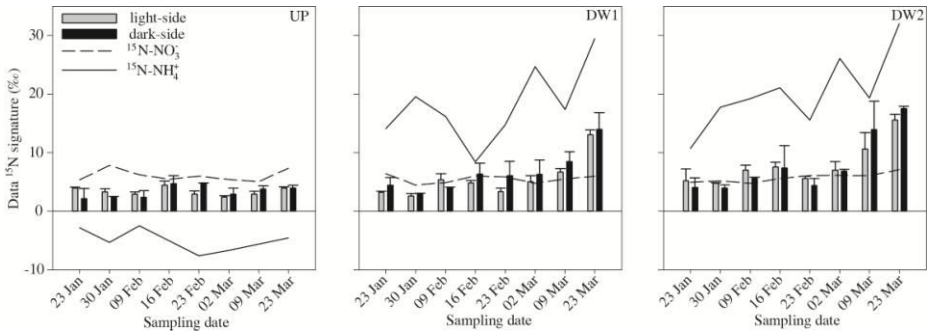

Figure 3.2: Temporal variation in ^{15}N natural abundance (expressed as $\delta^{15}N$ in ‰) of both dissolved inorganic N forms in water and biofilms during the study period at UP, DW1, and DW2. Graphs show the mean values (n=3) for biofilms on the light (grey bars) and dark (black bars) sides of cobbles. Lines above the bars are the standard error of the mean. Doted line shows ^{15}N natural abundance of nitrate, and continuous line shows ^{15}N natural abundance of ammonium.

Chl *a* showed slightly different accrual patterns than those observed for AFDM (Figure 3.3). As expected, the light-side biofilms showed significantly higher Chl *a* content than the dark-side biofilms (Table 3.1). Results from the two-way ANOVA with repeated measures also indicated a significant effect of the sampling date on Chl *a*, which varied among sites (Table 3.1). At the UP site, a nearly exponential increase of Chl *a* was observed over the study period in the light-side biofilm (Figure 3.3). At the DW1 and DW2 sites, Chl *a* reached steady-state after the 5th sampling week (Figure 3.3). Chl *a* content in the dark-side biofilm was higher at DW2 than at DW1 and UP sites (Table 3.1).

Sampling site, side of the cobble, and sampling date had all a significant effects on the biofilm N content (as a percentage of dry weight), with no significant interactions among these factors (two-way ANOVA with repeated measures, Table 3.1). N percentage in biofilms gradually increased over time at all sites

Table 3.1. Statistical results form two-way ANOVAs with repeated measures for biofilm AFDM, chlorophyll *a* content, nitrogen content (as percentage of dry weight), and ^{15}N as dependent variables. Independent factors were sampling site (i.e., UP, DW1, and DW2) and side of the cobble (i.e., light and dark); and sampling date was considered as a within effect factor. Values highlighted in bold indicate factors or interaction among factors with significant effects (i.e., $p<0.05$).

	AFDM		Chlorophyll *a*		%N		^{15}N	
	F	*P*	*F*	*p*	*F*	*P*	*F*	*p*
Intercept	22.6	**0.02**	484.6	**0.00**	0.0	0.85	11896.3	**0.00**
Site	3.0	0.19	2.0	0.23	7.7	**0.02**	324.2	**0.00**
Part	31.6	**0.01**	209.0	**0.00**	111.0	**0.00**	1.8	0.31
Site x part	0.7	0.57	9.3	**0.02**	1.2	0.35	18.4	0.05
Week	2.5	0.05	13.5	**0.00**	4.2	**0.00**	49.4	**0.00**
Week x site	1.4	0.22	2.9	**0.01**	0.8	0.64	9.8	**0.00**
Week x part	1.5	0.22	0.6	0.74	0.9	0.50	9.4	**0.00**
Week x site x part	1.6	0.16	1.5	0.16	0.4	0.98	7.2	**0.00**

.

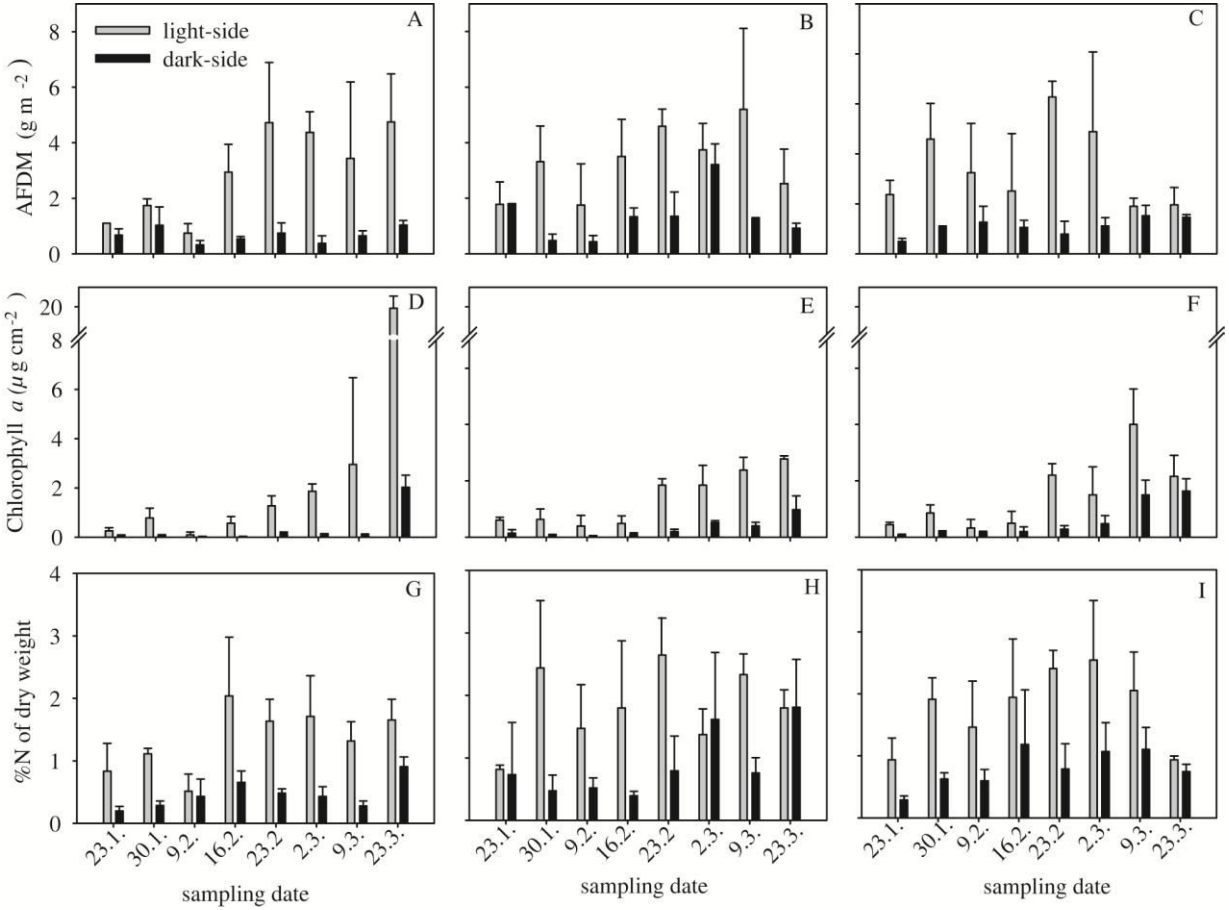

Figure 3.3: Temporal variation in AFDM, chlorophyll *a* content, and N content during the study period at the (A, D, G) UP, (B, E, H) DW1, and (C, F, I) DW2 sites.
Graphs show the mean values (n=3) for biofilms on the light (grey bars) and dark (black bars) sides of cobbles. Lines above the bars are the standard error of the mean.

(Figure 3.3), and was 2.5 times higher in the light-side than in the dark-side biofilms for all sites. In addition, N percentage in light- and dark-side biofilms at the DW1 and DW2 sites (average 2.0 % in light-side and 0.9 % in dark-side) was 1.5 and 1.9 times higher, respectively, than at the UP site (average: 1.3 % in light-side and 0.5 % in dark-side).

We observed a significant interaction effect among the 3 factors considered (sampling site, side of the cobble and sampling time) on the biofilm $\delta^{15}N$ (two-way ANOVA with repeated measures, Table 3.1). The $\delta^{15}N$ values showed different temporal patterns at each sampling site, but no significant differences between the light and dark-sides of the cobbles (Figure 3.2). At the UP site, the $\delta^{15}N$ values of dark- and light-side biofilms were similar and relatively stable over time, and averaged 3.35±0.85‰ (Figure 3.2). This value was significantly lower than $\delta^{15}N\text{-}NO_3^-$ (6.07±1.00‰, Wilcoxon matched pair test, p=0.012) and higher than $\delta^{15}N\text{-}NH_4^+$ (-4.94±0.61‰; Wilcoxon matched pair test, p=0.012). At the downstream sites, values of biofilm $\delta^{15}N$ were similar to those at the UP site during the first four sampling weeks (Figure 3.2). From the 5th week onward, in contrast to the steady biofilm $\delta^{15}N$ values of the UP site, values at the downstream sites gradually increased on both cobble sides (Figure 3.2). This temporal pattern of biofilm $\delta^{15}N$ was more pronounced at the DW2 site (Figure 3.2). Finally, biofilm $\delta^{15}N$ of both the light and dark-sides of cobbles at the downstream sites was similar to $\delta\ ^{15}N\text{-}NO_3^-$ (Wilcoxon matched pair test, p>0.05) and lower than $\delta\ ^{15}N\text{-}NH_4^+$ (Wilcoxon matched pair test, p=0.011). Nevertheless, the temporal variation in $\delta\ ^{15}N$ of biofilm at these two sites was positively related with $\delta^{15}N\text{-}NH_4^+$ (Spearman correlations, n=16, r=0.65, p=0.007 for the light-side; and n=16, r=0.52, p=0.040 for the dark-side) and not related with $\delta\ ^{15}N\text{-}NO_3^-$.

Ammonia-oxidizing microbial assemblages. Results from qPCR indicated presence of ammonia oxidizer populations in all sites. However, *amoA* relative

abundance and patterns of distribution among sites and cobble sides largely differed between AOB and AOA (Figure 3.4). AOB were only detected at downstream sites and were significantly more abundant in dark- than in light-side biofilms (Kruskal-Wallis, p = 0.012). In addition, a*moA* copies of AOB from the dark-side biofilms were higher at DW2 than at DW1; and in the dark-side of DW2 a*moA* copies gradually increased over the study period.

Conversely, AOA were detected at both upstream and downstream sites. The relative number of *amoA* gene copies tended to be more abundant in the dark- than in the light-side biofilms (Figure 3.4). This pattern is clearly consistent for samples from the DW2 site, where we observed the highest abundance of AOA, especially in the dark-side of the cobbles.

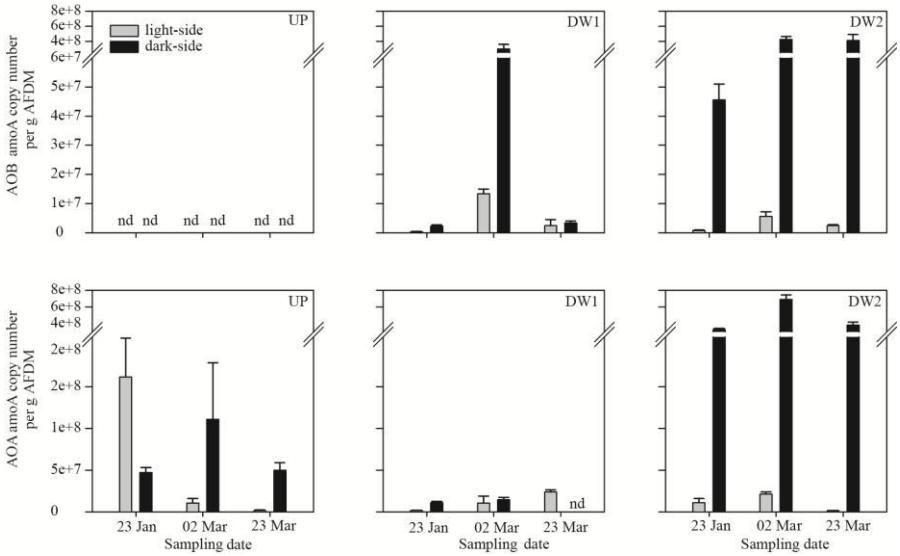

Figure 3.4: Temporal variation of bacterial and archaeal *amoA* copy number per gram AFDM of the biofilm during the study period at UP, DW1, and DW2. Data shown correspond to sampling weeks 1 (23 January), 6 (02 March), and 8 (23 March). Graphs show the mean values of methodological replicates (n=3) for biofilms on the light (grey bars) and dark (black bars) sides of cobbles. Lines above the bars are the standard error of the mean. At the UP site no bacterial *amoA* was detected over the study period. nd – not detected

3.4. Discussion

Influence on water chemistry. This study started under high flow conditions when downstream transport of nutrients usually dominates over in-stream nutrient uptake or transformation (Peterson et al. 2001; Argerich et al. 2008). Under these conditions, even though the dilution capacity of the stream was extraordinary high, the influence of the WWTP input was still remarkable. High NH_4^+-N and NO_3^--N concentrations measured in the WWTP effluent indicated that this was a relevant source of DIN to the stream. However, the influence of the WWTP input was more pronounced for NH_4^+-N, which increased by two orders of magnitude, than for NO_3^--N concentrations. Probably this is because upstream of the WWTP NH_4^+-N load was very low whereas NO_3^--N load was already high. Similar results have been reported by other studies in WWTP-influenced streams under baseflow conditions (Martí et al. 2004; Carey and Migiaccio 2009; Martí et al. 2010). Therefore, while NH_4^+-N concentration was mostly controlled by WWTP inputs, NO_3^--N concentration was controlled by soil runoff from the upstream catchment. The WWTP input also increased the ^{15}N signature of NH_4^+-N. This effect became more evident as discharge decreased. Stable isotopes have been successfully used to identify anthropogenic N sources in aquatic ecosystems due to their different ^{15}N signals (Lajtha and Michener 1994). Previous measurements of $\delta^{15}N$ in the study WWTP effluent for NH_4^+ and NO_3^- were 13.6-27.8‰ and 2.7-10.3‰, respectively (M. Ribot pers. comm.), indicating that DIN, especially NH_4^+, derived from the WWTP effluent was highly enriched in ^{15}N species. This is in agreement with previous studies (Robinson 2001; deBruyn and Rasmussen 2002), and supports the use of ^{15}N signatures of DIN forms in WWTP-influenced streams as tracers of WWTP-derived N.

The recovery of stream biofilm communities. Temporal changes of both stream hydrology and the relative influence of the WWTP inputs, lead to a structural and functional response of the biofilm communities. In general, biofilm

recovery was fast (i.e., 15 days) regardless of the site location. As the flood receded, biomass and Chl *a* content gradually increased and reached nearly steady-state after 1.5 months at all sites. Temperature, light and hydrological regime have been identified as important factors in algal and bacterial succession in river biofilms (Lyautey et al. 2005). At high flow conditions, such as in this study, early biofilms show low biomass accrual, whereas mature communities can show a decrease of biomass because of surface detachment (Battin et al. 2003; Rickard et al. 2004). Therefore, biofilm biomass is temporally variable and experiences successive accumulation, autogenic sloughing, and externally caused physical disturbances. These processes lead to the observed equilibrium in which accumulation and losses of biomass became relatively balanced (Biggs 1996). However, despite biofilms reached steady-state biomass, their influence on water column DIN concentrations along the downstream reach was negligible because no differences were observed either in NH_4^+-N or NO_3^- -N concentrations or in their ^{15}N signatures between the DW1 and DW2 sites probably due to the high discharge. This result clearly contrasts with previous findings in WWTP-influenced streams during low flow conditions in which significant declines of NH_4^+ and increases of NO_3^- concentrations and changes in their ^{15}N signature have been observed along downstream reaches (Merseburger et al. 2005; Lofton et al. 2007).

Our study also showed different recovery patterns between light- and dark-side biofilms, showing a differential spatial effect of WWTP inputs. As expected, biomass accrual on the dark-side was much lower than on the light exposed biofilms. Biofilms on the light-side reached similar steady-state biomass accrual at all sites regardless of differences in N concentrations. Only at the end of the study, we observed a consistent reduction of biomass at the DW2 site compared to the other sites. This decrease was likely due to high densities of macroinvertebrate grazers observed only at the DW2 site. Patterns of Chl *a* in light-side biofilms were also similar among sites and indicated an increasing

proportion of photoautotrophic organisms over the study period. Lack of differences in biomass and Chl *a* accrual among sites in the light-side biofilms could be explained by the fact that availability of DIN was already high upstream of the WWTP. In addition, riparian vegetation was leafless and sunlight reached stream surface along the study reach. Therefore, light-side communities of the different sites were neither limited by nutrient availability nor by light availability.

However, biomass accrual on the dark side was significantly higher at downstream than at upstream sites. This suggests that the additional N source from the WWTP favored the development of chemotrophic communities on the dark exposed sides. Biofilms below the WWTP had a higher percentage of N content, indicating that they were able to incorporate a fraction of the WWTP-supplied N. However, the light-side biofilm contained 2.5 times more N than the dark-side. This difference may be due to the ability of algae, which were restricted to the light-side of cobbles, to store nutrients, such as N and phosphorus, in very high concentrations in their vacuoles (luxury consumption), when it is not immediately required for growth (Sterner and Elser 2002).

The biofilm ^{15}N signature is a net result of all enzyme-driven N transformations carried out by the organisms and the degree of isotope fractionation associated to each process (Sulzman 2007). The boundary layer effect can be an additional physical factor leading to isotopic fractionation (MacLeod et al. 1998). Therefore, we expected clear differences in ^{15}N between light- and dark-side communities, especially in late stages of recovery, on the basis of the observed differences in AFDM, Chl *a*, and N content between the two communities at all sites. However, the results did not fit this expectation since light- and dark-side ^{15}N signatures were similar at each site. This similarity in ^{15}N signatures may indicate similar N sources and assimilation pathways and rates in the two communities. However, this may be unlikely because photoautotrophic

organisms were restricted to light-side communities whereas ammonia oxidizers were more abundant in the dark-side biofilm. These consistent differences in community composition more probably result in differences in N uptake rates at the community level. Alternatively, the different fractionation occurring in the two communities could have been somehow compensated resulting in similar ^{15}N signatures. Thus, for instance, the light-side biofilms could have been subjected to a higher boundary layer effect due to their higher biomass accrual, whereas fractionation associated to nitrification, which is widely known (Casciotti et al. 2003; Marshall et al. 2007; Baggs 2008), could have been more relevant in dark-side biofilms. Nevertheless, to our knowledge there is a lack of studies addressing the potential contrast of ^{15}N signatures in biofilms and the mechanisms driving it at this microhabitat scale to further support these hypotheses. Studies on later development stages during baseflow conditions may provide further insights as the biofilm matures and becomes even more distinct due to spatial segregation of resources and habitats (Jackson 2003). In contrast, biofilm ^{15}N differed among study sites following to the differences observed for ^{15}N signatures of NH_4^+ and NO_3^- which were basically driven by the WWTP input. At the UP site, biofilm ^{15}N signatures were closely related to those of NO_3^-, regardless of biofilm structural changes over the study period. At sites downstream of the WWTP input, biofilm ^{15}N signatures were similar to those of NO_3^- after the flood, but became more similar to those of NH_4^+ as discharge decreased and the influence of WWTP on NH_4^+ concentration was more pronounced. Overall, these results suggest a shift in the relative importance of NH_4^+ over NO_3^- utilization as a N source of biofilms between upstream and downstream sites, as well as over time at downstream sites. This provides further evidence of the biofilm capacity to regulate N inputs from point sources in these high-N loaded streams.

Distribution of ammonia-oxidizing microorgamisms in the biofilm. Our results showed that ammonia-oxidizing microorganisms were present in the biofilms at

all sites since early recovery stages, suggesting that in addition to photoautotrophic assimilation, nitrification could potentially contribute to the regulation of NH_4^+ loads downstream of the WWTP. This supports the hot-spot nitrification nature of high NH_4^+ loaded streams reported by previous studies (Merseburger et al. 2005; Martí et al. 2010).

The ammonia-oxidizing community in stream biofilms has been poorly studied, and former studies focused on the abundance and diversity of either bacteria (Wakelin et al. 2008) or archaea (Weidler et al. 2008; Herforth et al. 2009). Here, these phylogenetically-separated but physiologically-related populations were simultaneously detected co-existing in the biofilm assemblage. We observed, however, marked spatial differences in the relative abundance of these populations in a very short stream distance (i.e., <1 km) suggesting the existence of distinct physiological characteristics and ecological niches as previously proposed (Nicol et al. 2008). Thus, while AOA were found to be ubiquitous at nearly all sites and on both sides of cobbles, AOB were restricted to downstream sites and mostly found at the dark-side of cobbles. This distribution could be explained by a combination of factors operating at the stream reach and biofilm community scales. Low NH_4^+ concentration at the upstream site may be a limitation for AOB colonization. In addition, the WWTP effluent may also be a source of ammonia oxidizers and particularly of AOB as they represent the main nitrifying microorganisms in activated sludge (Wells et al. 2009). AOB from the effluent may easily colonize the downstream biofilm communities mostly at the dark cobble sides because of the intolerance to light caused by photo-oxidation of cytochrome *c* complex (Prosser 1989). We cannot rule out either the poor competition capacity of AOB against algae for NH_4^+ in the presence of light. In fact, it has been reported a decrease in nitrification activity and in abundance of AOB with increasing algae biomass in sediment biofilm mats (Risgaard-Petersen et al. 2004). Finally, as biofilms increased thickness, the diffusion of solutes from the water into the biofilm may be

reduced. For instance, a 10 cell thick biofilm would have 100 times longer diffusion times than that of a cell alone (Steward 2003). Therefore, NH_4^+-N and O_2 concentrations can become limiting *in situ* within the biofilm despite the high concentrations present in the water column, triggering competition among AOB, heterotrophic prokaryotes and photosynthetic organisms. This limitation was likely more relevant in light-side biofilms than in dark-side biofilms due to the highest biomass present in the former. Overall, these results indicate that dark-side conditions downstream of the WWTP are the most favorable for AOB because biofilm layer was thinner, photoautotrophic organisms were rare, and NH_4^+-N concentrations were high.

Unfortunately, for AOA in particular and for archaea in general (Auguet et al. 2010) there is a lack of comprehensive physiological information due to the lack of pure cultures in the laboratory. Recently Martens-Habbena et al. (2009) have shown that the ammonia-oxidizing archaeon *Nitrosupumilus maritimus* SCM1, and probably AOA in general, may have a remarkably high affinity for NH_4^+, that easily outcompete AOB and heterotrophic organisms under NH_4^+ limiting conditions. This high affinity for NH_4^+ may explain why AOA were found in all samples including those from the upstream site where NH_4^+ concentration was very low. This finding is confirmed by former studies from other environments, (i.e., oligotrophic marine waters) where AOA are the main ammonia oxidizing microorgamisms, outnumbering AOB by orders of magnitude (Beman et al. 2010). The abundance of AOA was in general much higher in dark side than in light side biofilm except on the first sampling date suggesting either intolerance to light or strong competition with other biofilm microorganisms, or both. Further investigations focused on the specific identity and activity of AOA and AOB populations are certainly needed to both explain the observed patterns and the spatial distribution within the biofilms and to easily scale from the cell level mechanisms to the whole-reach stream processes.

In this study we have shown that biofilm recovery was fast after an important hydrological disturbance, and that it was differentially affected by the continuous N inputs from a WWTP outflow. Thus, we found that biofilm structural properties (AFDM, Chl *a*) were less affected by WWTP inputs than their biogeochemical properties associated to N cycling (N content, and ^{15}N signature), and that the effects were more pronounced for microbial communities that developed on the dark side of cobbles. In particular, we observed that the input of a WWTP effluent modified the stream environment becoming more favorable for ammonia oxidizing bacteria at downstream sites and, at the same time, changing the dynamics of both bacterial and archaeal ammonia oxidizers in the biofilm. In the context of a future global change scenario with lower water availability, a better understanding on how stream ecosystems transform and retain human-derived nutrients and which mechanisms are driving these processes is certainly needed. The present work contributes to understand how WWTPs effluents modify both N uptake and biogeochemical transformations in streams, and shows an example of the tight link existing between stream biogeochemistry and microbial ecology.

Acknowledgments

We thank C. Gutierrez, M. Ribot, J. Pfann, L. Serrano, M. Raja, A. Poch, L. Haller, and N. Nomokonova for excellent field and laboratory assistance. We also acknowledge anonymous reviewers for valuable feedbacks and constructive comments on the manuscript. This study has been granted by the following projects to EM and EOC: Coupling biofilm diversity and ecosystem functioning: The role of COmmunication and MIXing in microbial landscapes-COMIX (European Science Foundation, Eurodiverstiy Collaborative Research Program, ref: 05_EDIV_FP065-COMIX); Multidisciplinary research consortium on GRadual and Abrupt Climate Changes, and their Impacts on the Environment- GRACCIE (Ministerio de Educación y Ciencia, Programa Consolider, CSD2007-00067); and Biology and Ecology of uncultured freshwater archaea- PIRENA (Ministero de Ciencia e Innovación, ref:

CGL2009-13318-C02-01). SM is supported by a JAE-predoctoral fellowship from the Spanish National Research Council (CSIC) and JCA is supported by a Juan de la Cierva fellowship from the Ministero de Ciencia e Innovación.

3.5. References

Agrich, A., E. Martí, F. Sabater, M. Ribot, D. von Schiller, and J. L. Riera. 2008. Combined effects of leaf litter inputs and a flood on nutrient retention in a Mediterranean mountain stream during fall. *Limnology and Oceanography* **53**: 631–641

APHA. 1995. Standard methods for the examination of water and wastewater, 19th ed. American Publishers Health Association, Washington DC, USA.

Auguet, J.-C., A. Barberán, and E. O. Casamayor. 2010. Global ecological patterns in uncultured Archaea. *ISME Journal* **4**: 182-190

Baggs, E. M. 2008. A review of stable isotope techniques for N_2O source partitioning in soils: recent progress, remaining challenges and future considerations. *Rapid Communications in Mass Spectrometry* **22**: 1664-1672.

Bates, B. C., Z. W. Kundzewics, S. Wu, and J. P. Palutikof [eds.]. 2008. Analyzing regional aspects of climate change and water resources, p. 77-114. *In* Climate change and water. IPCC Secretariat, Geneva.

Battin, T. J., L. A. Kaplan, D. Newbold, and C. M. E. Hansen. 2003. Contributions of microbial biofilms to ecosystem processes in stream mesocosms. *Nature* **426**: 439-442.

Beman, J. M., S. Rohan, and J. A. Fuhrman. 2010. Population ecology of nitrifying archaea and bacteria in the Southern California Bight. *Environmental Microbiology* **12**: 1282 - 1292

Besemer, K., G. Singer, R. Limberger, A.-K. Chlup, G. Hochedlinger, I. Hödl, C. Barany, and T. J. Battin. 2007. Biophysical controls on community succession in stream biofilms. Appl. *Environmental Microbiology* **73**: 4966-4974.

Biggs, B. J. F. 1996. Patterns in bentic algae of streams, p. 31-56. *In* R. J. Stevenson, M. L. Bothwell and R. L. Lowe [eds.], Algal ecology: *In* Freshwater benthic ecosystem. Academic Press.

Borchardt, M. A. 1996. Nutrients, p. 183-228. *In* R. J. Stevenson, M. L. Bothwell and R. L. Lowe [eds.], Algal ecology *In:* Freshwater benthic ecosystem. Academic Press.

Camargo, J. A., and Á. Alonso. 2006. Ecological and toxicological effects of inorganic nitrogen pollution in aquatic ecosystems: A global assessment. *Environment International* **32**: 831-849.

Carey, R., and K. W. Migiaccio. 2009. Contribution of wastewater treatment plant effluents to nutrient dynamics in aquatic systems: A review. *Environmental Management* **44**: 205-217.

Casciotti, K. L., D. M. Sigman, and B. B. Ward. 2003. Linking diversity and stable isotope fractionation in ammonia-oxidizing bacteria. *Geomicrobiology Journal* **20**: 335 - 353.

DeBruyn, A. M. H., and J. B. Rasmussen. 2002. Quantifying assimilation of sewage-derived organic matter by riverine benthos. *Ecological Applications* **12**: 511-520.

Dumestre, J. F., E. O. Casamayor, R. Massana, and C. Pedrós-Alió. 2002. Changes in bacterial and archaeal assemblages in an equatorial river induced by the water eutrophication of Petit Saut dam reservoir (French Guiana). *Aquatic Microbial Ecology* **26**: 209-221.

Epstein, S., and J. Rossel. 1995. Enumeration of sandy sediment bacteria: search for optimal protocol. *Marine Ecology Progress Series* **117**: 289-298.

Falkowski, P. G., T. Fenchel, and E. F. Delong. 2008. The microbial engines that drive earth's biogeochemical cycles. *Science* **320**: 1034-1039.

Hall, R. O. J., and J. Tank. 2003. Ecosystem metabolism controls nitrogen uptake in streams in Grand Teton National Park, Wyoming. *Limnology and Oceanography* **48**: 1120-1128

Herfort, L., K. Jung-Hyun, M. Coolen, B. Abbas, S. Schouten, G. J. Herndl, and J. S. S. Damsté. 2009. Diversity of Archaea and detection of crenarchaeotal *amoA* genes in the rivers Rhine and Têt. *Aquatic Microbial Ecology* **55**: 189–201.

Holmes, R. M., J. W. McClelland, D. M. Sigman, B. Fry, and B. J. Peterson. 1998. Measuring 15N-NH+4 in marine, estuarine and fresh waters: an adaptation of the ammonia diffusion method for samples with low ammonium concentrations. *Marine Chemistry*: 60.

Jackson, C. 2003. Changes in community properties during microbial succession. Oikos **101**: 444-448.

Koops, H.-P., and A. Pommerening-Röser. 2001. Distribution and ecophysiology of the nitrifying bacteria emphasizing cultured species. *FEMS Microbiology Ecology* **37:** 1-9.

Lajtha, K., and R. H. Michener. 1994. Stable isotopes in ecology and environmental science. 1st edition. Blackwell Scientific Publications.

Lock, M. A., R. R. Wallace, J. W. Costerton, R. M. Ventullo, and S. E. Charlton. 1984. River epilithon: toward a structural-functional model. *Oikos* **42**: 10-22.

Lofton, D. D., A. E. Hershey, and S. C. Whalen. 2007. Evaluation of denitirification in an urban stream receiving wastewater effluent. *Biogeochemistry* **86**: 77-90.

Loreau, M., S. Naeem, P. Inchausti, J. Bengtsson, J. P. Grime, A. Hector, D. U. Hooper, M. A. Huston, D. Raffaelli, B. Schmid, D. Tilman, and D. A. Wardle. 2001. Biodiversity and ecosystem functioning: Current knowledge and future challenges. *Science* **294**: 804-808.

Lyautey, E., C. R. Jackson, J. Cayrou, J. L. Rols, and F. Garabétian. 2005. Bacterial community succession in natural river biofilm assemblages. *Microbial Ecology* **50**: 601.

MacLeod, N. A., and D. R. Barton. 1998. Effects of light intensity, water velocity, and species composition on carbon and nitrogen stable isotope ratios in periphyton. *Can. J. Fish. Aquat. Sci*. **55**: 1919–1925.

Marshall, J. D., J. R. Brooks, and K. Lajthal. 2007. Sources of variation in the stable isotopic composition of plants, p. 1 – 22. *In* R. Michener and K. Lajthal [eds.], Stable isotopes in ecology and environmental science. Blackwell Scientific Publisher.

Martens-Habbena, W., P. M. Berube, H. Urakawa, J. R. de la Torre, and D. A. Stahl. 2009. Ammonia oxidation kinetics determine niche separation of nitrifying Archaea and Bacteria. Nature **461**: 976-979

Martí, E., J. Aumatell, J. Gode, M. Poch, and F. Sabater. 2004. Nutrient retention efficiency in streams receiving inputs from wastewater treatment plants. *Journal of Environmental Quality* **33**: 285-293.

Martí, E., J. L. Riera, and F. Sabater. 2010. Effects of wastewater treatment plants on stream nutrient dynamics under water scarcity conditions, p 173-195. *In* S. Sabater and D. Barceló [eds.], The handbook of environmental chemistry: Water scarcity in the Mediterranean area. Springer.

Merseburger, G., E. Martí, and F. Sabater. 2005. Net changes in nutrient concentraitons below a point source input in two streams draining catchments with contrasting land uses. *Science of the Total Environment* **347**: 217-229.

Mulholland, P. J., A. M. Helton, G. C. Poole, R. O. Hall Jr, S. K. Hamilton, B. J. Peterson, J. L. Tank, L. R. Ashkenas, L. W. Cooper, C. N. Dahm, W. K. Dodds, S. E. G. Findlay, S. V. Gregory, N. B. Grimm, S. L. Johnson, W. H. McDowell, J. L. Meyer, H. M. Valett, J. R. Webster, C. P. Arango, J. J. Beaulieu, M. J. Bernot, A. J. Burgin, C. L. Crenshaw, L. T. Johnson, B. R. Niederlehner, J. M. O'Brien, J. D. Potter, R. W. Sheibley, D. J. Sobota, and S. M. Thomas. 2008. Stream denitrification across biomes and its response to anthropogenic nitrate loading. *Nature* **452**: 202-205.

Nicol, G. W., L. Sven, C. Schleper, and J. I. Prosser. 2008. The influence of soil pH on the diversity, abundance and transcriptional activity of ammonia oxidizing archaea and bacteria. *Environmental Microbiology* **10**: 2966-2978.

Peterson, B. J., W. M. Wollheim, P. J. Mulholland, J. R. Webster, J. L. Meyer, J. L. Tank, E. Martí, W. B. Boden, H. M. Valett, A. E. Hershey, W. H. McDowell, W. K. Dodds, S. K. Hamilton, S. Gregory, and D. D. Morrall. 2001. Control of nitrogen export from watersheds by headwater streams. *Science of the Total Environment* **292:** 86-91.

Prosser, J. I. 1989. Autotrophic nitrification in bacteria, p. 125-181. *In* A. H. Rose, and D. W. Tempest [eds.], Advances in microbial physiology. Academic Press.

Prosser, J. I., B. J. M. Bohannan, T. P Curtis, R. J. Ellis, M. K. Firestone, R. P. Freckleton, J. L. Green, L. E. Green, K. Killham, J. J. Lennon, A. M. Osborn, M. Solan, C. J. van der Gast, and J. P. W. Young. 2007. The role of ecological theory in microbial ecology. *Naure Review Microbiology*. **5**: 384-392.

Rickard, A. H., A. J. McBain, A. T. Stead, and P. Gilbert. 2004. Shear rate moderates community diversity in freshwater biofilms. *Applied and Environmental Microbiology*. **70**: 7426-7435.

Risgaard-Petersen, N., M. H. Nicolaisen, N. P. Revsbec, and B. A. Lomstein. 2004. Competition between ammonia-oxidizing bacteria and benthic microalgae. *Applied and Environmental Microbiology*. **70**: 5528-5537.

Robinson, D. 2001. δ15N as an integrator of the nitrogen cycle. *Trends in Ecology & Evolution* **16**: 153-162.

Rotthauwe, J.-H., K-P., Witzel, and W. Liesack. 1997. The ammonia monooxygenase structural gene *amoA* as a functional marker: Molecular fine-scale analysis of natural ammonia oxidizing populations. *Applied and Environmental Microbiology* **63**: 4704-4712.

Sánchez-Pérez, J.-M., M. Gerino, S. Sauvage, P. Dumas, E. Maneux, F. Julien, P. Winterton, and P. Vervier. 2009. Effects of wastewater treatment plant

pollution on in-stream ecosystems functions in an agricultural watershed. *Annales de Limnology – International Journal of Limnology*. **45**: 79-92.

Sigman, D. M., R. Michener, D. C. McCorkle, B. Fry, and R. M. Holmes. 1997. Natural abundance-level measurement of the nitrogen isotopic composition of oceanic nitrate: an adaptation of the ammonia diffusion method. *Marine Chemistry* **57**: 227-242.

Singer, G., K. Besemer, P. Schmitt-Kopplin, I. Hödl, and T. J. Battin. 2010. Physical heterogeneity increases biofilm resource use and its molecular diversity in stream mesocosms. *PLoS ONE* **5**: e9988, doi:10.1371/journal.pone.0009988

Spang, A., R. Hatzenpichler, C. Brochier-Armanet, T. Rattei, P. Tischler, E. Spieck, W. Streit, D. A. Stahl, M. Wagner, and C. Schleper. 2010. Distinct gene set in two different lineages of ammonia-oxidizing archaea supports the phylum Thaumarchaeota. *Trends in Microbiology* **18**: 331-340.

Steinman, A. D., and G.A. Lamberti. 1996. Biomass and pigments of benthic algae, p. 295 – 314. *In* F. R. Hauer, and G. A. Lamberti [eds.], Methods in stream ecology. Academic Press.

Sterner, R. W., and J. J. Elser. 2002. Ecologic stoichiometry: the biology of elements from molecules to the biosphere. Princton University Press.

Stewart, P. S. 2003. Diffusion in biofilms. *Journal of Bacteriology*. **185**: 1485-1491.

Sulzman, E. W. 2007. Stable isotope chemistry and measurement: a primer, p: 1-14. *I:* R. Michner and K. Lajatha, [eds.], Stable isotopes in ecology and environmental science. Blackwell.

Tourna, M., T. E. Freitag, G. W. Nicol, and J. I. Prosser. 2008. Growth, activity and temperature responses of ammonia-oxidizing archaea and bacteria in soil microcosms. *Environmental Microbiology* **10:** 1357-1364.

von Schiller, D., E. Martí, and J. L. Riera. 2009. Nitrate retention and removal in Mediterranean streams bordered by contrasting land uses: a ^{15}N tracer study. *Biogeosciences* **6**: 181–196.

von Schiller, D., E. MartÍ, J. L. Riera, and F. Sabater. 2007. Effects of nutrients and light on periphyton biomass and nitrogen uptake in Mediterranean streams with contrasting land uses. *Freshwater Biology* **52**: 891-906.

Wakelin, S. A., M. J. Colloff, and R. S. Kookana. 2008. Effect of Wastewater Treatment Plant Effluent on Microbial Function and Community Structure in the Sediment of a Freshwater Stream with Variable Seasonal Flow. *Applied and Environmental Microbiology* **74**: 2659-2668.

Walsh, C., A. H. Roy, J. W. Feminella, P. D. Cottingham, P. M. Groffman, and R. P. Morgan. 2005. The urban stream syndrome: current knowledge and the search for a cure. *Journal of the North American Benthological Society* **24**: 706-723

Weidler, G. W., F. W. Gerbl, and H. Stan-Lotter. 2008. Crenarchaeota and their role in the nitrogen cycle in a subsurface radioactive thermal spring in the Austrian Central Alps. . *Applied and Environmental Microbiology*. **74**: 5934-5942.

Wells, G. F., H.-D. Park, C.-H. Yeung, B. Eggleston, C. A. Francis, and C. S. Criddle. 2009. Ammonia-oxidizing communities in a highly aerated full-scale activated sludge bioreactor: betaproteobacterial dynamics and low relative abundance of Crenarchaea. *Environmental Microbiology* **11:** 2310-2328.

Wessén, E., K. Nyberg, J. K. Jansson, and S. Hallin. 2009. Responses of bacterial and archaeal ammonia oxidizers to soil organic and fertilizer amendments under long-term management. *Applied Soil Ecology* **45:** 193-200.

Wastewater treatment plants effluents change abundance and composition of ammonia-oxidizing microorganisms in Mediterranean urban stream biofilms

4

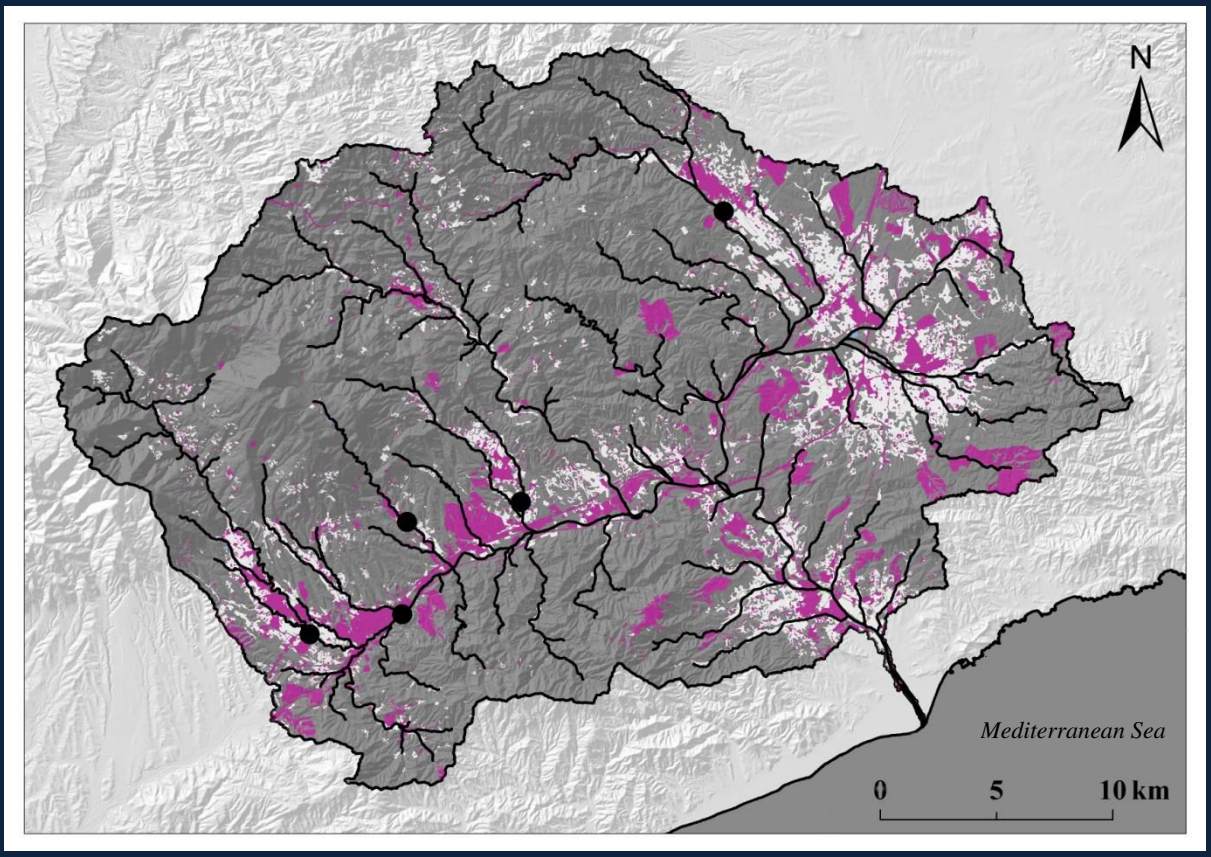

Original publication of Stephanie N Merbt, Jean-Christophe Auguet, Alba Blesa, Eugènia Martí and Emilio O Casamayor. 2014. Wastewater Treatment Plant Effluents Change Abundance and Composition of Ammonia-Oxidizing Microorganisms in Mediterranean Urban Stream Biofilms. *Microbial Ecology*: 1-9. DOI 10.1007/s00248-014-0464-8

Cover: Map of the catchment of the Tordera River (NE Spain, highlighted in dark grey). Indicated are urban (violet) and agricultural (white) land uses, as well as the effluents of the waste water treatment plants (black dots), which have been sampled in this study. Map design by Aitana Oltra Codina.

4.1. Abstract

Natural streams affected by wastewater treatment plants (WWTP) effluents are hotspots of nitrification. We analyzed the influence of WWTP inputs on the abundance, distribution and composition of epilithic ammonia-oxidizing (AO) assemblages in five Mediterranean urban streams by qPCR and *amoA* gene cloning and sequencing of both archaea (AOA) and bacteria (AOB). The effluents significantly modified streams chemical parameters, and changes in longitudinal profiles of both NH_4^+ and NO_3^- indicated stimulated nitrification activity. WWTP effluents were an allocthonous source of both AOA, essentially from the *Nitrosotalea* cluster, and mostly of AOB, mainly *Nitrosomonas oligotropha, N. communis,* and *Nitrosospira* spp. changing the relative abundance and the natural composition of AO assemblages. Under natural conditions, *Nitrososphaera* and *Nitrosopumilus* AOA dominated AO assemblages and AOB were barely detected. After the WWTP perturbation, epilithic AOB increased by orders of magnitude whereas AOA did not show quantitative changes but a shift in population composition to dominance of *Nitrosotalea* spp. The foraneous AOB successfully settled in downstream biofilms and probably carried out most of the nitrification activity. *Nitrosotalea* were only observed downstream and only in biofilms exposed to either darkness or low irradiance. In addition to other potential environmental limitations for AOA distribution, this result suggests *in situ* photosensitivity as previously reported for *Nitrosotalea* under laboratory conditions.

4.2. Introduction

Nitrification is a key process in nitrogen (N) cycling of any ecosystems bridging reduced with oxidized forms of dissolved inorganic nitrogen (DIN), and affecting *in situ* N uptake and transformation pathways. Studies from headwater streams show that nitrification rates can vary substantially among streams; however, overall nitrification contributes to a relatively low proportion of total ammonium (NH_4^+) removed (Peterson et al., 2001). In contrast, streams affected by inputs from urban waste-water treatment plants (WWTP) may have nitrification as the most relevant N cycling process (Martí et al., 2004; Merseburger et al., 2005; Martí et al., 2010; Ribot et al., 2012). In general, in large rivers WWTP effluent plumes are substantially diluted and the main river characteristics remain mostly unaffected. However, in headwater streams, especially from arid and semi-arid regions, the WWTP effluent can contribute from 3 to 100% of total stream flow and create strong physical and chemical discontinuities (Martí et al., 2004; Merseburger et al., 2005). In fact, during low natural flow conditions, the WWTP effluent tends to dominate the stream chemistry (Martí et al., 2004; Merbt et al., 2011).

Small streams can retain and transform up to 50 % N inputs from the catchment (Peterson et al., 2001), being microbial assemblages on streambed substrata (i.e., biofilms) and in sediments the most active component of N cycling (Teissier et al., 2007). Biofilms are highly, metabolic active, complex structures of algae, bacteria, archaea and fungi embedded in a polysaccharide matrix growing on submerged substrata, mostly cobbles and pebbles (Lock et al., 1984; Battin et al., 2003). Ammonia oxidizing archaea (AOA) and bacteria (AOB) play a key role in the N cycle catalyzing the oxidization of NH_4^+ to nitrite, the first and rate-limiting step of nitrification. Both phyla encode for the alpha subunit of the enzyme ammonia mono-oxygenase (*amoA*) that can be traced with specific primers (Rotthauwe et al., 1997; Francis et al., 2005). AOA and

AOB present intrinsic and distinctive adaptations to natural habitats (Fernàndez-Guerra and Casamayor, 2012) and to environmental conditions such as NH_4^+ availability (Martens-Habbena et al., 2009) and irradiance (Merbt et al., 2012), which can modulate their abundance and distribution in streams.

In the present study, we analyzed the influence of WWTP inputs on the abundance, distribution and composition of ammonia oxidizing assemblages, both AOA and AOB, in epilithic biofilms of small Mediterranean urban streams. In particular, we aimed to examine consistent patterns among WWTP-influenced streams and five streams affected by different WWTPs were studied to provide a general pattern for this type of ecosystems. In addition, we hypothesized that changes observed in nitrification rates in urban streams could be related to a substantial modification of the abundance and composition of ammonia-oxidizing microorganisms.

4.3. Material and Methods

Selected streams sampling and analyses. The streams were located in the catchment of La Tordera river (NE Spain) and were of similar size (Table 4.1). The study was conducted at the beginning of autumn (October 2009) when the influence from WWTP inputs was remarkable due to low stream flow conditions (see details in Tables 4.1 and 4.2). The selected stream reaches were comparable in hydrology and streambed substrates, which were dominated by cobbles and some patches of sand. The canopy cover from riparian vegetation was dense at all streams, and light conditions reaching stream surface were < 4 % of total incident irradiance in the surrounding landscape.

At each stream we selected a ca. 1 km reach and we identified one site upstream (UP) of the WWTP input and eight sites along the reaches (DW1-DW8, spread at ca. 100 m from each other) and the WWTP effluent itself (WWTP). At each site we measured water temperature and conductivity using a portable

conductivity meter (WTW Weilheim) and collected a water sample for analysis of $N\text{-}NH_4^-$, $N\text{-}NO_2^-$ and $N\text{-}NO_3^-$. At sampling site UP and DW8 we estimated discharge by measuring both water depth and velocity at 50 cm intervals, respectively, using a tape and a velocity meter (Schiltknecht Messtechnik). Longitudinal profiles of dissolved inorganic nitrogen (DIN) concentrations were used to estimate net uptake velocity (V_f, mm min^{-1}) at which nutrients are removed from the water column. V_f was calculated by estimating the stream-specific uptake length (m) using the slope of the regression of the ln-transformed and background corrected nutrient:conductivity ratio versus distance (8 sampling points downstream of the WWTP) and then further correction for stream-specific discharge (that is, discharge $width^{-1}$) (Hall et al., 2002; Webster and Valett, 2006; von Schiller et al., 2008). V_f is an indicator of nutrient demand or production relative to concentration in the water column and allows for comparison among different streams. To measure biofilm metrics we randomly collected three fist sized cobbles from riffle-run areas at sites UP, DW1, and DW8. For the measurement of biofilm biomass (expressed as ash free dry mass – AFDM) and for molecular analysis we scraped separately light-exposed (here after referred as light side biofilm) and the sediment facing side of the cobbles (here after referred as dark side biofilm) with a sterile metallic brush. The biofilm sludge of the three cobbles was pooled in a sterile plastic beaker and filtered onto an ignited, preweighted glass fiber filters (FVF). The total surface scraped was estimated after covering cobbles with aluminum foil and following a weight-to-area relationship. Filters for AFDM were dried (60 °C) until constant weight (ca. 0.1 mg, Sartorius analytical balance, model MC1). For the quantification of the ammonia oxidizers, the remaining biofilm sludge was transported to the laboratory on ice within 2 h after sampling. In the lab to estimate AFDM, biofilm samples collected on glass fiber filters were combusted at 500 °C for 5 h and weighted as indicated above. The AFDM was estimated as

Table 4.1: Physical and chemical parameters of water samples and epilithic concentrations of *amoA* genes for the five waste water treatment plant (WWTP)-influenced streams analyzed in this study; --: UP – upstream of the WWTP effluent, DW1 – 100 m downstream and DW8 – 800 m downstream of the effluent of the WWTP; --: not detected; nd: not determined. See Table S4.1 for AOA-AOB concentrations in WWTP effluent .

Urban stream	Site	Location		Cond.	Dis.	T	O_2	DIN	NH_4	NO_3	NO_2	AOB		AOA	
		(N)	(E)	µS/cm²	L s-1	°C	%	mg N L-1				copies m^{-2}		copies m^{-2}	
												Light-side	Dark-side	Light-side	Dark-side
BRE	UP			677	0	13.2	38.9	0.19	0.04	0.15	0	3.6 x 10^6	40.8 x 10^6	--	--
	WWTP	41°	2°	618	nd	20.6	78.7	13.07	0.81	10.64	1.62				
	DW1	44.181	34.127	615	nd	20.9	71.1	12.82	0.95	4.23	7.64	28.5 x 10^6	0. 6 x 10^6	161 x 10^6	200 x 10^6
	DW8			576	4.27	17.3	58.6	9.85	0.28	7.97	1.61	27.9 x 10^6	>300	3346 x 10^6	--
CEL	UP			742	0	19	93	0.49	0.05	0.44	0.01	3.2 x 10^6	3.2 x 10^6	--	9 x 10^6
	WWTP	41°	2°	1087	nd	22.4	94.3	2.72	2.38	0.28	0.06				
	DW1	41,537	30,466	836	nd	19.8	81.2	1.29	0.69	0.56	0.04	7.3 x 10^6	1.4 x 10^6	705 x 10^6	467 x 10^6
	DW8			987	27	21.8	75	2.75	1.36	1.21	0.18	24.0 x 10^6	26.1 x 10^6	437 x 10^6	215 x 10^6

Table 4.1. continued

Urban stream	Site	Location		Cond.	Dis.	T	O_2	DIN	NH_4	NO_3	NO_2	AOB		AOA	
												Light-side	Dark-side	Light-side	Dark-side
COL	UP			316	0	16.4	95.4	3.42	0.01	3.4	0	29.3 x 10^6	22.7 x 10^6	6.9 x 10^6	50 x 10^6
	WWTP	41°	2°	657	nd	20.5	72.7	4.62	3.97	0.54	0.11				
	DW1	51.005	40.399	408	nd	17.5	93.7	2.28	1.09	1.15	0.04	1.5 x 10^6	0.4 x 10^6	105 x 10^6	659 x 10^6
	DW8			415	69.06	18.5	91.2	2.22	0.75	1.43	0.05	4.1 x 10^6	1.0 x 10^6	175 x 10^6	234 x 10^6
GUA	UP			149	14.86	17.3	97.2	0.33	0.02	0.32	0	4.5 x 10^6	1.8 x 10^6	--	--
	WWTP	41°	2°	635	nd	19.6	93.6	10.01	9.18	0.62	0.21				
	DW1	43,702	30,596	203	nd	18.5	84.2	3.98	3.46	0.44	0.08	0	40.4 x 10^6	1982 x 10^6	3249 x 10^6
	DW8			164	36.01	19.3	96	1.08	0.02	1.05	0.01	10.3 x 10^6	--	103 x 10^6	--
SMP	UP			316	0.79	16.6	67.2	7.46	0.03	7.43	0.01	15.5 x 10^6	1.7 x 10^6	--	--
	WWTP	41°	2°	490	nd	20.4	89.4	1.76	0.64	1.00	0.12				
	DW1	41.049	27.598	474	nd	20.3	84.7	2.42	0.49	1.91	0.02	6.1 x 10^6	1.7 x 10^6	127 x 10^6	122 x 10^6
	DW8			478	35.12	19.1	103.1	2.61	0.05	2.54	0.03	0.02 x 10^6	23.5 x 10^6	75.5 x 10^6	1828 x 10^6

Table 4.2: Characterization of the WWTP effluents from the five selected study sites.

	BRE	**CEL**	**COL**	**GUA**	**SMP**
Mean daily discharge (m^3/day)	*800*	*6000*	*3250*	*190*	*2500*
Population supplied (hab.)	*3707*	*17510*	*11090*	*1065*	*11474*
Treatment	*Biological*	*Biological & N,P elimin.*	*Biological & N elimin.*	*Soft*	*Biological & N,P elimin.*
Equivalent population (h-e)	*5600*	*30000*	*14667*	*1035*	*15841*
Discharge (L s^{-1})	5.2	69.44[a]	37.6[a]	4.6	23.4
Temperature (°C)	20.6	22.4	20.5	19.6	20.4
O_2 (mg L^{-1})	7.00	8.08	6.47	8.40	7.94
DOC (mg L^{-1})	11.76	6.75	6.89	8.28	3.94
SRP (mgP L^{-1})	4.82	0.11	1.46	4.70	25.96
NH_4-N (mgN L^{-1})	0.81	2.38	3.97	9.18	0.64
NO_3-N (mgN L^{-1})	10.64	0.28	0.54	0.62	1.00
% DIN as NH_4	6.2	87.6	86.0	91.7	36.3
amoA AOA (copies L^{-1})	36.92	47.88	42.62	193.70	81.65
amoA AOB (copies L^{-1})	3221.38	783.67	646.86	343.98	313.35

Data in italics was taken from the Catalonian water agency (ACA, 2009) derived from the WWTP informational sheets. [a] *values taken from the Catalonian water agency (ACA, 2009) database of annual average discharges,*

the mass difference between dry and combusted filters and was reported per unit of surface area (g m^{-2}).

For molecular analysis the remaining biofilm sludge was incubation with Tween 20 detergent (10^{-6} % w v^{-1}) for 5 min followed by soft sonication (Sonopuls ultrasonic homogenizer HD 2070) with 20^{-s} pulses at 10% power (Epstein and Rossel, 1995). Sludge was filtered through a 0.2-mm pore size polycarbonate membrane (Millipore). Filters were incubated with lysozyme, proteinase K, and sodium dodecyl sulfate in lysis buffer (40 mmol L^{-1} ethylenediaminetetra-acetic acid, 50 mmol L^{-1} Tris, pH 8.3, and 0.75 mol L^{-1} sucrose), and phenol extracted as previously described (Dumestre, 2002).

amoA gene analysis. AOA and AOB abundances among streams and cobble sides were measured by quantitative PCR of *amoA* genes using different primers pairs (see details in Table 4.4) following methods by (Merbt et al., 2011). For *amoA* gene composition analysis, we selected SMP as representative stream. Archaeal *amoA* genes were amplified with the primer sets Arch-amoAF - Arch-amoAR (635-bp fragment; Francis et al., 2005), and bacterial *amoA* using primers amoA-1F - amoA-2R (491-bp fragment; Rotthauwe et al., 1999; see details in Table 4.4). PCR products were purified with the QIAquick PCR Purification kit (Qiagen) and cloned with the TOPO TA cloning kit (Invitrogen) following the manufacturer's instructions. The presence of inserts was checked by ampicillin resistance and blue/white selection on LB plates supplemented with ampicillin (100 lg mL^{-1}) and X-gal (40 µg mL^{-1}) as previously reported (Demergasso et al., 2008). Sequencing was carried out using external facilities (http://www.macrogen.com). The *amoA* gene sequences were manually checked with BioEdit (Hall, 1999) and submitted for matching in the protein database using translated nucleotide sequences (BLASTX, www.ncbi.nlm. nih.gov; Altschul et al., 1990) to check for protein identity. Next, sequences were clustered at 95% identity in nucleotides with Mothur (Schloss et al., 2009). Multiple sequence alignment, phylogenetic inference by maximum likelihood

and calculation of *amoA* gene identity matrices was carried out as recently reported (Auguet et al., 2011). Sequences were deposited in GenBank under accession numbers between FR773891 and FR773972 (AOB) and HG937834 to HG938130 (AOA). Additional biofilm samples were collected from SMP after leaf-fall, when riparian canopy cover was open and full light intensity reached the stream channel, to further explore the influence of irradiance on the composition of AOA.

Data analysis: Data set was tested on normal distribution by using Shapiro-Wilk Normality test. All data failed requirements and nonparametric tests were applied. The effect of the WWTP inputs on stream was assessed by comparing $N\text{-}NH_4^+$ and $N\text{-}NO_3^-$ concentrations, temperature among sites by using Kruskal–Wallis ANOVA nonparametric test (site as a factor). This test was also used to compare AOA and AOB *amoA* gene copy numbers among sites (site as a factor), and AFDM among streams, sites and SMP among season and sites. Spearman rank R nonparametric correlations were used to examine relationships among N concentrations, AFDM, and AOA and AOB *amoA* gene copy numbers. Wilcoxon matched paired test was used to test differences among AOA and AOB *amoA* gene copy numbers content of firstly, light and dark side of biofilms of sites and rivers and secondly, of WWTP outfall. Distance matrices for *amoA* genes were constructed with UniFrac and comparison of AOA and AOB communities were based on the UniFrac metric (http://bmf.colorado.edu/unifrac) (Lozupone and Knight, 2005). UniFrac is a betadiversity metric that quantifies community similarity based on the phylogenetic relatedness. To assess the sources of variation in *amoA* UniFrac matrices, we carried out permutational multivariate analysis of variance based on 1000 permutations (McArdle and Anderson, 2001), using the function adonis in vegan package (Oksanen et al., 2007). Results were considered significant for $p < 0.05$. All statistical analyses were done using R project for statistical computing.

4.4 Results and Discussion

The contribution of WWTP effluents to the flow of the streams ranged between 59 and 99 % and, consequently, physical and chemical parameters (conductivity, temperature, oxygen, flow, nutrients) increased strongly (Table 4.1). In particular, stream water $N\text{-}NH_4^+$ concentration increased significantly by one order of magnitude (Kruskal-Wallis ANOVA, $p < 0.05$), NO_3^- between 3 to 300 %, and NO_2^- between 3 and 30%. Thus, a significant decrease in the $N\text{-}NO_3^-$:$N\text{-}NH_4^+$ ratio was observed between UP and DW sites (Figure 4.1A). Increases in DIN concentration (mainly $N\text{-}NH_4^+$) are commonly observed in streams affected by WWTPs urban effluents, especially if a tertiary treatment is missing (Martí et al., 2010), as it was the case for the study streams. In addition, the high $N\text{-}NH_4^+$ concentration present downstream favored nitrification (Merseburger et al., 2005), and, in agreement with these previous findings, we observed concomitant decreases in $N\text{-}NH_4^+$ and increasing $N\text{-}NO_3^-$ along the reach in all five streams. However, net uptake velocities (V_f) varied substantially among the five streams and ranged from 0.030 to 3.483 and -0.011 to -1.492 mm per min for $N\text{-}NH_4^+$ and $N\text{-}NO_3^-$ respectively (Table 4.3).

Table 4.3: Net nutrient uptake velocity (V_f) in downstream reaches (DW1-DW8). V_f indicates the velocity at which a nutrient is removed from the water column (mm min^{-1}) [17]. * Velocity was calculated from DW3 – DW8 because water column was not well mixed. Significant linear regression over distance in bold face.

(mm min^{-1})	nutrient	BRE	CEL	COL	GUA	SMP
V_f	$N\text{-}NH_4^+$	**0.951**	**0.115***	**0.030**	**3.483**	**0.177**
V_f	$N\text{-}NO_3^-$	**-0.329**	**-0.542***	-0.011	**-1.492**	-0.022

Nevertheless, $N\text{-}NH_4^+$ demand (V_f $N\text{-}NH_4^+$) and $N\text{-}NO_3^-$ production (V_f $N\text{-}NO_3^-$) were correlated ($p<0.05$; $R^2=0.857$) indicating nitrification activity. Furthermore V_f $N\text{-}NO_3^-$ and V_f $N\text{-}NH_4^+$ increased with increasing $N\text{-}NH_4^+$ concentration.

These results indicate that streams with higher $N\text{-}NH_4^+$ concentration have higher demand of $N\text{-}NH_4^+$ being nitrification hotspots.

AOA and AOB were present in the epilithic biofilms of the streams, with abundances estimated by qPCR data ranging between 10^6-10^9 *amoA* gene copies m^{-2} (Figure 4.1B). All five WWTP effluents also contained ammonia-oxidizing prokaryotes (c. 40-3000 *amoA* gene copies L^{-1}), being concentrations of AOB one order of magnitude higher than those of AOA (Table S4.1).

This finding is in agreement with previous studies showing the presence of AOA and AOB within WWTP reactors (Zhang et al., 2009; Mußmann et al., 2011), although their particular contribution to nitrification in the plants is still under discussion and seems to be closely related to the organic matter quality, oxygen and substrate availability within the wastewater (Mußmann et al., 2011; Bai et al., 2012; Short et al., 2013). Presence of AOA and AOB in the effluents further indicates that WWTP effluents are potential sources of ammonia-oxidizers (Sonthiphand et al., 2013). In fact, the AOB:AOA ratio in epilithic biofilms downstream the WWTPs was closer to the ratio in the WWTP effluent than in upstream sites (Figure 4.1C).

In downstream biofilms, the shift in the AOB:AOA ratio was associated with increases in AOB abundance. While AOB were rarely detected in biofilms of the five upstream sites, they were highly abundant in biofilms downstream (Table 4.1). Conversely, AOA abundances were relatively similar among biofilms, regardless of the stream site location. These results indicated a remarkable influence of the WWTP inputs on the in-stream ammonia oxidizing assemblages of such urban small streams, especially for AOB. In addition, results further indicate that ammonia-oxidizers from the WWTPs, especially

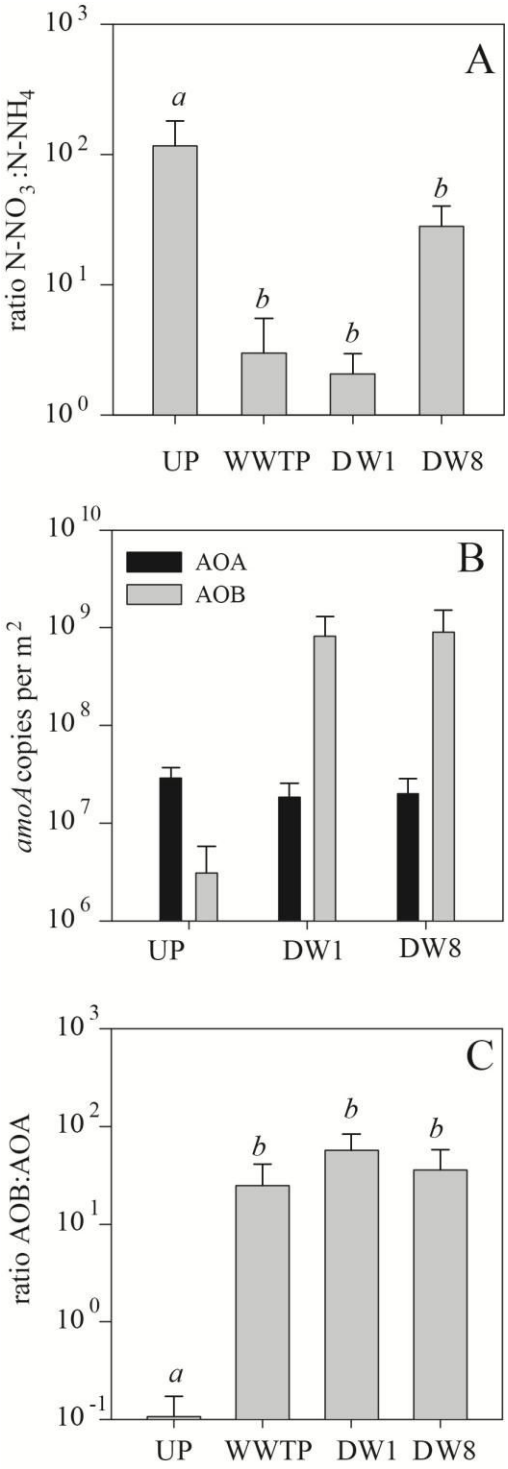

Figure 4.1. **(A)** ratio of $N\text{-}NO_3^-$:$N\text{-}NH_4^+$ concentration in stream water column and the WWTP effluent; **(B)** Mean abundance of archaeal (grey bars) and bacterial (black bars) *amoA* gene per m² in biofilms (for simplification sum of light and dark side biofilms) **(C)** ratio of *amoA* AOB:AOA copies in stream biofilm and in the WWTP effluent. All y-*aches* in log scale. UP– upstream of the WWTP effluent, DW1 – 100 m and DW8 – 800 m downstream of the effluent of the WWTP, and the WWTP effluent itself. Lines above the bars are the standard error for 5 streams. Different letters (*a* or *b*) above the bars indicate significant differences among ratios (Kruskal wallis, $p<0.05$).

AOB, can successfully settle in the biofilms of WWTP affected streams and indicates the AOB colonizing capacity is consistent among affected streams and could be a general pattern in this type of ecosystems. Higher abundances of ammonia-oxidizing prokaryotes downstream of the WWTP inputs is in accordance with the high nitrification activity mentioned above and may explain the net changes in $N\text{-}NH_4^+$ and $N\text{-}NO_3^-$ concentrations along the streams.

To additionally test the impact of the WWTP inputs on the composition of the AOA-AOB, we selected SMP as representative stream for cloning and sequencing (Figure 4.2). This site has already a solid background on hydrology, nutrient biogeochemistry and microbial assemblage from previous studies (see (Merseburger et al., 2005; Merbt et al., 2011; Ribot et al., 2012; Mußmann et al., 2013). We selected biofilms developed on the side of cobbles facing the streambed sediments (i.e., dark-side biofilms). These biofilms are exposed to shaded conditions, and thus we minimized the effect of additional controlling factors such as light inhibition (Merbt et al., 2012) or nutrients competition with photoautotrophic algae (Risgaard-Petersen et al., 2004). Similarly to qPCR results, AOB were only detected in downstream sites located after the inlet of the WWTP effluent. Although AOB communities harbored specific clusters to each site (i.e. *N. communis* cluster detected only in the WWTP outflow and *N. europea* cluster detected only in downstream biofilms), we found a strong compositional overlap between them (UNIFRAC significance pairwise test, $p > 0.05$). Indeed, *amoA* sequences belonging to the two dominant clusters in the outflow of the WWTP (i.e. *Nitrosospira* and *N. oligotropha* clusters) represented a significant proportion of AOB communities in downstream sites (i.e. 37 % at DWD1 and 80 % at DWD8) (Figure 4.2A). Most interesting, more than 50 % of downstream site sequences had their closest Blast match with sequences retrieved from waste waters indicating a strong influence of the waste water treatment plant downstream (data not shown). In contrast to AOB, AOA were found along all stream sites and differences were observed in the

composition of the AOA assemblages (UNIFRAC significance pairwise test, $p < 0.01$). At the upstream site, AOA were dominated by soil-related archaea mainly affiliated to *Nitrososphaera* cluster (former 1.1b group; Figure 4.2B), which probably derived from soil runoff. At the downstream sites, AOA additionally included *Nitrosotalea* (former 1.1a cluster, Restrepo-Ortiz et al., 2014; 44% of all sequences), which probably derived from the WWTP effluent where it was the dominant AOA (88 % of all sequences; Figure 4.2).

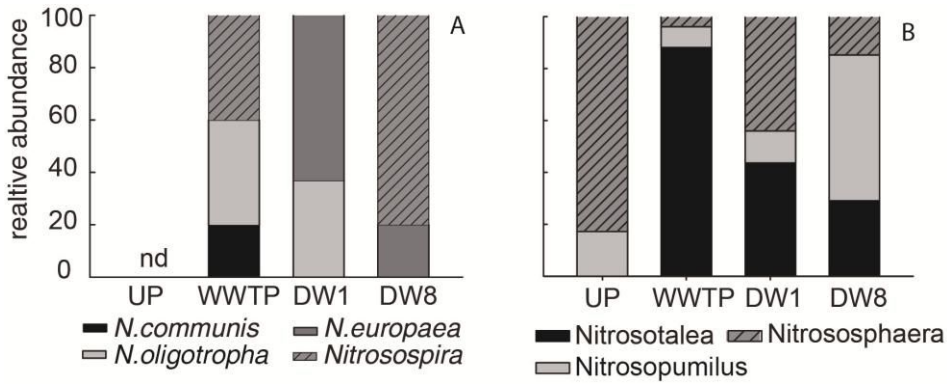

Figure 4.2: Changes in the relative abundance of *amoA* gene for AOB (panel A) and AOA (panel B) in dark side stream biofilms along the stream reach and composition of the WWTP outflow in the urban stream SMP.

Together, these results suggest that niche separation among different clusters of AOA occurs in stream biofilms in response to differences in physical and chemical conditions (Pester et al., 2012). Changes in pH are within the neutral range in these systems and one driving factor for such separation could be the significant difference in $N\text{-}NH_4^+$ availability among sites (Auguet et al., 2011; Herrmann et al., 2011; Verhamme et al., 2011). Low $N\text{-}NH_4^+$ concentration in upstream sites may probably limit AOB development due to their lower $N\text{-}NH_4^+$ affinity compared to AOA (Martens-Habbena et al., 2009). Within AOA, information derived from pure cultures indicates that *Nitrosophaera* and *Nitrosopumilus* are more active at low $N\text{-}NH_4^+$ concentrations ($K_m < 0.133$ nM total ammonium, (Hatzenpichler et al., 2008; Martens-Habbena et al., 2009), while *Nitrosotalea* may be better adapted to higher $N\text{-}NH_4^+$ concentrations

(growing at 500 µM ammonium, Lehtovirta-Morley et al., 2011). This may be one of the reasons why lineages affiliated to *Nitrosotalea* cluster occur only downstream of the WWTP input. In any case, biofilms are very complex structures that provide multiple biological and physiological factors shaping their spatial configuration and also interact with the surrounding environment (Battin et al., 2007). All these variability should be considered to further understand microbial composition of these assemblages. For instance, chemical conditions can change within mm from top to deepest layer, e.g. $N\text{-}NH_4^+$ decreased from about 650 µM to 500 µM and oxygen decreased from 50 % to anoxic conditions (0 % oxygen air) in the deepest layer in nitrifying model biofilms (Gieseke et al., 2005). These gradients can determine the successful colonization of nitrifiers from WWTP inputs as well as the composition of the nitrifier assemblages that will ultimately influence N cycling in the streams.

Other additional factors to be considered for the observed niche separation of AOA clusters are related to the season of sampling (Auguet et al., 2011) and particularly temperature, river discharge and irradiance. Here, we analyzed the effect of these seasonal parameters by comparison of the AOA assemblage composition on the up-side of cobbles exposed to natural light conditions (light-side biofilm) with those dark-exposed on the down-side of cobbles facing the streambed sediment (dark-side biofilm). We sampled the two biofilm types in summer, when riparian canopy cover shaded the stream (irradiance 60 µE m^{-2} s^{-1}), and in autumn after leaf fall, when full irradiance reached the stream channel (irradiance 1500 µE m^{-2} s^{-1}). The samples were treated with two different primers sets targeting AOA, i.e., T (Tourna et al., 2008), and F (Francis et al., 2005) to maximize the coverage. Results showed that temperature, river discharge and light irradiance were significant driving factors ($p < 0.01$, PERMANOVA test) for the AOA assemblage structure (Figure 4.3). In summer, temperature and biofilm biomass were higher and light irradiance and discharge were lower than in autumn (summer temperature: 19 °C, discharge:

35 L s^{-1}). Under these conditions, members of the *Nitrosotalea* cluster originating from the WWTP effluent dominated AOA communities of both sides of the cobbles (Figure 4.3). In contrast, in autumn, discharge was much higher (autumn temperature: 9 °C, discharge: 152 L s^{-1}) and diluted the WWTP effluent decreasing its influence on the stream. In addition to the dilution effect, full light-exposed biofilms were less suitable for *Nitrosotalea* like sequences as illustrated by their segregation between both faces of the cobbles. These results suggested in situ photosensitivity for AOA, particularly for *Nitrosotalea* like sequences, as previously reported under laboratory conditions (Merbt et al., 2012). The molecular and physiological factors involved in the photoinhibiton of AOA remain, however, to be determined.

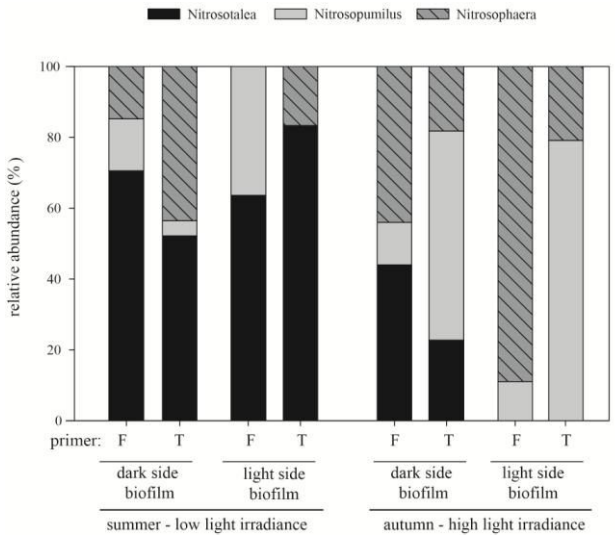

Figure 4.3. Changes in the relative abundance of *amoA* gene for AOA present in the light and dark side biofilm of sampling site DW1 (100m downstream of the WWTP effluent) in SMP urban stream in summer (low irradiance and discharge, high temperature) and in autumn (high irradiance and discharge, lower temperature). AOA composition tested with primers set F (Arch-amoAF/ Arch-amoAR, from Francis et al., 2005), and T (CrenamoA23f/ CrenamoA616r, from Tourna et al., 2008).

Overall, epilithic ammonia oxidizing assemblages developed in small Mediterranean streams showed a strong influence by wastewater treatment plant effluents both quantitatively, mostly for AOB, and qualitatively, mainly for AOA. Overall, these results potentially explain the hot spot nitrification nature of WWTP-influenced streams and also provide a mechanistic approach of actual nitrification relevance in urban streams affected by WWTP effluents. Environmental constrain factors both natural (i.e., temperature, river discharge and irradiance) and anthropogenically driven (i.e., WWTP inputs), determine the abundance and composition of AOB and AOA in stream biofilms, which will ultimately influence the rate at which supplied ammonium will be transformed into nitrate at the ecosystem level.

Acknowledgment

We thank C. Gutierrez, M. Ribot, and N. Nomokonova, for field, and laboratory assistance. S.N.M. was supported by a JAE predoctoral fellowship from the Spanish National Research Council (CSIC) and J.-C.A. by a Juan de la Cierva fellowship from the Spanish Office for Research (MINECO). This research was granted by DARKNESS CGL2012-32747 to EOC and MED_FORESTREAM CGL2011-30590-CO2-02 (MINECO) and REFRESH-244121 (7th Framework Programme EU Comission) to EM.

4.5. References

Altschul, S.F., Gish, W., Miller, W., Myers, E.W., and Lipman, D.J. (1990) Basic local alignment search tool. *Journal of Molecular Biology* **215**: 403-410.

Auguet, J.-C., Nomokonova, N., Camarero, L., and Casamayor, E.O. (2011) Seasonal Changes of Freshwater Ammonia-Oxidizing Archaeal Assemblages and Nitrogen Species in Oligotrophic Alpine Lakes. *Appl Environ Microbiol* **77**: 1937-1945.

Bai, Y., Sun, Q., Wen, D., and Tang, X. (2012) Abundance of ammonia-oxidizing bacteria and archaea in industrial and domestic wastewater treatment systems. *FEMS Microbiology Ecology* **80**: 323-330.

Battin, T.J., Kaplan, L.A., Denis Newbold, J., and Hansen, C.M.E. (2003) Contributions of microbial biofilms to ecosystem processes in stream mesocosms. *Nature* **426**: 439-442.

Battin, T.J., Sloan, W.T., Kjelleberg, S., Daims, H., Head, I.M., Curtis, T.P., and Eberl, L. (2007) Microbial landscapes: new paths to biofilm research. *Nat Rev Micro* **5**: 76-81.

Demergasso, C., Escudero, L., Casamayor, E., Chong, G., Balagué, V., and Pedrós-Alió, C. (2008) Novelty and spatio–temporal heterogeneity in the bacterial diversity of hypersaline Lake Tebenquiche (Salar de Atacama). *Extremophiles* **12**: 491-504.

Dumestre, J.F., E.O Casamayor, R. Massana, C. Pedrós-Alió (2002) Changes in bacterial and archaeal assemblages in an equatorial river induced by the water eutrophication of Petit Saut dam reservoir (French Guiana). *Aquatic Microbial Ecology* **26**: 209-221.

Epstein, S.S., and Rossel, J. (1995) Enumeration of sandy sediment bacteria: search for optimal protocol. *MARINE ECOLOGY PROGRESS SERIES* **117**: 289-298.

Fernàndez-Guerra, A., and Casamayor, E.O. (2012) Habitat-Associated Phylogenetic Community Patterns of Microbial Ammonia Oxidizers. *PLoS ONE* **7**: e47330.

Francis, C.A., Roberts, K.J., Beman, J.M., Santoro, A.E., and Oakley, B.B. (2005) Ubiquity and diversity of ammonia-oxidizing archaea in water columns and sediments of the ocean. *Proceedings of the National Academy of Sciences of the United States of America* **102**: 14683-14688.

Gieseke, A., Nielsen, J.L., Amann, R., Nielsen, P.H., and De Beer, D. (2005) In situ substrate conversion and assimilation by nitrifying bacteria in a model biofilm. *Environmental Microbiology* **7**: 1392-1404.

Hall, R.O., Bernhardt, E.S., and Likens, G.E. (2002) Relating nutrient uptake with transient storage in forested mountain streams. *Limnology and Oceanography* **47**: 255-265.

Hall, T.A. (1999) BioEdit: a user-friendly biological sequence alingment editor and analysis program for Windows 95/98/ NT. *Nucleic Acid Symp Ser* **41**: 95–98.

Hatzenpichler, R., Lebedeva, E.V., Spieck, E., Stoecker, K., Richter, A., Daims, H., and Wagner, M. (2008) A moderately thermophilic ammonia-oxidizing crenarchaeote from a hot spring. *Proceedings of the National Academy of Sciences* **105**: 2134-2139.

Herrmann, M., Scheibe, A., Avrahami, S., and Küsel, K. (2011) Ammonium Availability Affects the Ratio of Ammonia-Oxidizing Bacteria to Ammonia-

Oxidizing Archaea in Simulated Creek Ecosystems. *Applied and Environmental Microbiology* **77**: 1896-1899.

Lehtovirta-Morley, L.E., Stoecker, K., Vilcinskas, A., Prosser, J.I., and Nicol, G.W. (2011) Cultivation of an obligate acidophilic ammonia oxidizer from a nitrifying acid soil. *Proceedings of the National Academy of Sciences* **108**: 15892-15897.

Lock, M., Wallace, R., Costerton, J., Ventullo, R., and Charlton, S. (1984) River epilithon: toward a structural-functional model. *Oikos*: 10-22.

Lozupone, C., and Knight, R. (2005) UniFrac: a new phylogenetic method for comparing microbial communities. *Applied and Environmental Microbiology* **71**: 8228-8235.

Martens-Habbena, W., Berube, P.M., Urakawa, H., de la Torre, J.R., and Stahl, D.A. (2009) Ammonia oxidation kinetics determine niche separation of nitrifying Archaea and Bacteria. *Nature* **461**: 976-979.

Martí, E., Riera, J., and Sabater, F. (2010) Effects of Wastewater Treatment Plants on Stream Nutrient Dynamics Under Water Scarcity Conditions. In *Water Scarcity in the Mediterranean*. Sabater, S., and Barceló, D. (eds): Springer Berlin Heidelberg, pp. 173-195.

Martí, E., Aumatell, J., Gode, L., Poch, M., and Sabater, F. (2004) Nutrient retention efficiency in streams receiving inputs from wastewater treatment plants. *J Environ Qual* **33**: 285-293.

McArdle, B.H., and Anderson, M.J. (2001) Fitting multivariate models to community data: a comment on distance-based redundancy analysis. *Ecology* **82**: 290-297.

Merbt, S.N., Jean-Christophe Auguet, Emilio O. Casamayor, and Martı, E. (2011) Biofilm recovery in a wastewater treatment plant-influenced stream and spatial segregation of ammonia-oxidizing microbial populations. *Limnol Oceanogr* **56**: 1054–1064

Merbt, S.N., Stahl, D.A., Casamayor, E.O., Martí, E., Nicol, G.W., and Prosser, J.I. (2012) Differential photoinhibition of bacterial and archaeal ammonia oxidation. *FEMS Microbiology Letters* **327**: 41-46.

Merseburger, G., Martí, E., and Sabater, F. (2005) Net changes in nutrient concentrations below a point source input in two streams draining catchments with contrasting land uses. *Science of the total environment* **347**: 217-229.

Mußmann, M., Ribot, M., Schiller, D., Merbt, S.N., Augspurger, C., Karwautz, C. et al. (2013) Colonization of freshwater biofilms by nitrifying bacteria from activated sludge. *FEMS Microbiology Ecology* **85**: 104-115.

Mußmann, M., Brito, I., Pitcher, A., Sinninghe Damsté, J.S., Hatzenpichler, R., Richter, A. et al. (2011) Thaumarchaeotes abundant in refinery nitrifying sludges express amoA but are not obligate autotrophic ammonia oxidizers. *Proceedings of the National Academy of Sciences* **108**: 16771-16776.

Oksanen, J., Kindt, R., Legendre, P., O'Hara, B., Stevens, M.H.H., Oksanen, M.J., and Suggests, M. (2007) The vegan package. *Community ecology package*.

Pester, M., Rattei, T., Flechl, S., Gröngröft, A., Richter, A., Overmann, J. et al. (2012) amoA-based consensus phylogeny of ammonia-oxidizing archaea and deep sequencing of amoA genes from soils of four different geographic regions. *Environmental Microbiology* **14**: 525-539.

Peterson, B.J., Wollheim, W.M., Mulholland, P.J., Webster, J.R., Meyer, J.L., Tank, J.L. et al. (2001) Control of nitrogen export from watersheds by headwater streams. *Science* **292**: 86-90.

Restrepo-Ortiz, C.X., Auguet, J.-C., and Casamayor, E.O. (2014) Targeting spatiotemporal dynamics of planktonic SAGMGC-1 and segregation of ammonia-oxidizing thaumarchaeota ecotypes by newly designed primers and quantitative polymerase chain reaction. *Environmental Microbiology* **16**: 689-700.

Ribot, M., Martí, E., von Schiller, D., Sabater, F., Daims, H., and Battin, T.J. (2012) Nitrogen processing and the role of epilithic biofilms downstream of a wastewater treatment plant. *Freshwater Science* **31**: 1057-1069.

Risgaard-Petersen, N., Nicolaisen, M.H., Revsbech, N.P., and Lomstein, B.A. (2004) Competition between Ammonia-Oxidizing Bacteria and Benthic Microalgae. *Appl Environ Microbiol* **70**: 5528-5537.

Rotthauwe, J.-H., Witzel, K.-P., and Liesack, W. (1997) The ammonia Monooxygenase Structural Gene amoA as a Functional Marker: Molecular Fine-Scale Analysis of Natural Ammonia Oxidizing Populations. *Applied and environmental microbiologie* **63**: 4704-4712.

Schloss, P.D., Westcott, S.L., Ryabin, T., Hall, J.R., Hartmann, M., Hollister, E.B. et al. (2009) Introducing mothur: open-source, platform-independent, community-supported software for describing and comparing microbial communities. *Applied and Environmental Microbiology* **75**: 7537-7541.

Short, M.D., Abell, G.C.J., Bodrossy, L., and van den Akker, B. (2013) Application of a Novel Functional Gene Microarray to Probe the Functional Ecology of Ammonia Oxidation in Nitrifying Activated Sludge. *PLoS ONE* **8**: e77139.

Sonthiphand, P., Cejudo, E., Schiff, S.L., and Neufeld, J.D. (2013) Wastewater Effluent Impacts Ammonia-Oxidizing Prokaryotes of the Grand River, Canada. *Applied and Environmental Microbiology* **79**: 7454-7465.

Teissier, S., Torre, M., Delmas, F., and Garabétian, F. (2007) Detailing biogeochemical N budgets in riverine epilithic biofilms. . *Journal of the North American Benthological Society* **26**: 178-190.

Tourna, M., Freitag, T.E., Nicol, G.W., and Prosser, J.I. (2008) Growth, activity and temperature responses of ammonia-oxidizing archaea and bacteria in soil microcosms. *Environmental Microbiology* **10**: 1357-1364.

Verhamme, D.T., Prosser, J.I., and Nicol, G.W. (2011) Ammonia concentration determines differential growth of ammonia-oxidising archaea and bacteria in soil microcosms. *ISME J* **5**: 1067-1071.

von Schiller, D., Martí, E., Riera, J.L., Ribot, M., Argerich, A., Fonollà, P., and Sabater, F. (2008) Inter-annual, annual, and seasonal variation of P and N retention in a perennial and an intermittent stream. *Ecosystems* **11**: 670-687.

Webster, J., and Valett, H. (2006) Solute dynamics. In *Methods in stream ecology*. Hauer FR, and Lamberti GA, E. (eds). San Diego,USA: Academic Press, pp. 169-185.

Zhang, T., Jin, T., Yan, Q., Shao, M., Wells, G., Criddle, C., and Fang, H.H.P. (2009) Occurrence of ammonia-oxidizing Archaea in activated sludges of a laboratory scale reactor and two wastewater treatment plants. *Journal of Applied Microbiology* **107**: 970-977.

4.6 Supplement Material

Table S4.1. Average archaeal and bacterial *amoA* gene abundance in the WWTP effluents (copies L^{-1}) for the five urban streams analyzed. SD: Standard deviation

gene	COL	SMP	GUA	CEL	BRE
amoA AOB	647	313	344	784	3221
SD *amoA* AOB	144	42	96	70	369
amoA AOA	43	82	194	48	37
SD *amoA* AOA	35	38	20	59	27

PART II

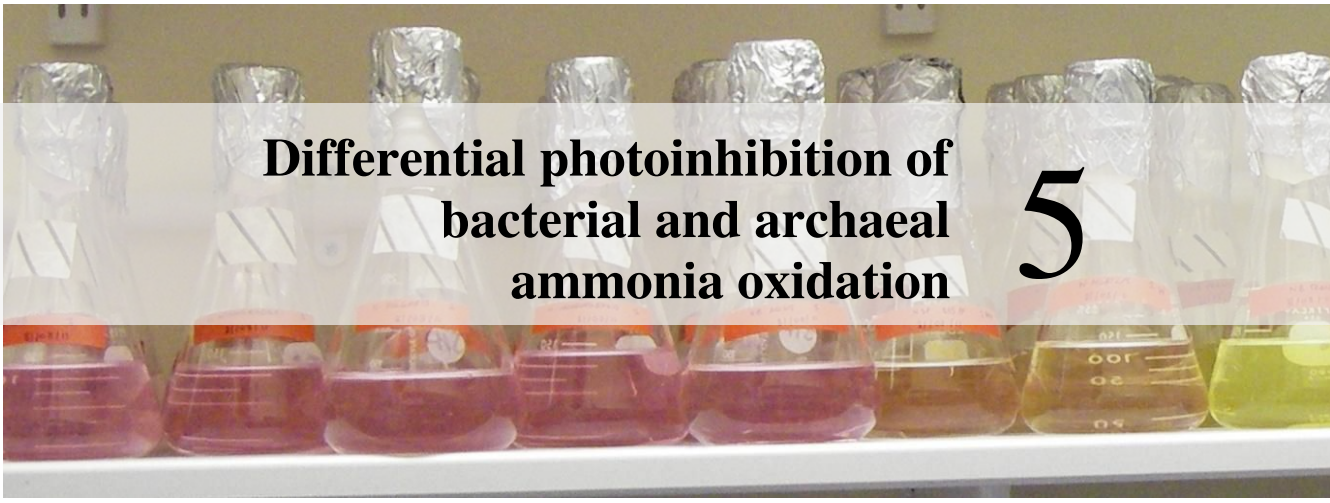

5 Differential photoinhibition of bacterial and archaeal ammonia oxidation

With permission of Stephanie N. Merbt, David A. Stahl, Emilio O. Casamayor, Eugenia Martí, Graeme W. Nicol1 and James I. Prosser1 (2012) Differential photoinhibition of bacterial and archaeal ammonia oxidation. FEMS Letters 327, 41 – 46

Cover: Laboratory cultures. Photography by SN Merbt

5.1 Abstract

Inhibition by light potentially influences the distribution of ammonia oxidizers in aquatic environments and is one explanation for nitrite maxima near the base of the euphotic zone of oceanic waters. Previous studies of photoinhibition have been restricted to bacterial ammonia oxidizers, rather than archaeal ammonia oxidizers, which dominate in marine environments. To compare the photoinhibition of bacterial and archaeal ammonia oxidizers, specific growth rates of two ammonia-oxidizing archaea (*Nitrosopumilus maritimus* and *Nitrosotalea devanaterra*) and bacteria (*Nitrosomonas europaea* and *Nitrosospira multiformis*) were determined at different light intensities under continuous illumination and light/dark cycles. All strains were inhibited by continuous illumination at the highest intensity (500 μE m^{-2} s^{-1}). At lower light intensities, archaeal growth was much more photosensitive than bacterial growth, with greater inhibition at 60 μE m^{-2} s^{-1} than at 15 μE m^2 s^{-1}, where bacteria were unaffected. Archaeal ammonia oxidizers were also more sensitive to cycles of 8-h light/16-h darkness at two light intensities (60 and 15μE m^{-2} s^{-1}) and, unlike bacterial strains, showed no evidence of recovery during dark phases. The findings provide evidence for niche differentiation in aquatic environments and reduce support for photoinhibition as an explanation of nitrite maxima in the ocean.

5.2 Introduction

Nitrification is a key process in the cycling of nitrogen interrestrial and aquatic ecosystems. The first, rate-limiting step of nitrification, the oxidation of ammonia (NH_3) to nitrite (NO_2), is carried out by both ammonia-oxidizing bacteria (AOB, Koops & Pommerening-Röser, 2001) and archaea belonging to the recently described thaumarchaea group (AOA, Spang et al., 2010). The first step in ammonia oxidation is catalysed by ammonia monooxygenase, and the subunit A gene (*amoA*) is the most commonly used marker for tracking ammonia oxidizers in environmental samples. Although sharing a common function, bacterial and archaeal amo genes are phylogenetically distinct, suggesting different evolution and phenotypic characteristics between AOB and AOA (Nicol & Schleper 2006). AOB were traditionally considered to be responsible for most ammonia oxidation in natural environments, but AOA *amoA* genes are now known to be ubiquitous and to outnumber those of AOB in many environments, including soils (Leininger et al., 2006), oceans (Wuchter et al., 2006), streams (Merbt et al., 2011) and alpine lakes (Auguet et al., 2011). Although AOA and AOB coexist in many ecosystems, differential sensitivities to pH (Nicol et al., 2008), temperature (Tourna et al., 2008) and ammonium concentration (Martens-Habbena et al., 2009; Verhamme et al., 2011) appear to control their relative abundances and activities, suggesting distinct physiological adaptations for each group. Photoinhibition of ammonia oxidation has been investigated in laboratory cultures of AOB (e.g. Hooper & Terry, 1974, Guerrero & Jones, 1996a, b). Hyman & Arp (1992) found that light may completely inhibit nitrite production and de novo synthesis of ammonia monooxygenase is required after exposure of cultures to light, leading to suggestions that light may be responsible for the inhibition of nitrification in ocean surface waters (Horrigan et al., 1981), coastal areas (Olson, 1981), estuaries (Horrigan & Springer, 1990) and eutrophic rivers (Lipschultz et al., 1985). The low availability of laboratory cultures has restricted physiological

studies of photoinhibition in AOB and, particularly, AOA. This has prevented assessment of the role of light exposure in niche separation and distribution of AOA and AOB in natural environments. Recent observations of the distribution of archaeal *amoA* genes in stream biofilms exposed to light and dark conditions (Merbt et al., 2011) and along a vertical profile in the Atlantic Ocean (Church et al., 2010) suggest, however, that AOA could also be sensitive to light and that sensitivity of AOA and AOB may differ. The aims of this study were to determine the effects of different light intensities on bacterial and archaeal ammonia oxidation using several laboratory cultures of AOA and AOB and to assess their potential to explain AOB and AOA differential distribution and activity in aquatic ecosystems.

5.3 Materials and methods

Strains and culture conditions Photoinhibition of two AOB (*Nitrosomonas europaea* ATCC19718 and *Nitrosospira multiformis* ATCC25196) and two AOA (*Nitrosopumilus maritimus* and *Nitrosotalea devanaterra*) strains was investigated during growth in batch culture. *Nitrosomonas europaea* and *N. multiformis* were obtained from NCIMB (http://www.ncimb.com/). *Nitrosopumilus maritimus* and *N. devanaterra* were obtained from existing laboratory cultures (Ko¨nneke et al., 2005; Lehtovirta-Morley et al., 2011). All strains were grown aerobically in 100-ml quartz flasks containing 50 mL inorganic growth medium. AOB were grown in Skinner & Walker (1961) medium containing 1.78 mM ammonia sulphate, adjusted to pH 8.0 with Na_2CO_3 (5% w/v). *Nitrosopumilus maritimus* was grown in HEPES buffered, synthetic medium (pH 7.6) (Martens-Habbena et al., 2009), and N. devanaterra was cultured in acidic (pH 4.5) freshwater medium as described by Lehtovirta-Morley et al. (2011). The media for AOA contained ammonium chloride at concentrations of 1 mM for *N. maritimus* and 0.5 mM for *N. devanaterra*.

Media were inoculated with 1% or 10% (v/v) of exponential-phase cultures of AOB or AOA, respectively. Bacterial cultures were sampled (1 mL) at intervals of 8 h for 5 days, and archaeal cultures were sampled daily for 10 days.

Experimental design and sample analysis. Photoinhibition was investigated in controlled temperature chambers maintained at 26 °C and illuminated by compact fluorescent lights (55 W) and clear strip lights (30 W) (International Lamps Ltd, Hertford, UK) emitting light with a wavelength spectrum of 400–680 nm with a maximum intensity at approximately 580 nm. Ammoniaoxidizing activity of the different cultures was measured under continuous illumination at an intensity of either 15, 60 or 500 μE m^2 $s^{-1}$and with diurnal cycles of 8-h light (15 or 60 μE m^{-2} s^{-1}) and 16-h dark conditions. Control cultures were incubated in the dark in the same incubator. Triplicate cultures were grown for all light treatments and controls. Light intensities were selected to reflect conditions prevailing in riparian zones of rivers and lakes, with highest light intensity (500 μE m^{-2} s^{-1}) simulating naturally occurring conditions during a clear summer day in open areas and the lower intensities (60 and 15 μE m^{-2} s^{-1}) simulating conditions in shaded areas. Ammonia-oxidizing activity was determined by measuring increases in nitrite (NO_2) concentration over time for each particular culture and light exposure treatment. Specific growth rate was estimated by linear regression during the linear phase of semi-logarithmic plots of nitrite concentration vs. time, as in previous studies (Powell & Prosser, 1992; Könneke et al., 2005; Lehtovirta- Morley et al., 2011). Estimated specific growth rates in control and illuminated cultures were compared using the Student's t-test (two-sample assuming unequal variances).

5.4 Results

All AOA and AOB strains grew exponentially during incubation in the dark. Initial increases in nitrite concentration were sometimes non-exponential, because of carryover of nitrite with inocula, but subsequent increases in nitrite concentration were exponential. Typical nitrite production kinetics are exemplified in Figure 5. 1 for cultures of *N. multiformis* and *N. devanaterra* under continuous light at 60 µE m^{-2} s^{-1} and dark controls. Nitrite production kinetics were analysed prior to limitation by reduction in pH (all strains except *N. devanaterra*) or high nitrite concentration (*N. devanaterra*). Continuous illumination at 60 µE m^{-2} s^{-1} reduced the specific growth rate of *N. multiformis* from 1.05 (±0.07) day ¯1 to 0.62 (±0.01) day ¯1 and completely inhibited that of *N. devanaterra*.

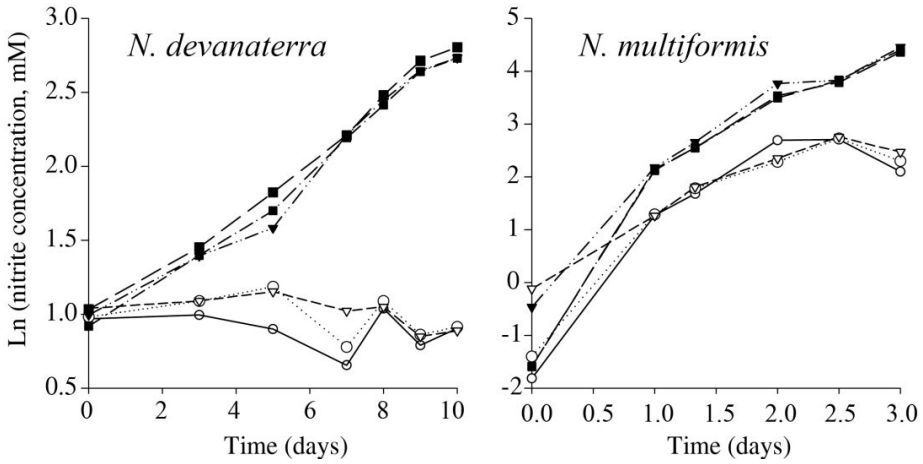

Figure 5.1. Semi-logarithmic plots of nitrite concentration vs. time during incubation of triplicate cultures of *Nitrosotalea devanaterra* and *Nitrosospira multiformis* in liquid batch culture in the dark (solid symbols) and under continuous illumination (open symbols) at an intensity of60 µE m^{-2} s^{-1}.

Effects of illumination and associated statistical analysis are summarized in Figure 5.2 and Table 5.1, respectively. AOA were more sensitive to illumination

than AOB. Continuous illumination at the lowest light intensity examined (15 μE m^{-2} s^{-1}) did not significantly affect the growth of the AOB, *N. europaea* and *N. multiformis*, but inhibited that of the AOA, *N. maritimus* (91% reduced growth rate compared with controls) and *N. devanaterra* (81%) (Figure 5.2a, Table 5.1). Continuous illumination at 60 μE m^{-2} s^{-1} completely inhibited growth of the two studied AOA species, but only partially inhibited growth of AOB strains (Figs 1 and 2, Table 5.1). The highest light intensity (500μEm^{-2} s^{-1}) completely inhibited growth of all AOB and AOA strains. Apparent differences in sensitivity to photoinhibition of AOA species were only observed at the lowest light intensity, where *N. devanaterra* was less sensitive than *N. maritimus*. For AOB, *N. europaea* was more sensitive than *N. multiformis*, with respective decreases in specific growth rate of 91% and 41% at 60 μE m^{-2} s^{-1} (Figure 5.1, Table 5.1).

In natural environments, diurnal cycles enable the recovery of ammonia oxidizers from photoinhibition and growth. This was therefore investigated for all strains using 8-h light/16-h dark cycles at the two lowest light intensities. At 15 μE m^2 s^{-1}, AOB were not significantly inhibited, as found under continuous illumination. At 60 μE m^2 s^{-1}, however, photoinhibition was lower than that under continuous illumination. There was no significant reduction in the specific growth rate of *N. europaea*, demonstrating an ability to recover during periods of darkness, while the growth of *N. multiformis* was reduced by only 14%, compared to 41% under continuous illumination (Figure 5.2), suggesting partial recovery. Photoinhibition of *N. maritimus* was not influenced by light cycling, with almost complete inhibition at both light intensities. There was evidence of some recovery of growth of *N. devanaterra* at 60 μE m^2 s^{-1}, where inhibition was only 63% and surprisingly lower than at 15 μE m^2 s^{-1} continuous ilumination.

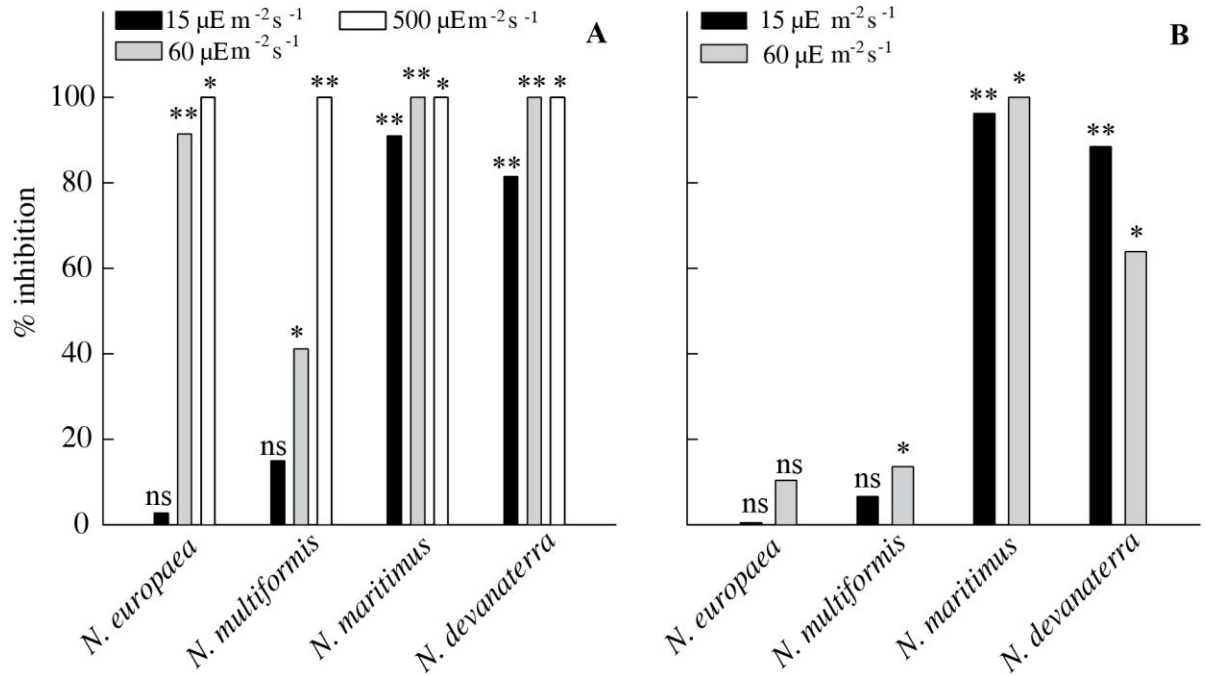

Figure 5.2. The reduction in estimated specific growth rate as the percentage of the control, dark-incubated cultures, during incubation of bacterial (*Nitrosomonas europaea* and *Nitrosospira multiformis*) and archaeal (*Nitrosopumilus maritimus* and *Nitrosotalea devanaterra*) ammonia oxidizers under (a) continuous illumination at three intensities (15, 60 and 500 µE m^{-2} s^{-1}) and under (b) 16-h light/8-h dark cycles at 15 and 60 µE m^{-2} s^{-1}. Data are presented as the mean and standard error of triplicate cultures, and significant differences between control and illuminated cultures are represented as ns (no significant difference), *$P < 0.05$ and **$P < 0.001$.

Table 5.1. Mean estimated specific growth rates of triplicate cultures of bacterial (*Nitrosomonas europaea* and *Nitrosospira multiformis*) and archaeal (*Nitrosopumilus maritimus* and *Nitrosotalea devanaterra*) ammonia oxidisers in liquid batch culture. Cultures were incubated in the dark (control), with continuous illumination or with light:dark cycles.

	Light intensity ($\mu E\ m^{-2}\ s^{-1}$)	*N. europaea*		*N. multiformis*		*N. maritimus*		*N. devanaterra*	
		Rate	std error	rate	std. error	rate	std error	rate	std. error
Continuous illumination	15	1.08	0.007	0.71	0.038	0.019	0.004	0.046	0.003
	control	1.11	0.017	0.83	0.024	0.21	0.005	0.246	0.008
	p-value	*ns*		*ns*		**		**	
	60	0.084	0.007	0.62	0.014	-0.008	0.004	-0.028	0.007
	control	0.99	0.015	1.05	0.071	0.26	0.001	0.206	0.003
	p-value	**		*		**		**	
	500	ng	ng	ng	ng	-0.017	0.005	-0.018	0.002
	control	0.62	0.023	1.37	0.010	0.16	0.020	0.081	0.008
	p-value	**		**		*		*	
8:16 h light : dark cycling	15	1.61	0.187	1.45	0.041	0.004	0.002	0.022	0.008
	control	1.54	0.128	1.56	0.080	0.109	0.003	0.190	0.009
	p-value	*ns*		*ns*		**		**	
	60	1.01	0.047	0.88	0.010	-0.004	0.025	0.052	0.007
	control	1.122	0.011	1.016	0.002	0.211	0.002	0.144	0.004
	p-value	*ns*		*		*		**	

ng, no growth detected; ns, no significant difference between control and treatment. *P < 0.05; **P < 0.001.

5.5 Discussion

Light plays a key role in the nitrogen cycle in aquatic ecosystems, stimulating uptake and excretion of inorganic nitrogen and inhibiting nitrification (Nelson & Conway, 1979; Hooper & Terry, 1973). The detrimental effect of light on ammonia-oxidizing bacteria (AOB) has been known for many years. Hooper & Terry (1973, 1974) demonstrated light inhibition of ammonia oxidation by N. europaea suspended cells, with maximum inhibition at short, near-UV wavelength (410 nm). Horrigan & Springer (1990) reported variability in the photosensitivity of ammonia oxidizers such as *Nitrosococcus oceanus* and strain SF-2, isolated from sea-surface films, and Guerrero & Jones (1996a) provided further evidence of species-specific and dose- and wavelength-dependent photoinhibition. Results from the present study support these previous findings.

Photoinhibition appears to operate on the initial step of ammonia oxidation, which is catalysed by ammonia monooxygenase. This step is common to both AOB and AOA, although subsequent metabolism of hydroxylamine, the product of initial ammonia oxidation, has not yet been determined for AOA. Broad similarities in AOA *amoA* gene sequences predict potentially similar AMO structure and therefore similar sensitivities to photoinhibition, while phylogenetic separation of AOA and AOB sequences and other physiological distinctions between archaea and bacteria suggest that levels of photoinhibition may differ and may give rise to niche differentiation, which is supported by our results. The effect of light on AOA has not previously been investigated. This study therefore provides the first evidence of photoinhibition in AOA and significantly greater inhibition of AOA than that of AOB. In addition, the study demonstrates differences in photosensitivity within AOB and AOA. Photoinhibition may therefore contribute to niche differentiation between and within AOA and AOB and may determine their distribution and diversity in light-affected ecosystems. Our findings influence explanations for several

phenomena in aquatic environments. Nitrite often accumulates at the base of the euphotic zone, forming the primary nitrite maximum, which is explained by either nitrate reduction to nitrite, by light-limited phytoplankton or by differential photoinhibition of ammonia oxidizers and nitrite oxidizers (Lomas & Lipschultz, 2006). While other environmental factors may drive the distribution of AOA and AOB, the latter hypothesis assumes a key role for photoinhibition of ammonia oxidizers in surface waters, which is relieved with increasing depth, as light intensity decreases. It further assumes that nitrite oxidizers are more photosensitive than ammonia oxidizers, leading to the accumulation of nitrite through greater inhibition of nitrite production and/or slower recovery following photoinhibition. Cultivation-based studies provide contradictory evidence for this hypothesis, indicating that AOB are more photosensitive than nitrite oxidizers (Guerrero & Jones, 1996a), but that they recover more quickly from photoinhibition when subsequently incubated in the dark (Guerrero & Jones, 1996b). However, this model was developed prior to the discovery of the dominance of AOA in marine ecosystems. Greater photoinhibition and slower recovery of AOA, compared with AOB, observed in our study suggest that the difference between photoinhibition of ammonia and nitrite oxidizers is less than previously thought, reducing confidence in this explanation of the nitrite maximum.

The light intensities investigated are similar to those causing in situ inhibition of nitrification in previous studies: 100 μE m^2 s^{-1} in the eutrophic Delaware River (Lipschultz et al., 1985) and approximately 40–70 μE m^2 s^{-1} in a Californian bight (Olson, 1981). In the mixed layer of natural aquatic systems, however, turbidity may promote nitrification both by protecting nitrifiers from photoinhibition and by limiting substrate competition with phytoplankton. Findings also provide a physiological explanation for the higher accumulation of AOA and AOB in river biofilms on the dark side, rather than on the illuminated side of cobbles (Merbt et al., 2011), and the greater abundance of

amoA genes with decreasing light intensity in the ocean (Church et al., 2010). Despite this evidence of photoinhibition in natural ecosystems, AOA *amoA* abundance is high in regions of high irradiance, such as surface waters of the Mediterranean Sea (Galand et al., 2010) and high mountain lakes (Auguet & Casamayor, 2008; Auguet et al., 2011). This may reflect differences in photosensitivity within AOA, which may also contribute to consistent phylogenetic changes observed in AOA along vertical gradients in the Gulf of Mexico from upper (0–100 m) to deeper layers (450 m) (Beman et al., 2008) and in a deep alpine lake in the Pyrenees (J.C. Auguet, X. Triado-Margarit, N. Nomokonova, L. Camarero & E.O.Casamayor, unpublished data). Although our findings provide a rationale for future ecological and physiological diversity studies, they were performed with a limited number of strains, of which only one, *N. maritimus*, was isolated from a marine ecosystem. In addition, photoinhibition was investigated in suspended batch culture and may be influenced in natural systems by growth in biofilms and aggregates. Although AOA appear to be more photosensitive, they outnumber AOB in the upper water column (Beman et al., 2008), with high transcriptional activity (Church et al., 2010), and other environmental factors undoubtedly contribute to their relative distributions. Studies of AOB also suggest that photoinhibition depends on wavelength (Hooper & Terry, 1974; Guerrero & Jones, 1996a), which, like intensity, will vary with water depth. Nevertheless, the findings suggest light as an additional factor determining niche differentiation in ammonia oxidizers that may determine their distribution and relative contributions to nitrogen cycling in aquatic ecosystems.

Acknowledgements

We thank Jenna McWilliam and David Hadwen for laboratory assistance. The project was financed by the GRACCIE project (Spanish Ministry of Science and Education Consolider Program, ref: CSD2007-00067). S.N.M. is supported by a JAE-pre-doctoral fellowship from the Spanish National Research Council (CSIC), and G.W.N. by a NERC Advanced Fellowship (NE/D010195/1). Additional support was from NSF Award MCB-0920741 to D.A.S.and M. Hackett and from NSF Award OCE-1046017 to D.A.S., A. Ingalls, E.V. Armbrust, A.H. Devol and J. Moffett.

5.6 References

Auguet J-C & Casamayor EO (2008) A hotspot for cold crenarchaeota in the neuston of high mountain lakes. *Environmental Microbiology* **10**: 1080–1086.

Auguet J-C, Nomokonova N, Camarero L & Casamayor EO (2011) Seasonal changes of freshwater ammonia-oxidizing archaeal assemblages and nitrogen species in oligotrophic alpine lakes. . *Applied and Environmental Microbiology* **77**: 1937–1945.

Beman JM, Popp BN & Francis CA (2008) Molecular and biogeochemical evidence for ammonia oxidation by marine Crenarchaeota in the Gulf of California. *ISME Journal* **2**: 429–441.

Church MJ, Wai B, Karl DM & DeLong EF (2010) Abundances of crenarchaeal amoA genes and transcripts in the Pacific Ocean. *Environmental Microbiology* **12**: 679–688.

Galand PE, Gutierrez-Provecho C, Massana R, Gasol JM & Casamayor EO (2010) Inter-annual recurrence of archaeal assemblages in the coastal NW Mediterranean Sea (BlanesBay Microbial Observatory). *Limnology and Oceanography* **55**: 2117–2125.

Guerrero M & Jones R (1996a) Photoinhibition of marine nitrifying bacteria. I. Wavelength dependent response. *Marine Ecology Progress Series* 141: 183–192.

Guerrero M & Jones R (1996b) Photoinhibition of marine nitrifying bacteria. II. Dark recovery after monochromatic or polychromatic irradiation. *Marine Ecology Progress Series.* **141**: 193–198.

Hooper AB & Terry KR (1973) Specific inhibitors of ammonia oxidation in Nitrosomonas. *Journal of Bacteriology* **115**: 480–485.

Hooper AB & Terry KR (1974) Photoinactivation of ammonia oxidation in Nitrosomonas. *Journal of Bacteriology* **119**: 899–906.

Horrigan SG & Springer AL (1990) Oceanic and estuarine ammonium oxidation: effects of light. *Limnology and Oceanography* **35**: 479–482.

Horrigan SG, Carlucci AF & Williams PM (1981) Light inhibition of nitrification in sea-surface films. *Journal of Marine Research.* **39**: 557–565.

Hyman MR & Arp DJ (1992) 14C2H2- and l4C02-1abeling studies of the de novo synthesis of polypeptides by Nitrosomonas europaea during recovery from acetylene and light inactivation of ammonia monooxygenase. *Journal of Biologcial Chemistry.* **267**: 1534–1545.

Könneke M, Bernhard AE, de la Torre JR, Walker JB, Waterbury CB & Stahl DA (2005) Isolation of an autotrophic ammonia-oxidizing marine archaeon. *Nature* **437**: 543–546.

Koops H-P & Pommerening-Röser A (2001) Distribution and ecophysiology of the nitrifying bacteria emphasizing cultured species. *FEMS Microbioal Ecology* **37**: 1–9.

Lehtovirta-Morley L, Stoecker K, Vilcinskas A, Prosser JI & Nicol GW (2011) Cultivation of an obligate acidophilic ammonia oxidizer from a nitrifying acid soil. *Proceedings of the National Academy of Science USA*. **108**: 15892–15897.

Leininger S, Urich T, Schloter M, Schwark L, Qi J, Nicol GW, Prosser JI, Schuster SC & Schleper C (2006) Archaea predominate among ammonia-oxidizing prokaryotes in soils. *Nature* **442**: 806–809.

Lipschultz F, Wofsy SC & Fox LE (1985) The effects of light and nutrients on rates of ammonium transformation in a eutrophic river. Mar Chem 16: 329–341.

Lomas MW & Lipschultz F (2006) Forming the primaryn itrite maximum: Nitrifiers or phytoplankton? *Limnology and Oceanography* **51**: 2453–2467.

Martens-Habbena W, Berube PM, Urakawa H, de la Torre JR & Stahl DA (2009) Ammonia oxidation kinetics determine niche separation of nitrifying Archaea and Bacteria. *Nature* **461**: 976–979.

Merbt SN, Auguet J-C, Casamayor EO & Martı´ E (2011) Biofilm recovery in a wastewater treatment plantinfluenced stream and spatial segregation of ammoniaoxidizing microbial populations. *Limnology and Oceanography* **56**: 1054–1064.

Nelson D & Conway HL (1979) Effects of the light regime on nutrient assimlation by phytoplankton in the Baja California and northwest Africa upwelling systems. *Journal of Marine Research.* **37**: 301–318.

Nicol GW & Schleper C (2006) Ammonia-oxidising Crenarchaeota: important players in the nitrogen cycle? *Trends Microbiol* **14**: 207–212.

Nicol GW, Leininger S, Schleper C & Prosser JI (2008) The influence of soil pH on the diversity, abundance and transcriptional activity of ammonia oxidizing archaea and bacteria. *Environmental Microbiology* **10**: 2966–2978.

Olson RJ (1981) 15N tracer studies of the primary nitrite maximum. *Journal of Marine Research.* **39**: 203–225.

Powell SJ & Prosser JI (1992) Inhibition of biofilm populations of Nitrosomonas europaea. *Microbial Ecolology* **24**: 43–50.

Skinner FA & Walker N (1961) Growth of Nitrosomonas europaea in batch and continuous culture. *Arch Mikrobiol* **38**: 339–349.

Spang A, Hatzenpichler R, Brochier-Armanet C, Rattei T, Tischler P, Spieck E, Streit W, Stahl DA, Wagner M & Schleper C (2010) Distinct gene set in two different lineages of ammonia-oxidizing archaea supports the phylum Thaumarchaeota. *Trends in Microbiology* **18**: 331–340.

Tourna M, Freitag TE, Nicol GW & Prosser JI (2008) Growth, activity and temperature responses of ammonia-oxidizing archaea and bacteria in soil microcosms. *Environmental Microbiology* **10**: 1357–1364.

Verhamme DT, Prosser JI & Nicol GW (2011) Ammonia concentration determines differential growth of ammoniaoxidising archaea and bacteria in soil microcosms. *ISME Journal* **5**: 1067–1071.

Wuchter C, Abbas B, Coolen MJL et al. (2006) Archaeal nitrification in the ocean. *Proceedings of the National Academy of Science USA* **103**: 12317– 12322.

Response to light of archaeal and bacteria ammonia oxidizers inhabiting natural epilithic stream biofilms

6

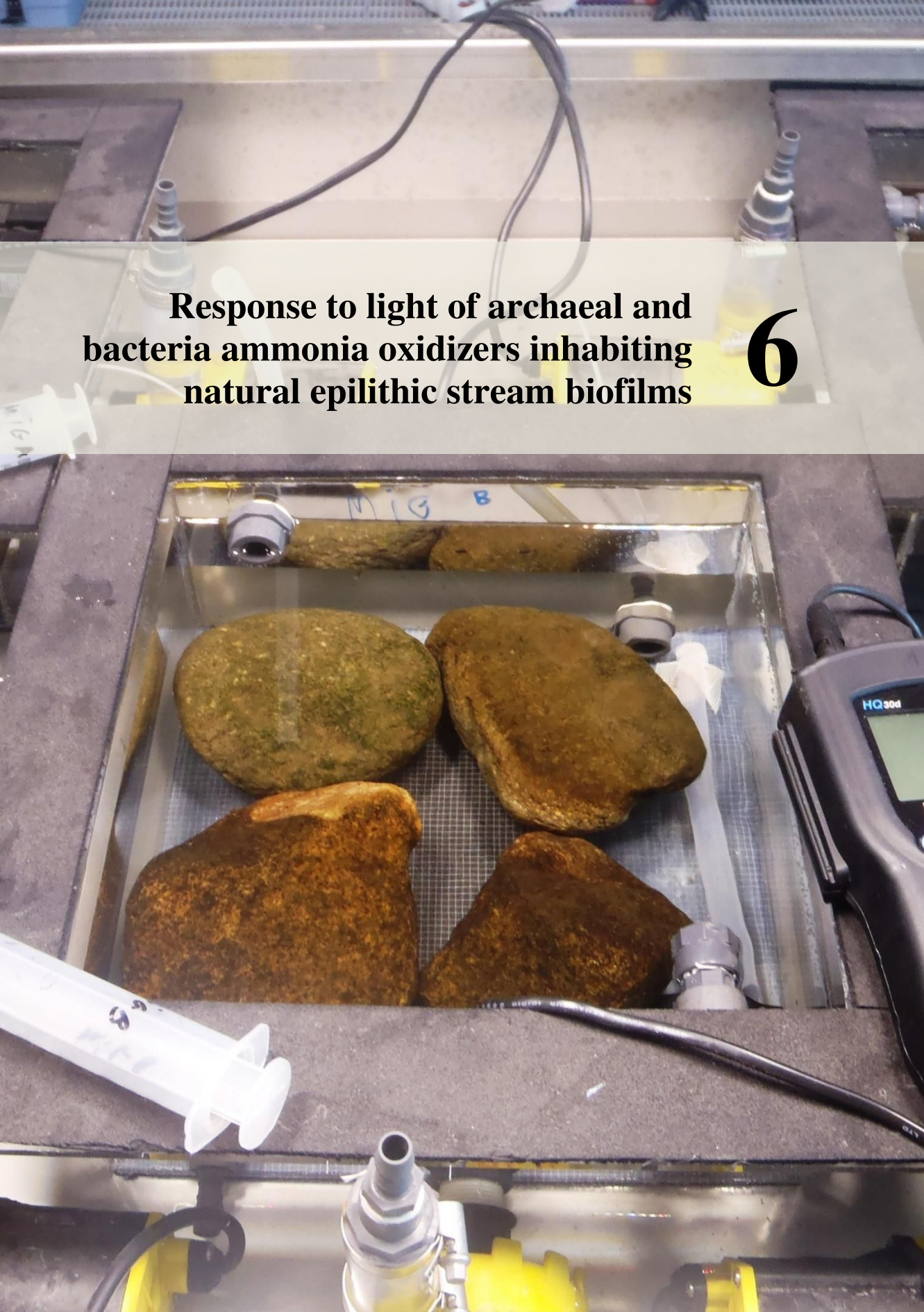

With permission from L. Proia, S. Bernal, E. Martí and E. O. Casamayor who were Co-authors of this study

Cover: Circulating chambers used for experimental setting in this chapter. Cobbles overgrown with biofilm. Photograph by Alexandra Serra.

6.1 Abstract

Nitrification (ammonia oxidation to nitrate) is a key process in nitrogen cycling. Both, archaeal (AOA) and bacterial (AOB) ammonia oxidizers (AO) carry out the first, rate-limiting, nitrification step, which is photoinhibited in strains cultured in the laboratory. We hypothesize that complex stream biofilms exert a natural protection against light inhibition *in situ*. To test it, we examined nitrification rates coupled to synthesis of AOA and AOB *amoA* gene transcripts. Biofilms grown *in situ* on cobbles in an urban stream differing significantly in natural NH_4^+ concentrations and AO abundance and composition were selected from both the upper cobble side (light-side biofilms) and sediment facing side (dark-side biofilms). Different light-dark manipulations and transplant experiments were carried out in microcosms. In biofilms dominated by AOB, nitrification rates were significantly higher and responses to changes in light regime were similar among treatments and always within the first few minutes. Under dark incubations, mean nitrification rates were 38 % higher in biofilms coming from the dark-side than from the light-side counterpart, and nitrification potential estimated as mRNA abundance was mostly driven by AOB. Under light incubations, both AOB activity and nitrification rates were reduced by 30-100 % in dark-side biofilms indicating photoinhibition susceptibility. Conversely, nitrification was not reduced in light-side biofilms suggesting either a putative umbrella effect from the thick photoautotrophic matrix or a natural photoadaptation in AO assemblages naturally exposed to sun irradiance. These results also show AO co-exist and successfully oxidize NH_4^+ in the presence of photoautotrophs (algae and cyanobacteria) and heterotrophic bacteria *in situ*.

6.2 Introduction

Ammonia oxidizing archaea (AOA) and bacteria (AOB) catalyze the oxidation of ammonia ($N\text{-}NH_4^+$) to nitrite ($N\text{-}NO_2^-$), the rate limiting step of nitrification. Under laboratory conditions, the activity of cultured representatives of both AOA and AOB is strongly inhibited by light (Hooper and Terry, 1973; Lomas and Lipschultz, 2006; French et al., 2012; Merbt et al., 2012). The ammonia monooxygenase (AMO) is the enzyme responsible for the oxidation of $N\text{-}NH_4^+$, and it has been reported that light completely inhibits the AMO enzyme in AOB and a *de-novo* protein biosynthesis is required to recover the activity (Hyman and Arp, 1992). Conversely, the biochemical mechanisms associated to light inhibition in AOA are still unknown, but genome annotations suggest that the copper containing AMO enzyme could possibly be oxidized leading to a full breakdown of metabolic activities (Walker et al., 2010).

Photoinhibition of the nitrification process may have important implication for the N cycle *in situ* (Lomas and Lipschultz, 2006). Accordingly, light has been suggested as one of the major environmental drivers shaping the distribution of ammonia oxidizers in the plankton of oceans (Beman et al., 2006; Santoro et al., 2010), and lakes (Restrepo-Ortiz et al., 2014).

In headwater streams AOA and AOB are part of the epilithic biofilms (Herrmann et al., 2011; Merbt et al., 2011; Merbt et al., 2014). Biofilms are substrata attached, matrix-embedded complex three dimensional structures of bacteria, algae and fungi that host a rich microbial community turning them to active bioreactors for nutrient cycling (Peterson et al., 2001; Battin et al., 2003). The biofilm matrix provides spatially heterogeneous space with highly diverse microenvironments varying significantly in physicochemical conditions where different microbes develop (Lock et al., 1984; Schramm et al., 2000; Battin et al., 2007).

In streams, nitrification can be a significant $N\text{-}NH_4^+$ sink where up to 60 % of the in-stream $N\text{-}NH_4^+$ is transformed to $N\text{-}NO_2^-$ and nitrate ($N\text{-}NO_3^-$) being biofilms an highly important compartment driving this process (Peterson et al., 2001; Bernhardt et al., 2002, Teissier et al., 2007). However, sun light penetrates the upper surface of the stream bed and hence, not only rules biofilm community composition (Schiller et al., 2007) but may also have an inhibitory affect on the activity of AOA and AOB *in situ.*

The present investigation aimed to test whether AOA and AOB from biofilms present in natural stream cobbles are inhibited by light and if this fact scales up changing the nitrifying patterns detected in the water column. We hypothesized that ammonia oxidization is higher in biofilms growing on the sediment-facing cobble side (dark-side) and hampered on the light-exposed upper cobble side (light-side). Therefore, if both sides are experimentally exposed to light, the nitrification process in the biofilm should be inhibited or at least substantially reduced. To test the hypothesis, we conducted microcosm experiments and followed potential nitrification rates after $N\text{-}NH_4^+$ additions under light and dark conditions. Our experimental setting encompassed stream biofilm communities grown *in situ* under differing light regimes and NH_4^+ concentrations aiming to cover different ammonia oxidizing assemblages (AOA and AOB dominated) embedded in distinct types of biofilm matrixes (Merbt et al., 2014). Nitrification rates were further supported after assessing abundance and activity of AOA and AOB by quantitative real time PCR (qPCR) and reverse transcriptase qPCR (rt-qPCR) on transcripts (mRNA) of the *amoA* gene, the molecular marker most commonly used for tracking ammonia oxidizers in environmental samples.

6.3 Material and Methods

Environmental samples and sampling reaches: To evaluate the response to light of AOA and AOB four different biofilm types developed *in-situ* on fist sized cobbles were chosen. The biofilms were naturally developed *in situ* under i) exposition to light on the light exposed, upper cobble side (light-side biofilms) or ii) in darkness on the sediment-facing cobble side (dark-side biofilms). Previous studies had shown that both biofilm types differ significantly in biomass, chlorophyll a content and ammonia oxidizing community composition (Merbt et al 2011, 2014).

Both biofilm types were collected from two stream reaches, which significantly differed in NH_4^+ loads in La Tordera River (NE, Spain). Previous studies had shown that biofilms from low NH_4^+ concentration reaches were dominated by AOA and biofilms from high NH_4^+ concentration reaches were dominated by AOB (Merbt et al., 2011; 2014). High NH_4^+ load was related to the local waste water treatment plant (WWTP) effluents of Santa Maria de Palautordera (41°41'3.47"N; 2°27'33.19"W). The sampling reaches were settled 50 m upstream and 900 m downstream of the WWTP perturbation. Sampling reaches differed in temperature, conductivity and discharge. The upstream reach had 0.02 mg N- NH_4^+ L^{-1} (here after referred as "low NH4 reach") and the downstream reach showed 350 times higher ammonium concentration (here after referred as "high NH4 reach"). Cobbles were collected from both reaches in January 2013 when riparian vegetation was leafless and the stream surface was under full sun irradiance. We carefully selected cobbles which were submerged but not embedded into the sediment, and transported them to the laboratory covered by stream water.

Experimental setting. Potential nitrification rates were estimated in experimental microcosms. Microcosms were transparent metacrylate chambers (30 x 30 x 10 cm) connected to a submergible peristaltic pump (24 V) and run under constant

room temperature (21 °C). Four LED light panels (Led's Grow 120W V.2) illuminated the experimental setting at 100 µE m^{-2} s^{-1} constant intensity.

To separately measure potential nitrification rates in light-side and dark-side biofilms we carefully removed the biomass from the respective cobble side. The biofilm was removed after scratching with a sterile metal brush and repeated washing steps with sterile distillated water followed by carefully dipping the scraped side in 70 % ethanol for 10 s and a final water washing step. For each experiment 3-4 cobbles were prepared. Experiments were run in triplicates (three chambers each) and controls (stream water alone) in duplicates. Manipulated cobbles were placed with the preserved biofilm side facing upwards in metacrylate chambers filled with 8 L of stream water.

The microbial communities present in the biofilms were exposed to different light conditions. First, biofilms were pre-incubated for 12 h under the respective experimental conditions before the experiment of 8 h duration started. Table 6.1 summarizes the experimental light combinations applied. To determine the potential maximum nitrification rates biofilms were pre-incubated in the dark and the experiment was carried out in the dark (DD). To record the response to light and hence evaluate photoinhibition of ammonia oxidizers, both pre-incubation and the experiment were carried out in the light (LL). To further investigate the photoinhibition lag phase, biofilms were pre-incubated in the dark and experiment was carried out in the light (DL). And finally, to evaluate the recovery after photoinhibition, biofilms were pre-incubated in the light and the experiment was carried out in the dark (LD). Such light switching experiments were carried out exclusively with AOB dominated biofilms from the high NH_4^+ reach where, based on previous measurements (Merseburger et al., 2005), we expected highest nitrification rates and therefore the strongest experimental responses.

Table 6.1**:** Light conditions applied in the experimental design. * Treatments carried out exclusively with biofilms from high NH4 reach.

code	Pre-incubation (12 h)	Experiment (8 h)
LL	light	light
DD	dark	dark
LD*	light	dark
DL*	dark	light

Potential nitrification rate measurement: Potential nitrification rate was estimated by the nutrient addition technique (O'Brion and Dodds, 2008). P-PO_4^+ and N- NH_4^+ concentrations were increased 2-5 times by adding a spike of NH_4Cl and $NaH_2PO_4 \cdot H_2O$ and incubated for 8 h. Water temperature, conductivity, pH and O_2 concentration were recorded before, during and after the experiment (Supplemental material, Table S6.1). Water samples (60 mL) for analyzing changes in N- NH_4^+, N-NO_2, and N-NO_3 concentrations were taken after 2, 30, 60, 120, 180, 240, 300, 390, and 480 min, and were immediately filtered through a glass fiber filters (FVF; 0.7 μm pore size, Albet) and stored at – 20 °C for subsequent analysis following colorimetric methods (APHA, 1995).

The biogeochemical pattern of nitrification is described by a significant increase of NO_3^- or NO_2^- over time and a concomitantly decrease of NH_4^+. However, NH_4^+ and NO_3^-, NO_2^- are simultaneously assimilated by heterotrophs and photoautotrophs. Rates of potential nitrification can be therefore described by a first-order rate function with the equation:

$$C_x = C_0 + k_c t$$

where t is time, C_x is concentration at a time point from the injection start, C_0 is the concentration just after injection, and k_c is the first-order uptake rate coefficient (h^{-1}, Ensign and Doyle, 2006).

In microcosms containing biofilms from the low NH_4^+ reach, the experimentally added NH_4^+ was fully consumed within the first 120 min and thus nitrification constant (k) was calculated after integrating the response within this time interval (Figure 6.1, panels A and B). Here we used $N\text{-}NO_2^-$ rather than $N\text{-}NO_3^-$ dynamics over time because $N\text{-}NO_3^-$ concentrations either remained constant or decrease during the experiment in all chambers. To calculate nitrification dynamics $N\text{-}NO_2^-$ and $N\text{-}NH_4^+$ dynamics were *log* transformed (1+x) to fit a linear regression.

For the microcosms setting with biofilms from the high NH_4 reach, the experimentally added $N\text{-}NH_4^+$ was not fully consumed during the experimental time and thus k was calculated integrating the whole 480 min of experimental period (Figure 6.1C and D). Here we used $N\text{-}NO_3^-$ dynamics over time because in contrast to microcosms from low NH_4 reach no increase of $N\text{-}NO_2^+$ concentrations over time was observed.

The contribution of nitrification to decreasing $N\text{-}NH_4^+$ concentrations was estimated by a nitrification constant, which is the k_{NO3}:k_{NH4} ratio. Assuming that during the nitrification process one molecule of NH_4^+ is transformed first to NO_2 and then to NO_3^+, the ratio of k_{NOx}:k_{NH4} would be 1 if all ammonia is nitrified (e.g. laboratory cultures, Martens-Habbena et al., 2009).

Mass balance: We used a mass balance approach to infer the net result of the N cycling during each experiment. For each chamber, we calculated the net change in dissolved inorganic nitrogen (ΔDIN, in %) at the end of the experiment with:

$$\Delta\mathrm{DIN} = 100 \times \left[\left(\frac{\mathrm{DINf}}{\mathrm{DINo}}\right) - 1\right]$$

where DIN_f and DIN_o are DIN concentration (in mg L^{-1}) at the end and at the beginning of the experiment, respectively. We expect no changes in ΔDIN when the added N-NH_4^+ is mainly used by nitrifiers and there is no assimilatory uptake by photoautotrophs and heterotrophs. High assimilatory uptake will result in ΔDIN>0, while ΔDIN<0 will indicate that indirect nitrification (from mineralized N-NH_4^+) was high during the experiment.

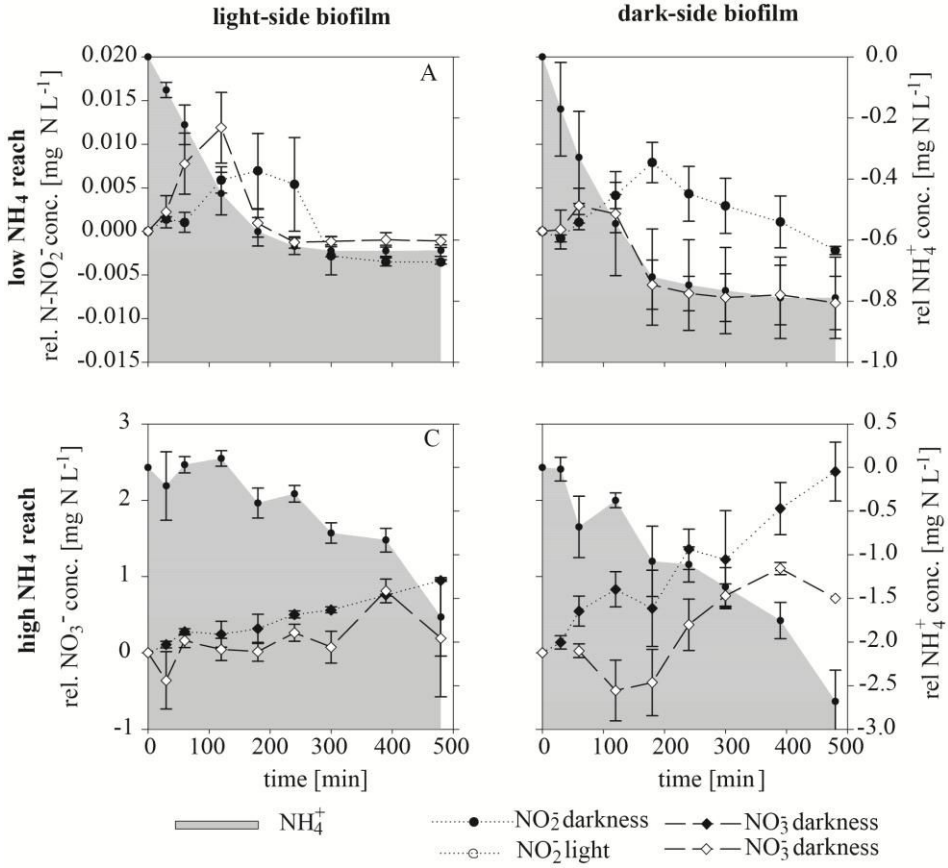

Figure 6.1: N dynamics in light-side (A and C) and dark-side biofilms (B, D) measured as relative N-NO_2^- and N-NO_3^- production over time collected from low NH_4 reach (A, B) and high NH4 reach (C, D) respectively. Open symbols indicate biofilms hold under light conditions (LL) and closed symbols indicate biofilms hold in darkness (DD). Grey shaded area indicates the N-NH_4^+ consumption over time. Lines above the dotes indicates the standard error of the mean out of 3 independent biological replicates for N-NO_2^- and N-NO_3^- and 6 replicates for N-NH_4^+

Biofilm measurements: Once the addition experiment concluded, the concentration (µg cm^{-2}) of chlorophyll *a* (Chl *a*) was measured by triplicate in each cobble using a Bentotorch (BBE, Germany). Afterwards, each cobble was scraped with a sterile metallic brush and washed into a sterile plastic beaker for measurement of biofilm biomass and molecular analysis. One biofilm composite sample per chamber was obtained and treated as an independent, biological replicate. The total surface scraped was estimated by a weight-to-area relationship after covering cobbles surface with aluminum foil.

For the measurement of biofilm biomass (expressed as ash free dry mass –in g AFDM m^{-2}) 20 mL of the biofilm sludge was filtered onto ignited, pre-weighted glass fiber filters (FVF), and dried (60 °C) until constant weight (ca. 0.1 mg, Sartorius analytical balance, model MC1) and subsequently combusted at 500°C for 5 h and re-weighted. The AFDM was estimated as the difference between dry and combusted filters masses and expressed per unit area (Hauer and Lamberti, 2011). The autotrophic index (AI) was calculated as the AFDM:Chl *a* ratio, and biofilms were considered dominated by autotrophs for AI < 200 (Steinman and Lamberti, 1996).

For the quantification of the transcript and gene abundance of the ammonium monooxigenase gene (*amo*A) 5 mL of the biofilm sludge was immediately filtered onto a 0.2 µm polycarbonate filter (Milipore). The filter was air dried and stored in 1 mL RTL buffer (Quiagen) containing 10 µl ß-Mercaptoethanol and immediately frozen in ethanol 96 % at – 80 °C. Samples were stored at – 80 °C until further processing.

RNA and DNA extraction and quantitative PCR analysis of amoA genes and transcripts: RNA and DNA were extracted using MOBIO RNApower soil and DNA accessory kit following the manufacturer's instructions. Extracted DNA and RNA were quantified with Qubit fluorometer (Invitrogen). To generate cDNA, RNA was treated with AMBION Turbo DNA free to digest carry over

DNA (Invitrogen). cDNA was synthesized from 10-100 ng of RNA with random hexamer primers (160 pmol per reaction) using Superscript II reverse transcriptase (BIORAD). Two negative controls were carried out along the process. The first control contained all DNase/RT reagents and the RNA template but no RT enzyme, to confirm that the RNA extract was DNA free. The second control combined all DNase/RT reagents but no RNA template (water only) to check for reagents contamination (Nicol et al., 2008).

The presence and quantification of *amoA* gene in the genomic DNA extract and transcripts abundance was estimated by quantitative real-time polymerase chain reaction (qPCR). The qPCR assays were carried out as described in Merbt et al (2011). Briefly, bacterial *amoA* (AOB) gene and transcript were targeted by the primers amoA-1F (59-GGGTTTCTACTGGTGGT-39) and amoA-2R (59-CCCCTCKGSAAAGCCTTCTTC-39) that generated a 491 base-pair (bp) fragment (Rotthauwe et al., 1997). Archaeal *amoA* (AOA) gene and transcripts were targeted by the primer sets CrenamoA23f (59-ATGGTCTGGCTWAGACG-39) and CrenamoA616r (59-GCCATCCATCTGTATGTCCA-39) that amplified a 628- bp fragment (Tourna et al., 2008). The quantification was run in a final volume of 10 µL containing a 5 µL solution of SsoFast EvaPhotoautotrophic supermix (BioRad), 1 ng of template genomic DNA and 2 - 3 ng of cDNA, 200 nmol L^{-1} of each corresponding primer, 0.3 mg mL^{-1} BSA, and molecular biology-grade water (Sigma). The qPCR was run on a DNA Engine thermal cycler (Bio-Rad, Hercules) equipped with a Chromo 4 Real-Time Detector (Bio-Rad). The cycling included an initial denaturation step of 2 min at 98°C, followed by 45 cycles of denaturation for 5 s at 98°C, annealing for 20 s at 57 °C and 58°C for AOA and AOB respectively, and elongation for 15 sec at 72°C. After cycling a 1 min denaturation hold at 95 ° was included followed by a 1 min at 65 °C to guarantee a stringent coupled PCR product. All qPCR runs were double checked on amplicon specificity by applying a melting curve from 55 to 95°C

and by agarose gel electrophoresis. Each run was compared with a standard curves from 10^7 to 10^2 copies μL^{-2} of *amoA* DNA from an available environmental clone. qPCR data were used when run efficiency ranged from 85 to 110 %. Controls without templates resulted in undetectable values and no unspecific PCR products such as primer dimers or gene fragments of unexpected length were observed. Results from molecular analysis of *amoA* AOA and AOB transcript analysis were displayed as RNA:DNA ratios to normalize for the differences in abundances among sampling reaches and biofilm types.

Statistical analysis: Differences in AFDM, Chl *a*, AOA and AOB concentrations in light-side and dark-side biofilms from high and low NH_4 reaches were tested applying a two-way ANOVA (biofilm type and sampling reach as factors). The test was run using *log*-transformed values to fit normality requirements, and normality of ANOVA residues were tested applying Shapiro test to accept the results. $N\text{-}NH_4^+$ and the respective $N\text{-}NO_3^-$ or $N\text{-}NO_2^-$ kinetics were fitted to a linear regression using Sigma Plot 11.0. The slope of the regression (k_c) was considered only when the *p*-value of the regression was significant ($p<0.05$). If the regression was not significant the respective k_c value was set to zero. k_c values, mass balance, and bacterial and archaeal RNA:DNA ratios from DD and LL were compared among the different biofilm types (AOA and AOB dominated in light and dark-side biofilms respectively using Kruskal-Wallis Test because values did not fulfill normality requirements (Shapiro and Levene test). When significant differences were observed we conducted additionally an ANOVA test with subsequent test of normality of the ANOVA residues. When this analysis fulfilled normality requirements (Shapiro test) than a Tukey post-hoc test was run to determine differences between samples. k_c values, mass balance, and bacterial and archaeal RNA:DNA ratios. Results from light switching experiments (DL and LD) were tested on normal distribution using Shapiro and Levene test and data were further compared among the

different biofilm types using unpaired, Student T test (Shapiro and Levene test). All tests, except kinetic tests were carried out in R project.

6.4 Results

Biofilm characterization. Light-side and dark-side biofilms from the two reaches differed significantly in AFDM and Chl *a*. AFDM and Chl *a* were higher in light-side biofilms than in dark-side biofilms (Table 6.2). Moreover AFDM was higher in biofilms at the low NH_4 reach compared to the high NH_4 reach. In terms of ammonia oxidizers (AO) abundance, AOB dominated the AO community from high NH_4 reach (here after AOB dominated biofilms) and were more abundant in light-side biofilms. In turn, AOA were equally abundant in the two reaches and in the biofilm types but dominated the AO community from low NH_4 reach (here after AOA dominated biofilms). Moreover we found a significant effect of the interaction between cobble side and sampling reach for AOA abundance (Table 6.2 and 6.3).

Table 6.2: Characterization of light and dark side biofilm collected from high and low NH4 reach ± indicates the standard error of the mean.

		low NH_4 reach (n=6)		high NH_4 reach (n=12)	
	unit	light-side	dark-side	light-side	dark-side
AFDM	g m^{-2}	7.7±1.2	1.1± 0.1	4.4±0.4	3.7±0.6
Chl *a*	µg cm^{-2}	9.2±1.9	0.1±0.0	7.9±0.7	0.5±0.2
AI		114±34	1155±202	60±7	1477±2267
AOB	copies cm^{-2}	$2.6 \times 10^4 \pm 2.9 \times 10^3$	$5.4 \times 10^3 \pm 3.8 \times 10^3$	$1.3 \times 10^6 \pm 2.3 \times 10^6$	$1.6 \times 10^6 \pm 6.0 \times 10^5$
AOA	copies cm^{-2}	$6.34 \times 10^4 \pm 2.3 \times 10^4$	$6.9 \times 10^3 \pm 5.8 \times 10^3$	$4.8 \times 10^3 \pm 2.8 \times 10^3$	$3.4 \times 10^3 \pm 1.4 \times 10^3$

Table 6.3: Statistical results from two-way ANOVA of biofilm chacteristics of light-side and dark-side biofilms (biofilm type) from high and low NH4 reach (reach). Values in bold highlight significant differences.

	ln AFDM		*ln* Chl *a*		*ln* AOA copies cm^{-2}		*ln* AOB copies cm^{-2}	
	F	P	F	p	F	p	F	p
biofilm type	1	**0.00**	174	**0.00**	1	0.34	11	**0.01**
reach	24	**0.05**	1	0.29	3	0.06	34	**0.00**
biofilm type: reach	1	**0.00**	3	0.08	6	**0.01**	3	0.11

Nitrification in biofilms under dark conditions. In the dark experiments (DD) all biofilms assimilated N-NH_4^+ and active nitrification was indicated by increase of N-NO_2^- and N-NO_3^- concentrations in biofilms from low and high NH_4 reach respectively. However we found substantial differences in N dynamics among biofilm types. The typical N dynamics are illustrated in Figure 6.1 and summarized in Table 6.4 and Figure 6.2 A-D.

next page:_____

Figure 6.2. Data from biofilms grown on the light-side (white bars) and dark-side (black bars) of the cobbles differing in ammonia oxidizing community composition (AOA and AOB dominated) under constant irradiance (E-H) and darkness control (A-D). Panel A and E show the ratio of k_{NO3}:k_{NH4} for AOB dominated biofilms and k_{NO2}:k_{NH4} for AOA dominated biofilms. Panel B and F show the mass balance of initial and final DIN concentration; Panel C and G show the ratio of bacterial and panel D and H the ratio of archeal *amoA* transcripts against gene copy abundance. Bars represent the mean of three independent biological replicates, line above the bars is the standard error of the mean. Letters indicate sig differences ($p<0.05$) between samples (Kruskal-Wallis test, nonparametric test)→

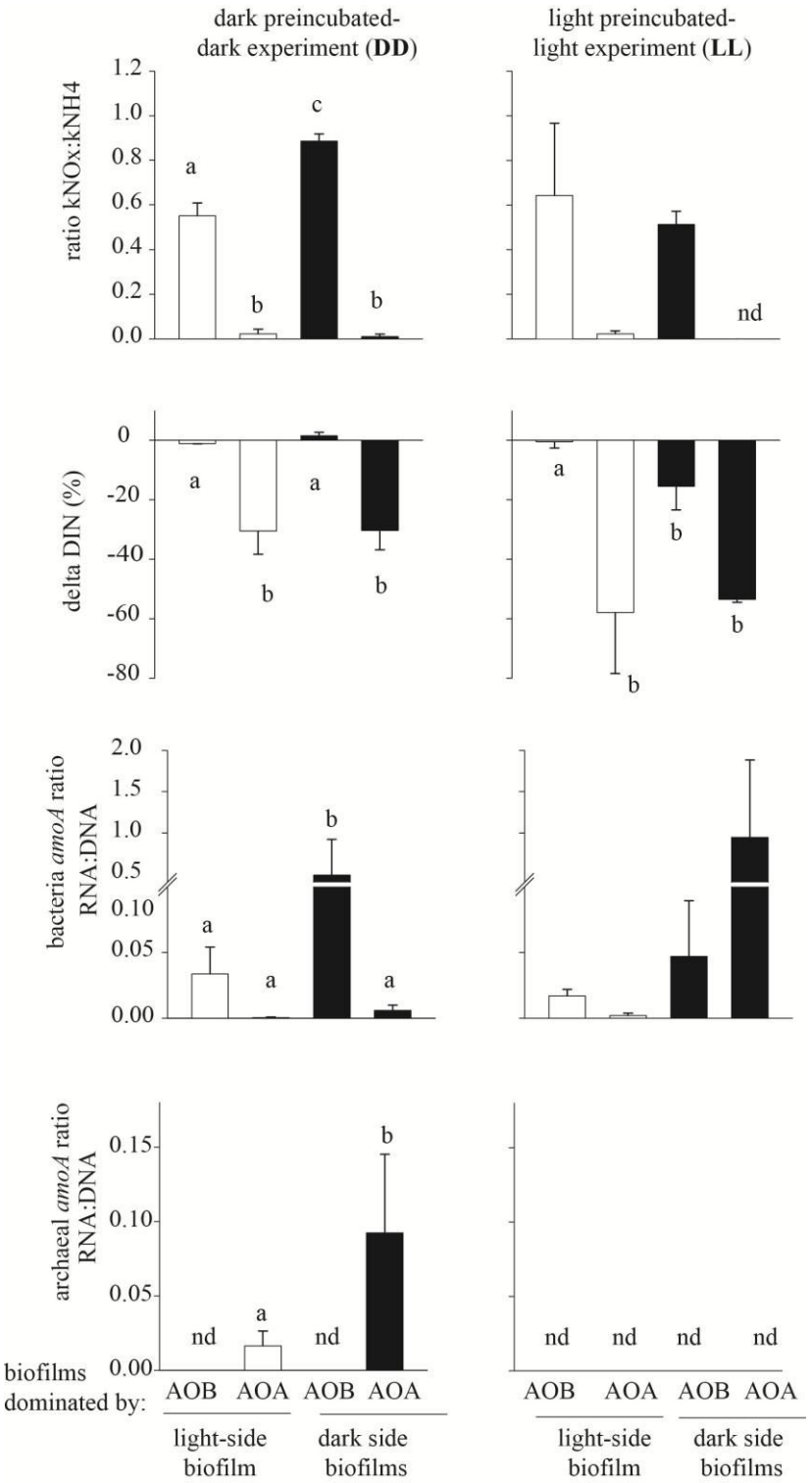
dark preincubated-
dark experiment (DD)
light preincubated-
light experiment (LL)
ratio kNOx:kNH4
1.2
1.0
0.8
0.6
0.4
0.2
0.0
a
b
c
b
nd
delta DIN (%)
0
-20
-40
-60
-80
a
b
a
b
a
b
b
b
bacteria amoA ratio
RNA:DNA
2.0
1.5
1.0
0.5
0.10
0.05
0.00
a
a
b
a
archaeal amoA ratio
RNA:DNA
0.15
0.10
0.05
0.00
nd
a
nd
b
nd
nd
nd
nd
biofilms
dominated by:
AOB
AOA
AOB
AOA
light-side
biofilm
dark side
biofilms
AOB
AOA
AOB
AOA
light-side
biofilm
dark side
biofilms

In AOB dominated biofilms, k_{NH4} and k_{NO3} were in the same range but k_{NO3} was significantly higher in dark-side than in light-side biofilms. Conversely in the AOA dominated biofilms k_{NH4} and k_{NO2} were similar in both, light-side and dark-side biofilms. However, k_{NO2} was 2-orders of magnitude lower than k_{NH4} in this AOA dominated biofilms (Table 6.4). Accordingly, the ratio k_{NO3}:k_{NH4} indicating the amount of $N\text{-}NH_4^+$ transformed to $N\text{-}NO_2^-$ and $N\text{-}NO_3^-$ respectively was highest in AOB dominated dark-side biofilms were it was close to one indicating high nitrifying activity (Figure 6.2 A). In addition, in AOB dominated the ratio was 38 % higher dark-side than light-side biofilms. In contrast in AOA dominated biofilms the ratio k_{NO2}:k_{NH4} was below 0.04 indicating that only up to 4 % of the inorganic $N\text{-}NH_4^+$ was oxidized to $N\text{-}NO_2^-$ (Figure 6.2 A). Therefore the DIN mass balance differed significantly between biofilm types. In AOB dominated biofilms DIN was close to zero. In contrast in both AOA dominated biofilm types 60 % of DIN was assimilated (Figure 6.2 B). The highest AOB activity was observed in AOB dominated dark-side biofilms with on average 0.5 *amoA* transcripts per *amoA* gene. All other biofilms did not differ in AOB activity (Figure 6.2C). The highest AOA activity was observed in AOA dominated dark-side biofilms with on average 0.1 *amoA* AOA transcripts per *amoA* gene. In AOA dominated light-side biofilm it was on averaged 5 times lower than in dark-side biofilms. In both AOB dominated biofilms however archael *amoA* transcripts were below detection limit (not detected, Figure 6.2 D).

Nitrification in biofilms under constant irradiance. To investigate the response to light of AOA and AOB within the biofilm matrix we exposed all biofilm types to constant irradiance (LL). Effects of illumination are summarized in Table 6.4 and Figure 6.2 E-H.

Table 6.4: Mean estimates and the standard error of k value [h^{-1}] of $N\text{-}NH_4^+$, $N\text{-}NO_2^-$ and $N\text{-}NO_3^-$ of triplicate microcosms containing light-side or dark-side biofilms of low NH4 and high NH4 reach. We applied unpaired Student T test and (*) Kruskal Wallis test respectively to analyze statistical differences between treatments from biofilms grown in low NH4 reach. For data from high NH4 site we used ANOVA to determine differences between all four treatments. Values in *bold* highlight significant and *ns* indicate no significant differences between treatments.

	k(c) [h^{-1}]	treatment	light-side	dark-side
AOA dominated biofilms from low NH4 reach	k_{NH4}	DD	-0.134 ±0.002	-0.132±0.012
		LL	-0.288±0.032	-0.116±0.024
			0.008	ns
	k_{NO2}	DD	0.003±0.001	0.004±0.004
		LL	0.003±0.002	0
		P	ns	ns*
AOB dominated biofilms from high NH4 reach	k_{NH4}	DD	-0.204±0.021	-0.34±0.04
		LL	-0.148±0.017	-0.324±0.024
		DL	-0.57±0.059	-0.507±0.039
		LD	-0.622±0.137	-0.47±0.054
		P	**0.003**	**0.009**
		F	17.52	10
	k_{NO3}	DD	0.11±0.002	0.302±0.038
		LL	0.084±0.042	0.164±0.011
		DL	0	0
		LD	0.198±0.021	0.442±0.091
		P	0.277	**0.003**
		F	1.641	15.96

Continuous illumination did significantly increase and decrease k_{NH4} of AOA and AOB dominated light-side biofilms, respectively. However k_{NH4} remained constant in dark-side biofilms (Table 6.4). k_{NO3} and the ratios k_{NO3}:k_{NH4} from AOB dominated as well k_{NO2} and the ratio k_{NO2}:k_{NH4} from AOA dominated biofilms were not affected by continuous illumination in light-side biofilms but decreased in by 100 % in AOA dominated and 55 % in AOB dominated dark-side biofilms respectively (Table 6.4, Figure 6.2 E). Moreover $N\text{-}NO_2^-$ production stopped in AOA dominated dark-side biofilms. However, due to

high variability, k_{NO3}:k_{NH4} and k_{NO2}:k_{NH4} respectively resulted were similar in all biofilms under constant illumination but tended to be highest in both AOB dominated biofilms (Figure 6.2E). Similarly to N dynamics AOB activity was not affected in light-side biofilms but decreased from 0.5 in darkness to 0.05 *amoA* AOB transcripts per *amoA* gene abundance in AOB dominated dark-side biofilms (Figure 6.2F, Student T test). In contrast, in AOA dominated dark-side biofilms bacterial *amoA* transcript was highly variable, yet the mean ratio RNA:DNA was one and hence tended to be the highest value compared to other biofilm types. Therefore, due to high variability we observed no significant differences among biofilm types in AOB activity (Figure 6.2F). In all biofilms under continuous illumination AOA transcripts were not detected (Figure 6.2 F and G).

Photoinhibition lag phase and nitrification activity recovery after photoinhibition. To investigate the lag-phase of the response to light we additionally carried out light switching experiments on AOB dominated biofilms consisting of a pre-incubation in darkness and experimental conditions under full light conditions (DL). $N\text{-}NH_4^+$ was constantly consumed in all chambers. $N\text{-}NO_3^-$ concentrations in contrast showed irregular dynamics and no consisted conclusion on the lag-phase of photoinhibition could be drawn. The dynamics in light-side biofilms consisted in decrease on $N\text{-}NO_3^-$ concentrations for 60 min and a subsequent but low increase the rest of the experimental period. In dark- side biofilms, $N\text{-}NO_3^-$ concentrations firstly increased during approx 60 min, subsequently declined and increased repeatedly after 120 min. Therefore in all the cases, $N\text{-}NO_3^-$ pool remained constant and hence k_{NO3} as well as the ratio k_{NO3}:k_{NH4} was equal to zero (Figure 6.3 A, Supplement Figure 6.1). In both, light-side and dark-side biofilms 20-40 % of DIN was assimilated. AOB activity was similar in both biofilm types and ranged from 1-5 *amoA* transcripts per *amoA* gene. AOA transcripts were not detected (Figure 6.3).

To investigate the recovery from light inhibition the biofilms were pre-incubated in the light and the experiment run in the dark (LD). In both, light-side and dark-side biofilms $N\text{-}NH_4^+$ and $N\text{-}NO_3^-$ were assimilated and produced similar to DD experiments (Supplement Figure 6.1). $N\text{-}NH_4^+$ was consistently consumed in both biofilm types. In light-side biofilms resulting k_{NH4} rates were highest in this LD compared to other treatments with 0.602 h^{-1}. $N\text{-}NO_3^-$ concentration increased immediately in both biofilm types. However, k_{NO3} was higher in dark-side than in light-side biofilms and 40 % higher in LD than in DD (Table 6.4). The ratio k_{NO3}:k_{NH4} was similar in both biofilm types and ranged from 0.5 – 1 indicating high nitrifying activity (Figure 6.3 D). AOB activity was highly variable and ranged from 0.3 - 12 *amoA* transcripts per *amoA* gene copy in both biofilm types.

6.5 Discussion

Nitrification is a crucial step in the N cycle because it links reduced and oxidized forms of N and enhances the water column NO_3 pool triggering denitrification. Therefore, understanding its environmental modulation *in situ* is of major interest. The fact, that ammonia oxidizers (AO) are significantly photoinhibited in laboratory cultures (French et al., 2012; Merbt et al., 2012) imprints on *in situ* activities, ruling their spatial distribution in lakes and the oceans (Lipschultz et al., 1985; Beman et al., 2012; Small et al., 2013). However, in streams AOA and AOB are embedded in the biofilm matrix and the consequences of their intrinsic susceptibility to light on N cycling within the biofilm matrix are not described.

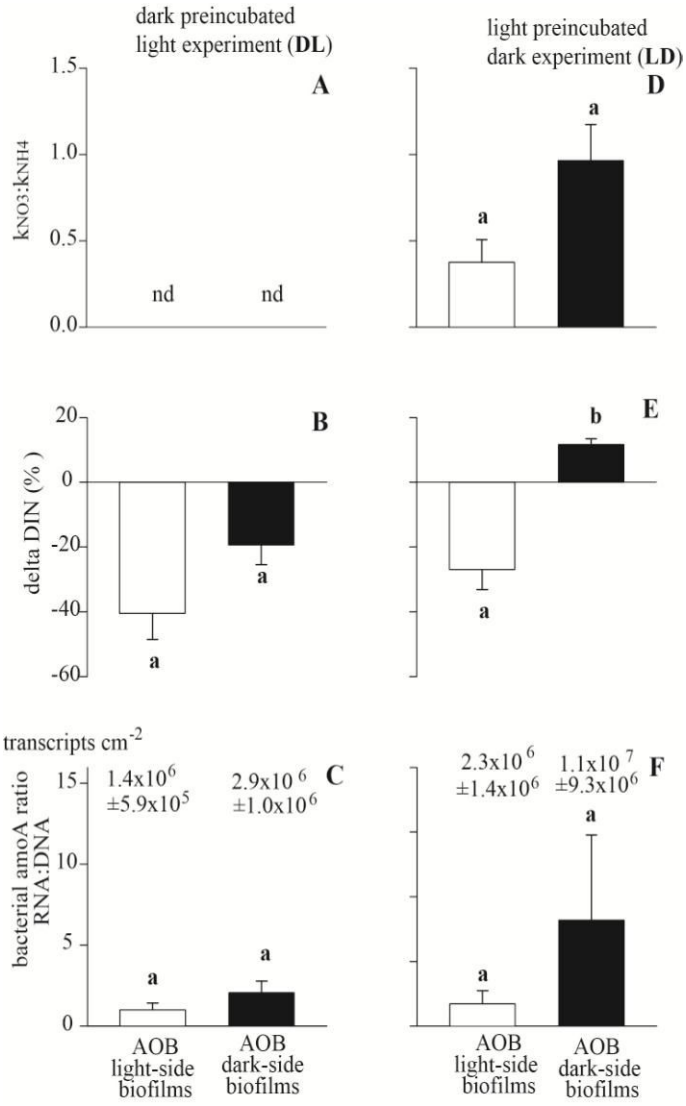

Figure 6.3. Data from biofilms grown on the light-side (white bars) and dark-side (black bars) of the cobbles differing in ammonia oxidizing community composition (AOA and AOB dominated) under varining light conditons. Panels A – C show data of biofilms pre-incubated in darkness and experimental conditions under illumination (DL). Panels D – F show data of biofilms pre-incubated under illumination and experimental conditions in darkness (LD). Represented are the ratio of k_{NO3}:k_{NH4} (panel A, D), mass balance of initial and final DIN concentration (panel B and E); ratio of bacterial *amoA* transcripts against gene copy abundance (panel C and F). Bars represent the mean of three independent biological replicates, line above the bars is the standard error of the mean. Letters indicate sig differences ($p<0.05$) between samples (Student T test, un-paired)

To fill this gap we used four biofilm types differing in structure and in ammonia oxidizing community composition. These differences were the result of the light and NH_4^+ availability under which the biofilms were grown *in situ*. Biofilms developed on the upper, sun light exposed side of the cobbles (light-side) were dominated by photoautotrophs. In contrast, the Chlorophyll *a* content was low in biofilms grown on the sediment facing side of the cobbles (dark-side) and thus, they were classified as heterotrophic biofilms. Moreover, both biofilm types contained ammonia oxidizers (AO) and their community composition depended on N-NH_4^+ availability, with AOB and AOA dominance in high and low NH_4^+ concentrations respectively (Merbt et al 2011, 2014). Figure 6.4 shows a simplified illustration of the structure of both biofilm types used in this study.

All three major components of the biofilm assemblages, heterotrophs, chemotrophs and phototrophs assimilate N-NH_4^+ though their particular contribution to N-NH_4^+ assimilation is ruled by light availability. For instance, irradiance stimulates photoautotrophic N uptake (Reuter et al., 1986) but inhibits the activity of AOA and AOB in laboratory cultures (Merbt et al., 2012). Therefore we hypothesized that in stream biofilms both, AOA and AOB would be more abundant and active in light-protected environments, i.e. dark-side biofilms.

In concordance, despite the fact that AO were predominately more abundant in light-side than in dark-side biofilms, under optimum conditions (in darkness) potential nitrification rates were higher in AOB dominated dark-side than in light-side biofilms. This finding suggests that dark-side biofilms were the most relevant habitat for nitrifiers. Conversely, this segregation of ammonia oxidizing activity was not observed in AOA dominated bioflms. However, the overall ammonia oxidizing efficiency was much lower in AOA than in AOB dominated biofilms. This is probably due to the metabolic nature of AOA, which despite its

high NH_4^+ affinity show lower rates than AOB (Martens-Habbena et al., 2009, French et al., 2012).

Nonetheless, photoinhibition was similar on both, AOA and AOB and appeared to operate only in dark-side biofilms, while in light-side biofilms ammonia oxidation and *amoA* transcript abundances were not affected by light exposition. This fact confirmed the intrinsic negative effect of light on natural AO assemblages and suggested a shadow effect with putative light protective role by the photosynthetic biofilm matrix itself.

In particular, previous structural investigations from nitrifying model biofilms grown in the dark showed that AOB were restricted to the upper 50 µm, oxic narrow zone (Schramm et al., 1996; Gieseke et al., 2005). Consequently, at least the first layer of ammonia oxidizing community growing in dark-side biofilm was probably fully exposed to light during our experiments, explaining the significant and immediate decrease of ammonia oxidizing activity under illumination.

In contrast, in light-side biofilms, the structural organization may be different enabling the growth and active ammonia oxidation under illumination. Here photoautotrophs are possibly located in the first layer of the biofilms converting irradiance into phototrophic energy and concomitantly providing shade for underlying AOA and AOB (*umbrella effect*). This light protective feature has been described previously for algae to maintain photoautotrophic activity under high irradiances (Boston and Hill, 1991; Guasch and Subater, 1995) and thus may also be applicable for ammonia oxidizers. Alternatively, light-adapted AO ecotypes may have naturally colonized the light-side biofilms. In fact, recent investigations have potentially shown light-adapted phylotypes present within AOA (Merbt et al., 2014; Pedneault et al., 2014; Restrepo-Ortiz et al., 2014).

The response to light was investigated with light switching experiments (DL - dark pre-incubation, experiment in light). Interestingly, $N\text{-}NO_3^-$ production was not recorded in any biofilm avoiding further conclusions. Nonetheless, albeit the lack of $N\text{-}NO_3^-$ accumulation in the water column, ammonia oxidation was active under DL conditions, as shown by high abundance of bacterial *amoA* transcripts in both, light-side and dark-side biofilms. Moreover, the transcript abundance was higher than in LL. Similar patterns were observed in culture studies. Here bacterial ammonia oxidation was not photoinhibted in a 16-8h dark/light cycle indicating either a good recovery from photoinhibition or the photoinhibition takes longer than the experimental time. Therefore, taking into account that ammonia oxidation takes place under DL conditions, the reason for the lack of NO_3^- accumulation could be explained by a higher assimilation of N species by photoautotrophs and heterotrophs.

Especially in light-side biofilms photoautotrophs are starved after a dark phase and light enhances N assimilation (Reuter et al., 1986). This idea is supported by the observed higher DIN uptake in DL compared to LL. Together the sustained nitrification activity during light exposition in light-side biofilms suggests that AOA and AOB are active and successfully co-exist in presence of photoautotrophs. This result contrasts previous findings from algal overgrown Fjord sediments and marine sediments in low N conditions showing that slow growing ammonia oxidizers are outcompeted by algae (Henriksen and Kemp, 1988; Risgaard-Petersen et al., 2004) and confirms the finding from biofilms of higher river order (Teissier et al., 2007).

However, in dark-side biofilms light cycles (DL and LD) changed N dynamics significantly being either a N sink under light exposition or a N source in darkness. This reinforces the idea that ammonia oxidizers are highly active and co-exist with heterotrophs in darkness, while under light conditions, ammonia oxidizers are limited and heterotrophic NH_4^+ uptake possibly increases (Figure 6.4). Interactions between heterotrophs and ammonia oxidizers have been

investigated intensively showing that under low C:N ratio (< 9.6) both groups co-exist in culture, sediments and biofilms despite the fact that heterotrophs grow faster and are more abundant than ammonia oxidizers (Prosser, 1989; Verhagen and Laanbroek, 1991; Okabe et al., 2005). Moreover cross-feeding has been demonstrated where heterotrophs efficiently degraded dead biomass and metabolites deriving from AOB (Okabe et al., 2005) leading to increased heterotrophic activity under active nitrification (Gieseke et al., 2005).

The recovery from photoinhibition can only be described using data from dark-side biofilms, because in light-side biofilms no photoinhibition was detected. Our results indicated that similar to laboratory cultures biofilms dominated by AOB recovered immediately and high amounts of bacterial *amoA* transcripts were detected.

Figure 6.4 summarizes schematically the N dynamics in dark-side and light-side biofilms governed by irradiance. In light-side biofilms ammonia oxidation is independent form irradiance due to the *umbrella effect* carried out by the biofilm structure itself. Irradiance activates photoautotrophs and the assimilation of inorganic N-NH_4^+, mineralized N-NH_4^+ provided by heterotrophs and produced N-NO_3 by nitrifyers enhances (Figure 6.4A). In darkness, photoautotrophic N assimilation is lower and only NH_4^+ can be assimilated because for NO_3 uptake additional energy is needed (Reuter et al., 1986; Dortch, 1990). Hence, the NO_3 originally produced by nitrifiers is released to the stream water column (Figure 6.4a). In dark-side biofilms ammonia oxidation is inhibited by irradiance and NO_3 is predominately produced in darkness (N source). However, when dark-side biofilms were exposed to light biofilms behave as N sink (Figure 6.4b).

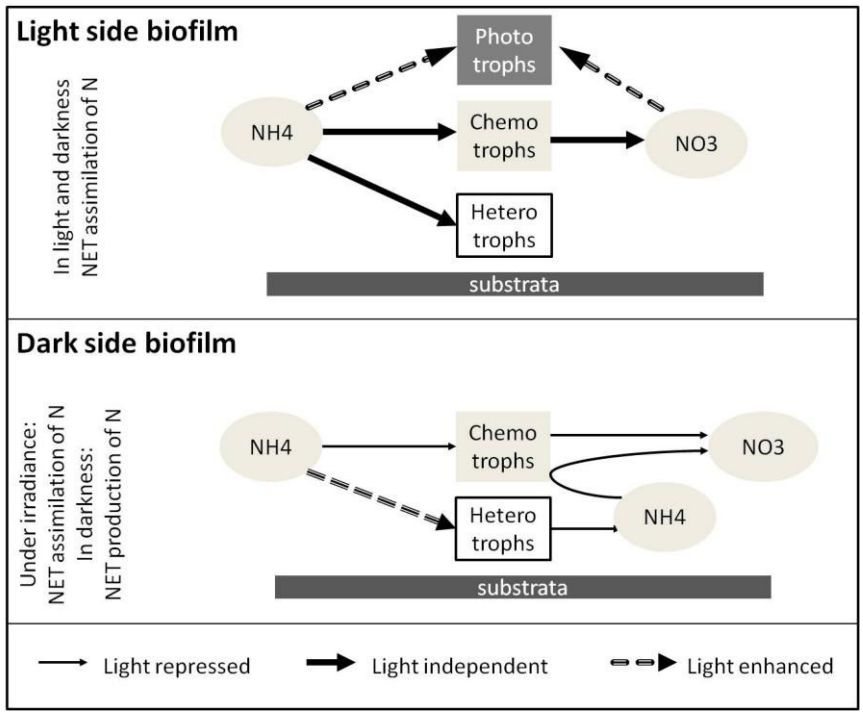

Figure 6.4. Schematic illustration of light driven N processes in light-side and dark-side biofilm respectively. Fine lines show processes repressed by light, dashed lines processes enhanced by light and bold lines processes, which are not affected by irradiance.

In conclusion, as previously observed in laboratory cultures, matrix bound AOA and AOB are significantly inhibited by irradiance. To overcome this intrinsic photoinhibition AO follow a light avoiding strategy preferentially accumulating in light protected sites. Therefore results from this study support experimentally that light is a driving factor for the distribution of AOA and AOB *in situ* and highlight that ammonia oxidizers co-exists with heterotrophs and photoautotrophs under high nutrient conditions.

Acknowledgments: We thank Roser Ventosa for excellent technical assistence. S.N.M. was supported by a JAE predoctoral fellowship from the Spanish National Research Council (CSIC) and S.B. by a Juan de la Cierva fellowship from the Spanish Office for Research (MINECO). This research was granted by DARKNESS CGL2012-32747 to EOC and MED_FORESTREAM CGL2011-30590-CO2-02 (MINECO) and REFRESH-244121 (7th Framework Programme EU Comission) to EM.

.

6.5 References

APHA (1995) Standard methods for the examination of water and wastewater. *American Public Health Association, Washington, USA*.

Battin, T.J., Kaplan, L.A., Denis Newbold, J., and Hansen, C.M.E. (2003) Contributions of microbial biofilms to ecosystem processes in stream mesocosms. *Nature* **426**: 439-442.

Battin, T.J., Sloan, W.T., Kjelleberg, S., Daims, H., Head, I.M., Curtis, T.P., and Eberl, L. (2007) Microbial landscapes: new paths to biofilm research. *Nat Rev Micro* **5**: 76-81.

Beman, J.M., Rohan, S., and Jed, A.F. (2006) Population ecology of nitrifying *Archaea* and *Bacteria* in the Southern California Bight. *Environmental Microbiology,* **12,** 1282-1292.

Beman, J.M., Popp, B.N., and Alford, S.E. (2012) Quantification of ammonia oxidation rates and ammonia-oxidizing archaea and bacteria at high resolution in the Gulf of California and eastern tropical North Pacific Ocean. *Limnol Oceanogr* **57**: 711-726.

Bernhardt, E.S., Hall Jr, R.O., and Likens, G.E. (2002) Whole-system estimates of nitrification and nitrate uptake in streams of the Hubbard Brook Experimental Forest. *Ecosystems* **5**: 419-430.

Boston, H., and Hill, W. (1991) Photosynthesis-light relations of stream periphyton communities. *Limnology and Oceanography* **36**: 644-656.

Dortch, Q. (1990) The interaction between ammonium and nitrate uptake in phytoplankton. *Marine ecology progress series Oldendorf* **61**: 183-201.

Ensign, S.H., and Doyle, M.W. (2006) Nutrient spiraling in streams and river networks. *Journal of Geophysical Research: Biogeosciences* **111**: G04009.

French, E., Kozlowski, J.A., Mukherjee, M., Bullerjahn, G., and Bollmann, A. (2012) Ecophysiological Characterization of Ammonia-Oxidizing Archaea and Bacteria from Freshwater. *Applied and Environmental Microbiology* **78**: 5773-5780.

Gieseke, A., Nielsen, J.L., Amann, R., Nielsen, P.H., and De Beer, D. (2005) In situ substrate conversion and assimilation by nitrifying bacteria in a model biofilm. *Environmental Microbiology* **7**: 1392-1404.

Guasch, H., and Subater, S. (1995) Seasonal varioation isn photosynthesis-irradiance response by biofilms in mediterranean streams. *Journal of Phycology* **31**: 727-735.

Hauer, F.R., and Lamberti, G.A. (2011) *Methods in stream ecology*: Academic Press.

Henriksen, K., and Kemp, W.M. (1988) Nitrification in estuarine and coastal marine sediments. In *Nitrogen cycling in coastal marine environments*. Blackburn, H., and Sorensen, J. (eds). Wiley, Indianapolis, Indiana., pp. 201–249.

Hooper, A.B., and Terry, K.R. (1973) Specific Inhibitors of Ammonia Oxidation in Nitrosomonas. *Journal of Bacteriology* **115**: 480-485.

Hyman, M.R., and Arp, D.J. (1992) 14C2H2- and 14CO2-labeling studies of the de novo synthesis of polypeptides by Nitrosomonas europaea during recovery from acetylene and light inactivation of ammonia monooxygenase. *Journal of Biological Chemistry* **267**: 1534-1545.

Lipschultz, F., Wofsy, S.C., and Fox, L.E. (1985) The effects of light and nutrients on rates of ammonium transformation in a eutrophic river. *Marine Chemistry* **16**: 329-341.

Lock, M., Wallace, R., Costerton, J., Ventullo, R., and Charlton, S. (1984) River epilithon: toward a structural-functional model. *Oikos*: 10-22.

Lomas, M.W., and Lipschultz, F. (2006) Forming the primaryn itrite maximum: Nitrifiers or phytoplankton? *Limnology and Oceanography* **51**: 2453-2467.

Martens-Habbena, W., Berube, P.M., Urakawa, H., de la Torre, J.R., and Stahl, D.A. (2009) Ammonia oxidation kinetics determine niche separation of nitrifying Archaea and Bacteria. *Nature* **461**: 976-979.

Merbt, S.N., Jean-Christophe Auguet, Emilio O. Casamayor, and Martı, E. (2011) Biofilm recovery in a wastewater treatment plant-influenced stream and spatial segregation of ammonia-oxidizing microbial populations. *Limnology and Oceanography* **56**: 1054–1064

Merbt, S.N., Auguet, J.-C., Blesa, A., Martí, E., and Casamayor, E. (2014) Wastewater Treatment Plant Effluents Change Abundance and Composition of Ammonia-Oxidizing Microorganisms in Mediterranean Urban Stream Biofilms. *Microbial Ecology*: 1-9.doi: 10.1007/s00248-014-0464-8

Merbt, S.N., Stahl, D.A., Casamayor, E.O., Martí, E., Nicol, G.W., and Prosser, J.I. (2012) Differential photoinhibition of bacterial and archaeal ammonia oxidation. *FEMS Microbiology Letters* **327**: 41-46.

Merseburger, G., Martí, E., and Sabater, F. (2005) Net changes in nutrient concentrations below a point source input in two streams draining catchments with contrasting land uses. *Science of the total environment* **347**: 217-229.

Nicol, G.W., Sven, L., Christa, S., and James, I.P. (2008) The influence of soil pH on the diversity, abundance and transcriptional activity of ammonia oxidizing archaea and bacteria. *Environmental Microbiology* **10**: 2966-2978.

O´Brion, J.M., and Dodds, W.K. (2008) Ammonium uptake and mineralization in prairie streams: chamber incubation and short-term nutrient addition experiments. *Freshwater Biology* **53**: 102-112

Okabe, S., Kindaichi, T., and Ito, T. (2005) Fate of 14C-labeled microbial products derived from nitrifying bacteria in autotrophic nitrifying biofilms. *Applied and Environmental Microbiology* **71**: 3987-3994.

Pedneault, E., Galand, P.E., Potvin, M., Tremblay, J.-É., and Lovejoy, C. (2014) Archaeal amoA and ureC genes and their transcriptional activity in the Arctic Ocean. *Scientific reports* **4**.

Peterson, B.J., Wollheim, W.M., Mulholland, P.J., Webster, J.R., Meyer, J.L., Tank, J.L. et al. (2001) Control of Nitrogen Export from Watersheds by Headwater Streams. *Science of The Total Environment* **292** 86-91.

Prosser, J.I. (1989) Autotrophic Nitrification in Bacteria. In *Advances in Microbial Physiology*. Rose, A.H.T., D. W. (ed): Academic Press, pp. 125–181.

Restrepo-Ortiz, C.X., Auguet, J.-C., and Casamayor, E.O. (2014) Targeting spatiotemporal dynamics of planktonic SAGMGC-1 and segregation of ammonia-oxidizing thaumarchaeota ecotypes by newly designed primers and quantitative polymerase chain reaction. *Environmental Microbiology* **16**: 689-700.

Reuter, J.E., Loeb, S.L., and Goldman, C.R. (1986) Inorganic nitrogen uptake by epilithic periphyton in a N-deficient lake. *Limnolology and Oceanography* **31**: 149-160.

Risgaard-Petersen, N., Nicolaisen, M.H., Revsbech, N.P., and Lomstein, B.A. (2004) Competition between Ammonia-Oxidizing Bacteria and Benthic Microalgae. . *Applied and Environmental Microbiology* **70**: 5528-5537.

Rotthauwe, J.-H., Witzel, K.-P., and Liesack, W. (1997) The ammonia Monooxygenase Structural Gene amoA as a Functional Marker: Molecular Fine-Scale Analysis of Natural Ammonia Oxidizing Populations. *Applied and Environmental Microbiologie* **63**: 4704-4712.

Santoro, A.E., Casciotti, K.L., and Francis, C.A. (2010) Activity, abundance and diversity of nitrifying archaea and bacteria in the central California Current. *Environmental Microbiology* **12**: 1989-2006.

Schiller, D.v., Martí, E., Riera, J.L., and Sabater, F. (2007) Effects of nutrients and light on periphyton biomass and nitrogen uptake in Mediterranean streams with contrasting land uses. *Freshwater Biology* **52**: 891-906.

Schramm, A., De Beer, D., Gieseke, A., and Amann, R. (2000) Microenvironments and distribution of nitrifying bacteria in a membrane-bound biofilm. *Environmental Microbiology* **2**: 680-686.

Schramm, A., Larsen, L.H., Revsbech, N.P., Ramsing, N.B., Amann, R., and Schleifer, K.H. (1996) Structure and function of a nitrifying biofilm as determined by in situ hybridization and the use of microelectrodes. *Applied and Environmental Microbiology* **62**: 4641-4647.

Small, G.E., Bullerjahn, G.S., Sterner, R.W., Beall, B.F., Brovold, S., Finlay, J.C. et al. (2013) Rates and controls of nitrification in a large oligotrophic lake. *Limnology and Oceanography* **58**: 276-286.

Steinman, A.D., and Lamberti, G.A. (1996) Biomass and pigments of benthic algae. In *Methods in stream ecology*. Lamberti, F.R.H.a.G.A. (ed). California: academic Press.

Teissier, S., Torre, M., Delmas, F., and Garabétian, F. (2007) Detailing biogeochemical N budgets in riverine epilithic biofilms. *Journal of the North American Benthological Society* **26**: 178-190.

Tourna, M., Freitag, T.E., Nicol, G.W., and Prosser, J.I. (2008) Growth, activity and temperature responses of ammonia-oxidizing archaea and bacteria in soil microcosms. *Environmental Microbiology* **10**: 1357-1364.

Verhagen, F.J.M., and Laanbroek, H.J. (1991) Competition for Ammonium between Nitrifying and Heterotrophic Bacteria in Dual Energy-Limited Chemostats. *Applied and Environmental Microbiology* **57**: 3255-3263.

Walker, C., De La Torre, J., Klotz, M., Urakawa, H., Pinel, N., Arp, D. et al. (2010) Nitrosopumilus maritimus genome reveals unique mechanisms for nitrification and autotrophy in globally distributed marine crenarchaea. *Proceedings of the National Academy of Sciences* **107**: 8818-8823.

6.7 Supplemental material

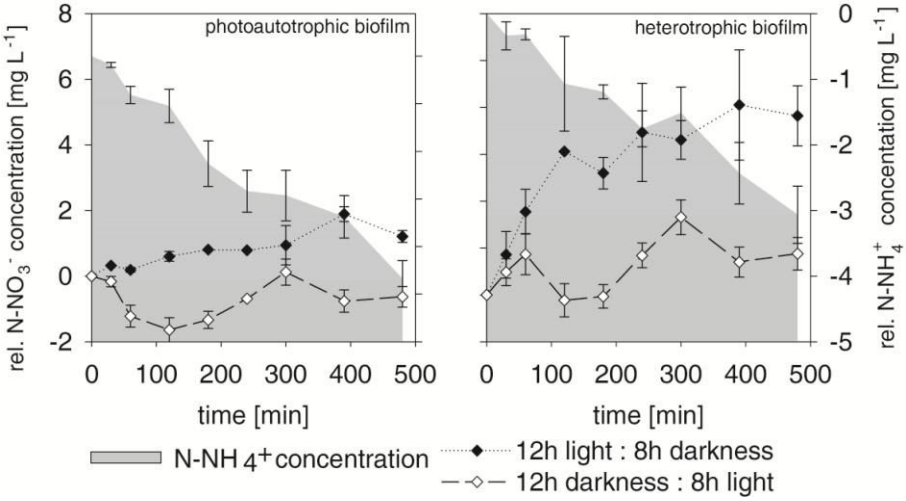

Supplements Figure6.1: nitrification kinetics (relative $N\text{-}NO_3^-$ producction [mg L-1]) in biofilms acclimatized during 12 h in darkness and measured under light exposition (open diamonds) versus nitrification kinetecs measured in biofilms acclimatized during 12 h under light exposition and measured in drakness (closed circles) in circulation chambers containing exlusively green (left) and black (right) biofilms, respectively. Lines above the dotes indicates the stadard error of the mean out of 3 independent biological replicates.

Supplement table 6.1: electrical conductivity, temperature, oxygen and pH before and after each experiment with light-side and dark-side biofilms respectively. Biofilms were either collected from high, or low NH4 reach. Experiments differed in light conditions. LL- preincubation in light, experimental conditions in light; DD- preincubation in dark, experimental conditions in dark, DL- preincubation in dark, experimental conditions in light, LD- preincubation in light, experimental conditions in dark. Data represent the mean of three independent biological replicates and standard error (SE) of physical paramenters in chamber experiments (Exp) A-F in green and black biofilms. Measurements were done before and after the addition experiment (8h).

				Cond [µS cm-2]		T [°C]		O2 [mg L-1]		ph	
				avg	SE	avg	SE	avg	SE	avg	SE
from low NH4 reach	LL	light side	before	217	1.2	22.5	0.3	8.6	0.1	8.1	0
			after	219	1.2	20.8	0.6	8.7	0.4	8	0.1
		dark side	before	225	2.5	23.6	0.6	8.3	0.1	8	0
			after	221	1.2	20.9	0.9	6.9	0.4	7.6	0.1
	DD	light side	before	218	1.2	20.1	0.7	8	0.4	8	0.1
			after	217	1.5	21.7	0.7	7.5	0.3	8	0.1
		dark side	before	221	1	21.8	1	34.9	26.7	8	0.1
			after	221	0.9	19.7	0.8	8.5	0.2	8	0

Supplement Table 6.1 continued

				Cond [µS cm-2]		T [°C]		O2 [mg L-1]		ph	
				avg	SE	avg	SE	avg	SE	avg	SE
from high NH4 reach	LL	light side	before	457	0.9	24.9	0.9	NA	NA	8.1	0.3
			after	455	2.1	24.1	0.2	NA	NA	8.1	0.1
		dark side	before	508	0.6	24.7	0	NA	NA	6.2	2
			after	504	2.2	24.8	0.1	NA	NA	8	0.1
	DD	light side	before	415	4.6	21.8	0.3	8.5	0.3	7.8	0
			after	424	0.7	22.1	0.7	8.9	0.1	8.1	0
		dark side	before	475	1.2	22.4	0.7	8.8	0.1	8	0
			after	460	6.4	22.3	0.4	8.6	0.2	7.7	0
	LD	light side	before	525	1.5	24.4	1.2	8.3	0.1	7.8	0.1
			after	523	4.4	21.8	0.6	6.9	0.6	7.5	0.1
		dark side	before	518	2.3	22.8	0.4	8	0.3	7.8	0.1
			after	518	2.3	22.8	0.4	8	0.3	7.8	0.1
	DL	light side	before	500	1.9	22.4	0.6	8	0.5	7.9	0.1
			after	510	9.6	20	0.6	6.4	0.4	7.6	0.2
		dark side	before	481	5.7	24.5	0.5	8.1	0.1	7.9	0.1
			after	491	##	22	0.4	5.6	1.5	7.5	0.1

Light avoidance of ammonia oxidizers contributes to sustain nitrification in an urban stream.

7

With permissions from Miquel Ribot, Emilio O. Casamayor, Eugènia Martí, and Susana Bernal, who are co-authors of this study.

Cover: La Tordera river at Santa Maria de Palautordera downstream of the input of the wastewater treatment plant effluent in summer (upper picture) and winter (lower picture). Photographs by SN Merbt.

7.1 Abstract

We examined the effects of light availability and its diurnal regime on nitrification rates at whole-reach scale and on the in-stream distribution and abundance of archaeal (AOA) and bacterial (AOB) ammonia oxidizers. Because of the intrinsic photoinhibition of both, AOA and AOB we hypothesized that either nitrification would be higher under low light intensity and during nighttime than under high light intensities during daytime. Alternatively, nitrification rates could be independent from light regime if ammonia oxidizers accumulate in light protected habitats, such as the sediment facing side of the cobbles (dark-side biofilms) and the sediments. To test this hypothesis, we measured uptake rates of ammonium (NH_4) and nitrification rates (based on NO_2) (U_{NH4}, and U_{NIT}; mg N m^{-2} h^{-1}) at whole-reach scale using short term NH_4 and chloride injections in two stream reaches contiguously located, but differing in canopy cover (shaded versus open). Furthermore, we estimated the abundance of AOA and AOB in the episamic and epilithic biofilms using quantitative PCR. We analyzed epilithic biofilms developed on the dark-side and the light-exposed side of the cobbles (light-side) separately. The metabolism of the two studied reaches was dominated by heterotrophic activity and N dynamics were similar in the two reaches. U_{NH4} tended to be higher during the day than during the night. U_{NIT} did not show diurnal variations. The ratio of U_{NO2}:U_{NH4} tended to be higher during the night. Against expectations, AOA and AOB were highly abundant in all three habitats with a significant dominance in dark-side biofilms. This assigns a light protective feature to the light-side biofilms, which is more pronounced when biofilm biomass exceeded the threshold of 0.166 g cm^{-2}. Altogether, results indicate that at reach scale, spatial distribution of AOA and AOB rather than differences in irradiance between reaches is a critical factor determining whole-reach nitrification in high N loaded streams.

7.2. Introduction

Sunlight is a major energy source for photoautotrophic primary production in aquatic ecosystems, which can drive the metabolic balance between production and respiration in these ecosystems (Nelson and Conway, 1979; Reuter et al., 1986). Conversely, the activity of chemoautotrophic primary producers, such as ammonia oxidizing bacteria (AOB) and archaea (AOA), is strongly inhibited by light availability (French et al., 2012; Merbt et al., 2012). AOB and AOA rely on ammonia (NH_4^+) as a chemical energy source, which is transformed into nitrite (NO_2^-) using the enzyme ammonia monooxygenase (*amoA*; Prosser, 1989; Spang et al., 2010). The susceptibility of ammonia oxidizers (AO) to light is considered to be the mechanism responsible for the vertical zonation of ammonia oxidizing activity in lakes and oceans, where it mainly occurs in the bottom of the euphotic zones (Lomas and Lipschultz, 2006; Beman et al., 2012; Small et al., 2013). While in AOA the biochemical mechanism of photoinhibition is not fully understood, in AOB light denaturalizes the ammonia monooxigenase (Hyman and Arp, 1992) leading to a full inactivation of ammonia oxidation in culture (French et al., 2012, Merbt et al., 2012). In stream ecosystems, however, the potential influence of light on regulating the activity and spatial distribution of AO has been barely explored (but see, Merbt et al., 2014).

The oxidization of NH_4^+ to NO_2^- is the first and rate-limiting step of nitrification, which represents the only oxidative step in the N cycle and plays a pivotal role in aquatic ecosystems by linking N inputs (N fixation and mineralization) and outputs (denitrification, anamox) to and from the water column. In streams, nitrification can significantly increase stream water nitrate (NO_3^-) concentrations (Bernhardt et al., 2002), especially in high N loaded streams such as those receiving effluents from wastewater treatment plant (WWTP) effluents (Merseburger et al., 2005; Ribot et al., 2012). In these

streams, AOA and AOB develop within benthic microbial assemblages (i.e. biofilms) coating streambed substrata (i.e., cobbles, pebbles and sediment) (Merbt et al., 2011; Sonthiphand et al., 2013). In these relatively small-size streams, water depth is not deep; and thus, light can directly penetrate into the streambed. Therefore under these conditions, AO located in light exposed epilithic biofilms may be especially vulnerable to irradiance. Yet, light intensity is strongly regulated by riparian vegetation coverage, which can reduce irradiance up to 95 % during full canopy cover (Hill et al., 1995). Thus, riparian canopy could provide shaded conditions to stream AO, which could contribute to sustain in-stream nitrification at least during the vegetative period. Despite nitrification is a crucial step of the stream N cycle, to the best of our knowledge there are no studies examining the influence of light on nitrification at whole-reach scale.

This study aimed to fill this gap of knowledge by testing if light influences in-stream nitrification at whole-reach scale. Based on the severe photoinhibition experienced by AO under laboratory experiments (French et al., 2012; Merbt et al., 2012), we hypothesized that in-stream nitrification will be higher under low than under high irradiances. Thus, we expected nitrification rates to be higher (i) in shaded than in open stream reaches, and (ii) at night than at daytime within a reach. Alternatively, we expected in-stream nitrification rates to be independent of light irradiance if AO mainly grow in habitats where light availability is low (e.g., in biofilms colonizing surface of cobbles facing the sediments and in stream sediments). To test these hypotheses, we measured whole-reach nitrification rates using short-term constant rate additions of NH_4^+, which were conducted during day and night time in two contiguous reaches differing in the degree of riparian canopy cover; and thus, in light availability. Further, we investigated the abundance of AOA and AOB in stream episamic and epilithic biofilms both light-exposed and non-exposed, by using the gene encoding for

the subunit A of the ammonia monooxygenase gene (*amoA*) as a molecular tracer of AOA and AOB (Rotthauwe et al., 1997; Francis et al., 2005).

7.3 Material and Methods

Study site

The study was carried out in the Tordera river (NE of Barcelona, Spain). The study site corresponds to a third order stream located below the input of the WWTP facility of the Santa Maria de Palautordera village (41°41´3.47´´N, 2°27´33.19´´W). The WWTP does not have a tertiary treatment; and thus, its partial nitrification capacity results in an effluent with high NO_3^- and NH_4^+ concentrations. Previous studies at this stream site have shown that the receiving stream has a high nitrification capacity, which is evidenced by consistent decreases in NH_4^+ concentration and increases in NO_3^- concentration along the receiving stream (Merseburger et al., 2005; Ribot et al., 2012). In addition, we have also found that biofilms developed on cobbles in this stream have a high abundance of AOA and AOB (Merbt et al. 2011).

At the study site, we selected two 100 m long reaches, which were contiguously located at 600 and 900 m downstream of the WWTP effluent input. The location of these reaches was selected to ensure similar NH_4^+ concentration in both two reaches and to avoid the strong gradients in NH_4^+ concentration, which were observed closer to the WWTP effluent (Ribot et al., 2012). The two reaches had similar channel morphology and streambed substrata composition. During the study, the up-stream reach was 3.9 ± 0.7 m [average ± standard deviation] wide, and the streambed substrata were composed of 55±10 % of cobbles, 16±14 % of gravel and 19±21 % of fine sediment. The down-stream reach was 4.5 ± 0.6 m wide and the streambed substrata were composed of 3±3% rocks, 72±5 % of cobbles, 9±2 % of gravel, and 17±9 % of fine sediment.

However, the two reaches significantly differed in the density of riparian canopy cover. The up-stream reach was covered by a dense riparian canopy (hereafter referred as to the shaded reach), while riparian canopy was very sparse at the down-stream reach (hereafter referred as the open reach).

Field measurements

The study was conducted in September 2013, before riparian tree leaf fall. At each reach, discharge (Q, in L s^{-1}) was measured by a mass balance approach based on slug additions of a conservative tracer (NaCl; Gordon et al., 1992). Stream channel width (w, in m) was calculated as the average from measurements done at 7 sampling sites along each reach. Irradiance at each reach was measured at 20 min intervals over the study period using five data loggers (HOBO UA-002-64) evenly distributed along the reaches. Daily photosynthetic active radiation (PAR, in mol m^{-2} d^{-1}) was computed by integrating averaged instantaneous irradiance data from the five data loggers over the daytime hours.

We measured whole-reach metabolism in each reach to characterize the two reaches in terms of their metabolic balance (i.e., photoautotrophic and heterotrophic activity). The light influence on metabolism between the two reaches was then compared with that on whole-reach nitrification rates. To measure daily rates of in-stream metabolism, at each reach we recorded dissolved oxygen (DO) concentration, water temperature, and atmospheric pressure at 5 min intervals at the top and at the bottom of the reach with oxygen meter probes (Hach HQ 30d). These data were used to estimate daily rates of ecosystem respiration (ER) and gross primary production (GPP) (see description below). Probes were left in the stream during the 4 consecutive days when measurements of whole-reach NH_4^+ uptake and nitrification rates were conducted.

Whole-reach NH_4^+ uptake and nitrification rates were measured by conducting short-term constant rate additions of ammonium (as NH_4Cl) together with a conservative tracer (i.e., NaCl) following the method by Webster and Valett (2006). At each reach, we conducted 4 additions, 2 during daytime (starting at 1 pm) and 2 during nighttime (starting at 1 am) on 2 consecutive days. Each addition consisted on adding a solution of NH_4Cl and NaCl at constant rate using a peristaltic pump (200 ml min^{-1}), which elevated the ambient concentration of NH_4^+ to approximately 1.5 mg L^{-1}. Despite this concentration were two orders of magnitude higher than ambient NH_4^+ concentration at the study reaches, it is a very common concentration in this stream during all seasons due to the inputs of NH_4^+ from the WWTP effluent (Merseburger et al., 2005; Merbt et al., 2011; Ribot et al., 2012). In addition, this plateau concentration was targeted to be able to track nitrification along the study reaches by analyzing the longitudinal increase in both NO_2^- and NO_3^- concentrations during plateau in the NH_4^+ addition experiments. Along each reach, we identified 7 evenly distributed sampling stations along. Before each addition, we collected water samples at each sampling station and at an upstream of the addition point to measure ambient concentrations of NH_4^+, NO_2^- and NO_3^-, and we recorded water temperature and conductivity. Once the conductivity at the last station of the reach achieved plateau conditions (approximately after 1.5 h), we collected water samples and recorded conductivity and temperature at each sampling station. All water samples were immediately filtered on a 0.7 µm pore size FVF glass fiber filters (Albet) and stored on ice for further chemical analysis.

We characterized epilithic biofilms by measuring biomass, Chlorophyll *a* content (Chl a), and *amoA* gene abundance. At each reach, we collected a composite sample of three cobbles from 3 different sampling stations (1, 5, and 7). Epilithic biofilms were scratched with a sterile metallic brush and washed into a sterile 250 ml plastic beaker using stream water. We scratched the light-

exposed (i.e., light-side) and no light-exposed (i.e., dark-side) sides of each cobble separately. Additionally, we collected samples of light-side biofilms from 10 cobbles at each reach to examine in more detail the relationship between *amoA* gene abundance and biofilm biomass. For these samples we followed the same sampling protocol as described above. The biofilm sludge of each sample was filtered onto ignited, pre-weighted glass fiber filters (FVF). The total surface scraped was estimated by covering cobbles with aluminum foil and applying a weight-to-area relationship. At each reach, we also collected samples from sediments to characterize them in terms of biomass and *amoA* gene abundance. A composite sample (3 locations within each sampling station) of approximately 100 g of sediments from the 0-5 cm surface layer was collected from the same three sampling stations used for sampling epilithic biofilms. Each composite sample was well mixed and a 30 g subsample was placed into an aluminum tray for biomass estimation and a 1g subsample was placed into a falcon tube for posterior molecular analysis.

Laboratory methods

Stream water samples were analyzed for NH_4^+, NO_2^- and NO_3^- concentrations following standard colorimetric methods (APHA, 1995) on a FUTURA autoanalyzer at the Analytical Services of Nutrients of the CEAB-CSIC.

Biomass of epilithic (on cobbles) and episamic (in sediments) biofilms was measured as ash free dry mass (AFDM). We dried samples at 60 °C until constant weight (ca. 0.1 mg, Sartorius analytical balance, model MC1), and dried samples were then combusted at 500 °C for 5 h, and weighted again as indicated previously. AFDM was computed as the difference between dry and combusted mass and was reported per unit of surface area (g AFDM m^{-2}) and per unit of dry weight (g AFDM g DW^{-1}) for epilithic and episamic biofilms. Filters with epilithic biofilms were extracted with acetone and chlorophyll *a* content (Chl *a*, in µg cm^{-2}) was determined by spectrophotometry (UV-2401PC,

ultraviolet–visible spectrometer, Shimadzu), after correction for phaeopigments, following (Steinman and Lamberti, 1996).

To estimate the abundance of AOB and AOA in epilithic biofilms, 5 ml of well mixed biofilm sludge was filtered through a 0.2-mm pore size polycarbonate membrane (Millipore), dried and placed in lysis buffer (40 mmol L^{-1} ethylenediaminetetra-acetic acid, 50 mmol L^{-1} Tris, pH 8.3, and 0.75 mol L^{-1} sucrose). To estimate the abundance of AOB and AOA in sediments, approximately 1 g of wet sediment was weighted and similarly placed in lysis buffer. The two sample types were stored at -80° C. DNA was extracted by incubating biofilm filters and sediments with lysozyme, proteinase K, and sodium dodecyl sulfate in lysis buffer (see indications above) and were further extracted with phenol-chloroform (Dumster et al 2002).

Abundance of AOA and AOB in epilithic biofilms and sediments from the two reaches was estimated by quantitative real time polymerase chain reaction (qPCR). For AOA we used the primes CrenamoA23f (5´-ATGGTCTGGCTWAGACG-3´) and CrenamoA616r (5´-GCCATCCATCTGTATGTCCA-3´; Tourna et al., 2008). For AOB we used the primers amoA-1F (5´-GGGTTTCTACTGGTGGT-3´) and amoA-2R (5´-CCCCTCKGSAAAGCCTTCTTC-3´; Rotthauwe et al., 1997). The two primer pairs were previously tested for qPCR approaches (Merbt et al., 2011). The final reaction mixture (20 µl) contained 10 µl of Sso Fast EVA Green Mix (BioRad), 1 ng genomic DNA, 300 ng μl^{-1} BSA and 200 nmol L^{-1} of each primer and was carried out in 96 well plates with adhesive seals (Bio-Rad) in a DNA Engine thermal cycler (Bio-Rad, Hercules) equipped with a Chromo 4 Real-Time Detector (Bio-Rad). The cycling protocol started with 2 min at 98 °C, followed by 45 cycles of 98 °C for 5 sec, annealing at 58 °C and 57 °C for AOB and AOA, respectively, for 15 sec. An additional elongation step was included at 72 °C for 15 sec. After cycling, a 1 min denaturation hold at 95 °C was included followed by 1 min at 65 °C to assure a stringent coupled PCR product. All

qPCR runs were double checked on amplicon specificity by applying a melting curve from 55 to 95 °C and by agarose gel electrophoresis. Each run was compared with standard curves from 10^7 to 10^2 copies μl^{-1} of *amoA* DNA from available environmental clones. The standard DNA was purified (QIAquick, QIAGEN), quantified (Qubit fluorometer, Invitrogen), and serially diluted for standard curves (r^2 = 0.99). qPCR was accepted when run efficiency ranged from 85 to 110%, controls without templates resulted in undetectable values, and no unspecific PCR products such as primer dimers or gene fragments of unexpected length occurred.

To compare between reaches and among sample types, *amoA* copy abundance was expressed per g AFDM. To further explore the relationship between *amoA* abundance and biomass for epilithic biofilms, *amoA* copy abundance was expressed per surface area (cm^2).

Parameter calculation

Daily rates of whole-reach metabolism: For each reach, we measured daily rates of GPP and ER by integrating changes in DO concentration between the top and the bottom of the reach during a 24 h period following the two-stations method (Bott et al., 2006). Instantaneous net DO change rates between the two stations were corrected for reaeration DO fluxes by calculating the product of the DO deficit, the reaeration coefficient, the water travel time, and the Q (Mulholland et al., 2001). DO concentration at saturation was estimated using average water temperature and the atmospheric pressure provided by the DO probes between the two sites within each reach. DO at saturation was compared to measured DO values to estimate the DO deficit. Reaeration coefficients for each reach were estimated based on the night-time method (Young and Huryn, 1996) using the relationship between instantaneous net DO change rates and DO deficits measured at night-time. The average of the instantaneous net DO change rates, corrected by reaeration fluxes, at night was extrapolated to 24 h to estimate

daily rates of ER. We computed daily rates of GPP by integrating the difference between the instantaneous corrected net DO change rates during daytime hours and the averaged instantaneous rate at night. Daily rates of GPP and ER were expressed per unit of streambed area (g O_2 m^{-2} d^{-1}). For each reach, values of ER were available for 4 consecutive days; however, values of GPP were only available for 2 of the 4 sampling dates at each stream, due to malfunction of probes during some daytime readings. The ratio between GGP and ER was estimated for dates were both values were available (n=2) to examine the relative dominance of autotrophic and heterotrophic activity on whole-reach metabolism rates.

Whole-reach NH_4 uptake and nitrification rates: We used data from the 4 short-term NH_4^+ additions performed at each reach to estimate rates of NH_4^+ uptake and nitrification at the whole-reach scale. In-stream NH_4^+ uptake rates were calculated from longitudinal declines in NH_4^+ concentration at plateau. In-stream nitrification rates were calculated from longitudinal increases in NO_2^- concentration along the reach at plateau. No longitudinal change in stream NO_3^- concentration was observed at plateau in any of the additions; and thus, data of NO_3^- concentration was not used in further stream nutrient spiraling calculations.

The coefficient of NH_4^+ uptake (k_{NH4}) and NO_2^- release (as a proxy of nitrification, k_{NIT}) per unit of reach length (both in m^{-1}) were estimated following Webster and Valett, (2006). These mass-transfer coefficients were calculated as the slope of the regression between the distance of each sampling station from the addition point and the *ln*-transformed concentration of either NH_4^+ or NO_2^- at plateau, corrected by i) the average ambient concentration along the reach, and ii) the groundwater inputs along the reach (inferred from changes in conductivity at plateau corrected by background conductivity). We multiplied the absolute value of the inverse of *k* by the specific discharge (Q/w) and average ambient concentration along the reach to compute areal rates of gross

NH_4^+ uptake (U_{NH4}, mg N s^{-1} m^{-2}; Webster and Valett, 2006) and nitrification (U_{NIT}, mg N s^{-1} m^{-2}). The U_{NIT}:U_{NH4} ratio was used as a proxy of the relative contribution of nitrification to total NH_4^+ uptake rate.

Statistical data analysis

We explored whether differences in average daily PAR, stream water temperature, conductivity, and dissolved inorganic N (DIN) concentrations were statistically significant between the open and shaded reach by using Student T test, after confirming normality of the data with the Shapiro test and variance equality with the Levene test (Zar, 1996). Data of DIN concentrations were log transformed to achieve normality requirements. To explore whether GPP, ER, U_{NH4}, and U_{NIT} differed between the open and shaded reaches, we used the confidence interval of 95%, because standard statistics could not be applied due to the low degree of freedom of the data (Zar, 1996). This approach was also used to compare U_{NH4} and U_{NIT} between daytime and nighttime experiments. For each substrata type, we explored differences between the two reaches for AFDM, Chl *a* (only for epilithic biofilms) using Student T-test separately for each substrate type. Differences between reaches and among substrata types (light-side, dark-side and sediments) in AOA and AOB abundance per g AFDM were analyzed using a two-way ANOVA (substrata type and reach as factors) with *log*-transformed data to fulfill normality requirements. For epilithic biofilms we further explored the relationship between total *amoA* abundance (AOA + AOB) and biomass (AFDM) in both light-side and dark-side biofilms separately by using non-linear regression analysis. The inflection point of the curve was calculated by estimating the second derivative of the best-fitted model. All statistical analyses were done using R project for statistical computing

7.4 Results

Characterization of the open and shaded reaches: The two reaches differed significantly in daily PAR and average daily water temperature, values being higher in the open than in the shaded reach (Table 7.1). Conductivity was slightly higher in the shaded than in the open reach. Average DIN concentration was high and dominated by $N\text{-}NO_3^-$ at the two reaches (Table 7.1). $N\text{-}NH_4^+$ concentration showed high variability during the experiments at the two reaches, and was marginally higher in the shaded than in the open reach. Concentrations of $N\text{-}NO_3^-$ and $N\text{-}NO_2^-$ were significantly higher in the shaded than in the open reach (Table 7.1).

Table 7.1: Average ± standard error of daily photosynthetic active radiation (PAR), water temperature, conductivity, and concentrations of NH_4^+, NO_3^- and NO_2^- at the open and shaded reaches. Bold *p*-values indicate significant differences between the two reaches (Student T test).

	unit	Open	Shaded	*p*-value
PAR	mol m^{-2} d^{-1}	32.5±4.5	9.2±1.5	**0.00**
Temperature	°C	21.5±0.6	19.7±0.7	**0.00**
Conductivity	µS cm^{-1}	500±12	533±5	**0.05**
$N\text{-}NH_4^+$	mg N L^{-1}	0.03±0.01	0.14±0.04	0.08
$N\text{-}NO_3^-$	mg N L^{-1}	2.65±0.11	4.10±0.41	**0.00**
$N\text{-}NO_2^-$	mg N L^{-1}	0.01±0.00	0.04±0.01	**0.00**

Daily rates of whole-reach metabolism were dominated by heterotrophic activity at the two reaches, being daily rates of ER ca. one order of magnitude higher than those of GPP (Table 7.2). Daily rates of GPP were slightly higher at the open than at the shaded reach, while the opposite pattern was observed for ER (Table 7.2), resulting in slightly higher GPP:ER ratio in the open that in the shaded reach.

Table 7.2: Gross primary production (GPP), ecosystem respiration (ER), and the GPP:ER ratio measured at the open and shaded reach during 2 consecutive days (n=2). The whole-reach NH_4^+ uptake rate (U_{NH4}), nitrification rate (U_{NIT}), and the U_{NIT}:U_{NH4} ratio for each reach are also shown. All data correspond to mean values ± coefficient interval (95%) of day and night experiments pooled together (n=4 for each reach).

	unit	open	shaded
GPP	g O2 m^{-2} d^{-1}	3.6±0.2	2.3±1.1
ER	g O2 m^{-2} d^{-1}	15.8±6.7	18.7±2.3
GPP:ER		0.3 ±0.1	0.1±0.01
U_{NH4}	mg N m^{-2} h^{-1}	0.3 ±0.3	6.3±13.8
U_{NIT}	mg N m^{-2} h^{-1}	2.6 ± 3.2	9.0 ± 11.8
U_{NIT}:U_{NH4}		7.7 ± 6.0	4.6 ± 7.6

Comparison of U_{NH4} and U_{NIT} between the open and shaded reach: In-stream N processing rates were highly variable within each reach, especially in the shaded reach. Consequently, we found no statistical differences between the two reaches for either U_{NH4} or U_{NIT} when data from daytime and nighttime at each reach was pooled together (Table 7.2). In-stream N processing rates also showed no statistical differences between daytime and nighttime when data from the two reaches were pooled together (Figure 7.1). In all cases U_{NIT} was higher than U_{NH4}, resulting in U_{NIT}:U_{NH4} ratios >1. However, the U_{NIT}:U_{NH4} ratio was 2-folds higher during nighttime than during daytime, suggesting that the relative contribution of nitrification to total NH_4^+ uptake was more pronounced at nighttime (Figure 7.1).

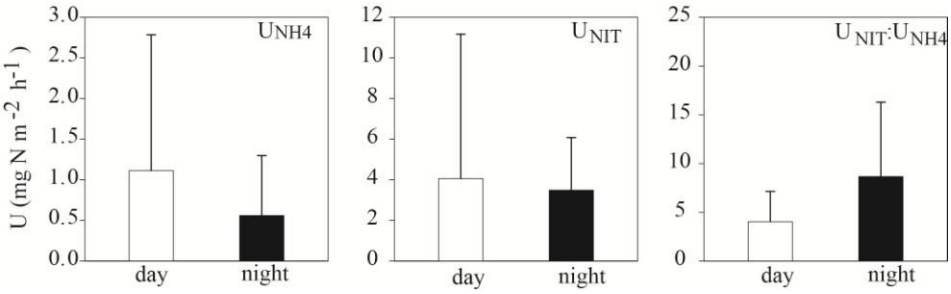

Figure 7.1: Mean values of NH_4^+ uptake rate (U_{NH4}), nitrification rate (U_{NIT}), and the U_{NIT}:U_{NH4} ratio for the day and night experiments pooling data from the tow reaches together (n=4). Whiskers indicate the coefficient interval (95%) of the mean.

Comparison of streambed substrata characteristics between the open and shaded reach: AFDM content in sediments and light-side biofilms was similar in the shaded and open reach. However, AFDM content in dark-side biofilms was significantly higher in the open than in the shaded reach (Student T test, n=3, Figure 7.2). In the two reaches, AFDM content was higher in light-side than in dark-side biofilms ($p<0.05$, Student T test, n=3). Content of Chl *a* in dark-side biofilms was significantly higher in the open than in the shaded reach. Conversely, content of Chl *a* in light-side biofilms was significantly higher in the shaded than in the open reach (Student T test, n=3, Figure 7.2). In the two reaches, Chl *a* was higher in light-side than in dark-side biofilms ($p<0.05$, Student T test, n=3). Results from two-way ANOVA indicated that the abundance of AOA and AOB per g AFDM was similar between the shaded and open reach for all substrate types (Figure 7.2). These results also indicated that the abundance of both AOA and AOB differed among substrata types, with highest values dark-side biofilms (two-way ANOVA, AOA~substrat, $p<0.05$, $F=5.16$ and for AOB~ substrat, $p<0.05$, $F=24.89$).

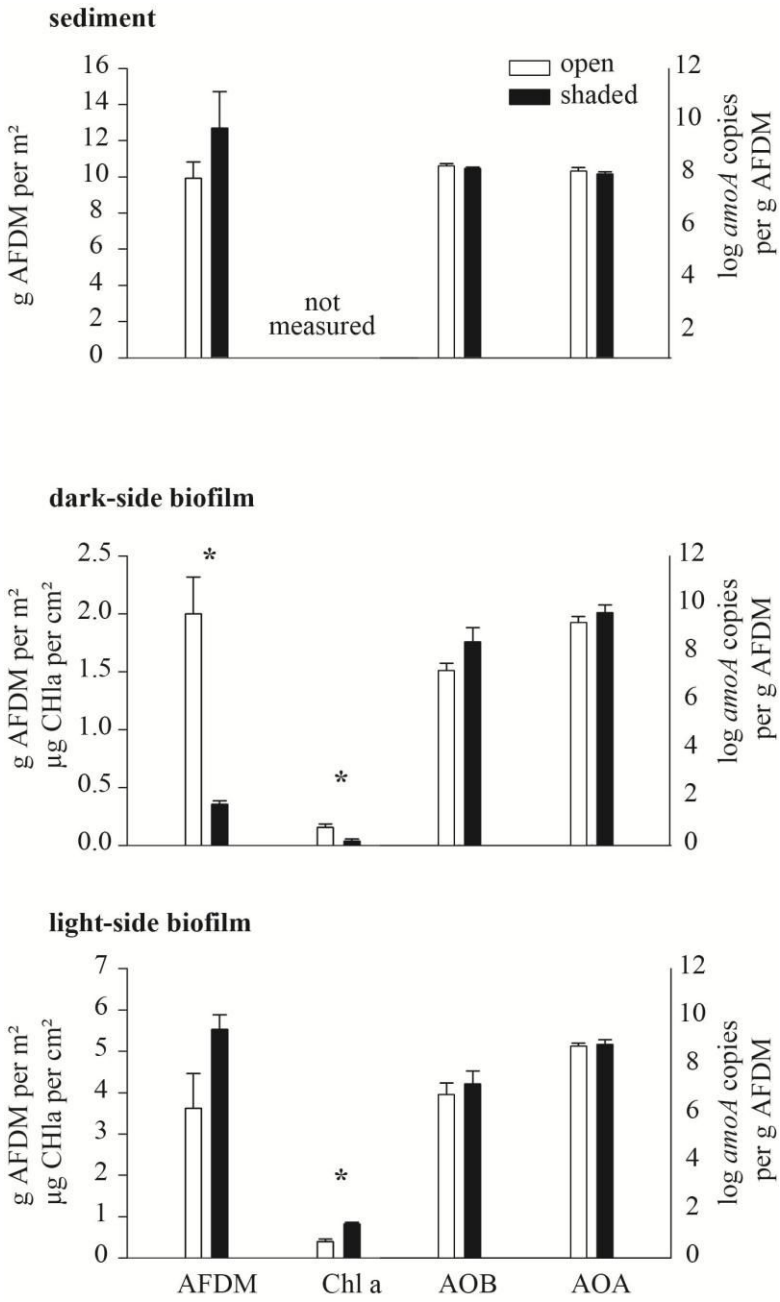

Figure 7.2: Substrata characteristics at the open and shaded reach. Differences in ash free dry mass (AFDM), Chl a, archaeal (AOA) and bacterial (AOB) *amoA* gene abundance are represented in sediment (upper), dark-side biofilm (middle) and light-side biofilm (bottom). Bars are means (n=3) and whiskers are the standard error of the mean. Stars indicate significant differences between open and shaded data sets (Student T test, $p<0.05$, amoA AOA and AOB copy abundances are log-transformed).

To analyze the relationship between the abundance of *amoA* copies (AO) and AFDM in the epilithic biofilms, we used data from this study and also from a previous study in nearby streams (Merbt et al., 2014). We did not find a significant relationship between AFDM and *amoA* abundance in dark-side biofilms (Figure 7.3). In contrast, we found a significant relationship netween AFDM and *amoA* abundance in light-side biofilms.

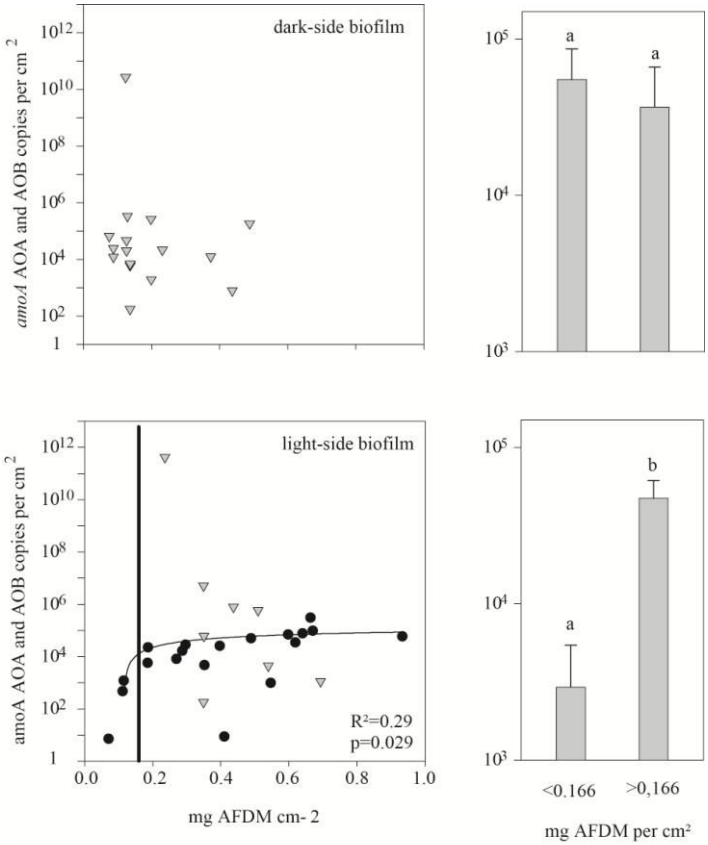

Figure 7.3: Relationship between *amoA* gene abundance (AOA+AOB) and biofilm biomass (AFDM) in dark-side and light-side biofilms (upper and lower panels, respectively). Bar plots (right panels) show the average abundance of *amoA* genes below and above a threshold of 0.166 mg AFDM cm^{-2}. Different letters in right panels indicate statistically significant differences between groups (Wilcoxon test, $p<0.05$). Black dots are data from this study and grey triangles are data from Merbt et al. (2014).

In these substrata, abundance of *amoA* increased with increasing AFDM below values of 0.166 mg AFDM cm^{-2}; above this threshold, *amoA* abundance remained relatively constant around 10^4 copies per cm^2, regardless of changes in AFDM (Figure 7.3). This result was reinforced by statistically comparing *amoA* gene abundance above and below the AFDM threshold. We found that *amoA* gene abundance was significantly higher at AFDM>0.166 mg AFDM cm^{-2} for biofilms in the light-side, whereas we did not observed this difference for biofilms in the dark-side (Figure 7.3).

7.5 Discussion

In high N loaded streams, such as urban streams receiving inputs from WWTP effluents nitrification accounts for a high proportion of the NH_4^+ uptake. Therefore they have been documented as hotspots of nitrification (Groffman et al., 2005; Merseburger et al., 2005; Ribot et al., 2012). This increased nitrifying activity is due to the prevailing NH_4 excess in the water column as well as due to the inoculation of nitrifying organisms from the WWTPs that are able to colonize substrata in the receiving streams (Merbt et al., 2014). Additionally, changes induced by WWTP inputs on other environmental factors, such as pH, temperature, dissolved organic carbon (DOC), oxygen availability, can influence the nitrification capacity of the receiving streams (Hill et al., 1995; Sabater et al., 2000; Mulholland et al., 2006). Besides these controlling factors observed at whole-reach scale, laboratory experiments with monoespecific cultures of ammonia oxidizing bacteria (AOB) and archea (AOA) have shown that light can strongly inhibit the activity of these organisms (Merbt et al., 2012). This suggests that under similar inputs from WWTP effluents, the nitrification capacity of the receiving stream could vary depending on the light availability and also between daytime and night. How light influences the nitrifying capacity of receiving streams can help understanding the in-stream capacity to regulate N inputs from WWTP, which have implications for N

exports to downstream ecosystems. However, to our knowledge, the effect of light on whole-reach nitrification has never been tested; and thus, this study aimed to fill this gap

Nitrification under different light regimes: Results of this study indicated that in-stream nitrification in the receiving stream was more subjected to variation in the chemical conditions of the stream water (probably due to changes in the effluent input) than to differences in light availability between the two reaches. Differences in light intensities between the two reaches, due to differences in riparian canopy cover, affected significantly stream water temperature and algal abundance, which is probably due to the saturation of photosynthetic activity in open reaches (Boston and Hill, 1991; Guasch and Subater, 1995). However, biomass and AO abundances in the different substrata types as well as ecosystem metabolism, NH_4^+ uptake rates, and nitrification rates did not clearly differ between the two reaches. This was possibly the result of the overall dominance of the WWTP inputs in both reaches.

Previous studies showed that the inputs from WWTP effluents increase DOC concentration, which enhances heterotrophic activity in receiving streams, and probably shifts overall stream metabolism (Bernhardt and Likens, 2002). In addition, enhanced heterotrophic activity results in increased mineralization, which in turn can increase NH_4^+ availability (Bernhardt and Likens, 2002; Daniel et al., 2002; Teissier et al., 2007). Therefore, it is reasonable to expect that in the two reaches nitrification was significantly fueled by both $NH_4^+$from the effluent as well as by in-stream mineralized NH_4^+. This is supported by the fact that rates of NO_2^- release from NH_4^+additions were consistently higher than NH_4^+ uptake rates.

Furthermore, we did not observe NO_3^- release during the NH_4^+. This contrasts with the sensitivity of NO_3^- concentration to short-term NH_4^+ additions in pristine streams (Bernhard et al., 2005 ; Arango et al., 2008), and could be

explained by the fact that the high NO_3^- background concentration may have masked any potential change from nitrification of the NH_4^+ added in the additions.

Responses to light availability were more obvious when comparing day and night time measurements than when comparing the two reaches. As expected, NH_4^+ uptake rates tended to be higher during the day than during the night due to photoautotrophic N demand (Fellows et al., 2006; Mulholland et al., 2006). In addition, despite similar nitrification rates between daytime and nighttime the U_{NH4}:U_{NIT} ratio tended to be higher during the night. This suggests that the relative contribution of nitrification to gross NH_4^+ uptake was more important during the night. Together, these results suggest that activity of AO seem to be more optimal during nighttime hours, in agreement with their intrinsic photosensitivity.

Light avoiding strategy of ammonia oxidizers: In the streambed of the two reaches ammonia oxidizers were highly abundant in all the study substrata, regardless of the differences in light intensity. This finding indicates that all tested substrata types provide a light protected environment and hence are suitable for the development of AO. As expected, in biofilms developed under natural dark conditions (dark-side biofilms) AO abundance was highest. However, despite their intrinsic susceptibility to light, AO were similarly abundant in light-side biofilms, which were grown under natural light exposition and in the sediments, which are considered as dark environments. The reason therefore may be found in the three-dimensional layer structure and the particular self-shading capacity for algae and AO of the light-side biofilm matrix (Chapter 6, Boston and Hill, 1991; Guasch and Sabater, 1995). Accordingly, our data indicated that the establishment of AO community depends on the biomass accrual and below the biomass threshold of 0.16 g AFDM m² the AO abundance was significantly reduced. This hypothesis was further supported by the fact that nitrifying activity and bacterial *amoA*

transcript abundance in mature light-side biofilms were not inhibited by artificial light exposure (Chapter 6). In contrast, in dark-side biofilms no relationship between biomass accrual and AO abundances was found and AO were already present in the early stages of dark-side biofilms indicating that the self-shading capacity is exclusively assigned to light-side biofilms. However, mature epilithic biofilms create chemical microenvironments with significant vertical gradients of oxygen, and N availability (Schramm et al., 2000; Battin et al., 2003; Gieseke et al., 2005), which provide niches for specialists and is the basis for the high microbial diversity observed in this biofilms (Besemer et al., 2013; Widder et al., 2014). This could explain the asymptotic pattern exhibited by AOA and AOB abundance as biofilms have higher AFDM.

Results from this study indicate high AO abundance in all substrata types, anticipating similar high nitrifying potential for each substratum. However, particular contribution of each substratum to whole-reach nitrification remains unsolved and may be regulated by other factors such as transient storage and oxygen concentration rather than light irradiance.

In conclusion, nitrification is a highly important process in urban streams receiving high N loads from WWTP inputs. Light can be the driver of shifts of biogeochemical processes in streams indicated by higher NH_4^+ uptake rates during the day than during the nighttime, but despite intrinsic photosensitivity of AOA and AOB, our results suggests that nitrification at whole-reach scale is not hampered by differences in light availability between stream reaches. Our findings suggest that AOA and AOB, the key players of nitrification, overcome their intrinsic photosensitivity because they accumulate in shaded environments (i.e., dark-side biofilms or biofilms in sediments), or are protected by the shield offered by the biofilm matrix in light-side biofilms. These two light-avoiding strategies enable in-stream nitrification during light hours, minimizing the strong inhibitory effect of light on the activity of AO reported for batch cultures (French et al., 2012; Merbt et al., 2012).

Acknowledgments:

We thank Dr A. Serra, C. Romero for excellent field assistance. This research was granted by DARKNESS CGL2012-32747 to EOC and MED_FORESTREAM CGL2011-30590-CO2-02 (MINECO) and REFRESH-244121 (7th Framework Programme EU Comission) to EM. S.N.M. is supported by a JAE predoctoral fellowship from the Spanish National Research Council (CSIC).

7.6. References

APHA (1995) Standard methods for the examination of water and wastewater. *American Public Health Association, Washington, USA*.

Arango, C., Tank, J., Johnson, L., and Hamilton, S. (2008) Assimilatory uptake rather than nitrification and denitrification determines nitrogen removal patterns in streams of varying land use. *Limnology and Oceanography* **53**: 2558–2572.

Battin, T.J., Kaplan, L.A., Denis Newbold, J., and Hansen, C.M.E. (2003) Contributions of microbial biofilms to ecosystem processes in stream mesocosms. *Nature* **426**: 439-442.

Beman, J.M., Popp, B.N., and Alford, S.E. (2012) Quantification of ammonia oxidation rates and ammonia-oxidizing archaea and bacteria at high resolution in the Gulf of California and eastern tropical North Pacific Ocean. *Limnol Oceanogr* **57**: 711-726.

Bernhard, A.E., Donn, T., Giblin, A.E., and and Stahl, D.A. (2005) Loss of diversity of ammonia-oxidizing bacteria

correlates with increasing salinity in an estuary system. *Environmental Microbiology* **7**: 1289–1297.

Bernhardt, E.S., and Likens, G.E. (2002) Dissolved organic carbon enrichment alters nitrogen dynamics in a forest stream. *Ecology* **83**: 1689-1700.

Bernhardt, E.S., Hall Jr, R.O., and Likens, G.E. (2002) Whole-system estimates of nitrification and nitrate uptake in streams of the Hubbard Brook Experimental Forest. *Ecosystems* **5**: 419-430.

Besemer, K., Singer, G., Quince, C., Bertuzzo, E., Sloan, W., and Battin, T.J. (2013) Headwaters are critical reservoirs of microbial diversity for fluvial networks. *Proceedings of the Royal Society B: Biological Sciences* **280**.

Boston, H., and Hill, W. (1991) Photosynthesis-light relations of stream periphyton communities. *Limnology and Oceanography* **36**: 644-656.

Bott, T.L., Newbold, J.D., and Arscott, D.B. (2006) Ecosystem metabolism in Piedmont streams: reach geomorphology modulates the influence of riparian vegetation. *Ecosystems* **9**: 398-421.

Camargo, J.A., and Alonso, Á. (2006) Ecological and toxicological effects of inorganic nitrogen pollution in aquatic ecosystems: A global assessment. *Environment International* **32**: 831-849.

Daniel, M.H., Montebelo, A.A., Bernardes, M.C., Ometto, J.P., De Camargo, P.B., Krusche, A.V. et al. (2002) Effects of urban sewage on dissolved oxygen, dissolved inorganic and organic carbon, and electrical conductivity of small streams along a gradient of urbanization in the Piracicaba river basin. *Water, Air, and Soil Pollution* **136**: 189-206.

Fellows, C.S., Valett, H., Dahm, C., Mulholland, P., and Thomas, S. (2006) Coupling nutrient uptake and energy flow in headwater streams. *Ecosystems* **9**: 788-804.

Francis, C.A., Roberts, K.J., Beman, J.M., Santoro, A.E., and Oakley, B.B. (2005) Ubiquity and diversity of ammonia-oxidizing archaea in water columns and sediments of the ocean. *Proceedings of the National Academy of Sciences* **102**: 14683-14688.

French, E., Kozlowski, J.A., Mukherjee, M., Bullerjahn, G., and Bollmann, A. (2012) Ecophysiological Characterization of Ammonia-Oxidizing Archaea and Bacteria from Freshwater. *Applied and Environmental Microbiology* **78**: 5773-5780.

Gieseke, A., Nielsen, J.L., Amann, R., Nielsen, P.H., and De Beer, D. (2005) In situ substrate conversion and assimilation by nitrifying bacteria in a model biofilm. *Environmental Microbiology* **7**: 1392-1404.

Gordon, N., McMahon, T., and Finlayson, B. (1992) How to have a field day and still collect some useful information. In *Stream hydrology, an introduction for ecologists*. ND, G., TA, M., and BL, F. (eds). Chichester, England: John Wiley & Sons, pp. 127–214.

Groffman, P.M., Dorsey, A.M., and Mayer, P.M. (2005) N processing within geomorphic structures in urban streams. *Journal of the North American Benthological Society* **24**: 613-625.

Guasch, H., and Subater, S. (1995) Seasonal variation in photosynthesis-irradiance response by biofilms in mediterranean streams. *Journal of Phycology* **31**: 727-735.

Hill, W.R., Ryon, M.G., and Schilling, E.M. (1995) Light limitation in a stream ecosystem: responses by primary producers and consumers. *Ecology*: 1297-1309.

Hyman, M.R., and Arp, D.J. (1992) 14C2H2- and 14CO2-labeling studies of the de novo synthesis of polypeptides by Nitrosomonas europaea during recovery from acetylene and light inactivation of ammonia monooxygenase. *Journal of Biological Chemistry* **267**: 1534-1545.

Lomas, M.W., and Lipschultz, F. (2006) Forming the primaryn itrite maximum: Nitrifiers or phytoplankton? *Limnology and Oceanography* **51**: 2453-2467.

Merbt, S.N., Jean-Christophe Auguet, Emilio O. Casamayor, and Martı, E. (2011) Biofilm recovery in a wastewater treatment plant-influenced stream and spatial segregation of ammonia-oxidizing microbial populations. *Limnology and Oceanography* **56**: 1054–1064

Merbt, S.N., Auguet, J.-C., Blesa, A., Martí, E., and Casamayor, E. (2014) Wastewater Treatment Plant Effluents Change Abundance and Composition of Ammonia-Oxidizing Microorganisms in Mediterranean Urban Stream Biofilms. *Microbial Ecology*: 1-9.

Merbt, S.N., Stahl, D.A., Casamayor, E.O., Martí, E., Nicol, G.W., and Prosser, J.I. (2012) Differential photoinhibition of bacterial and archaeal ammonia oxidation. *FEMS Microbiology Letters* **327**: 41-46.

Merseburger, G., Martí, E., and Sabater, F. (2005) Net changes in nutrient concentrations below a point source input in two streams draining catchments with contrasting land uses. *Science of the total environment* **347**: 217-229.

Mulholland, P., Fellows, C.S., Tank, J., Grimm, N., Webster, J., Hamilton, S. et al. (2001) Inter-biome comparison of factors controlling stream metabolism. *Freshwater Biology* **46**: 1503-1517.

Mulholland, P.J., Thomas, S.A., Valett, H.M., Webster, J.R., and Beaulieu, J. (2006) Effects of light on NO3-uptake in small forested streams: diurnal and day-to-day variations. *Journal of the North American Benthological Society* **25**: 583-595.

Nelson, D., and Conway, H.L. (1979) Effects of the light regime on nutrient assimilation by phytoplankton in the Baja California and northwest Africa upwelling systems *Journal of Marine Research* **37**: 301-318.

Nicol, G.W., Sven, L., Christa, S., and James, I.P. (2008) The influence of soil pH on the diversity, abundance and transcriptional activity of ammonia oxidizing archaea and bacteria. *Environmental Microbiology* **10**: 2966-2978.

Prosser, J.I. (1989) Autotrophic Nitrification in Bacteria. In *Advances in Microbial Physiology*. Rose, A.H.T., D. W. (ed): Academic Press, pp. 125–181.

Reuter, J.E., Loeb, S.L., and Goldman, C.R. (1986) Inorganic nitrogen uptake by epilithic periphyton in a N-deficient lake. *Limnology and Oceanography* **31**: 149-160.

Ribot, M., Martí, E., von Schiller, D., Sabater, F., Daims, H., and Battin, T.J. (2012) Nitrogen processing and the role of epilithic biofilms downstream of a wastewater treatment plant. *Freshwater Science* **31**: 1057-1069.

Rotthauwe, J.-H., Witzel, K.-P., and Liesack, W. (1997) The ammonia Monooxygenase Structural Gene amoA as a Functional Marker: Molecular Fine-Scale Analysis of Natural Ammonia Oxidizing Populations. *Applied and environmental microbiologie* **63**: 4704-4712.

Sabater, F., Butturini, A., MartÍ, E., Muñoz, I., Romaní, A., Wray, J., and Sabater, S. (2000) Effects of riparian vegetation removal on nutrient retention in a Mediterranean stream. *Journal of the North American Benthological Society*: 609-620.

Schramm, A., De Beer, D., Gieseke, A., and Amann, R. (2000) Microenvironments and distribution of nitrifying bacteria in a membrane-bound biofilm. *Environmental Microbiology* **2**: 680-686.

Small, G.E., Bullerjahn, G.S., Sterner, R.W., Beall, B.F., Brovold, S., Finlay, J.C. et al. (2013) Rates and controls of nitrification in a large oligotrophic lake. *Limnology and Oceanography* **58**: 276-286.

Sonthiphand, P., Cejudo, E., Schiff, S.L., and Neufeld, J.D. (2013) Wastewater Effluent Impacts Ammonia-Oxidizing Prokaryotes of the Grand River, Canada. *Applied and Environmental Microbiology* **79**: 7454-7465.

Spang, A., Hatzenpichler, R., Brochier-Armanet, C., Rattei, T., Tischler, P., Spieck, E. et al. (2010) Distinct gene set in two different lineages of ammonia-oxidizing archaea supports the phylum Thaumarchaeota. *Trends in Microbiology* **18**: 331-340.

Steinman, A.D., and Lamberti, G.A. (1996) Biomass and pigments of benthic algae. In *Methods in stream ecology*. Lamberti, F.R.H.a.G.A. (ed). California: academic Press.

Strauss, E.A., Mitchell, N.L., and Lamberti, G.A. (2002) Factors regulating nitrification in aquatic sediments: effects of organic carbon, nitrogen availability, and pH. *Canadian Journal of Fisheries and Aquatic Sciences* **59**: 554-563.

Strauss, E.A., Richardson, W.B., Bartsch, L.A., Cavanaugh, J.C., Bruesewitz, D.A., Imker, H. et al. (2004) Nitrification in the Upper Mississippi River: patterns, controls, and contribution to the NO3-budget. *Journal of the North American Benthological Society* **23**: 1-14.

Teissier, S., Torre, M., Delmas, F., and Garabétian, F. (2007) Detailing biogeochemical N budgets in riverine epilithic biofilms. . *Journal of the North American Benthological Society* **26**: 178-190.

Tourna, M., Freitag, T.E., Nicol, G.W., and Prosser, J.I. (2008) Growth, activity and temperature responses of ammonia-oxidizing archaea and bacteria in soil microcosms. *Environmental Microbiology* **10**: 1357-1364.

Webster, J., and Valett, H. (2006) Solute dynamics. In *Methods in stream ecology*. Hauer FR, and Lamberti GA, E. (eds). San Diego, USA: Academic Press, pp. 169-185.

Widder, S., Besemer, K., Singer, G.A., Ceola, S., Bertuzzo, E., Quince, C. et al. (2014) Fluvial network organization imprints on microbial co-occurrence networks. *Proceedings of the National Academy of Sciences*.

Young, R.G., and Huryn, A.D. (1996) Interannual variation in discharge controls ecosystem metabolism along a grassland river continuum. *Canadian Journal of Fisheries and Aquatic Sciences* **53**: 2199-2211.

Zar, J.H. (1996) *Biostatistical analysis.* Prentice–Hall, Upper Saddle River, New Jersey, USA.

General discussion 8

Cover: Barranc de Remediano, Taüll (Lleida, Spain). Photograph by SN Merbt

8.1. General discussion

The overall goal of this dissertation was to improve the current knowledge on in-stream nitrification, a biogeochemical process that links the cycling of reduced and oxidized forms of dissolved inorganic N, by bringing together perspectives of two independent disciplines, stream biogeochemistry and molecular ecology. This has allowed introducing the "key actors" into the in-stream nitrification "play". This knowledge is crucial to further understand controlling factors and mechanisms of the nitrification process, which is frequently an important sink of ammonium (NH_4^+), especially in high N loaded streams.

Existing studies on nitrification in streams have been focused on measurements of rates at habitat or whole-reach scale (Peterson et al., 2001; O'Brien and Dodds, 2008). The observed variability in the rates has been examined within the context of environmental variables to infer controlling factors of this process. Using this regression-based approach, stream discharge, water temperature, and concentrations of oxygen, dissolved organic carbon (DOC) and NH_4^+ have been reported as important factors controlling nitrification in streams (Jones et al., 1995; Bernhardt et al., 2002; Strauss et al., 2002; O'Brien and Dodds, 2008; Levi et al., 2013). Nevertheless, a mechanistic understanding of in-stream nitrification is still lacking.

At the same time, microbial ecology studies have increasingly contribute to understand the physiologic properties and phylogenetic separation between and within ammonia oxidizing archaea (AOA) and bacteria (AOB), (Chain et al., 2003; Spang et al., 2010; Walker et al., 2010; Fernàndez-Guerra and Casamayor, 2012), but implications of this knowledge for in-stream nitrification remains unexplored. Currently, only a few studies explicitly deal with abundance and potential role of AOA and AOB in streams (Cebron et al., 2003;

Mußmann et al., 2013; Sonthiphand et al., 2013). In this PhD dissertation, we merged the two perspectives, molecular ecology and biogeochemistry, to characterize the abundance and distribution of AOA and AOB in streams and provide mechanistic insights on in-stream nitrification.

This general discussion chapter will consider together the results from each particular study to provide a) an overview synthesis on the abundance, identity, distribution and function of AOA and AOB in streams, both at habitat and whole reach scales; b) insights on the effect of a particular factor (irradiance) on the activity of nitrifiers and how this cell-level effect scales up to whole-reach patterns of nitrification; and c) an evaluation of the contribution of AOA and AOB from different streambed habitats (cobbles and sediments) to whole reach nitrification. It is worth noting that results from this PhD mostly come from streams receiving high inputs of NH_4^+ from wastewater treatment plant (WWTP) effluents. We selected these sites because previous studies indicated nitrification as a relevant process in theses streams (Merseburger et al., 2005), thus offering optimal conditions and excellent study scenarios to address the objectives of this PhD.

8.2. Chemical conditions in the stream water column drive AOA and AOB abundance and distribution and activity in stream biofilms.

Physical and chemical conditions in streams and rivers change with increasing stream order and concomitantly shape the composition of benthic and pelagic microbial assemblages (Besemer et al., 2013; Widder et al., 2014). Therefore, it should be expected that the abundance and identity of ammonia oxidizing organism along the fluvial continuum vary gradually encompassing changes in physical and chemical conditions. However, inputs from WWTP effluents create abrupt physical and chemical disruptions by increasing stream discharge,

water temperature and concentrations of DOC, and inorganic nutrients, especially NH_4^+ (Martí et al., 2010; Merbt et al., 2011; Mußmann et al., 2013). We used such anthropogenically induced shifts to study in-stream dynamics of epilithic ammonia oxidizing assemblages under heterogeneous chemical conditions.

Results of this PhD showed that ammonium oxidizers (AOA and AOB) can be ubiquitously abundant in epilithic biofilms along the stream continuum. Moreover, these organisms are already present at early stages of biofilm development (i.e., after severe floods), and in mature biofilms both in summer and winter seasons, suggesting that nitrification may contribute to in-stream NH_4^+ regulation throughout the year (Merbt et al., 2011, 2014). Concordantly, in a stream receiving high NH_4^+ loads from WWTP inputs we consistently observed a gradual decrease of NH_4^+ concentration accompanied by an increase of NO_3^- concentrations regardless of the time of the year (Figure 8.1).

In this high N loaded stream, nitrifying activity was of paramount importance accounting for up to 90 % of the NH_4^+ uptake and was mostly driven by AOB, from *Nitrosospira* and *N. oligotropha* clusters. In turn, at more pristine reaches, with relatively low NH_4^+ concentrations, AOA from the *Nitrososophaera* cluster predominated, and biofilm nitrification rates were relatively low accounting for only 2 % of NH_4^+ uptake. AOB abundance was low and frequently negligible at these pristine sites. These differences in nitrifying activity in high and low N loaded reaches suggested that NH_4^+ availability rule AOA and AOB distribution and activity.

Results from culture studies on the physiology of AOA and AOB can help explaining the differences in relative abundance of the two phyla among sites. Their intrinsic ecophysiological adaptations such as NH_4^+ affinity and pH tolerance have been shown to determine the AOA-AOB interactions

(Fernàndez-Guerra and Casamayor, 2012). AOB are known to have lower NH_4^+ affinity than AOA and hence, AOB are frequently more abundant and active in high NH_4^+ environments, such as agricultural soils and sludge of WWTPs (Koops et al., 2006; Di et al., 2009; Martens-Habbena et al., 2009; Herrmann et al., 2011). Conversely, AOA, the most widely distributed microorganism group in the planet driving nitrification, tends to develop in low N loaded ecosystems like the ocean (Yool et al., 2007; Beman et al., 2012), oligotrophic mountain lakes (Restrepo-Ortiz et al., 2014), neutral and acidic soils (Leininger et al., 2006; Nicol et al., 2008) and in extreme environments such as hot springs (Hatzenpichler et al., 2008). Our results suggesting NH_4^+ availability to shape relative abundance of AOA and AOB in stream biofilms are in agreement with these previous expectations.

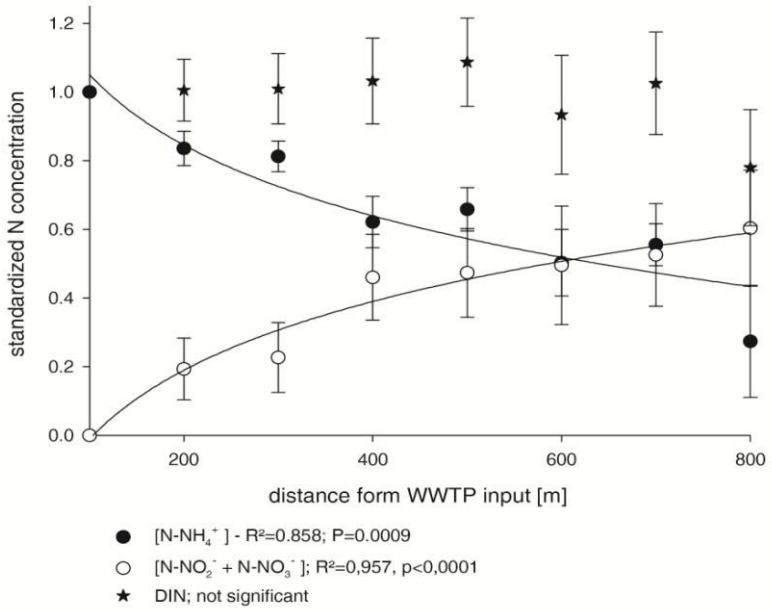

Figure 8.1: Relative change in stream water $N\text{-}NH_4^-$ (black dots), $N\text{-}NO_2^+ + N\text{-}NO_3^-$ (white dots), and dissolved inorganic N (DIN, stars) concentrations along the 800m-reach downstream of the WWTP in La Tordera stream at Santa Maria de Palautordera. Circles represent means and Whiskers standard error of the mean (n=9, March-September 2013). Lines indicate the significant non-linear regression over distance.

In addition, shifts in nitrifying assemblages between stream reaches differing in NH_4^+ concentrations were also explained by the inoculation of both, AOA and AOB, through the WWTP effluent. Once in the stream, their capacity to settle in the biofilms and their nitrifying activity was probably dictated by the *in situ* chemical conditions. For instance, downstream of the WWTP input AOB abundance increased by orders of magnitude and exhibited high activity, while the community composition of AOA was different from that at upstream sites and showed low activity. This indicates that AOA from either more pristine sites probably poorly adapted to the disturbed conditions; and hence, confirms previous statements about the high phylogenetic diversity of AOA (Thaumarcheaota) with remarkably specialized lineages (Auguet et al., 2009; Spang et al., 2010).

Despite the present PhD thesis was focused on ammonia oxidizers, results from a collaborative study indicated that chemical conditions also influence other organisms crucial to nitrification process (i.e., nitrite oxidizing bacteria, NOB) (Mußmann et al., 2013). NOB catalyze the second step of nitrification, the oxidation of NO_2^- to NO_3^-. Similarly to AOB, they were mainly observed downstream of WWTP effluents (Mußmann et al., 2013) and microscopic observations showed they develop in close contact with AOB in stream biofilms (Figure 8.2). This co-localization most probably favors the high nitrifying capacity observed in mesocosm incubations. In contrast, upstream of the WWTP effluent NOB were absent; and therefore, in mesocosm incubations those biofilms only produced NO_2^- while NO_3^- concentrations remained constant.

Together our findings suggest that the chemical conditions in the water column influence nitrifying assemblages and associated activity along the stream and river continuum, which subsequently determines the dominant pathways of in-stream N cycling.

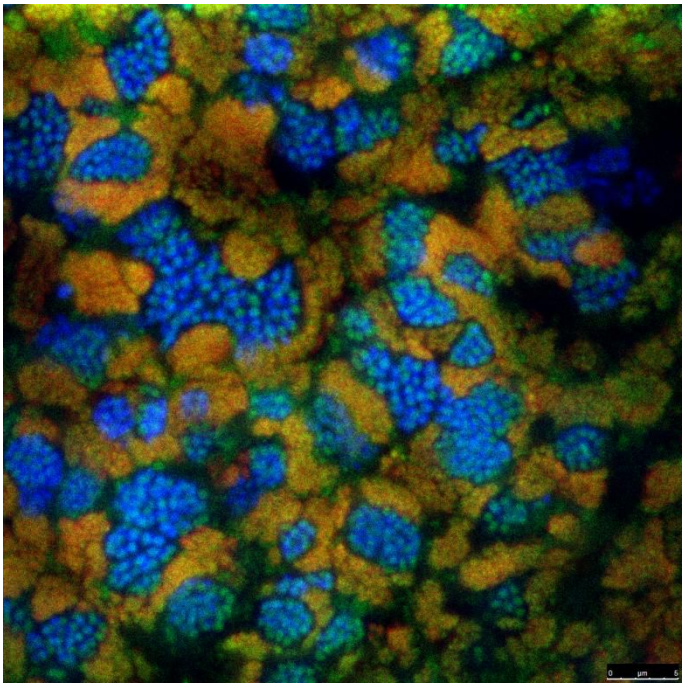

Figure 8.2: Fluorescent in situ hybridization of dark-side biofilms. Yellow – *Nitrosospira* (NOB : probe NTSP1431), blue – *Nitrosomonas europaea* (AOB – probe NEU) and green – all bacteria (probe EUB338). Biofilms were grown in darkness *in situ* during 4 weeks on roughed glass fiber plates, fixed, hybridized and visualized as previously described (Daims and Wagner, 2011). AOA were below detection limit (probe Arch915).

8.3. Distribution of AOA and AOB at habitat scale

We found a spatial segregation of AOA and AOB in epilithic biofilms developed on both sides of the cobbles (i.e., light- and dark-exposed sides), highlighting that the conditions in different habitats can rule the spatial distribution of AOA and AOB within stream reaches.

In particular, the abundance of ammonia oxidizers relative to the total biofilm biomass was predominantly higher in the dark-side than in the light-side, regardless of the season of the year (Figure 8.3). Only in summer, when riparian canopy cover was dense, there were no differences in AOA abundance between the cobble sides (Figure 8.3). This suggests that environmental conditions in dark-side biofilms are more suitable for ammonia oxidizers; and thus, these habitats can be considered as hot spots for nitrifyers within the stream reaches. Accordingly, nitrification rates measured in dark-side biofilms were higher than those in light-side biofilms.

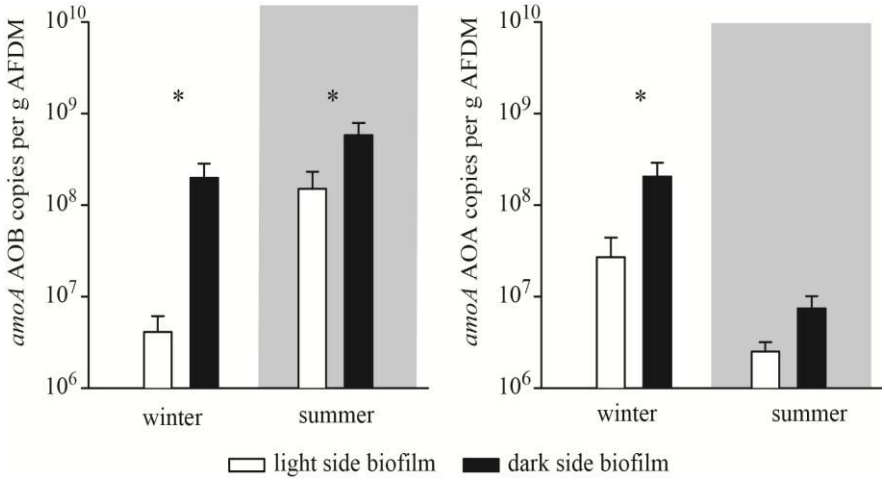

Figure 8.3: mean *amoA* AOB (A) and *amoA* AOA (B) copy abundance per g AFDM in light-side and dark-side biofilms in winter (n=9, Chapter 3, Merbt et al 2011) and summer (n=18, Chapter 4, Merbt et al 2014). For statistical analysis data were *log*-transformed to fulfill normality requirements. Lines above the bars indicate the standard error of the mean. * indicate significant differences between light-side and dark-side biofilms (paired, Student T test, $p < 0.05$).

To extrapolate the standing stock of AOA and AOB at the stream reach scale it has to be taken into account that, in light-side biofilms, AOA and AOB abundance does not increase linearly with biofilm biomass and their abundances rather remain in steady state from a certain biomass threshold (1.6 g AFDM m^{-2}). Similarly in dark-side biofilms, AOA and AOB abundance level off already

in early stage biofilms and do not increase further with increasing biomass. However, it is necessary to estimate the total abundance of AOA and AOB within the biofilms to apply regression analysis with environmental factors aiming to further unveil driving factors of in-stream nitrification.

To overcome this problem; and thus, to estimate the standing stock of AOA and AOB in the biofilms, we expressed their abundance per unit of colonized surface area (per m²), and found that values were predominately similar for both biofilm types both in winter and summer (Figure 8.4).

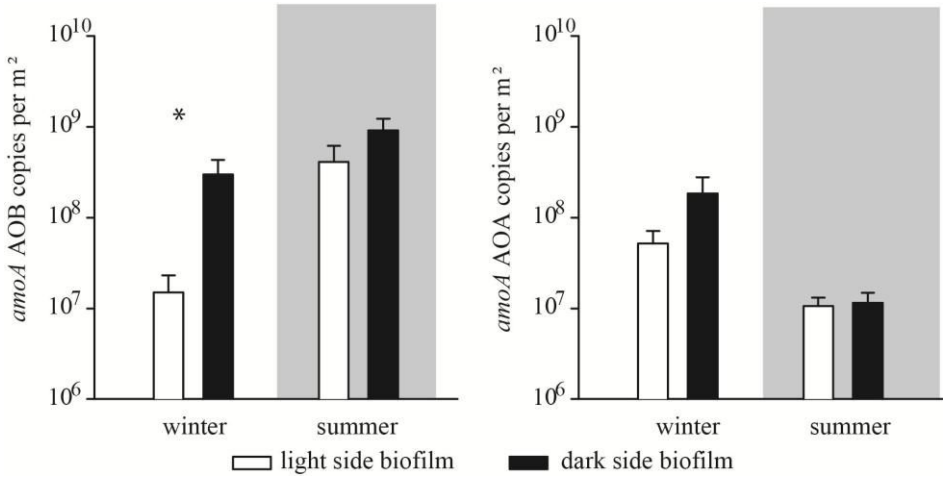

Figure 8.4: mean *amoA* AOB (A) and *amoA* AOA (B) copy abundance per m² of cobbles in light-side and dark-side biofilms in winter (n=9, Chapter 3, Merbt et al 2011) and summer (n=18, Chapter 4, Merbt et al 2014). For statistical analysis data were log-transformed to fulfill normality requirements. Lines above the bars indicate the standard error of the mean. * indicate significant differences between light-side and dark-side measurements (paired, Student T test, $p < 0.05$).

This unexpected finding appeared counterintuitive because of the reported photoinhibition in laboratory strains of both AOA and AOB (Hooper and Terry, 1974; Merbt et al., 2012). The fact that light is not a ruling factor for the distribution and activity of AOA and AOB in biofilms *in situ* can be further explained after carefully exploring the spatial structure and configuration of the

biofilm matrix. Mature biofilms provide a complex, three dimensional layer structure (Schramm et al., 1996; Battin et al., 2003; Gieseke et al., 2005), which possibly provides shaded microenvironments suitable for the photo-sensitive ammonia oxidizers; and thus, enable successful development of ammonia oxidizers regardless biofilms can be exposed to full light conditions. This feature of the light-side biofilm matrix has been proposed as a protective *umbrella effect* and seems to operate above a certain biomass accrual threshold (1.6 g AFDM m^{-2}) turning light-exposed biofilms into a favorable habitat for AOA and AOB. Besides the *umbrella effect*, the mature biofilm matrix provides microhabitats where chemical conditions change significantly within micrometers and significant vertical gradients of oxygen, NH_4, RedOx and pH are present (Schramm et al., 2000; Gieseke et al., 2005; Battin et al., 2007). This may be one reason why AOA and AOB abundance does not increase linearly with biofilm biomass, but follow a saturation curve.

In contrast to light-side biofilms, this protective *umbrella effect* was not evident in dark-side biofilms and both nitrification rates and AOA-AOB *amoA* transcripts decreased significantly when biofilms were exposed to light. The *umbrella effect* of the light-side biofilm matrix was further supported at the whole-reach scale since in-stream nitrification rates were similar between day and night and between reaches under low and high *in situ* irradiance. Biofilms growing in the sediment (episamic biofilms) also host ammonia oxidizing organism and may significantly contribute to whole-reach nitrification (Jones et al., 1995; Dahm et al., 1998; Butturini et al., 2000; Levi et al., 2013). However, there is not a complete understanding of the contribution from different stream compartments (i.e. biofilms and sediments) to whole-reach nitrification. We aimed to cover this gap providing a direct comparison among stream compartments.

8.4. Up-scaling nitrification from habitat to whole-reach

In this part of the general discussion we aim to complete the picture of urban stream nitrification. We provide a direct comparison of ammonia oxidizing community composition and nitrifying activity between epilithic and episamic biofilms within the same stream. Furthermore, we scale the habitat-specific findings into the context of whole-reach nitrification aiming to unveil the nitrifying hotspots at whole-reach scale. Interestingly, the episamic biofilms were dominated by AOA, while the epilithic biofilms were dominated by AOB (Chapter 7). Therefore, the intrinsic ecophysiology and niche separation between AOA and AOB suggests that these habitats differ in physical and chemical conditions, which may have a significant impact on the nitrifying activity (Prosser and Nicol, 2008).

The abundance of ammonia oxidizing organism (AOA and AOB) per cm^2 of colonized surface was highest in the dark-side biofilms and lowest in the episamic biofilms indicating high spatial heterogeneity among habitats (Figure 8.5). To extrapolate these numbers to the whole-reach scale we estimated the total colonizable surface area of each compartment assuming a typical Mediterranean streambed (as in La Tordera, Spain) consisting of approximately 55 % cobbles and rocks and 100 % of underling sediments of the total reach area. After integrating the first five centimeters of the sediment as colonizable surface for AO, the surface provided by the sediments was 80 times higher than the surface provided by cobbles and rocks. Therefore, 98 % of all the ammonia oxidizers within the reach are located in the sediment and only the remaining 2 % split into the two epilithic biofilms. The results from this exercise give an overwhelming picture and point to episamic biofilms as the major contributors to in-stream nitrification at whole-reach scale.

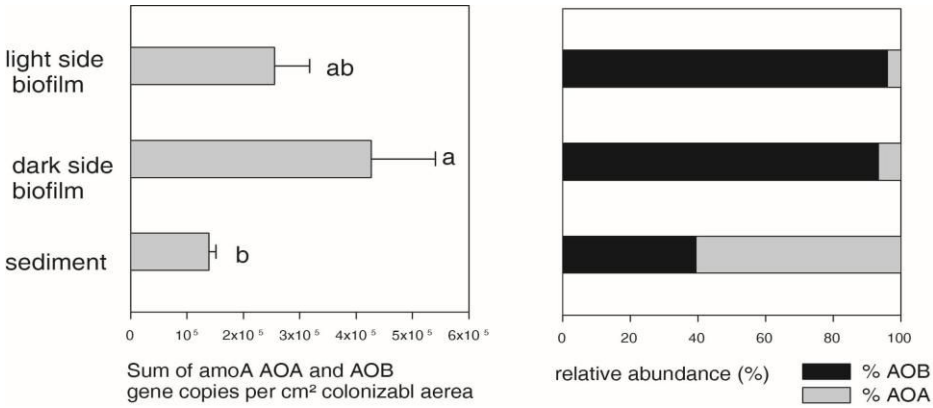

Figure 8.5: left panel reflects the abundance of AOA and AOB *amoA* gene in light-side, dark-side biofilms and the sediment. Values averaged out of 6 independent, biological replicates, and line above the bar indicates the standard error of the mean. Letters above the bars indicate significant differences between biofilm types (ANOVA, $p<0.05$). Right panel indicates the relative abundance (%) of AOA and AOB in the habitats.

However, when comparing N processing rates measured in mesocosms among the three habitats, the highest gross NH_4^+ uptake rates (k_{NH4} [min^{-1}]) were observed in dark-side biofilms (Figure 8.6). In addition, nitrification rates, estimated from the increase of either NO_2^- or NO_3^- over time in the mesocosms, were comparable in the sediments and in the dark-side biofilms (Figure 8.6). This suggests that dark-side biofilms, dominated by AOB, have a high potential for nitrification, which could partially counterbalance the relatively low distribution of these biofilms in the reach in terms of surface area.

To evaluate the relative contribution of the different habitats to whole-reach nitrification, we used data from habitat-specific nutrient cycling measured in mesocosms (Figure 8.6, Chapter 6) and scaled them to whole-reach values. We used stream velocity and ambient DIN concentrations measured at the reach of the Tordera River were we collected the samples for measuring AO abundance in biofilm and sediments (Figure 8.1 and Table 8.1). The habitat-specific N uptake rates for biofilms on the light-side ($U_{light\text{-}side}$), dark-side ($U_{dark\text{-}side}$) and sediment ($U_{sediment}$) were calculated in three steps. First, for each biofilm type we

converted the uptake constant rate per unit of time (k_t, min^{-1}) from mesocosms experiments into the uptake constant rate per unit of reach length (k_s, m^{-1}) by dividing it for the stream velocity (m s^{-1}). Second, we calculated the expected concentrations of NH_4^+, NO_2^- and NO_3^- at the bottom of the reach (C_{bot}, in mg N L^{-1}) based on a first order equation following nutrient spiraling theory (Webster and Vallett, 2006) as follows:

$$C\,(bot) = C\,(top) \times e^{(ks \times X)}$$

where C_{top} is the concentration of NH_4^+, NO_2^- and NO_3^- at the top of the reach (mg N L^{-1}), k_s is the uptake rate coefficient per unit reach length (m^{-1}) and X is the length of the selected reach (i.e., 700 m, in this case). Third, we considered that the amount of NH_4^+, NO_2^- and NO_3^- either removed from or released to the water column by each particular habitat was the difference between C_{bot} and C_{top} (Δc, mg N L^{-1}). Finally, the habitat-specific uptake rates (U_i) were calculated following (Webster and Valett, 2006) and reach weighted.

$$Ui = \Delta c * \left(\frac{Q}{stream\ surface * surface\ (compartment)}\right)$$

where Q is the discharge as measured *in situ* (L s^{-1}), *stream surface* (m^2) is the total surface area of the reach (467 m^2, in this case), and *surface (compartment)* (m^2) represents the percent of reach surface area covered by each habitat type (55% for epilithic biofilms and 100% for sediments). All calculations were repeated for each of the nine sampling days conducted from March to September 2013 to provide statistical consistency (Table 8.1).

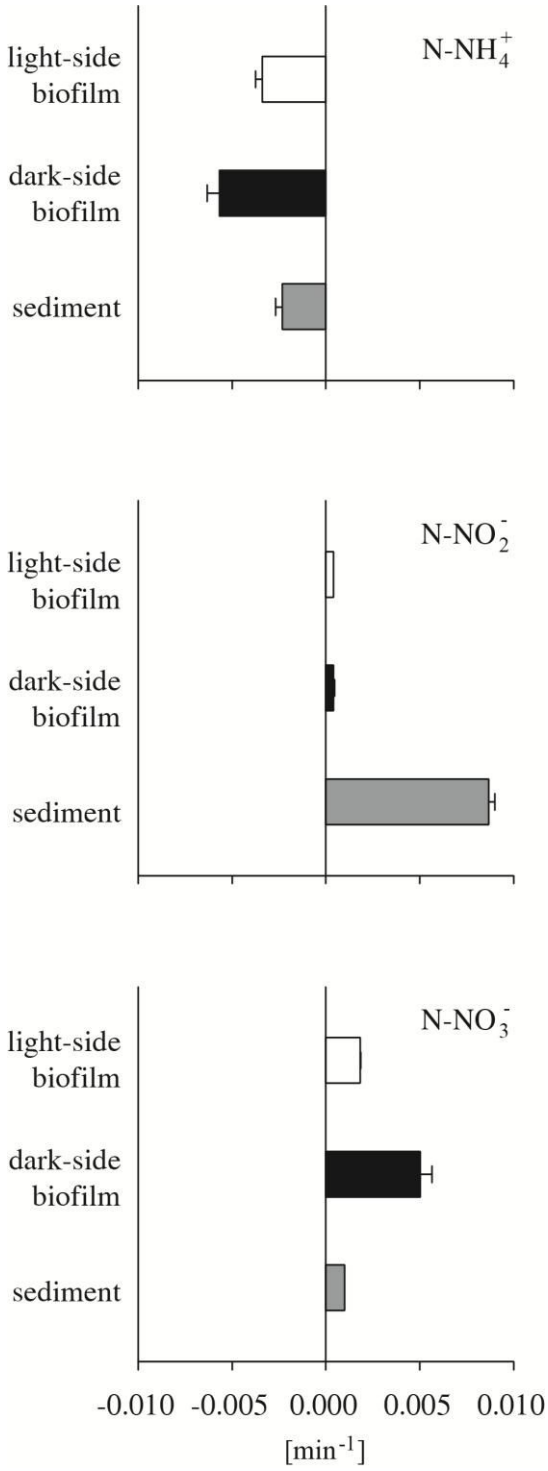

Figure 8.6: Habitat-specific N dynamics for $N\text{-}NH_4^+$ – left panel, $N\text{-}NO_2^-$ – middle panel and $N\text{-}NO_3^-$ – right panel. Bars chart indicate mean uptake rate coefficients (min^{-1}) for epilithic biofilms from light-side, dark-side of the cobbles and episamic biofilm from the sediment (n=3). Lines above the bars indicate the standard error of the mean. Data are from the mesocosm experiment in chapter 6. Sediment data presented with permission of A. Segarra, Master Thesis (2014), University of Girona. All experiments were carried out in darkness and under similar recirculation conditions.

According to these calculations, dark-side biofilm accounted for the largest amount of NH_4^+ uptake (46 %) at whole-reach scale, while light-side biofilms and sediments accounted for 31 % and 23 %, respectively (Figure 8.7). Thus, the scale-up of habitat-specific N uptake rates unveiled an unexpected result and highlighted the key importance of dark-side biofilms at whole-reach scale. Moreover, nitrification was higher in dark-side biofilms with major production rate of NO_3^- per m² (68 %), while light-side biofilm and sediment accounted for the 21 % and 11 % of released NO_3^-, respectively (Figure 8.7). Surprisingly the sediments contributed to the highest release of NO_2^- (94 %), and NO_2^- release by the epilithic biofilms was negligible. However, the total release of NO_2^- represented only 3 % of total DIN uptake rates, while the release of NO_3^- accounted for 68 % of total DIN uptake. At the whole-reach scale, the two types of epilithic biofilms, especially those on the dark-side were unveiled as the main habitats releasing NO_3 (Figure 8.7).

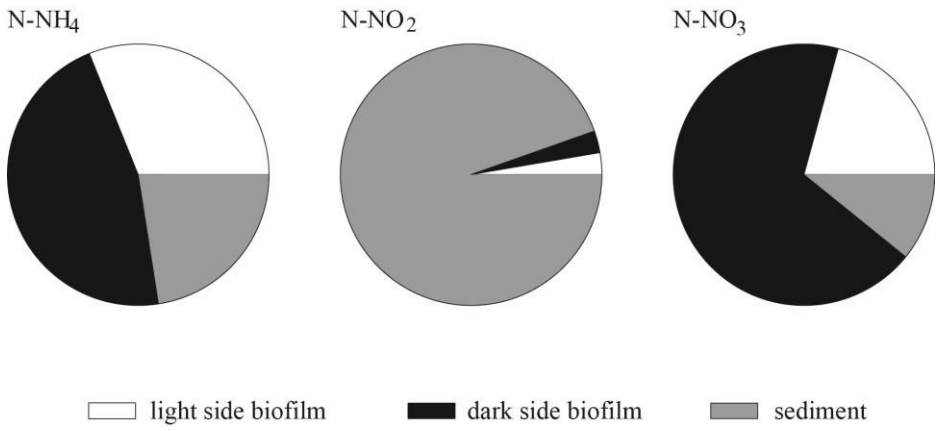

Figure 8.7: Whole-reach weighted habitat-specific uptake rates for $N\text{-}NH_4^-$ – left panel, release rates for $N\text{-}NO_2^-$ – middle panel and for $N\text{-}NO_3^-$ – right panel. Rates are expressed in mg N m^{-2} s^{-1}. White – biofilm on light-side, black – biofilms on dark-side and grey – biofilms in the sediment.

Table 8.1: Physical and chemical data from the Tordera downstream of the WWTP input of Santa Maria Palautordera. Over the period of May to September 2013, 9 longitudinal samplings along a 800-m reach beginning at 100 m downstream of the WWTP effluent were carried out. Along this reach samples were collected at 100 m intervals. On each sampling date and at each sampling site we measured discharge, water width, conductivity and velocity, and collected water sample as previously described Merbt et al. (2011). Water samples were immediately filtered using a 0.7µm pore size glass-fiber filter and analyzed following colorimetric standard procedures (APHA, 1995). Values indicate the mean of the different sampling sites. BS – background sampling.

	unit	BS1	BS2	BS3	BS4	BS5	BS6	BS7	BS8	BS9
date, 2013		7-05	13-05	21-05	4-06	11-06	18-06	25-06	5-08	27-09
discharge	$L\ s^{-1}$	597	200	752	208	212	120	89	19	21
wetted width	m	5.5	5.2	6.5	4.9	4.6	4.3	4.3	4	4.5
velocity	$m\ s^{-1}$	0.53	0.37	0.49	0.29	0.29	0.18	0.18	0.19	0.19
Conductivity	$\mu S\ cm^{-2}$	182	166	161	224	217	325	281	530	533
Temperature	°C	14	15	13	15	16	19	19	--	21
NH_4^+	$mg\ N\ L^{-1}$	0.21	0.49	0.25	0.35	0.23	0.79	1.03	1.07	0.23
NO_3^-	$mg\ N\ L^{-1}$	0.74	0.91	0.42	1.11	1.30	2.44	2.93	3.12	3.52

These calculations indicate that the relative contribution of ammonia oxidizers within the sediments to whole-reach nitrification is disproportionally lower than expected based on their abundance at reach scale, suggesting a low nitrification activity of these biofilms under in situ conditions. This can be explained by differences in chemical conditions between epilithic and episamic biofilms possibly related to differences in water column exchange with sediments that can drive nutrient availability and oxygen conditions in the sediments.

The hydrologic exchange between water column and the sediments is controlled by the channel morphology with higher transient storage in pools compared to riffle and run zones (Gücker and Boëchat, 2004). If surface-sediment hydrologic exchange is low the replenishment of sediment with surface nutrients and oxygen is constrained, which leads to low metabolic activity in stream sediments, and hence, a reduced contribution of this compartment to whole-reach metabolis (Jones and Holmes, 1996). This is in line with the dominance of AOA in the sediments, which are able to develop in low oxygen and NH_4^+ environments (Molina et al., 2010; Hatzenpichler, 2012). This idea is further supported by the fact that in sediments release of NO_2^- predominated over release of NO_3^-, suggesting the limitation of nitrite oxidizing bacteria in this habitat. Overall, these results support the idea that differing chemical conditions between epilithic and episamic biofilms can drive spatial heterogeneity of nitrification within the stream reaches (Lücker et al., 2010, Prosser and Nicol, 2008, 2012).

In turn, the complex three dimensional structures of epilithic biofilms provide voids and flow pathways in the channel system to transport water and solutes through the structure, leading to high water and solute transient storage capacity (Battin et al., 2003). Therefore, epilithic biofilms have been recently claimed as important compartment for nutrient processing in streams (Battin et al., 2003; Teissier et al., 2007; O'Brien and Dodds, 2008). These structural characteristics

induce differences in chemical condition, which probably drive the observed differences in relative abundance of AOA and AOB and associated activity.

We acknowledge that the up-scaling exercise we have proposed here provides many weaknesses and can be biased because data are based on mesocosm values of biofilms developed under optimal conditions for nitrification. To evaluate the goodness of our calculations, we compared the sum of the scale up habitat-specific aereal uptake rates to net DIN uptake rates obtained from changes in ambient N concentrations along the 700-m reach of La Tordera river. The sum of the habitat-specific areal uptake rate was two times higher for NH_4^+ and NO_3^- release rates than the net areal N uptake rates calculated from the longitudinal profiles (Table 8.2).

Table 8.2. Net areal N uptake rates at whole-reach scale obtained from ambient longitudinal patterns in N concentrations and sum of scale-up habitat-specific uptake rates from empirical calculation exercise (data from Figure 8.7).

mg N m^{-2} s^{-1}	net-areal uptake rates at whole-reach scale	Sum of habitat-specific scale-up rates
NH_4^+	0.011 ± 0.003	0.029
NO_2^-	not detected	0.003
NO_3^-	0.028 ± 0.007	0.067

This difference was expected because at whole-reach scale nutrients are transported downstream and do not remain in place in the same way as in the mesocosms. In addition, measures in the mesocosms basically reflected gross processing rates, due to the fact that they responded to the spike additions of NH_4^+, whereas in the longitudinal profiles we measured net rates. Moreover, at whole-stream scale multiple processes may influence N concentrations, which are not taken into account in the mesocosms experiments (Webster et al., 2003), and counterbalance the net longitudinal changes in the stream. However, our

data were within the same range as previous studies from pristine streams draining lands with heterogeneous uses, giving additional support to our empirical findings (Hall and Tank, 2003; Arango et al., 2008).

The up-scaling exercise unveiled the relevance of dark-side epilithic biofilms as nitrifying hotspots at reach scale in high N loaded urban streams. This suggests that further research should include the activity of the highly diverse microbial assemblages at reach-scale to fully understand and predict N cycling in lotic systems. Overall, by linking mechanistic and functional approaches of nitrifying assemblages, the investigations carried out in this PhD thesis have shown the mechanism why urban streams are hot spots of nitrification, which enable the transformation of high NH_4^+ loads, deriving from human activities, into NO_3^- loads downstream. Despite nitrifiers were ubiquitously distributed in the stream reach, epilithic biofilms were unveiled as a suitable habitat for ammonia oxidizers to settle and to drive in-stream nitrification, especially of WWTP-receiving streams.

8.5 General conclusions

- AOA and AOB are nearly ubiquitously present in stream biofilms, from early to mature stage, ands growing both on the light exposed upper side (light-side) and the sediment facing side (dark-side) of the cobbles.
- Their spatial segregation, community composition, and activity depend on NH_4 availability due to different NH_4 affinities; and secondly it depends on irradiance, due to intrinsic photoinhibition of both, AOA and AOB.
- WWTP effluents were an allochthonous source of both AOA, essentially from the *Nitrosotalea cluster*, and AOB, mainly *Nitrosomonas oligotropha*, *Nitrosomonas communis*, and *Nitrosospira* spp. changing the relative abundance and the natural composition of ammonia oxidizing assemblages of the WWTP-receiving streams.
- Downstream of the WWTP inputs, AOA shifted population composition and AOB abundance increased by orders of magnitude within stream biofilms suggesting AOB were more adapted to colonize streams with high nutrient concentrations.
- In laboratory cultures, AOA and AOB were significantly inhibited by light and AOB showed better ability to recover.
- AOA and AOB embedded in the biofilm matrix were similarly inhibited by light. However, active archaeal and bacterial ammonia oxidation was measured under illumination indicating an umbrella effect by the biofilm matrix.
- Due to this light avoiding strategy the intrinsic susceptibility to light of AOA and AOB did not have implications for in-stream nitrification at whole reach scale. However, we were able to show that nitrification rates within the reach show a spatial heterogeneity distribution associated to habitat-specific conditions.

8.6 References

Arango, C., Tank, J., Johnson, L., and Hamilton, S. (2008) Assimilatory uptake rather than nitrification and denitrification determines nitrogen removal patterns in streams of varying land use. *Limnology and Oceanography* 53: 2558–2572.

Auguet, J.-C., Barberan, A., and Casamayor, E.O. (2009) Global ecological patterns in uncultured Archaea. *ISME J* 4: 182-190.

Battin, T.J., Kaplan, L.A., Denis Newbold, J., and Hansen, C.M.E. (2003) Contributions of microbial biofilms to ecosystem processes in stream mesocosms. *Nature* 426: 439-442.

Battin, T.J., Sloan, W.T., Kjelleberg, S., Daims, H., Head, I.M., Curtis, T.P., and Eberl, L. (2007) Microbial landscapes: new paths to biofilm research. *Nat Rev Micro* 5: 76-81.

Beman, J.M., Popp, B.N., and Alford, S.E. (2012) Quantification of ammonia oxidation rates and ammonia-oxidizing archaea and bacteria at high resolution in the Gulf of California and eastern tropical North Pacific Ocean. *Limnol Oceanogr* 57: 711-726.

Bernhardt, E.S., Hall Jr, R.O., and Likens, G.E. (2002) Whole-system estimates of nitrification and nitrate uptake in streams of the Hubbard Brook Experimental Forest. *Ecosystems* 5: 419-430.

Besemer, K., Singer, G., Quince, C., Bertuzzo, E., Sloan, W., and Battin, T.J. (2013) Headwaters are critical reservoirs of microbial diversity for fluvial networks. *Proceedings of the Royal Society B: Biological Sciences* 280.

Butturini, A., Battin, T.J., and Sabater, F. (2000) Nitrification in stream sediment biofilms: the role of ammonium concentration and DOC quality. *Water Research* 34: 629-639.

Cebron, A., Berthe, T., and Garnier, J. (2003) Nitrification and Nitrifying Bacteria in the Lower Seine River and Estuary (France). *Appl Environ Microbiol* 69: 7091-7100.

Chain, P., Lamerdin, J., Larimer, F., Regala, W., Lao, V., Land, M. et al. (2003) Complete genome sequence of the ammonia-oxidizing bacterium and obligate chemolithoautotroph Nitrosomonas europaea. *Journal of Bacteriology* 185: 2759-2773.

Dahm, C.N., Grimm, N.B., Marmonier, P., Valett, H.M., and Vervier, P. (1998) Nutrient dynamics at the interface between surface waters and groundwaters. *Freshwater Biology* 40: 427-451.

Daims, H., and Wagner, M. (2011) 8 In Situ Techniques and Digital Image Analysis Methods for Quantifying Spatial Localization Patterns of Nitrifiers and Other Microorganisms in Biofilm and Flocs. *Methods in enzymology* 496: 185.

Di, H., Cameron, K., Shen, J.P., Winefield, C., O'Callaghan, M., Bowatte, S., and He, J. (2009) Nitrification driven by bacteria and not archaea in nitrogen-rich grassland soils. *Nature Geoscience* 2: 621-624.

Fernàndez-Guerra, A., and Casamayor, E.O. (2012) Habitat-Associated Phylogenetic Community Patterns of Microbial Ammonia Oxidizers. *PLoS ONE* 7: e47330.

Gieseke, A., Nielsen, J.L., Amann, R., Nielsen, P.H., and De Beer, D. (2005) In situ substrate conversion and assimilation by nitrifying bacteria in a model biofilm. *Environmental Microbiology* 7: 1392-1404.

Gücker, B., and Boëchat, I.G. (2004) Stream morphology controls ammonium retention in tropical headwaters. *Ecology* 85: 2818-2827.

Hall, R.O., Jr., and Tank, J.L. (2003) Ecosystem Metabolism Controls Nitrogen Uptake in Streams in Grand Teton National Park, Wyoming. *Limnology and Oceanography* 48: 1120-1128.

Hatzenpichler, R. (2012) Diversity, physiology and niche differentiation of ammonia-oxidizing archaea. *Applied and Environmental Microbiology*.

Hatzenpichler, R., Lebedeva, E.V., Spieck, E., Stoecker, K., Richter, A., Daims, H., and Wagner, M. (2008) A moderately thermophilic ammonia-oxidizing crenarchaeote from a hot spring. *Proceedings of the National Academy of Sciences* 105: 2134-2139.

Herrmann, M., Scheibe, A., Avrahami, S., and Küsel, K. (2011) Ammonium Availability Affects the Ratio of Ammonia-Oxidizing Bacteria to Ammonia-Oxidizing Archaea in Simulated Creek Ecosystems. *Applied and Environmental Microbiology* 77: 1896-1899.

Hooper, A.B., and Terry, K.R. (1974) Photoinactivation of Ammonia Oxidation in Nitrosomonas. *J Bacteriol* 119: 899-906.

Jones, J.B., and Holmes, R.M. (1996) Surface-subsurface interactions in stream ecosystems. *Trends in ecology & evolution* 11: 239-242.

Jones, J.B., Fisher, S.G., and Grimm, N.B. (1995) Nitrification in the hyporheic zone of a desert stream ecosystem. *Journal of the North American Benthological Society*: 249-258.

Koops, H.-P., Purkhold, U., Pommerening-Röser, A., Timmermann, G., and Wagner, M. (2006) The Lithoautotrophic Ammonia-Oxidizing Bacteria. In *The Prokaryotes*. Dworkin, M., Falkow, S., Rosenberg, E., Schleifer, K.-H., and Stackebrandt, E. (eds): Springer New York, pp. 778-811.

Leininger, S., Urich, T., Schloter, M., Schwark, L., Qi, J., Nicol, G.W. et al. (2006) Archaea predominate among ammonia-oxidizing prokaryotes in soils. *Nature* 442: 806-809.

Levi, P.S., Tank, J.L., Tiegs, S.D., Chaloner, D.T., and Lamberti, G.A. (2013) Biogeochemical transformation of a nutrient subsidy: salmon, streams, and nitrification. *Biogeochemistry* 113: 643-655.

Lücker, S., Wagner, M., Maixner, F., Pelletier, E., Koch, H., Vacherie, B. et al. (2010) A Nitrospira metagenome illuminates the physiology and evolution of globally important nitrite-oxidizing bacteria. *Proceedings of the National Academy of Sciences* 107: 13479-13484.

Martens-Habbena, W., Berube, P.M., Urakawa, H., de la Torre, J.R., and Stahl, D.A. (2009) Ammonia oxidation kinetics determine niche separation of nitrifying Archaea and Bacteria. *Nature* 461: 976-979.

Martí, E., Riera, J., and Sabater, F. (2010) Effects of Wastewater Treatment Plants on Stream Nutrient Dynamics Under Water Scarcity Conditions. In *Water Scarcity in the Mediterranean*. Sabater, S., and Barceló, D. (eds): Springer Berlin Heidelberg, pp. 173-195.

Merbt, S.N., Jean-Christophe Auguet, Emilio O. Casamayor, and Martı, E. (2011) Biofilm recovery in a wastewater treatment plant-influenced stream and spatial segregation of ammonia-oxidizing microbial populations. *Limnol Oceanogr* 56: 1054–1064

Merbt, S.N., Stahl, D.A., Casamayor, E.O., Martí, E., Nicol, G.W., and Prosser, J.I. (2012) Differential photoinhibition of bacterial and archaeal ammonia oxidation. *FEMS Microbiology Letters* 327: 41-46.

Merbt, S.N., Auguet, J.-C., Blesa, A., Martí, E., and Casamayor, E. (2014) Wastewater Treatment Plant Effluents Change Abundance and Composition of Ammonia-Oxidizing Microorganisms in Mediterranean Urban Stream Biofilms. *Microbial Ecology*: 1-9.doi: 10.1007/s00248-014-0464-8

Molina, V., Belmar, L., and Ulloa, O. (2010) High diversity of ammonia-oxidizing archaea in permanent and seasonal oxygen-deficient waters of the eastern South Pacific. *Environmental Microbiology* 12: 2450-2465.

Mußmann, M., Ribot, M., Schiller, D., Merbt, S.N., Augspurger, C., Karwautz, C. et al. (2013) Colonization of freshwater biofilms by nitrifying bacteria from activated sludge. *FEMS Microbiology Ecology* 85: 104-115.

Nicol, G.W., Sven, L., Christa, S., and James, I.P. (2008) The influence of soil pH on the diversity, abundance and transcriptional activity of ammonia oxidizing archaea and bacteria. *Environmental Microbiology* 10: 2966-2978.

O'Brien, J.M., and Dodds, W.K. (2008) Ammonium uptake and mineralization in prairie streams: chamber incubation and short-term nutrient addition experiments. *Freshwater Biology* 53: 102-112.

Prosser, J.I., and Nicol, G.W. (2008) Relative contributions of archaea and bacteria to aerobic ammonia oxidation in the environment. *Environmental Microbiology* 10: 2931-2941.

Prosser, J.I., and Nicol, G.W. (2012) Archaeal and bacterial ammonia-oxidisers in soil: the quest for niche specialisation and differentiation. *Trends in Microbiology* **20**: 523-531.

Restrepo-Ortiz, C.X., Auguet, J.-C., and Casamayor, E.O. (2014) Targeting spatiotemporal dynamics of planktonic SAGMGC-1 and segregation of ammonia-oxidizing thaumarchaeota ecotypes by newly designed primers and quantitative polymerase chain reaction. *Environmental Microbiology* 16: 689-700.

Schramm, A., De Beer, D., Gieseke, A., and Amann, R. (2000) Microenvironments and distribution of nitrifying bacteria in a membrane-bound biofilm. *Environmental Microbiology* 2: 680-686.

Schramm, A., Larsen, L.H., Revsbech, N.P., Ramsing, N.B., Amann, R., and Schleifer, K.H. (1996) Structure and function of a nitrifying biofilm as determined by in situ hybridization and the use of microelectrodes. *Applied and Environmental Microbiology* 62: 4641-4647.

Sonthiphand, P., Cejudo, E., Schiff, S.L., and Neufeld, J.D. (2013) Wastewater Effluent Impacts Ammonia-Oxidizing Prokaryotes of the Grand River, Canada. *Applied and Environmental Microbiology* 79: 7454-7465.

Spang, A., Hatzenpichler, R., Brochier-Armanet, C., Rattei, T., Tischler, P., Spieck, E. et al. (2010) Distinct gene set in two different lineages of ammonia-oxidizing archaea supports the phylum Thaumarchaeota. *Trends in Microbiology* 18: 331-340.

Strauss, E.A., Mitchell, N.L., and Lamberti, G.A. (2002) Factors regulating nitrification in aquatic sediments: effects of organic carbon, nitrogen availability, and pH. *Canadian Journal of Fisheries and Aquatic Sciences* 59: 554-563.

Teissier, S., Torre, M., Delmas, F., and Garabétian, F. (2007) Detailing biogeochemical N budgets in riverine epilithic biofilms. . *Journal of the North American Benthological Society* 26: 178-190.

Walker, C., De La Torre, J., Klotz, M., Urakawa, H., Pinel, N., Arp, D. et al. (2010) Nitrosopumilus maritimus genome reveals unique mechanisms for nitrification and autotrophy in globally distributed marine crenarchaea. *Proceedings of the National Academy of Sciences* 107: 8818-8823.

Webster, J., and Valett, H. (2006) Solute dynamics. In *Methods in stream ecology*. Hauer FR, and Lamberti GA, E. (eds). San Diego, USA: Academic Press, pp. 169-185.

Webster, J.R., Mulholland, P.J., Tank, J.L., Valett, H.M., Dodds, W.K., Peterson, B.J. et al. (2003) Factors affecting ammonium uptake in streams–an inter-biome perspective. *Freshwater Biology* 48: 1329-1352.

Widder, S., Besemer, K., Singer, G.A., Ceola, S., Bertuzzo, E., Quince, C. et al. (2014) Fluvial network organization imprints on microbial co-occurrence networks. *Proceedings of the National Academy of Sciences* 111: 12799-12804.

Yool, A., Martin, A.P., Fernandez, C., and Clark, D.R. (2007) The significance of nitrification for oceanic new production. *Nature* 447: 999-1002.

Appendix 1: Publication Chapter 1

Limnol. Oceanogr., 56(3), 2011, 1054–1064

doi:10.4319/lo.2011.56.3.1054

Biofilm recovery in a wastewater treatment plant-influenced stream and spatial segregation of ammonia-oxidizing microbial populations

Stephanie N. Merbt,* Jean-Christophe Auguet, Emilio O. Casamayor, and Eugènia Martí

Biogeodynamics & Biodiversity Group, Centre d'Estudis Avançats de Blanes (CSIC), Blanes, Spain

Abstract

We monitored the effects of wastewater treatment plant (WWTP) inputs on the recovery of stream biofilms after a large flood event that eroded most of the former biofilm communities. We monitored biomass recovery, chlorophyll *a*, nitrogen content, and stable isotope natural abundance (^{15}N) over 8 weeks in light- and dark-exposed biofilms upstream and downstream from WWTP inputs, respectively, as well as the abundance of ammonia oxidizers by quantitative polymerase chain reaction. Biomass and chlorophyll *a* recovered quickly (< 2 weeks), and were significantly higher for light- than for dark-exposed biofilms. There was no consistent effect of WWTP inputs on these parameters, except for the biomass on dark-exposed biofilm that was higher at the WWTP-influenced sites. The influence of the WWTP inputs on stream-water ammonium concentration and its isotopic ^{15}N signature increased as the flood receded. Biofilm ^{15}N downstream of WWTP increased over time, tracking the increase in ^{15}N-ammonium from the WWTP waters. Bacterial and archaeal ammonia oxidizers were present within the biofilm assemblages from early stages of postflood recovery. However, spatial distribution of these two clades was clearly segregated among sites and between light- and dark-exposed biofilms, probably related to ammonium availability and the development of photoautotrophic organisms.

Streams transport dissolved and particulate materials from adjacent terrestrial ecosystems to larger rivers and coastal zones. Human activity alters stream nutrient concentrations through nutrient-rich sources through point (e.g., effluents from wastewater treatment plants [WWTP]) or diffuse (e.g., from agricultural activities) inputs. In urban areas, nutrient point sources can be a significant cause of the urban stream syndrome (Walsh et al. 2005). High nutrient concentrations in WWTP-influenced streams lead to decreasing nutrient retention efficiency and loss of species diversity, which ultimately results in eutrophication of downstream ecosystems (Martí et al. 2004; Camargo and Alonso 2006; Sánchez-Pérez et al. 2009). However, these streams have also been reported as hot spots for microbial nitrification when they are subjected to large inputs of ammonium (NH_4^+) from the WWTPs (Merseburger et al. 2005). In the Mediterranean region, both water scarcity, a common feature that drives the hydrological regime of these streams, and relatively constant anthropogenic inputs from WWTPs have a very pronounced effect on stream ecology and biogeochemistry because of the reduced diluting capacity (Martí et al. 2010). Moreover, the Intergovernmental Panel to Climate Change has predicted for the Mediterranean region consistent decreases in precipitation and annual runoff (Bates et al. 2008), which will further exacerbate the local effects of anthropogenic inputs.

Increases in nitrogen concentration (mainly NH_4^+) are commonly observed in streams loaded with inputs from urban WWTP effluents (Martí et al. 2010). NH_4^+ is the preferential N source for primary uptake and a potential limiting nutrient for stream communities (Borchardt 1996; Hall and Tank 2003). However, even at relatively low concentrations, NH_4^+ can be highly toxic to aquatic organisms, whereas at high concentrations it may promote eutrophication (Camargo and Alonso 2006). Stream microbial communities (biofilms) can play a key role controlling bioreactive N loads since microbes mostly mediate the processes of N transformation and retention (Peterson et al. 2001; Falkowski et al. 2008; Mulholland et al. 2008). In benthic ecosystems, biofilms are a substrata-attached, matrix-embedded, complex mixture of algae, bacteria, fungi, and microzoans (Lock et al. 1984; Battin et al. 2003). Their three-dimensional layer structure, compositional heterogeneity, and biomass accrual depend on flow velocity, light, and nutrient availability (Besemer et al. 2007; von Schiller et al. 2007; Singer et al. 2010). Microbial diversity and identity in biofilms determine the efficiency at which N is uptaken and transformed; and thus, it may influence N biogeochemistry at the whole-reach scale (Loreau et al. 2001; Prosser et al. 2007).

Understanding both the structure of the biofilm and how it processes N inputs can provide insights on the mechanisms driving global stream N cycling. In particular, excess of NH_4^+ inputs can be biologically modulated by both assimilation and microbial nitrification associated with biofilms (Merseburger et al. 2005). Nitrification is a key process in highly N-loaded streams since the end product (i.e., nitrate; NO_3^-) can be further transformed under anaerobic conditions into N_2 gas through denitrification, which finally results in a net loss of N to the atmosphere. Microbial nitrification is a two-step oxidation process of NH_4^+ to NO_3^- via nitrite (NO_2^-). Ammonia oxidation is the rate-limiting step of nitrification. This step is carried out by two phylogenetically distant groups, which include three genera of the Bacteria domain (*Nitrosomonas, Nitrosococcus,* and *Nitrosospira;* Koops and Pommerening-Röser 2001) and a few recently described members of the domain Archaea, apparently restricted to the highly diverse *Thaumarchaeota* phylum (Spang et al. 2010). Both bacterial

* Corresponding author: smerbt@ceab.csic.es

and archaeal ammonia oxidizers encode for the alpha subunit of the enzyme ammonium mono-oxygenase; however, the gene sequence is different enough to easily distinguish ammonia-oxidizing archaea (AOA) from bacteria (AOB).

In the present study, we examined the patterns of biofilm development from emerging to mature communities in a WWTP-influenced stream after an unusually high flood disturbance. Development of the biofilm was separately examined for communities coating the light- and dark-exposed sides of cobbles since we expected they would differently respond to the influence of WWTP inputs. For this study we followed a multiparametric approach considering several structural and biogeochemical parameters. To the best of our knowledge, there is a lack of combined stream ecology and microbial ecology studies addressing the development, structure, and function of biofilm communities in high-N-loaded streams. The information provided here is relevant for understanding the fate of external N inputs, especially in WWTP-influenced streams.

Methods

Study site—The study was conducted in La Tordera river catchment (41°41′3.47″N, 2°27′33.19″W; NE Spain) from January to March 2009. We selected a 850-m reach along the mainstream located near the village of Santa Maria de Palautordera, which receives the inputs from the local WWTP effluent (population 8235 inhabitants). The WWTP was not submitted to tertiary treatment and had a partial nitrifying capacity. Over the study period, average concentrations of NO_3^- and NH_4^+ in the WWTP effluent were 4.9 ± 2.6 mg N L^{-1} and 5.7 ± 1.7 mg N L^{-1}, respectively, and average effluent outflow was 32.6 ± 5.5 L s^{-1} (data provided by the Santa Maria de Palautordera WWTP management agency). A previous study indicated that the selected reach was a hot spot for chemotrophic activity (i.e., nitrification; Merseburger et al. 2005). The reach had a channel with low sinuosity and a slope close to 1%. The streambed substrate was dominated by cobbles (34%), pebbles (22%), and boulders (22%). Three sampling sites were defined along the reach on the basis of the distance to the WWTP. The first sampling site was located 75 m upstream of the point source (hereafter referred to as UP) and was used as the reference site. The other two sampling sites were located 150 m and 850 m downstream from the WWTP input, respectively (hereafter referred to as DW1 and DW2, respectively). These two sites were selected to represent different availabilities of NO_3^--N and NH_4^+-N due to the high rates of nitrification previously observed along this reach (Merseburger et al. 2005). Thus, dominance of NH_4^+-N was expected at DW1, whereas dominance of NO_3^--N was expected at DW2.

Early in January 2009, a large storm event lasting 2 weeks caused an abrupt and remarkable increase in stream discharge, which completely eroded the biofilm from the surface of cobbles. The sampling sites were sampled weekly from 23 January to 23 March (a total of eight sampling dates). During this period, stream flow gradually decreased, except from the occurrence of another rainfall event between the third (30 January 2009) and fourth (09 February 2009) sampling weeks, which resulted in another flood of minor intensity.

Field measurements and sample collection—On each sampling date, discharge was estimated at sites UP and DW2 by measuring both water depth and velocity at 50-cm intervals, respectively, using a tape and a velocity meter (Schiltknecht Messtechnik) in a selected channel transect. Water temperature and conductivity were measured at all sites using a portable conductivity meter (WTW Weilheim).

At each site we collected 5-liter water samples for the analysis of NO_3^--N and NH_4^+-N, and their respective ^{15}N isotope signatures. The samples were stored on ice for less than 2 h and once in the laboratory were immediately filtered through ignited glass fiber filters (FVF; 0.7-μm pore size, Albet). Biofilm samples from riffle areas were collected from the surface of six randomly selected, fist-sized submerged cobbles not embedded into the sediment. Biofilm samples from the light-exposed side of the cobble (hereafter referred to as light side) and from the reverse side of the cobble facing the sediment (hereafter referred to as dark side) were separately treated.

For the measurement of biofilm biomass (expressed as ash-free dry mass [AFDM]), chlorophyll *a* (Chl *a*), N content, and ^{15}N isotopic signature, biofilm was sampled from three cobbles by scraping their surface and filtering the sludge onto ignited, preweighted glass fiber filters (FVF). The total surface scraped was estimated after covering cobbles with aluminum foil and following a weight-to-area relationship. Filters for Chl *a* analysis were stored at −20°C, whereas the remaining filters were dried (60°C) until constant weight (ca. 0.1 mg, Sartorius analytical balance, model MC1). For the quantification of the ammonia oxidizers, the biofilm of three additional cobbles was washed with MilliQ-water, scratched, and pooled together in a single 250-mL plastic beaker. All samples were transported to the laboratory on ice within 2 h after sampling.

Laboratory methods—NH_4^+-N concentration was analyzed with a Nova 60 Spectroquant (Merck) with the photometric ammonium test (Merck, 1.14752.0001). This method was sensitive enough for this analysis considering the high in situ concentrations. The concentration of NO_3^--N was analyzed using a Bran+Lubbe Aace 5.23 Technicon Autoanalyzer (Scientific-Technical Services). The two analyses were carried out following standard colorimetric methods (APHA 1995). The ^{15}N natural abundance of NH_4^+ and NO_3^- in the water was determined following the ammonia diffusion protocol by Holmes et al. (1998) and the sequential reduction and diffusion method by Sigman et al. (1997), respectively, as described in von Schiller et al. (2009). Briefly, a certain volume of filtered water sample containing ca. 100 μg of NH_4^+-N was poured into a high-density polyethylene (HDPE) bottle, and further amended with 3.0 g L^{-1} MgO, 50 g L^{-1} NaCl, and a Teflon filter packet, which contained a 1-cm-diameter ashed glass fiber filter (GF/D grade, Whatman,

Kent), acidified with 25 μL of 2.5 M $KHSO_4$. Water bottles were tightly capped and incubated in a shaker at 40°C for 4 weeks to allow the diffusion of volatilized NH_3 onto the acidified filter. To analyze ^{15}N natural abundance of NO_3^-, a volume of water sample containing ca. 100 μg of NO_3^--N was poured into a beaker; and it was amended with 3.0 g of MgO and 5.0 g of NaCl and boiled to remove the NH_4^+ and to concentrate the sample. The sample was then transferred into a HDPE bottle to which 0.5 g of MgO, 0.5 g of Devarda's alloy, and a Teflon filter packet were added. Bottles were tightly capped and incubated at 60°C for 48 h to reduce NO_3^- to NH_4^+, and then they were placed on a shaker for 7 d to allow for diffusion of NH_3 onto the acidified filter. Once the incubations were completed, filters were removed from the bottles, placed in scintillation vials, dried in a desiccator for 4 d, encapsulated in tins, and stored until ^{15}N analysis. A set of blanks and standards of known concentration for ^{15}N-NH_4^+ and ^{15}N-NO_3^- were processed along with the water samples.

To estimate AFDM (in g m^{-2}), biofilm samples collected on glass fiber filters were combusted at 500°C for 5 h and weighted as indicated above. The AFDM was estimated as the mass difference between dry and combusted filters and was reported per unit of surface area. Chl *a* (in μg cm^{-2}) was determined in acetone extracts by spectrophotometry (UV-2401PC, ultraviolet–visible spectrometer, Shimadzu) following Steinman and Lamberti (1996), and corrected for phaeopigments by further acidification. A subsample of the glass fiber filters (i.e., 1-cm-diameter) was placed in scintillation vials, dried in a desiccator for 4 d, weighted, encapsulated in tins, and stored until ^{15}N analysis. The filters for ^{15}N and N content analysis of NH_4^+, NO_3^-, and biofilm were sent to the University of California Stable Isotope Facility (Davis). The analysis was done by continuous-flow isotope ratio mass spectrometry (20–20 mass spectrometer; PDZ Europa) after sample combustion in an on-line elemental analyzer (PDZ Europa, ANCA-GSL). The ^{15}N content of the samples is reported as the $^{15}N:{}^{14}N$ ratio of the sample relative to the $^{15}N:{}^{14}N$ ratio of the standard (N_2 from the atmosphere) using the notation $\delta^{15}N$ (in ‰).

Deoxyribonucleic acid (DNA) extraction and quantification of ammonia-oxidizing microorganisms—A subset of selected biofilm samples from light and dark sides of sites UP, DW1, and DW2, and sampling weeks 1, 6, and 8 was processed. Microorganisms were detached from particles by incubation with Tween 20 detergent (10^{-6} % w v^{-1}) for 5 min followed by soft sonication (Sonopuls ultrasonic homogenizer HD 2070) with 20-s pulses at 10% power (Epstein and Rossel 1995). Supernatant was filtered through a 0.2-μm pore size polycarbonate membrane (Millipore). Filters were incubated with lysozyme, proteinase K, and sodium dodecyl sulfate in lysis buffer (40 mmol L^{-1} ethylenediaminetetra-acetic acid, 50 mmol L^{-1} Tris, pH 8.3, and 0.75 mol L^{-1} sucrose), and phenol-extracted as previously described (Dumestre et al. 2002).

Presence and quantification of AOB and AOA was based on *amoA* gene copy numbers estimated by quantitative real-time polymerase chain reaction (qPCR) amplification. The qPCR assays were run on 96-well transparent plates with adhesive seals (Bio-Rad) in a DNA Engine thermal cycler (Bio-Rad, Hercules) equipped with a Chromo 4 Real-Time Detector (Bio-Rad). The AOB primers amoA-1F (5′-GGGTTTCTACTGGTGGT-3′) and amoA-2R (5′-CCCCTCKGSAAAGCCTTCTTC-3′) generated a 491 base-pair (bp) fragment (Rotthauwe et al. 1997). The AOA primer sets CrenamoA23f (5′-ATGGTCTGGCTWAGACG-3′) and CrenamoA616r (5′-GCCATCCATCTGTATGTCCA-3′) amplified a 628-bp fragment (Tourna et al. 2008). The selected primer sets had been previously tested in the qPCR approach (Wessén et al. 2009). The quantification was run in a final volume of 20 μL containing a 10-μL solution of SsoFast EvaGreen supermix (BioRad), 20 ng of template genomic DNA, 10 μmol L^{-1} of each corresponding primer, and molecular biology-grade water (Sigma). The reaction started with an initial denaturation step of 2 min at 98°C, followed by 45 cycles of denaturation at 98°C for 5 s, annealing at 58°C for *amoA* of AOB and 57°C for *amoA* of AOA, respectively for 20 s, and elongation at 72°C for 15 s. Fluorescence signal was read after each elongation step. Finally, a denaturation step was done for 1 min at 98°C followed by 1 min at 65°C to ensure stringent coupled DNA fragments. All reactions were finished with a melting curve starting at 55°C and increasing by 0.5°C until 95°C to verify amplicon specificity. Each approach was run in triplicate with standard curves spanning from 10^2 to 10^8 copies of DNA *amoA* genes. Standards were obtained after conventional PCR amplification of available environmental clones. The standard was purified (QIAquick, QIAGEN), quantified (Qubit fluorometer, Invitrogen), and serially diluted for standard curves (r^2 = 0.99 for both standard curves). Overall, average efficiencies of all quantification reactions ranged from 74% to 99%. Controls without templates resulted in undetectable values in all samples. Specificity of the PCR reactions was confirmed by agarose gel electrophoresis (data not shown). No unspecific PCR products such as primer dimers or gene fragments of unexpected length were observed. The results of the qPCR analysis are expressed in copies of *amoA* per g of AFDM (i.e., organic matter) of the biofilm to allow comparison of results among sampling sites, cobble sides, and sampling dates.

Statistical analysis. The effect of the WWTP inputs on stream N concentration was assessed by comparing NH_4^+-N and NO_3^--N concentrations and their ^{15}N signatures among sites over the study period using a Kruskal–Wallis ANOVA nonparametric test (site as a factor). This test was also used to compare AOA and AOB *amoA* gene copy numbers on light- and dark-side biofilms between the sampling sites (side as a factor). Spearman rank *R* nonparametric correlations were used to examine relationships among hydrology, N concentrations, and ^{15}N signatures of dissolved inorganic N (DIN) forms. Comparison of AFDM, Chl *a* content, N content, and ^{15}N natural abundance among sites and between samples from light and dark sides was done using two-way ANOVA tests (site and cobble side as factors) with repeated measures (sampling week as the within effect). This allowed testing of the WWTP effect on the biofilms of both sides of cobbles

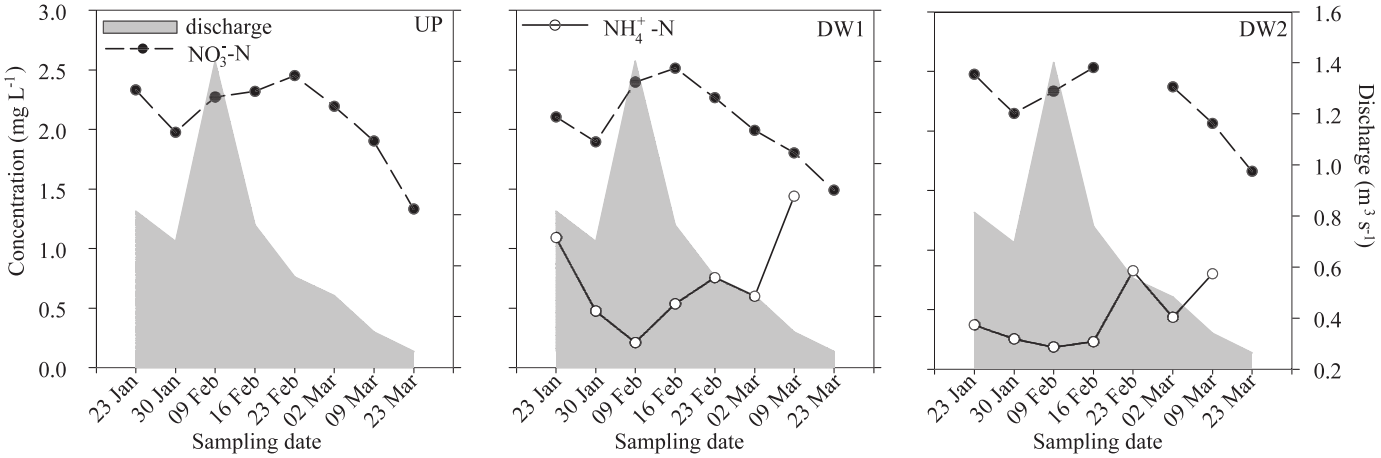

Fig. 1. Temporal variation in discharge (shaded area), and NH_4^+-N (white dots) and NO_3^--N (black dots) concentrations during the study period at UP, DW1, and DW2. Missing data are lost samples. NH_4^+-N concentration at UP site was below detection limits.

considering the patterns of temporal variation of the dependent variables after the flood disturbance. The test was done on Ln-transformed values to fit statistical requirements of normality. ^{15}N signatures of DIN forms and those of biofilms at each site were compared using a Wilcoxon matched pair test on data from light- and dark-side biofilm samples separately. Finally, relationships between temporal variation of ^{15}N signatures of DIN forms and those of biofilm were examined using Spearman rank R nonparametric correlations. For these last two tests we used average ^{15}N biofilm values from the three replicates collected on each date at each site and from each cobble side. Results were considered significant for $p < 0.05$. All statistical analyses were done using Statistica 6.0 (Statsoft).

Results

Physical and chemical parameters—Water discharge consistently decreased over time after the intense rainfalls of early January (Fig. 1). During the third sampling week, another storm event increased stream discharge again up to ~ 1.4 m^3 s^{-1}. By the end of the sampling period, despite observing a significant decrease in discharge, it was still relatively high compared with typical base flow levels (ca. < 0.1 m^3 s^{-1}). Conversely, the WWTP effluent discharge was relatively constant over the study period (data from the WWTP management agency) and its contribution to downstream discharge ranged from 2.3% at the beginning to 11.5% at the end of the study. As a result of this variation, discharge at UP and DW2 sites was similar at the beginning of the study, but it tended to be higher below the WWTP by the end of the study. At the UP site, water temperature decreased from 8.5°C to 6.2°C over the first sampling weeks, with a minimum value on the third sampling week, after the second flood. After this event, temperature gradually increased up to 9°C by the end of the study (data not shown). The pattern of temporal variation in water temperature was similar for all sites, but values were on average (± 1 SEM) 1.1°C ± 0.4°C higher at the DW1 and DW2 sites than at the UP site. Conductivity ranged between 88.5 and 132.7 μS cm^{-1} and had no clear temporal pattern at any site, although at the UP site it tended to decrease by the end of the study period. On average, conductivity was 1.4 times lower at the UP site than at the DW1 and DW2 sites (Kruskal–Wallis ANOVA, $p < 0.001$).

NO_3^--N concentration was already high at the UP site (i.e., $\sim$ 2 mg N L^{-1}, Fig. 1) and no significant differences were found among the three sites (Kruskal–Wallis ANOVA, $p > 0.05$). Temporal variation of NO_3^--N concentration was similar among sites and it was positively correlated with discharge (Spearman correlation, $n = 24$, $r = 0.65$, $p < 0.001$). Conversely, NH_4^+-N concentration was clearly affected by the WWTP input. At the UP site, NH_4^+-N concentration was consistently below detection limit (i.e., < 0.01 mg N L^{-1}). Downstream of the WWTP, NH_4^+-N concentration was significantly higher (Fig. 1), ranging from 0.2 to 1.4 mg N L^{-1} over the entire study period with no significant differences between DW1 and DW2 (Kruskal–Wallis ANOVA, $p > 0.05$). The N input from the WWTP represented an average increase in DIN concentration below the WWTP of 1.4 times the upstream concentration. It also represented a shift in the relative proportion of DIN as NO_3^--N from 99.9% at the UP site to 79.5% at the downstream sites. At these sites, temporal variation in NH_4^+-N concentration was negatively correlated with NO_3^--N concentration (Spearman correlation, $n = 14$, $r = -0.67$, $p = 0.008$) and with discharge (Spearman correlation, $n = 14$, $r = -0.63$, $p = 0.016$).

The $\delta^{15}N$ values of NO_3^--N in the water column had no significant variation both among sites (Kruskal–Wallis, $p > 0.05$) and over time (Fig. 2). Taking all sites and dates together, the average (± 1 SEM) of $\delta^{15}N$-NO_3^- was 5.75‰ ± 0.17‰. The $\delta^{15}N$ values of NH_4^+-N in the water column were significantly lower at the UP site than at the two downstream sites (Kruskal–Wallis, $p = 0.004$). No significant difference in $\delta^{15}N$-NH_4^+ was found between DW1 and DW2. At the UP site, the $\delta^{15}N$-NH_4^+ was relatively constant over time and averaged −4.92‰ ± 0.61‰ (Fig. 2). At the downstream sites, the $\delta^{15}N$-NH_4^+ increased over time from 14.1‰ to 29.5‰ at DW1 and from 10.7‰

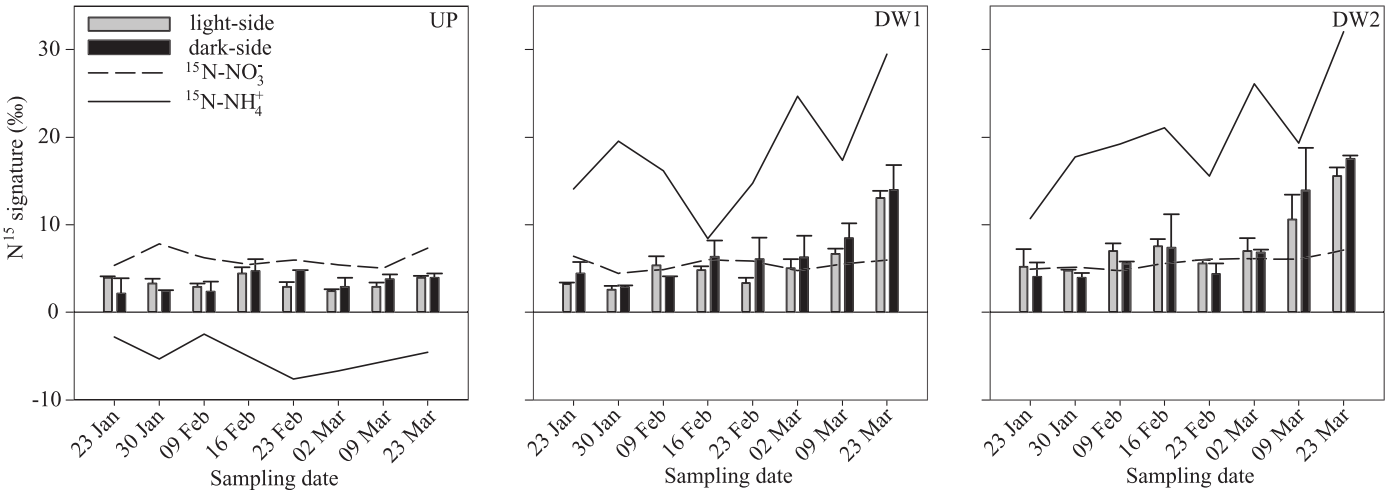

Fig. 2. Temporal variation in ^{15}N natural abundance (expressed as $\delta^{15}N$ in ‰) of both dissolved inorganic N forms in water and biofilms during the study period at UP, DW1, and DW2. Graphs show the mean values ($n = 3$) for biofilms on the light (gray bars) and dark (black bars) sides of cobbles. Lines above the bars are the standard error of the mean. Dotted line shows ^{15}N natural abundance of nitrate, and continuous line shows ^{15}N natural abundance of ammonium.

to 32.0‰ at DW2. The $\delta^{15}N\text{-}NH_4^+$ at these two sites was negatively correlated with stream discharge (Spearman correlation, $n = 16$, $r = -0.60$, $p = 0.013$).

Biofilm characterization—Biofilm biomass (expressed as AFDM) increased over time at all sites (Fig. 3). However, the increases in AFDM were more evident for biofilms on the light side, which showed a faster recovery after the flood, than on the dark side. For instance, 1 week after the flood, biofilm AFDM on the light side had increased by 75% at the UP site. After the fourth sampling week, AFDM accrual on the light side stabilized, reaching similar values at all sites. However, at the DW2 site, light-side AFDM decreased tremendously on the last two sampling weeks. Significant differences (two-way ANOVA) in AFDM accrual were found between light- and dark-side biofilms, but not among sites (Table 1). However, when sites were compared, we found that dark-side, but not light-side, biofilms had significantly higher AFDM at the downstream sites than at the UP site (one-way ANOVA, $p = 0.011$).

Chl *a* showed slightly different accrual patterns from those observed for AFDM (Fig. 3). As expected, the light-side biofilms showed significantly higher Chl *a* content than the dark-side biofilms (Table 1). Results from the two-way ANOVA with repeated measures also indicated a significant effect of the sampling date on Chl *a*, which varied among sites (Table 1). At the UP site, a nearly exponential increase of Chl *a* was observed over the study period in the light-side biofilm (Fig. 3). At the DW1 and DW2 sites, Chl *a* reached steady state after the fifth sampling week (Fig. 3). Chl *a* content in the dark-side biofilm was higher at DW2 than at DW1 and UP sites (Table 1).

Sampling site, side of the cobble, and sampling date had all significant effects on the biofilm N content (as a percentage of dry weight), with no significant interactions among these factors (two-way ANOVA with repeated measures, Table 1). N percentage in biofilms gradually increased over time at all sites (Fig. 3), and was 2.5 times higher in the light-side than in the dark-side biofilms for all sites. In addition, N percentage in light- and dark-side biofilms at the DW1 and DW2 sites (average 2.0% in light side and 0.9% in dark side) was 1.5 and 1.9 times higher, respectively, than at the UP site (average: 1.3% in light side and 0.5% in dark side).

We observed a significant interaction effect among the three factors considered (sampling site, side of the cobble, and sampling time) on the biofilm $\delta^{15}N$ (two-way ANOVA with repeated measures, Table 1). The $\delta^{15}N$ values showed different temporal patterns at each sampling site, but no significant differences between the light and dark sides of the cobbles (Fig. 2). At the UP site, the $\delta^{15}N$ values of dark- and light-side biofilms were similar and relatively stable over time, and averaged 3.35‰ ± 0.85‰ (Fig. 2). This value was significantly lower than $\delta^{15}N\text{-}NO_3^-$ (6.07‰ ± 1.00‰, Wilcoxon matched pair test, $p = 0.012$) and higher than $\delta^{15}N\text{-}NH_4^+$ (−4.94‰ ± 0.61‰; Wilcoxon matched pair test, $p = 0.012$). At the downstream sites, values of biofilm $\delta^{15}N$ were similar to those at the UP site during the first four sampling weeks (Fig. 2). From the fifth week onward, in contrast to the steady biofilm $\delta^{15}N$ values of the UP site, values at the downstream sites gradually increased on both cobble sides (Fig. 2). This temporal pattern of biofilm $\delta^{15}N$ was more pronounced at the DW2 site (Fig. 2). Finally, biofilm $\delta^{15}N$ of both the light and dark sides of cobbles at the downstream sites was similar to $\delta\ ^{15}N\text{-}NO_3^-$ (Wilcoxon matched pair test, $p > 0.05$) and lower than $\delta\ ^{15}N\text{-}NH_4^+$ (Wilcoxon matched pair test, $p = 0.011$). Nevertheless, the temporal variation in $\delta\ ^{15}N$ of biofilm at these two sites was positively correlated with $\delta^{15}N\text{-}NH_4^+$ (Spearman correlations, $n = 16$, $r = 0.65$, $p = 0.007$ for the light side; and $n = 16$, $r = 0.52$, $p = 0.040$ for the dark-side) and not correlated with $\delta\ ^{15}N\text{-}NO_3^-$.

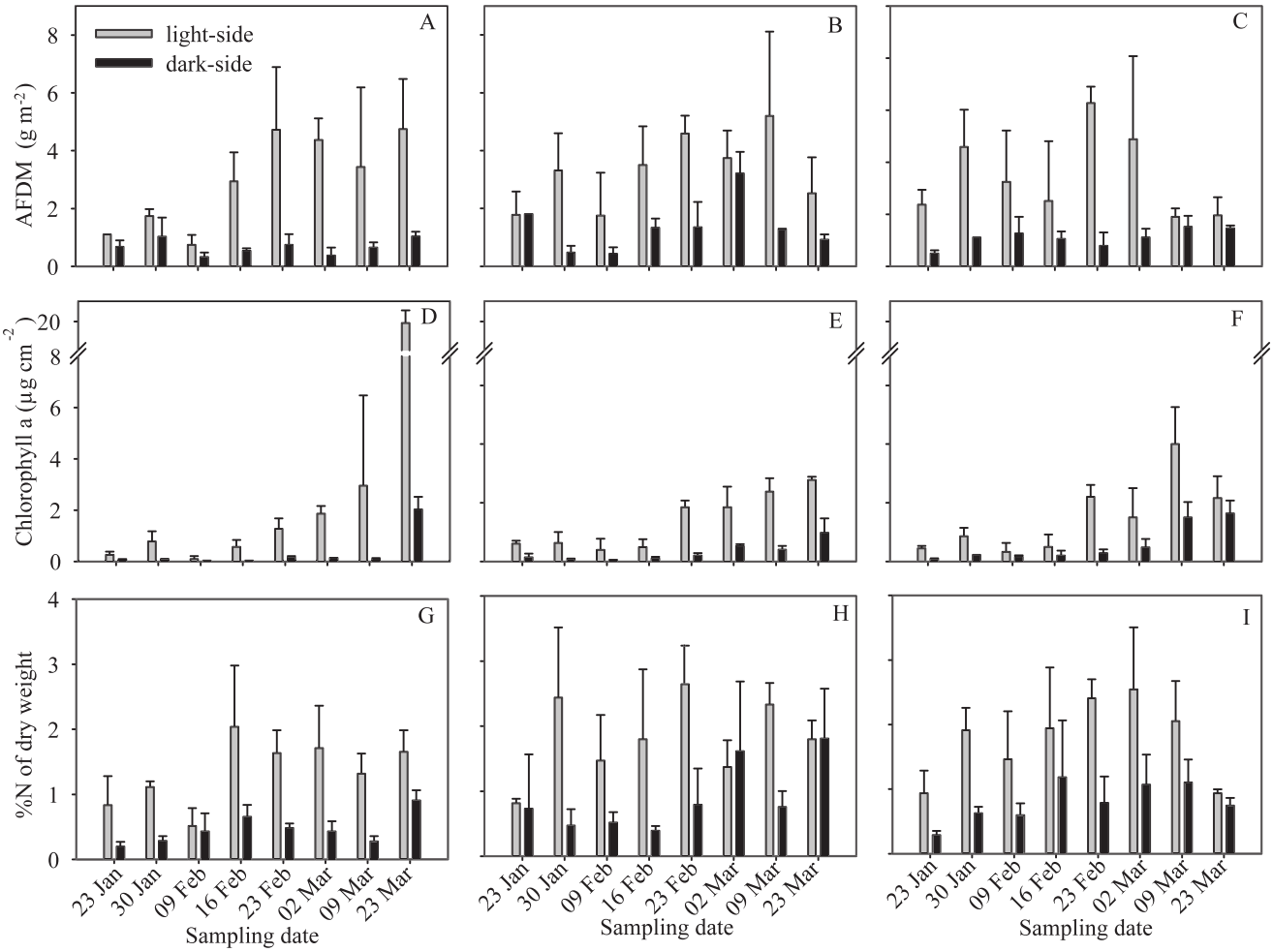

Fig. 3. Temporal variation in AFDM, chlorophyll *a* content, and N content during the study period at the (A, D, G) UP, (B, E, H) DW1, and (C, F, I) DW2 sites. Graphs show the mean values ($n = 3$) for biofilms on the light (gray bars) and dark (black bars) sides of cobbles. Lines above the bars are the standard error of the mean.

Ammonia-oxidizing microbial assemblages—Results from qPCR indicated presence of ammonia oxidizer populations in all sites. However, *amoA* relative abundance and patterns of distribution among sites and cobble sides largely differed between AOB and AOA (Fig. 4). AOB were only detected at downstream sites and were significantly more abundant in dark- than in light-side biofilms (Kruskal–Wallis, $p = 0.002$). In addition, a*moA* copies of AOB from the dark-side biofilms were higher at DW2 than at DW1; and in the dark-side of DW2 a*moA* copies gradually increased over the study period.

Conversely, AOA were detected at both upstream and downstream sites. The relative number of *amoA* gene copies tended to be more abundant in the dark- than in the light-side biofilms (Fig. 4). This pattern is clearly consistent for samples from the DW2 site, where we observed the highest abundance of AOA, especially in the dark side of the cobbles.

Discussion

Influence on water chemistry—This study started under high flow conditions when downstream transport of nutrients usually dominates over in-stream nutrient uptake or transformation (Peterson et al. 2001; Argerich et al. 2008). Under these conditions, even though the dilution capacity of the stream was extraordinarily high, the influence of the WWTP input was still remarkable. High NH_4^+-N and NO_3^--N concentrations measured in the WWTP effluent indicated that this was a relevant source of DIN to the stream. However, the influence of the WWTP input was more pronounced for NH_4^+-N, which increased by two orders of magnitude, than for NO_3^--N concentrations. Probably this is because upstream of the WWTP NH_4^+-N load was very low, whereas NO_3^--N load was already high. Similar results have been reported by other studies in WWTP-influenced streams under base-flow conditions (Martí et al. 2004, 2010; Carey and Migiaccio 2009). Therefore, although NH_4^+-N concentration was mostly controlled by WWTP inputs, NO_3^--N concentration was controlled by soil runoff from the upstream catchment. The WWTP input also increased the ^{15}N signature of NH_4^+-N. This effect became more evident as discharge decreased. Stable isotopes have been successfully used to identify anthropogenic N sources in aquatic ecosystems because of their different ^{15}N signals (Lajtha

Table 1. Statistical results from two-way ANOVAs with repeated measures for biofilm AFDM, chlorophyll *a* content, N content (as percentage of dry weight), and ^{15}N as dependent variables. Independent factors were sampling site (i.e., UP, DW1, and DW2) and side of the cobble (i.e., light and dark), and sampling date was considered as a within-effect factor. Values highlighted in bold indicate factors or interaction among factors with significant effects (i.e., $p < 0.05$).

	AFDM		Chlorophyll *a*		%N		^{15}N	
	F	*p*	*F*	*p*	*F*	*p*	*F*	*p*
Intercept	22.6	**0.02**	484.6	**0.00**	0.0	0.85	11896.3	**0.00**
Site	3.0	0.19	2.0	0.23	7.7	**0.02**	324.2	**0.00**
Part	31.6	**0.01**	209.0	**0.00**	111.0	**0.00**	1.8	0.31
Site × part	0.7	0.57	9.3	**0.02**	1.2	0.35	18.4	0.05
Week	2.5	0.05	13.5	**0.00**	4.2	**0.00**	49.4	**0.00**
Week × site	1.4	0.22	2.9	**0.01**	0.8	0.64	9.8	**0.00**
Week × part	1.5	0.22	0.6	0.74	0.9	0.50	9.4	**0.00**
Week × site × part	1.6	0.16	1.5	0.16	0.4	0.98	7.2	**0.00**

and Michener 1994). Previous measurements of $\delta^{15}N$ in the study of WWTP effluent for NH_4^+ and NO_3^- were 13.6–27.8‰ and 2.7–10.3‰, respectively (M. Ribot pers. comm.), indicating that DIN, especially NH_4^+, derived from the WWTP effluent was highly enriched in ^{15}N species. This is in agreement with previous studies (Robinson 2001; deBruyn and Rasmussen 2002), and supports the use of ^{15}N signatures of DIN forms in WWTP-influenced streams as tracers of WWTP-derived N.

Recovery of stream biofilm communities—Temporal changes of both stream hydrology and the relative influence of the WWTP inputs lead to a structural and functional response of the biofilm communities. In general, biofilm recovery was fast (i.e., 15 d) regardless of the site location. As the flood receded, biomass and Chl *a* content gradually increased and reached nearly steady state after 1.5 months at all sites. Temperature, light, and hydrological regime have been identified as important factors in algal and bacterial succession in river biofilms (Lyautey et al. 2005). At high flow conditions, such as in this study, early biofilms show low biomass accrual, whereas mature communities can show a decrease of biomass because of surface detachment (Battin et al. 2003; Rickard et al. 2004). Therefore, biofilm biomass is temporally variable and undergoes successive accumulation, autogenic sloughing, and externally caused physical disturbances. These processes lead to the observed equilibrium in which accumulation and losses of biomass became relatively balanced (Biggs 1996). However, despite biofilms reaching steady-state biomass, their influence on water-column DIN concentrations along the downstream reach was negligible because no differences were observed either in NH_4^+-N or NO_3^--N concentrations or in their ^{15}N signatures between the DW1 and DW2 sites probably because of the high discharge. This result clearly contrasts with previous findings in WWTP-influenced streams during low flow conditions in which significant declines of NH_4^+ and increases of NO_3^- concentrations and changes in their ^{15}N signature have been observed along downstream reaches (Merseburger et al. 2005; Lofton et al. 2007).

Our study also showed different recovery patterns between light- and dark-side biofilms, showing a differential spatial effect of WWTP inputs. As expected, biomass accrual on the dark side was much lower than on the light-exposed biofilms. Biofilms on the light side reached similar steady-state biomass accrual at all sites regardless of differences in N concentrations. Only at the end of the study did we observe a consistent reduction of biomass at the DW2 site compared with the other sites. This decrease was likely due to high densities of macroinvertebrate grazers observed only at the DW2 site. Patterns of Chl *a* in light-side biofilms were also similar among sites and indicated an increasing proportion of photoautotrophic organisms over the study period. Lack of differences in biomass and Chl *a* accrual among sites in the light-side biofilms could be explained by the fact that availability of DIN was already high upstream of the WWTP. In addition, riparian vegetation was leafless and sunlight reached stream surface along the study reach. Therefore, light-side communities of the different sites were neither limited by nutrient availability nor by light availability.

However, biomass accrual on the dark side was significantly higher at downstream than at upstream sites. This suggests that the additional N source from the WWTP favored the development of chemotrophic communities on the dark-exposed sides. Biofilms below the WWTP had a higher percentage of N content, indicating that they were able to incorporate a fraction of the WWTP-supplied N. However, the light-side biofilm contained 2.5 times more N than the dark-side. This difference may be due to the ability of algae, which were restricted to the light side of cobbles, to store nutrients such as N and phosphorus in very high concentrations in their vacuoles (luxury consumption) when it is not immediately required for growth (Sterner and Elser 2002).

The biofilm ^{15}N signature is a net result of all enzyme-driven N transformations carried out by the organisms and the degree of isotope fractionation associated with each process (Sulzman 2007). The boundary layer effect can be an additional physical factor leading to isotopic fractionation (MacLeod and Barton 1998). Therefore, we expected clear differences in ^{15}N between light- and dark-side communities, especially in late stages of recovery, on the basis of the observed differences in AFDM, Chl *a*, and N content between the two communities at all sites. However, the results did not fit this expectation since light- and dark-side ^{15}N signatures were similar at each site. This similarity

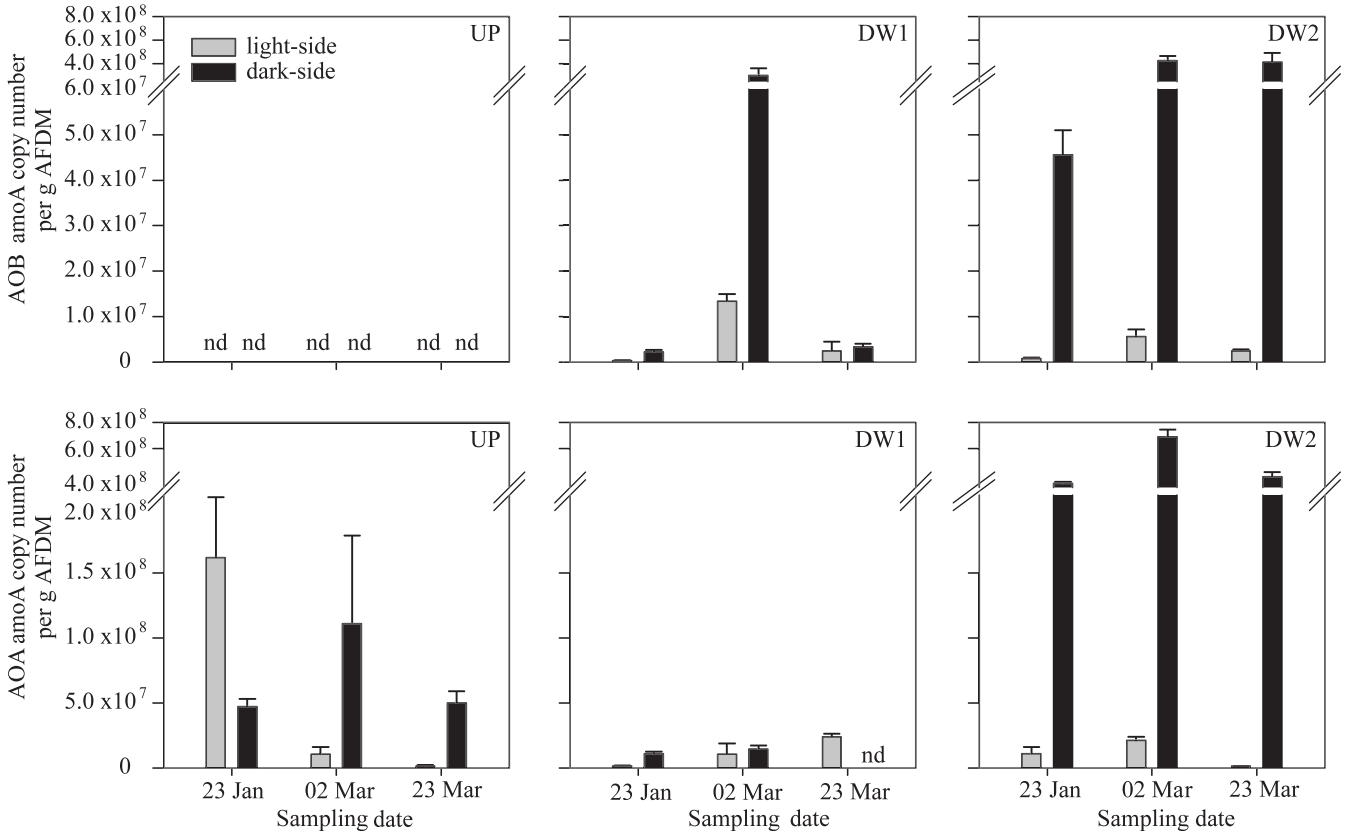

Fig. 4. Temporal variation of bacterial and archaeal *amoA* copy number per gram of AFDM of the biofilm during the study period at UP, DW1, and DW2. Data shown correspond to sampling weeks 1 (23 January), 6 (02 March), and 8 (23 March). Graphs show the mean values of methodological replicates ($n = 3$) for biofilms on the light (gray bars) and dark (black bars) sides of cobbles. Lines above the bars are the standard error of the mean. At the UP site no bacterial *amoA* was detected over the study period. nd, not detected.

in ^{15}N signatures may indicate similar N sources and assimilation pathways and rates in the two communities. However, this may be unlikely because photoautotrophic organisms were restricted to light-side communities, whereas ammonia oxidizers were more abundant in the dark-side biofilm. These consistent differences in community composition more probably result in differences in N uptake rates at the community level. Alternatively, the different fractionation occurring in the two communities could have been somehow compensated, resulting in similar ^{15}N signatures. Thus, for instance, the light-side biofilms could have been subjected to a higher boundary layer effect because of their higher biomass accrual, whereas fractionation associated with nitrification, which is widely known (Casciotti et al. 2003; Marshall et al. 2007; Baggs 2008), could have been more relevant in dark-side biofilms. Nevertheless, to our knowledge there is a lack of studies addressing the potential contrast of ^{15}N signatures in biofilms and the mechanisms driving it at this microhabitat scale to further support these hypotheses. Studies on later development stages during base-flow conditions may provide further insights as the biofilm matures and becomes even more distinct because of spatial segregation of resources and habitats (Jackson 2003). In contrast, biofilm ^{15}N differed among study sites following to the differences observed for ^{15}N signatures of NH_4^+ and NO_3^-, which were basically driven by the WWTP input. At the UP site, biofilm ^{15}N signatures were closely related to those of NO_3^-, regardless of biofilm structural changes over the study period. At sites downstream of the WWTP input, biofilm ^{15}N signatures were similar to those of NO_3^- after the flood, but became more similar to those of NH_4^+ as discharge decreased and the influence of WWTP on NH_4^+ concentration was more pronounced. Overall, these results suggest a shift in the relative importance of NH_4^+ over NO_3^- utilization as a N source of biofilms between upstream and downstream sites, as well as over time at downstream sites. This provides further evidence of the biofilm capacity to regulate N inputs from point sources in these high-N-loaded streams.

Distribution of ammonia-oxidizing microorgamisms in the biofilm—Our results showed that ammonia-oxidizing microorganisms were present in the biofilms at all sites since early recovery stages, suggesting that in addition to photoautotrophic assimilation, nitrification could potentially contribute to the regulation of NH_4^+ loads downstream of the WWTP. This supports the hot-spot nitrification nature of high-NH_4^+-loaded streams reported by previous studies (Merseburger et al. 2005; Martí et al. 2010).

The ammonia-oxidizing community in stream biofilms has been poorly studied, and former studies focused on the abundance and diversity of either bacteria (Wakelin et al.

2008) or archaea (Weidler et al. 2008; Herfort et al. 2009). Here, these phylogenetically separated but physiologically related populations were simultaneously detected coexisting in the biofilm assemblage. We observed, however, marked spatial differences in the relative abundance of these populations in a very short stream distance (i.e., < 1 km), suggesting the existence of distinct physiological characteristics and ecological niches as previously proposed (Nicol et al. 2008). Thus, although AOA were found to be ubiquitous at nearly all sites and on both sides of cobbles, AOB were restricted to downstream sites and mostly found at the dark side of cobbles. This distribution could be explained by a combination of factors operating at the stream reach and biofilm community scales. Low NH_4^+ concentration at the upstream site may be a limitation for AOB colonization. In addition, the WWTP effluent may also be a source of ammonia oxidizers and particularly of AOB as they represent the main nitrifying microorganisms in activated sludge (Wells et al. 2009). AOB from the effluent may easily colonize the downstream biofilm communities mostly at the dark cobble sides because of the intolerance to light caused by photo-oxidation of cytochrome *c* complex (Prosser 1989). We cannot rule out either the poor competition capacity of AOB against algae for NH_4^+ in the presence of light. In fact, there has been a report of a decrease in nitrification activity and in abundance of AOB with increasing algae biomass in sediment biofilm mats (Risgaard-Petersen et al. 2004). Finally, as biofilms increased in thickness, the diffusion of solutes from the water into the biofilm may be reduced. For instance, a 10-cell-thick biofilm would have 100 times longer diffusion times than that of a cell alone (Stewart 2003). Therefore, NH_4^+-N and O_2 concentrations can become limiting in situ within the biofilm despite the high concentrations present in the water column, triggering competition among AOB, heterotrophic prokaryotes, and photosynthetic organisms. This limitation was likely more relevant in light-side biofilms than in dark-side biofilms because of the highest biomass present in the former. Overall, these results indicate that dark-side conditions downstream of the WWTP are the most favorable for AOB because biofilm layer was thinner, photoautotrophic organisms were rare, and NH_4^+-N concentrations were high.

Unfortunately, for AOA in particular and for archaea in general (Auguet et al. 2010), there is a lack of comprehensive physiological information due to the lack of pure cultures in the laboratory. Recently Martens-Habbena et al. (2009) have shown that the ammonia-oxidizing archaeon *Nitrosupumilus maritimus* SCM1, and probably AOA in general, may have a remarkably high affinity for NH_4^+ that easily outcompetes AOB and heterotrophic organisms under NH_4^+-limiting conditions. This high affinity for NH_4^+ may explain why AOA were found in all samples including those from the upstream site where NH_4^+ concentration was very low. This finding is confirmed by former studies from other environments, (i.e., oligotrophic marine waters) where AOA are the main ammonia-oxidizing microorganisms, outnumbering AOB by orders of magnitude (Beman et al. 2010). The abundance of AOA was in general much higher in dark-side than in light-side biofilm except on the first sampling date, suggesting either intolerance to light or strong competition with other biofilm microorganisms, or both. Further investigations focused on the specific identity and activity of AOA and AOB populations are certainly needed to both explain the observed patterns and the spatial distribution within the biofilms and to easily scale from the cell-level mechanisms to the whole-reach stream processes.

In this study we have shown that biofilm recovery was fast after an important hydrological disturbance, and that it was differentially affected by the continuous N inputs from a WWTP outflow. Thus, we found that biofilm structural properties (AFDM, Chl *a*) were less affected by WWTP inputs than their biogeochemical properties associated with N cycling (N content and ^{15}N signature), and that the effects were more pronounced for microbial communities that developed on the dark side of cobbles. In particular, we observed that the input of a WWTP effluent modified the stream environment, becoming more favorable for AOB at downstream sites and, at the same time, changing the dynamics of both bacterial and archaeal ammonia oxidizers in the biofilm. In the context of a future global change scenario with lower water availability, a better understanding on how stream ecosystems transform and retain human-derived nutrients and which mechanisms are driving these processes is certainly needed. The present work contributes to understanding how WWTP effluents modify both N uptake and biogeochemical transformations in streams, and shows an example of the tight link existing between stream biogeochemistry and microbial ecology.

Acknowledgments

We thank C. Gutierrez, M. Ribot, J. Pfann, L. Serrano, M. Raja, A. Poch, L. Haller, and N. Nomokonova for excellent field and laboratory assistance. We also acknowledge anonymous reviewers for valuable feedback and constructive comments on the manuscript.

This study has been granted by the following projects to E.M. and E.O.C.: Coupling biofilm diversity and ecosystem functioning: The role of COmmunication and MIXing in microbial landscapes—COMIX (European Science Foundation, Eurodiverstiy Collaborative Research Program, ref: 05_EDIV_FP065-COMIX); Multidisciplinary research consortium on GRadual and Abrupt Climate Changes, and their Impacts on the Environment—GRACCIE (Ministerio de Educación y Ciencia, Programa Consolider, CSD2007-00067); and Biology and Ecology of uncultured freshwater archaea—PIRENA (Ministero de Ciencia e Innovación, ref: CGL2009-13318-C02-01). S.N.M. is supported by a JAE predoctoral fellowship from the Spanish National Research Council (CSIC) and J.-C.A. is supported by a Juan de la Cierva fellowship from the Ministero de Ciencia e Innovación.

References

Agerich, A., E. Martí, F. Sabater, M. Ribot, D. von Schiller, and J. L. Riera. 2008. Combined effects of leaf litter inputs and a flood on nutrient retention in a Mediterranean mountain stream during fall. Limnol. Oceanogr. **53:** 631–641, doi:10.4319/lo.2008.53.2.0631

APHA. 1995. Standard methods for the examination of water and wastewater, 19th ed. American Publishers Health Association.

Auguet, J.-C., A. Barberán, and E. O. Casamayor. 2010. Global ecological patterns in uncultured Archaea. ISME J. **4:** 182–190, doi:10.1038/ismej.2009.109

Baggs, E. M. 2008. A review of stable isotope techniques for N_2O source partitioning in soils: Recent progress, remaining challenges and future considerations. Rapid Commun. Mass Spectrom. **22:** 1664–1672, doi:10.1002/rcm.3456

Bates, B. C., Z. W. Kundzewics, S. Wu, and J. P. Palutikof [eds.]. 2008. Analyzing regional aspects of climate change and water resources, p. 77–114. *In* Climate change and water. IPCC Secretariat.

Battin, T. J., L. A. Kaplan, D. Newbold, and C. M. E. Hansen. 2003. Contributions of microbial biofilms to ecosystem processes in stream mesocosms. Nature **426:** 439–442, doi:10.1038/nature02152

Beman, J. M., S. Rohan, and J. A. Fuhrman. 2010. Population ecology of nitrifying archaea and bacteria in the Southern California Bight. Environ. Microbiol. **12:** 1282–1292, doi:10.1111/j.1462-2920.2010.02172.x

Besemer, K., G. Singer, R. Limberger, A.-K. Chlup, G. Hochedlinger, I. Hödl, C. Barany, and T. J. Battin. 2007. Biophysical controls on community succession in stream biofilms. Appl. Environ. Microbiol. **73:** 4966–4974, doi:10.1128/AEM.00588-07

Biggs, B. J. F. 1996. Patterns in bentic algae of streams, p. 31–56. *In* R. J. Stevenson, M. L. Bothwell, and R. L. Lowe [eds.], Algal ecology: Freshwater benthic ecosystem. Academic Press.

Borchardt, M. A. 1996. Nutrients, p. 183–228. *In* R. J. Stevenson, M. L. Bothwell, and R. L. Lowe [eds.], Algal ecology: Freshwater benthic ecosystem. Academic Press.

Camargo, J. A., and Á. Alonso. 2006. Ecological and toxicological effects of inorganic nitrogen pollution in aquatic ecosystems: A global assessment. Environ. Int. **32:** 831–849, doi:10.1016/j.envint.2006.05.002

Carey, R., and K. W. Migiaccio. 2009. Contribution of wastewater treatment plant effluents to nutrient dynamics in aquatic systems: A review. Environ. Manage. **44:** 205–217, doi:10.1007/s00267-009-9309-5

Casciotti, K. L., D. M. Sigman, and B. B. Ward. 2003. Linking diversity and stable isotope fractionation in ammonia-oxidizing bacteria. Geomicrobiol. J. **20:** 335–353, doi:10.1080/01490450303895

deBruyn, A. M. H., and J. B. Rasmussen. 2002. Quantifying assimilation of sewage-derived organic matter by riverine benthos. Ecol. Appl. **12:** 511–520, doi:10.1890/1051-0761(2002)012[0511:QAOSDO]2.0.CO;2

Dumestre, J. F., E. O. Casamayor, R. Massana, and C. Pedrós-Alió. 2002. Changes in bacterial and archaeal assemblages in an equatorial river induced by the water eutrophication of Petit Saut dam reservoir (French Guiana). Aquat. Microb. Ecol. **26:** 209–221, doi:10.3354/ame026209

Epstein, S., and J. Rossel. 1995. Enumeration of sandy sediment bacteria: Search for optimal protocol. Mar. Ecol. Prog. Ser. **117:** 289–298, doi:10.3354/meps117289

Falkowski, P. G., T. Fenchel, and E. F. Delong. 2008. The microbial engines that drive earth's biogeochemical cycles. Science **320:** 1034–1039, doi:10.1126/science.1153213

Hall, R. O. J., and J. Tank. 2003. Ecosystem metabolism controls nitrogen uptake in streams in Grand Teton National Park, Wyoming. Limnol. Oceanogr. **48:** 1120–1128, doi:10.4319/lo.2003.48.3.1120

Herfort, L., K. Jung-Hyun, M. Coolen, B. Abbas, S. Schouten, G. J. Herndl, and J. S. S. Damsté. 2009. Diversity of Archaea and detection of crenarchaeotal *amoA* genes in the rivers Rhine and Têt. Aquat. Microb. Ecol. **55:** 189–201, doi:10.3354/ame01294

Holmes, R. M., J. W. McClelland, D. M. Sigman, B. Fry, and B. J. Peterson. 1998. Measuring ^{15}N-NH_4^+ in marine, estuarine and fresh waters: An adaptation of the ammonia diffusion method for samples with low ammonium concentrations. Mar. Chem. **60:** 235–243, doi:10.1016/S0304-4203(97)00099-6

Jackson, C. 2003. Changes in community properties during microbial succession. Oikos **101:** 444–448, doi:10.1034/j.1600-0706.2003.12254.x

Koops, H.-P., and A. Pommerening-Röser. 2001. Distribution and ecophysiology of the nitrifying bacteria emphasizing cultured species. FEMS Microbiol. Ecol. **37:** 1–9, doi:10.1111/j.1574-6941.2001.tb00847.x

Lajtha, K., and R. H. Michener. 1994. Stable isotopes in ecology and environmental science, 1st ed. Blackwell Scientific.

Lock, M. A., R. R. Wallace, J. W. Costerton, R. M. Ventullo, and S. E. Charlton. 1984. River epilithon: Toward a structural–functional model. Oikos **42:** 10–22, doi:10.2307/3544604

Lofton, D. D., A. E. Hershey, and S. C. Whalen. 2007. Evaluation of denitrification in an urban stream receiving wastewater effluent. Biogeochemistry **86:** 77–90, doi:10.1007/s10533-007-9146-7

Loreau, M., and others. 2001. Biodiversity and ecosystem functioning: Current knowledge and future challenges. Science **294:** 804–808, doi:10.1126/science.1064088

Lyautey, E., C. R. Jackson, J. Cayrou, J. L. Rols, and F. Garabétian. 2005. Bacterial community succession in natural river biofilm assemblages. Microb. Ecol. **50:** 601, doi:10.1007/s00248-005-5032-9

MacLeod, N. A., and D. R. Barton. 1998. Effects of light intensity, water velocity, and species composition on carbon and nitrogen stable isotope ratios in periphyton. Can. J. Fish. Aquat. Sci. **55:** 1919–1925, doi:10.1139/cjfas-55-8-1919

Marshall, J. D., J. R. Brooks, and K. Lajthal. 2007. Sources of variation in the stable isotopic composition of plants, p. 1–22. *In* R. Michener and K. Lajthal [eds.], Stable isotopes in ecology and environmental science. Blackwell Scientific.

Martens-Habbena, W., P. M. Berube, H. Urakawa, J. R. de la Torre, and D. A. Stahl. 2009. Ammonia oxidation kinetics determine niche separation of nitrifying Archaea and Bacteria. Nature **461:** 976–979, doi:10.1038/nature08465

Martí, E., J. Aumatell, J. Gode, M. Poch, and F. Sabater. 2004. Nutrient retention efficiency in streams receiving inputs from wastewater treatment plants. J. Environ. Qual. **33:** 285–293, doi:10.2134/jeq2004.0285

———, J. L. Riera, and F. Sabater. 2010. Effects of wastewater treatment plants on stream nutrient dynamics under water scarcity conditions, p. 173–195. *In* S. Sabater and D. Barceló [eds.], The handbook of environmental chemistry: Water scarcity in the Mediterranean area. Springer.

Merseburger, G., E. Martí, and F. Sabater. 2005. Net changes in nutrient concentrations below a point source input in two streams draining catchments with contrasting land uses. Sci. Tot. Environ. **347:** 217–229, doi:10.1016/j.scitotenv.2004.12.022

Mulholland, P. J., and others. 2008. Stream denitrification across biomes and its response to anthropogenic nitrate loading. Nature **452:** 202–205, doi:10.1038/nature06686

Nicol, G. W., L. Sven, C. Schleper, and J. I. Prosser. 2008. The influence of soil pH on the diversity, abundance and transcriptional activity of ammonia oxidizing archaea and bacteria. Environ. Microbiol. **10:** 2966–2978, doi:10.1111/j.1462-2920.2008.01701.x

Peterson, B. J., and others. 2001. Control of nitrogen export from watersheds by headwater streams. Sci. Tot. Environ. **292:** 86–91.

Prosser, J. I. 1989. Autotrophic nitrification in bacteria, p. 125–181. *In* A. H. Rose and D. W. Tempest [eds.], Advances in microbial physiology. Academic.

———, and others. 2007. The role of ecological theory in microbial ecology. Nat. Rev. Microbiol. **5:** 384–392, doi:10.1038/nrmicro1643

Rickard, A. H., A. J. McBain, A. T. Stead, and P. Gilbert. 2004. Shear rate moderates community diversity in freshwater biofilms. Appl. Environ. Microbiol. **70:** 7426–7435, doi:10.1128/AEM.70.12.7426-7435.2004

Risgaard-Petersen, N., M. H. Nicolaisen, N. P. Revsbec, and B. A. Lomstein. 2004. Competition between ammonia-oxidizing bacteria and benthic microalgae. Appl. Environ. Microbiol. **70:** 5528–5537, doi:10.1128/AEM.70.9.5528-5537.2004

Robinson, D. 2001. δ^{15}N as an integrator of the nitrogen cycle. Trends Ecol. Evol. **16:** 153–162, doi:10.1016/S0169-5347(00)02098-X

Rotthauwe, J.-H., K.-P. Witzel, and W. Liesack. 1997. The ammonia monooxygenase structural gene *amoA* as a functional marker: Molecular fine-scale analysis of natural ammonia oxidizing populations. Appl. Environ. Microbiol. **63:** 4704–4712.

Sánchez-Pérez, J.-M., and others. 2009. Effects of wastewater treatment plant pollution on in-stream ecosystems functions in an agricultural watershed. Ann. Limnol. Int. J. Limnol. **45:** 79–92, doi:10.1051/limn/2009011

Sigman, D. M., R. Michener, D. C. McCorkle, B. Fry, and R. M. Holmes. 1997. Natural abundance-level measurement of the nitrogen isotopic composition of oceanic nitrate: An adaptation of the ammonia diffusion method. Mar. Chem. **57:** 227–242, doi:10.1016/S0304-4203(97)00009-1

Singer, G., K. Besemer, P. Schmitt-Kopplin, I. Hödl, and T. J. Battin. 2010. Physical heterogeneity increases biofilm resource use and its molecular diversity in stream mesocosms. PLoS ONE **5:** e9988, doi:10.1371/journal.pone.0009988

Spang, A., and others. 2010. Distinct gene set in two different lineages of ammonia-oxidizing archaea supports the phylum Thaumarchaeota. Trends Microbiol. **18:** 331–340, doi:10.1016/j.tim.2010.06.003

Steinman, A. D., and G. A. Lamberti. 1996. Biomass and pigments of benthic algae, p. 295–314. *In* F. R. Hauer and G. A. Lamberti [eds.], Methods in stream ecology. Academic.

Sterner, R. W., and J. J. Elser. 2002. Ecologic stoichiometry: The biology of elements from molecules to the biosphere. Princton Univ. Press.

Stewart, P. S. 2003. Diffusion in biofilms. J. Bacteriol. **185:** 1485–1491, doi:10.1128/JB.185.5.1485-1491.2003

Sulzman, E. W. 2007. Stable isotope chemistry and measurement: A primer, p. 1–14. *In* R. Michner and K. Lajatha [eds.], Stable isotopes in ecology and environmental science. Blackwell.

Tourna, M., T. E. Freitag, G. W. Nicol, and J. I. Prosser. 2008. Growth, activity and temperature responses of ammonia-oxidizing archaea and bacteria in soil microcosms. Environ. Microbiol. **10:** 1357–1364, doi:10.1111/j.1462-2920.2007.01563.x

von Schiller, D., E. Martí, and J. L. Riera. 2009. Nitrate retention and removal in Mediterranean streams bordered by contrasting land uses: a ^{15}N tracer study. Biogeosciences **6:** 181–196, doi:10.5194/bg-6-181-2009

———, ———, ———, and F. Sabater. 2007. Effects of nutrients and light on periphyton biomass and nitrogen uptake in Mediterranean streams with contrasting land uses. Freshw. Biol. **52:** 891–906, doi:10.1111/j.1365-2427.2007.01742.x

Wakelin, S. A., M. J. Colloff, and R. S. Kookana. 2008. Effect of wastewater treatment plant effluent on microbial function and community structure in the sediment of a freshwater stream with variable seasonal flow. Appl. Environ. Microbiol. **74:** 2659–2668, doi:10.1128/AEM.02348-07

Walsh, C., A. H. Roy, J. W. Feminella, P. D. Cottingham, P. M. Groffman, and R. P. Morgan. 2005. The urban stream syndrome: Current knowledge and the search for a cure. J. North Am. Benthol. Soc. **24:** 706–723.

Weidler, G. W., F. W. Gerbl, and H. Stan-Lotter. 2008. Crenarchaeota and their role in the nitrogen cycle in a subsurface radioactive thermal spring in the Austrian Central Alps. Appl. Environ. Microbiol. **74:** 5934–5942, doi:10.1128/AEM.02602-07

Wells, G. F., H.-D. Park, C.-H. Yeung, B. Eggleston, C. A. Francis, and C. S. Criddle. 2009. Ammonia-oxidizing communities in a highly aerated full-scale activated sludge bioreactor: Betaproteobacterial dynamics and low relative abundance of Crenarchaea. Environ. Microbiol. **11:** 2310–2328, doi:10.1111/j.1462-2920.2009.01958.x

Wessén, E., K. Nyberg, J. K. Jansson, and S. Hallin. 2009. Responses of bacterial and archaeal ammonia oxidizers to soil organic and fertilizer amendments under long-term management. Appl. Soil Ecol. **45:** 193–200, doi:10.1016/j.apsoil.2010.04.003

Associate editor: Ronnie Nøhr Glud

Received: 14 September 2010
Accepted: 04 February 2011
Amended: 21 February 2011

Appendix 2: Publication Chapter 2

Microb Ecol
DOI 10.1007/s00248-014-0464-8

ENVIRONMENTAL MICROBIOLOGY

Wastewater Treatment Plant Effluents Change Abundance and Composition of Ammonia-Oxidizing Microorganisms in Mediterranean Urban Stream Biofilms

Stephanie N. Merbt · Jean-Christophe Auguet · Alba Blesa · Eugènia Martí · Emilio O. Casamayor

Received: 9 May 2014 / Accepted: 9 July 2014

Abstract Streams affected by wastewater treatment plant (WWTP) effluents are hotspots of nitrification. We analyzed the influence of WWTP inputs on the abundance, distribution, and composition of epilithic ammonia-oxidizing (AO) assemblages in five Mediterranean urban streams by qPCR and *amoA* gene cloning and sequencing of both archaea (AOA) and bacteria (AOB). The effluents significantly modified stream chemical parameters, and changes in longitudinal profiles of both NH_4^+ and NO_3^- indicated stimulated nitrification activity. WWTP effluents were an allocthonous source of both AOA, essentially from the *Nitrosotalea* cluster, and mostly of AOB, mainly *Nitrosomonas oligotropha*, *Nitrosomonas communis*, and *Nitrosospira* spp. changing the relative abundance and the natural composition of AO assemblages. Under natural conditions, *Nitrososphaera* and *Nitrosopumilus* AOA dominated AO assemblages, and AOB were barely detected. After the WWTP perturbation, epilithic AOB increased by orders of magnitude whereas AOA did not show quantitative changes but a shift in population composition to dominance of *Nitrosotalea* spp. The foraneous AOB successfully settled in downstream biofilms and probably carried out most of the nitrification activity. *Nitrosotalea* were only observed downstream and only in biofilms exposed to either darkness or low irradiance. In addition to other potential environmental limitations for AOA distribution, this result suggests in situ photosensitivity as previously reported for *Nitrosotalea* under laboratory conditions.

Electronic supplementary material The online version of this article (doi:10.1007/s00248-014-0464-8) contains supplementary material, which is available to authorized users.

S. N. Merbt · J.-C. Auguet · A. Blesa · E. Martí · E. O. Casamayor (✉)
Integrative Freshwater Ecology Group, Centre of Advanced Studies of Blanes, CEAB-CSIC, Spanish Council for Scientific Research, Accés Cala St. Francesc 14, E-17300 Blanes, Spain
e-mail: casamayor@ceab.csic.es

J.-C. Auguet
Present Address: Equipe Environnement et Microbiologie, UMR CNRS-IPREM 5254, Université de Pau et des Pays de l'Adour, Pau, France

A. Blesa
Present Address: Centro de Biología Molecular Severo Ochoa (UAM-CSIC), Universidad Autónoma de Madrid, Madrid, Spain

Introduction

Nitrification is a key process in nitrogen (N) cycling of any ecosystem bridging reduced with oxidized forms of dissolved inorganic nitrogen (DIN) and affecting in situ N uptake and transformation pathways. Studies from headwater streams show that nitrification rates can vary substantially among streams; however, overall nitrification contributes to a relatively low proportion of total ammonium (NH_4^+) removed [1]. In contrast, streams affected by inputs from urban wastewater treatment plants (WWTP) may have nitrification as the most relevant N cycling process [2–5]. In general, in large rivers, WWTP effluent plumes are substantially diluted, and the main river characteristics remain mostly unaffected. However, in headwater streams, especially from arid and semiarid regions, the WWTP effluent can contribute from 3 to 100 % of total stream flow and create strong physical and chemical discontinuities [2, 3]. In fact, during low natural flow conditions, the WWTP effluent tends to dominate the stream chemistry [2, 6].

Small streams can retain and transform up to 50 % N inputs from the catchment [1], being microbial assemblages on streambed substrata (i.e., biofilms) and in sediments the most active component of N cycling [7]. Biofilms are highly, metabolic active, complex structures of algae, bacteria, archaea, and fungi embedded in a polysaccharide matrix growing on submerged substrata, mostly cobbles and pebbles [8, 9]. Ammonia-oxidizing archaea (AOA) and bacteria (AOB) play

Published online: 26 July 2014

a key role in the N cycle catalyzing the oxidization of NH_4^+ to nitrite the first and rate-limiting step of nitrification. Both phyla encode for the alpha subunit of the enzyme ammonia mono-oxygenase (*amoA*) that can be traced with specific primers [10, 11]. AOA and AOB present intrinsic and distinctive adaptations to natural habitats [12] and to environmental conditions such as NH_4^+ availability [13] and irradiance [14], which can modulate their abundance and distribution in streams.

In the present study, we analyzed the influence of WWTP inputs on the abundance, distribution, and composition of ammonia-oxidizing assemblages, both AOA and AOB, in epilithic biofilms of small Mediterranean urban streams. In particular, we aimed to examine consistent patterns among WWTP-influenced streams, and five streams affected by different WWTPs were studied to provide a general pattern for this type of ecosystems. In addition, we hypothesized that changes observed in nitrification rates in urban streams could be related to a substantial modification of the abundance and composition of ammonia-oxidizing microorganisms.

Material and Methods

Selected Stream Sampling and Analyses

The streams were located in the catchment of La Tordera river (NE Spain) and were of similar size (Table 1). The study was conducted at the beginning of autumn (October 2009) when the influence from WWTP inputs was remarkable due to low stream flow conditions (see details in Tables 1 and 2). The selected stream reaches were comparable in hydrology and streambed substrates, which were dominated by cobbles and some patches of sand. The canopy cover from riparian vegetation was dense at all streams, and light conditions reaching stream surface were <4 % of total incident irradiance in the surrounding landscape.

At each stream, we selected a ca. 1-km reach, and we identified one site upstream (UP) of the WWTP input and eight sites along the reaches (DW1–DW8, spread at ca. 100 m from each other) and the WWTP effluent itself (WWTP). At each site, we measured water temperature and conductivity using a portable conductivity meter (WTW Weilheim) and collected a water sample for analysis of $N\text{-}NH_4^-$, $N\text{-}NO_2^-$, and $N\text{-}NO_3^-$. At sampling sites UP and DW8, we estimated discharge by measuring both water depth and velocity at 50-cm intervals, respectively, using a tape and a velocity meter (Schiltknecht Messtechnik). Longitudinal profiles of DIN concentrations were used to estimate net uptake velocity (V_f, mm/min) at which nutrients are removed from the water column. V_f was calculated by estimating the stream-specific uptake length (m) using the slope of the regression of the ln-transformed and background corrected nutrient/conductivity ratio versus distance (eight sampling points downstream of the WWTP) and then further correction for stream-specific discharge (that is, discharge/width) [15–17]. V_f is an indicator of nutrient demand or production relative to concentration in the water column and allows for comparison among different streams.

To measure biofilm metrics, we randomly collected three fist-sized cobbles from riffle-run areas at sites UP, DW1, and DW8. For the measurement of biofilm biomass (expressed as ash-free dry mass (AFDM)) and for molecular analysis, we scraped separately light-exposed (here after referred as light side biofilm) and the sediment facing side of the cobbles (here after referred as dark side biofilm) with a sterile metallic brush. The biofilm sludge of the three cobbles was pooled in a sterile plastic beaker and filtered onto an ignited, preweighted glass fiber filters (FVF). The total surface scraped was estimated after covering cobbles with aluminum foil and following a weight-to-area relationship. Filters for AFDM were dried (60 °C) until constant weight (ca. 0.1 mg, Sartorius analytical balance, model MC1). For the quantification of the ammonia oxidizers, the remaining biofilm sludge was transported to the laboratory on ice within 2 h after sampling. In the lab to estimate AFDM, biofilm samples collected on glass fiber filters were combusted at 500 °C for 5 h and weighted as indicated above. The AFDM was estimated as the mass difference between dry and combusted filters and was reported per unit of surface area (g m^{-2}).

For molecular analysis, the remaining biofilm sludge was incubated with Tween-20 detergent (10^{-6} %*w*/*v*) for 5 min followed by soft sonication (Sonopuls ultrasonic homogenizer HD 2070) with 20^{-s} pulses at 10 % power [18]. Sludge was filtered through a 0.2-mm pore size polycarbonate membrane (Millipore). Filters were incubated with lysozyme, proteinase K, and sodium dodecyl sulfate in lysis buffer (40 mmol L^{-1} ethylenediaminetetra-acetic acid, 50 mmol L^{-1} Tris, pH 8.3, and 0.75 mol L^{-1} sucrose), and phenol extracted as previously described [19].

amoA Gene Analysis

AOA and AOB abundances among streams and cobble sides were measured by quantitative PCR of *amoA* genes using different primer pairs (see details in Table 4) following methods by Merbt et al. [6]. For *amoA* gene composition analysis, we selected SMP as representative stream. Archaeal *amoA* genes were amplified with the primer sets Arch-amoAF-Arch-amoAR (635-bp fragment; [10]) and bacterial *amoA* using primers amoA-1 F-amoA-

Table 1 Physical and chemical parameters of water samples and epilithic concentrations of *amoA* genes for the five wastewater treatment plant (WWTP)-influenced streams analyzed in this study

Urban Stream	Site	Location of the WWTP		conductivity	discharge	T	O_2	DIN	NH_4-N	NO_3-N	NO_2-N	AOA		AOB	
		Latitude (N)	Long (E)	µS cm^{-2}	L s^{-1}	°C	%	mg L^{-1}	mg L^{-1}	mg L^{-1}	mg L^{-1}	copies/m^2		copies m^{-2}	
												Light-side biofilm	Dark-side biofilm	Light-side biofilm	Dark-side biofilm
Breda (**BRE**)	UP			677	0.00	13.2	38.9	0.19	0.04	0.15	0.00	3.6×10^6	40.8×10^6	–	–
	WWTP	41° 44.181	2° 34.127	618	nd	20.6	78.7	13.07	0.81	10.64	1.62				
	DW1			615	nd	20.9	71.1	12.82	0.95	4.23	7.64	28.5×10^6	0.6×10^6	161.5×10^6	199.8×10^6
	DW8			576	4.27	17.3	58.6	9.85	0.28	7.97	1.61	27.9×10^6	>300	3346.9×10^6	–
Sant Celoni (**CEL**)	UP			742	0.00	19.0	93.0	0.49	0.05	0.44	0.01	3.2×10^6	3.2×10^6	–	9.3×10^6
	WWTP	41° 41,537	2° 30,466	1087	nd	22.4	94.3	2.72	2.38	0.28	0.06				
	DW1			836	nd	19.8	81.2	1.29	0.69	0.56	0.04	7.3×10^6	1.4×10^6	705.7×10^6	466.8×10^6
	DW8			987	27.00	21.8	75.0	2.75	1.36	1.21	0.18	24.0×10^6	26.1×10^6	437.1×10^6	215.0×10^6
Santa Coloma (**COL**)	UP			316	0.00	16.4	95.4	3.42	0.01	3.40	0.00	29.2 x 10^6	22.7×10^6	6.9×10^6	50.4×10^6
	WWTP	41° 51.005	2° 40.399	657	nd	20.5	72.7	4.62	3.97	0.54	0.11				
	DW1			408	nd	17.5	93.7	2.28	1.09	1.15	0.04	1.5 x 10^6	0.4×10^6	105.9×10^6	658.6×10^6
	DW8			415	69.06	18.5	91.2	2.22	0.75	1.43	0.05	4.1 x 10^6	1.0×10^6	175.1×10^6	234.3×10^6
Gualba (**GUA**)	UP			149	14.86	17.3	97.2	0.33	0.02	0.32	0.00	4.5×10^6	1.8×10^6	–	–
	WWTP	41° 43,702	2° 30,596	635	nd	19.6	93.6	10.01	9.18	0.62	0.21				
	DW1			203	nd	18.5	84.2	3.98	3.46	0.44	0.08	0	40.4×10^6	1981.9×10^6	3248.8×10^6
	DW8			164	36.01	19.3	96.0	1.08	0.02	1.05	0.01	10.3×10^6	–	102.7×10^6	–
Santa Maria Palautordera (**SMP**)	UP			316	0.79	16.6	67.2	7.46	0.03	7.43	0.01	15.5×10^6	1.7×10^6	–	–
	WWTP	41° 41.049	2° 27.598	490	nd	20.4	89.4	1.76	0.64	1.00	0.12				
	DW1			474	nd	20.3	84.7	2.42	0.49	1.91	0.02	6.1×10^6	1.7×10^6	127.0×10^6	122.1×10^6
	DW8			478	35.12	19.1	103.1	2.61	0.05	2.54	0.03	0.02×10^6	23.5×10^6	75.5×10^6	1828.0 x 10^6

UP upstream of the WWTP effluent, *DW1* 100 m downstream, *DW8* 800 m downstream of the effluent of the WWTP, – not detected, *nd* not determined

See Table S1 for AOA-AOB concentrations in WWTP effluent (copies L^{-1})

2R (491-bp fragment; [11]; see details in Table 4). PCR products were purified with the QIAquick PCR Purification kit (Qiagen) and cloned with the TOPO TA cloning kit (Invitrogen) following the manufacturer's instructions. The presence of inserts was checked by ampicillin resistance and blue/white selection on LB plates supplemented with ampicillin (100 lg mL^{-1}) and X-gal (40 μg mL^{-1}) as previously reported [20]. Sequencing was carried out using external facilities (http://www.macrogen.com). The *amoA* gene sequences were manually checked with BioEdit [21] and submitted for matching in the protein database using translated nucleotide sequences (BLASTX, www.ncbi.nlm.nih.gov; [22]) to check for protein identity. Next, sequences were clustered at 95 % identity in nucleotides with Mothur [23]. Multiple sequence alignment, phylogenetic inference by maximum likelihood, and calculation of *amoA* gene identity matrices were carried out as recently reported [24]. Sequences were deposited in GenBank under accession numbers between FR773891 and FR773972 (AOB) and HG937834 to HG938130 (AOA).

Additional biofilm samples were collected from SMP after leaf-fall, when riparian canopy cover was open and full light intensity reached the stream channel, to further explore the influence of irradiance on the composition of AOA.

Data Analysis

Dataset was tested on normal distribution by using Shapiro–Wilk normality test. All data failed requirements, and nonparametric tests were applied. The effect of the WWTP inputs on stream was assessed by comparing N-NH_4^+ and N-NO_3^- concentrations, temperature among sites by using Kruskal–Wallis ANOVA nonparametric test (site as a factor). This test was also used to compare AOA and AOB *amoA* gene copy numbers among sites (site as a factor), and AFDM among streams, sites and SMP among season and sites. Spearman rank *R* nonparametric correlations were used to examine relationships among N concentrations, AFDM, and AOA and AOB *amoA* gene copy numbers. Wilcoxon-matched paired test was used to test differences among AOA and AOB *amoA* gene copy number content of firstly light and dark side of biofilms of sites and rivers and secondly of WWTP outfall. Distance matrices for *amoA* genes were constructed with UniFrac, and comparison of AOA and AOB communities was based on the UniFrac metric (http://bmf.colorado.edu/unifrac) [25]. UniFrac is a betadiversity metric that quantifies community similarity based on the phylogenetic relatedness. To assess the sources of variation in *amoA* UniFrac matrices, we carried out permutational multivariate analysis of variance based on 1,000 permutations [26], using the function adonis in vegan package [27]. Results were considered significant for $p<0.05$. All statistical analyses were done using *R* project for statistical computing.

Results and Discussion

The contribution of WWTP effluents to the flow of the streams ranged between 59 and 99 %, and consequently, physical and chemical parameters (conductivity, temperature, oxygen, flow, nutrients) increased strongly (Table 1). In particular, stream water N-NH_4^+ concentration increased significantly by one order of magnitude (Kruskal–Wallis ANOVA, $p<0.05$), NO_3^- between 3 and 300 % and NO_2^- between 3 and 30 %. Thus, a significant decrease in the N-NO_3^-/N-NH_4^+ ratio was observed between UP and DW sites (Fig. 1a). Increases in DIN concentration (mainly N-NH_4^+) are commonly observed in streams affected by WWTP urban effluents, especially if a tertiary treatment is missing [4], as it was the case for the study streams. In addition, the high N-NH_4^+ concentration present downstream favored nitrification [3], and in agreement with these previous findings, we observed concomitant decreases in N-NH_4^+ and increasing N-NO_3^- along the reach in all five streams. However, net uptake velocities (V_f) varied substantially among the five streams and ranged from 0.030 to 3.483 and from -0.011 to -1.492 mm per min for N-NH_4^+ and N-NO_3^-, respectively (Table 3). Nevertheless, N-NH_4^+ demand (V_f N-NH_4^+) and N-NO_3^- production (V_f N-NO_3^-) were correlated ($p<0.05$, $R^2=0.857$) indicating nitrification activity. Furthermore V_f N-NO_3^- and V_f N-NH_4^+ increased with increasing N-NH_4^+ concentration. This results indicate that streams with higher N-NH_4^+ concentration have higher demand of N-NH_4^+ being nitrification hotspots.

AOA and AOB were present in the epilithic biofilms of the streams, with abundances estimated by qPCR data ranging between 10^6 and 10^9 *amoA* gene copies per m^2 (Fig. 1b). All five WWTP effluents also contained ammonia-oxidizing prokaryotes (c. 40–3,000 *amoA* gene copies per liter[1]), being concentrations of AOB one order of magnitude higher than those of AOA (Table S1). This finding is in agreement with previous studies showing the presence of AOA and AOB within WWTP reactors [28, 29], although their particular contribution to nitrification in the plants is still under discussion and seems to be closely related to the organic matter quality, oxygen, and substrate availability within the wastewater [29–31]. Presence of AOA and AOB in the effluents further indicates that WWTP effluents are potential sources of ammonia oxidizers [32]. In fact, the AOB/AOA ratio in epilithic biofilms downstream the WWTPs was closer to the ratio in the WWTP effluent than in upstream sites (Fig. 1c). In downstream biofilms, the shift in the AOB/AOA ratio was associated with increases in AOB abundance. While AOB were rarely detected in biofilms of the five upstream sites,

Table 2 Characterization of the WWTP effluents from the five selected study sites

	BRE	CEL	COL	GUA	SMP
Mean daily discharge ($m^3 day^{-1}$)	*800*	*6,000*	*3,250*	*190*	*2,500*
Population supplied (*hab.*)	*3707*	*17,510*	*11,090*	*1,065*	*11,474*
Treatment	*Biological*	*Biological & N,P elimin.*	*Biological & N elimin.*	*Soft*	*Biological & N,P elimin.*
Equivalent population (*h-e*)	*5,600*	*30,000*	*14,667*	*1,035*	*15,841*
Discharge (L s^{-1})	5.2	69.4[a]	37.6[a]	4.6	23.4
Temperature (°C)	20.6	22.4	20.5	19.6	20.4
O_2 (mg L^{-1})	7.00	8.08	6.47	8.40	7.94
DOC (mg L^{-1})	11.76	6.75	6.89	8.28	3.94
SRP (mg P L^{-1})	4.82	0.11	1.46	4.70	25.96
NH_4-N (mg N L^{-1})	0.81	2.38	3.97	9.18	0.64
NO_3-N (mg N L^{-1})	10.64	0.28	0.54	0.62	1.00
% DIN as NH_4	6	88	86	92	36
amoA AOA (copies L^{-1})	37	48	43	194	82
amoA AOB (copies L^{-1})	3221	784	647	344	313

Data in italics was taken from the Catalonian water agency (ACA, 2009) derived from the WWTP informational sheets

[a] Values taken from the Catalonian water agency (ACA, 2009) database of annual average discharges

they were highly abundant in biofilms downstream (Table 1). Conversely, AOA abundances were relatively similar among biofilms, regardless of the stream site location. These results indicated a remarkable influence of the WWTP inputs on the in-stream ammonia-oxidizing assemblages of such urban small streams, especially for AOB. In addition, results further indicate that ammonia oxidizers from the WWTPs, especially AOB, can successfully settle in the biofilms of WWTP-affected streams and indicate that the AOB-colonizing capacity is consistent among affected streams and could be a general pattern in this type of ecosystems. Higher abundances of ammonia-oxidizing prokaryotes downstream of the WWTP inputs are in accordance with the high nitrification activity mentioned above and may explain the net changes in N-NH_4^+ and N-NO_3^- concentrations along the streams.

To additionally test the impact of the WWTP inputs on the composition of the AOA–AOB, we selected SMP as representative stream for cloning and sequencing (Fig. 2). This site has already a solid background on hydrology, nutrient biogeochemistry, and microbial assemblage from previous studies (see [5, 33, 6, 3]). We selected biofilms developed on the side of cobbles facing the streambed sediments (i.e., dark side biofilms). These biofilms are exposed to shaded conditions, and thus, we minimized the effect of additional controlling factors such as light inhibition [14] or nutrient competition with photoautotrophic algae [34]. Similarly to qPCR results, AOB were only detected in downstream sites located after the inlet of the WWTP effluent. Although AOB communities harbored specific clusters to each site (i.e., *N. communis* cluster detected only in the WWTP outflow and *N. europea* cluster detected only in downstream biofilms), we found a strong compositional overlap between them (UNIFRAC significance pairwise test, $p>0.05$). Indeed, *amoA* sequences belonging to the two dominant clusters in the outflow of the WWTP (i.e., *Nitrosospira* and *N. oligotropha* clusters) represented a significant proportion of AOB communities in downstream sites (i.e., 37 % at DWD1 and 80 % at DWD2) (Fig. 2a). Most interesting, more than 50 % of downstream site sequences had their closest Blast match with sequences retrieved from wastewaters indicating a strong influence of the WWTP downstream (data not shown). In contrast to AOB, AOA were found along all stream sites, and differences were observed in the composition of the AOA assemblages (UNIFRAC significance pairwise test, $p<0.01$). At the upstream site, AOA were dominated by soil-related archaea mainly affiliated to *Nitrososphaera* cluster (former 1.1b group; Fig. 2b), which probably derived from soil runoff. At the downstream sites, AOA additionally included *Nitrosotalea* (former 1.1a cluster, [35]; 44 % of all sequences), which probably derived from the WWTP effluent where it was the dominant AOA (88 % of all sequences; Fig. 2). Together, these results suggest that niche separation among different clusters of AOA occurs in stream biofilms in response to differences in physical and chemical conditions [36]. Changes in pH are within the neutral range in these systems, and one driving factor for such separation could be the significant difference in N-NH_4^+ availability among sites [24, 37, 38]. Low N-NH_4^+ concentration in upstream sites may probably limit AOB development due to their lower N-NH_4^+ affinity compared to AOA [13]. Within AOA, information derived from pure cultures indicates that *Nitrosophaera* and *Nitrosopumilus* are more active at low N-NH_4^+ concentrations ($K_m<0.133$ nM total ammonium, [13, 39], while *Nitrosotalea* may be better

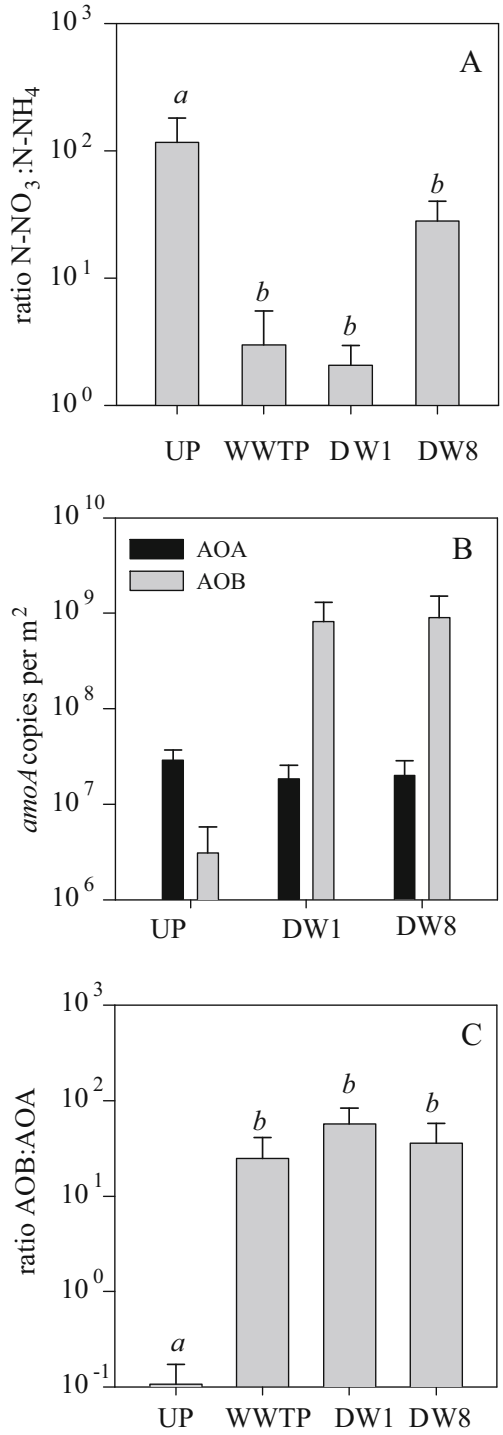

Fig. 1 **a** ratio of $N\text{-}NO_3^-/N\text{-}NH_4^+$ concentration in stream water column and the WWTP effluent; **b** mean abundance of archaeal (*dark bars*) and bacterial (*gray bars*) *amoA* gene per m^2 in biofilms (for simplification sum of light and dark side biofilms); **c** ratio of *amoA* AOB/AOA copies in stream biofilm and in the WWTP effluent. All y-axes in log scale. *UP* upstream of the WWTP effluent, *DW1* 100 m, and *DW8* 800 m downstream of the effluent of the WWTP, *WWTP*-the WWTP effluent itself. *Lines above the bars* are the standard error for five streams. *Different letters* (*a* or *b*) above the *bars* indicate significant differences among ratios (Kruskal–Wallis, $p<0.05$)

Table 3 Net nutrient uptake velocity (V_f) in downstream reaches (DW1–DW8)

	nutrient	BRE	CEL	COL	GUA	SMP
V_f (mm min^{-1})	$N\text{-}NH_4^+$	**0.951**	**0.115**[a]	**0.030**	**3.483**	**0.177**
V_f (mm min^{-1})	$N\text{-}NO_3^-$	**-0.329**	**-0.542**[a]	-0.011	**-1.492**	-0.022

V_f indicates the velocity at which a nutrient is removed from the water column (mm min^{-1}) [17]

[a] Velocity was calculated from DW3–DW8 because water column was not well mixed

Significant linear regression over distance in bold face

adapted to higher $N\text{-}NH_4^+$ concentrations (growing at 500 μM ammonium, [40]). This may be one of the reasons why lineages affiliated to *Nitrosotalea* cluster occur only downstream of the WWTP input. In any case, biofilms are very complex structures that provide multiple biological and physiological factors shaping their spatial configuration and also interact with the surrounding environment [41]. All this variability should be considered to further understand microbial composition of these assemblages. For instance, chemical conditions can change within mm from top to deepest layer, e.g., $N\text{-}NH_4^+$ decreased from about 650 to 500 μM and oxygen decreased from 50 % to anoxic conditions (0 % oxygen air) in the deepest layer in nitrifying model biofilms [42]. These gradients can determine the successful colonization of nitrifiers from WWTP inputs as well as the composition of the nitrifier assemblages that will ultimately influence N cycling in the streams.

Other additional factors to be considered for the observed niche separation of AOA clusters are related to the season of sampling [24] and particularly temperature, river discharge, and irradiance. Here, we analyzed the effect of these seasonal parameters by comparison of the AOA assemblage composition on the up-side of cobbles exposed to natural light conditions (light-side biofilm) with those dark-exposed on the downside of cobbles facing the streambed sediment (dark-side biofilm). We sampled the two biofilm types in summer, when riparian canopy cover shaded the stream (irradiance=60 μE m^{-2} s^{-1}), and in autumn after leaf fall, when full irradiance reached the stream channel (irradiance 1,500 μE m^{-2} s^{-1}). The samples were treated with two different primer sets (Table 4) targeting AOA, i.e., T [43] and F [10], to maximize the coverage. Results showed that temperature, river discharge, and irradiance were significant driving factors ($p<0.01$, PERMANOVA test) for the AOA assemblage structure (Fig. 3). In summer, temperature and biofilm biomass were higher, and light irradiance and discharge were lower than those in autumn (summer temperature 19 °C, discharge 35 L s^{-1}). Under these conditions, members of the *Nitrosotalea* cluster originating from the WWTP effluent

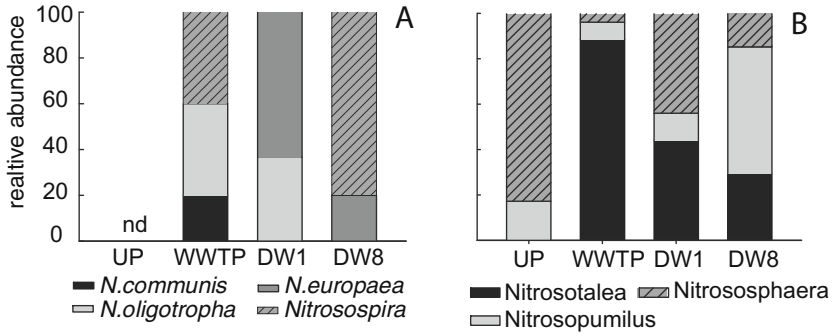

Fig. 2 Changes in the relative abundance of *amoA* gene for AOB (**a**) and AOA (**b**) in dark side stream biofilms along the stream reach and composition of the WWTP outflow in the urban stream SMP

Table 4 Primer used in this study for the *amoA* gene of bacteria (AOB) and archaea (AOA)

Target	Author	Name	Sequence	Annealing
amoA AOA	Tourna et al. [43]	CrenamoA23f CrenamoA616r	5′-ATGGTCTGGCTWAGACG-3′ 5′-GCCATCCATCTGTATGTCCA-3′	59.5 °C
amoA AOA	Francis et al. [10]	Arch-amoAF Arch-amoAR	5′-STAATGGTCTGGCTTAGACG-3′ (5′-GCGGCCATCCATCTGTATGT-3′	57°
amoA AOB	Rotthauwe et al [11]	amoA-1 F amoA-2R	5′-GGGTTTCTACTGGTGGT-3′ 5′-CCCCTCKGSAAAGCCTTCTTC-3′	58 °C

dominated AOA communities of both sides of the cobbles (Fig. 3). In contrast, in autumn, discharge was much higher (autumn temperature 9 °C, discharge 152 L s^{-1}) and diluted the WWTP effluent decreasing its influence on the stream. In addition to the dilution effect, full light-exposed biofilms were less suitable for *Nitrosotalea* like sequences as illustrated by their segregation between both faces of the cobbles. These results suggested in situ photosensitivity for AOA, particularly for *Nitrosotalea* like sequences, as previously reported under laboratory conditions [14]. The molecular and

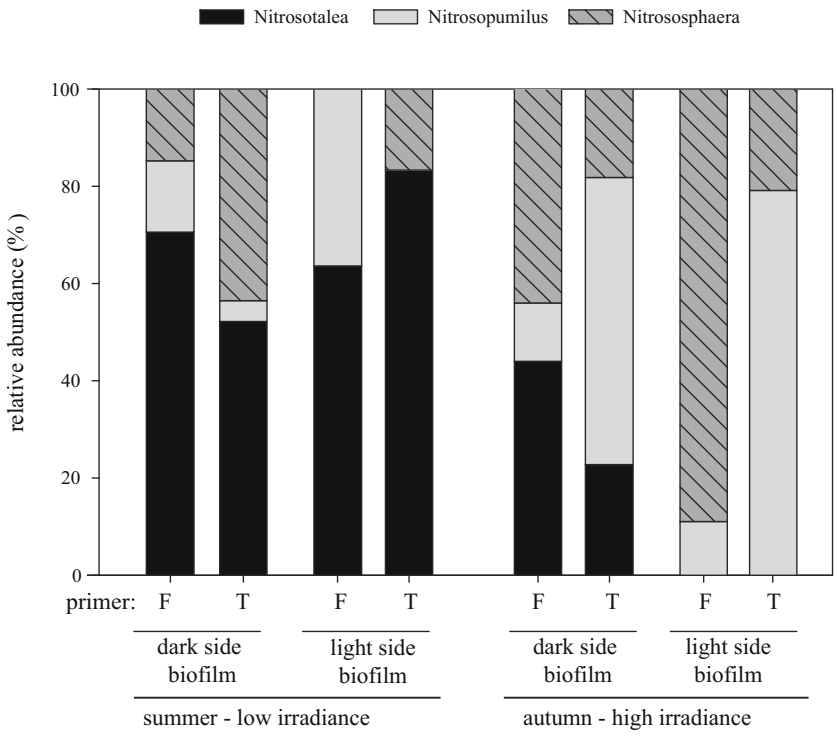

Fig. 3 Changes in the relative abundance of *amoA* gene for AOA present in the light and dark side biofilm of sampling site DW1 (100 m downstream of the WWTP effluent) in SMP urban stream in summer (low irradiance and discharge, high temperature) and in autumn (high irradiance and discharge, lower temperature). AOA composition tested with primers set F (Arch-amoAF/Arch-amoAR, from Francis et al. [10]) and T (CrenamoA23f/CrenamoA616r, from Tourna et al. [43])

physiological factors involved in the photoinhibiton of AOA remain, however, to be determined.

Overall, epilithic ammonia-oxidizing assemblages developed in small Mediterranean streams showed a strong influence by WWTP effluents both quantitatively, mostly for AOB, and qualitatively, mainly for AOA. Overall, these results potentially explain the hotspot nitrification nature of WWTP-influenced streams and also provide a mechanistic approach of actual nitrification relevance in urban streams affected by WWTP effluents. Environmental constrain factors, both natural (i.e., temperature, river discharge, and irradiance) and anthropogenically driven (i.e., WWTP inputs), determine the abundance and composition of AOB and AOA in stream biofilms, which will ultimately influence the rate at which supplied ammonium will be transformed into nitrate at the ecosystem level.

Acknowledgments We thank C. Gutierrez, M. Ribot, and N. Nomokonova for field and laboratory assistance. S.N.M. was supported by a JAE predoctoral fellowship from the Spanish National Research Council (CSIC) and J.-C.A. by a Juan de la Cierva fellowship from the Spanish Office for Research (MINECO). This research was granted by DARKNESS CGL2012-32747 to EOC and MED_FORESTREAM CGL2011-30590-CO2-02 (MINECO) and REFRESH-244121 (7th Framework Programme EU Comission) to EM.

References

1. Peterson BJ, Wollheim WM, Mulholland PJ, Webster JR, Meyer JL, Tank JL, Martí E, Boden WB, Valett HM, Hershey AE, McDowell WH, Dodds WK, Hamilton SK, Gregory S, Morrall DD (2001) Control of nitrogen export from watersheds by headwater streams. Science 292:86–91
2. Martí E, Aumatell J, Gode L, Poch M, Sabater F (2004) Nutrient retention efficiency in streams receiving inputs from wastewater treatment plants. J Environ Qual 33:285–293
3. Merseburger G, Martí E, Sabater F (2005) Net changes in nutrient concentrations below a point source input in two streams draining catchments with contrasting land uses. Sci Tot Environ 347:217–229
4. Martí E, Riera J, Sabater F (2010) Effects of wastewater treatment plants on stream nutrient dynamics under water scarcity conditions. In: Sabater S, Barceló D (eds) Water Scarcity in the Mediterranean. Springer Berlin Heidelberg, Berlin, pp 173–195
5. Ribot M, Martí E, von Schiller D, Sabater F, Daims H, Battin TJ (2012) Nitrogen processing and the role of epilithic biofilms downstream of a wastewater treatment plant. Freshwater Sci 31:1057–1069. doi:10.1899/11-161.1
6. Merbt SN, Auguet J-C, Casamayor EO, Martı E (2011) Biofilm recovery in a wastewater treatment plant-influenced stream and spatial segregation of ammonia-oxidizing microbial populations. Limnol Oceanogr 56:1054–1064. doi:10.4319/lo.2011.56.3.1054
7. Teissier S, Torre M, Delmas F, Garabétian F (2007) Detailing biogeochemical N budgets in riverine epilithic biofilms. JNABS 26:178–190
8. Lock M, Wallace R, Costerton J, Ventullo R, Charlton S (1984) River epilithon: toward a structural-functional model. Oikos 10–22
9. Battin TJ, Kaplan LA, Newbold JD, Cheng X, Hansen C (2003) Effects of current velocity on the nascent architecture of stream microbial biofilms. Appl Environ Microbiol 69:5443–5452. doi:10.1128/aem.69.9.5443-5452.2003
10. Francis CA, Roberts KJ, Beman JM, Santoro AE, Oakley BB (2005) Ubiquity and diversity of ammonia-oxidizing archaea in water columns and sediments of the ocean. PNAS 102:14683–14688. doi:10.1073/pnas.0506625102
11. Rotthauwe J-H, Witzel K-P, Liesack W (1997) The ammonia monooxygenase structural gene amoA as a functional marker: molecular fine-scale analysis of natural ammonia oxidizing populations. Appl Environ Microbiol 63:4704–4712
12. Fernàndez-Guerra A, Casamayor EO (2012) Habitat-associated phylogenetic community patterns of microbial ammonia oxidizers. PLoS ONE 7:e47330
13. Martens-Habbena W, Berube PM, Urakawa H, de la Torre JR, Stahl DA (2009) Ammonia oxidation kinetics determine niche separation of nitrifying Archaea and Bacteria. Nature 461:976–979
14. Merbt SN, Stahl DA, Casamayor EO, Martí E, Nicol GW, Prosser JI (2012) Differential photoinhibition of bacterial and archaeal ammonia oxidation. FEMS Microbiol Lett 327:41–46. doi:10.1111/j.1574-6968.2011.02457.x
15. Hall RO, Bernhardt ES, Likens GE (2002) Relating nutrient uptake with transient storage in forested mountain streams. Limnol Oceanogr 47:255–265
16. von Schiller D, Martí E, Riera JL, Ribot M, Argerich A, Fonollà P, Sabater F (2008) Inter-annual, annual, and seasonal variation of P and N retention in a perennial and an intermittent stream. Ecosystems 11:670–687
17. Webster J, Valett H (2006) Solute dynamics. In: Hauer FR, Lamberti GA (eds) Methods in stream ecology. Academic Press, San Diego, pp 169–185
18. Epstein SS, Rossel J (1995) Enumeration of sandy sediment bacteria: search for optimal protocol. Mar Ecol Prog Ser 117:289–298
19. Hervàs A, Casamayor EO (2009) High similarity between bacterioneuston and airborne bacterial community compositions in a high mountain lake area. FEMS Microbiol Ecol 67:219–228
20. Ferrera I, Massana R, Casamayor EO, Balagué V, Sánchez O, Pedrós-Alió C, Mas J (2004) High-diversity biofilm for the oxidation of sulfide-containing effluents. Appl Microbiol Biotech 64:726–734
21. Hall TA (1999) BioEdit: a user-friendly biological sequencealingment editor and analysis program for Windows 95/98/NT. Nucleic Acid Symp Ser 41:95–98
22. Altschul SF, Gish W, Miller W, Myers EW, Lipman DJ (1990) Basic local alignment search tool. J Mol Biol 215:403–410
23. Schloss PD, Westcott SL, Ryabin T, Hall JR, Hartmann M, Hollister EB, Lesniewski RA, Oakley BB, Parks DH, Robinson CJ (2009) Introducing mothur: open-source, platform-independent, community-supported software for describing and comparing microbial communities. Appl Environ Microbiol 75:7537–7541
24. Auguet J-C, Nomokonova N, Camarero L, Casamayor EO (2011) Seasonal changes of freshwater ammonia-oxidizing archaeal assemblages and nitrogen species in oligotrophic alpine lakes. Appl Environ Microbiol 77:1937–1945. doi:10.1128/aem.01213-10
25. Lozupone C, Knight R (2005) UniFrac: a new phylogenetic method for comparing microbial communities. Appl Environ Microbiol 71:8228–8235
26. McArdle BH, Anderson MJ (2001) Fitting multivariate models to community data: a comment on distance-based redundancy analysis. Ecology 82:290–297
27. Oksanen J, Kindt R, Legendre P, O'Hara B, Stevens MHH, Oksanen MJ, Suggests M (2007) Vegan: community ecology package. R package version 1:8–5. http://cran.r-project.org/
28. Zhang T, Jin T, Yan Q, Shao M, Wells G, Criddle C, Fang HHP (2009) Occurrence of ammonia-oxidizing Archaea in activated sludges of a laboratory scale reactor and two wastewater treatment plants. J Appl Microbiol 107:970–977

29. Mußmann M, Brito I, Pitcher A, Sinninghe Damsté JS, Hatzenpichler R, Richter A, Nielsen JL, Nielsen PH, Müller A, Daims H, Wagner M, Head IM (2011) Thaumarchaeotes abundant in refinery nitrifying sludges express amoA but are not obligate autotrophic ammonia oxidizers. PNAS 108:16771–16776. doi:10.1073/pnas.1106427108
30. Short MD, Abell GCJ, Bodrossy L, van den Akker B (2013) Application of a novel functional gene microarray to probe the functional ecology of ammonia oxidation in nitrifying activated sludge. PLoS ONE 8:e77139
31. Bai Y, Sun Q, Wen D, Tang X (2012) Abundance of ammonia-oxidizing bacteria and archaea in industrial and domestic wastewater treatment systems. FEMS Microbiol Ecol 80:323–330. doi:10.1111/j.1574-6941.2012.01296.x
32. Sonthiphand P, Cejudo E, Schiff SL, Neufeld JD (2013) Wastewater effluent impacts ammonia-oxidizing prokaryotes of the Grand River, Canada. Appl Environ Microbiol 79:7454–7465. doi:10.1128/aem.02202-13
33. Mußmann M, Ribot M, von Schiller D, Merbt SN, Augspurger C, Karwautz C, Winkel M, Battin TJ, Martí E, Daims H (2013) Colonization of freshwater biofilms by nitrifying bacteria from activated sludge. FEMS Microbiol Ecol. doi:10.1111/1574-6941.12103
34. Risgaard-Petersen N, Nicolaisen MH, Revsbech NP, Lomstein BA (2004) Competition between ammonia-oxidizing bacteria and benthic microalgae. Appl Environ Microbiol. doi:10.1128/aem.70.9.5528-5537.2004
35. Restrepo-Ortiz CX, Auguet J-C, Casamayor EO (2014) Targeting spatiotemporal dynamics of planktonic SAGMGC-1 and segregation of ammonia-oxidizing thaumarchaeota ecotypes by newly designed primers and quantitative polymerase chain reaction. Environ Microbiol 16:689–700. doi:10.1111/1462-2920.12191
36. Pester M, Rattei T, Flechl S, Gröngröft A, Richter A, Overmann J, Reinhold-Hurek B, Loy A, Wagner M (2012) amoA-based consensus phylogeny of ammonia-oxidizing archaea and deep sequencing of amoA genes from soils of four different geographic regions. Environ Microbiol. doi:10.1111/j.1462-2920.2011.02666.x
37. Herrmann M, Scheibe A, Avrahami S, Küsel K (2011) Ammonium availability affects the ratio of ammonia-oxidizing bacteria to ammonia-oxidizing archaea in simulated creek ecosystems. Appl Environ Microbiol 77:1896–1899. doi:10.1128/aem.02879-10
38. Verhamme DT, Prosser JI, Nicol GW (2011) Ammonia concentration determines differential growth of ammonia-oxidising archaea and bacteria in soil microcosms. ISME J 5:1067–1071
39. Hatzenpichler R, Lebedeva EV, Spieck E, Stoecker K, Richter A, Daims H, Wagner M (2008) A moderately thermophilic ammonia-oxidizing crenarchaeote from a hot spring. PNAS 105:2134–2139. doi:10.1073/pnas.0708857105
40. Lehtovirta-Morley LE, Stoecker K, Vilcinskas A, Prosser JI, Nicol GW (2011) Cultivation of an obligate acidophilic ammonia oxidizer from a nitrifying acid soil. PNAS 108:15892–15897. doi:10.1073/pnas.1107196108
41. Battin TJ, Sloan WT, Kjelleberg S, Daims H, Head IM, Curtis TP, Eberl L (2007) Microbial landscapes: new paths to biofilm research. Nat Rev Microbiol 5:76–81
42. Gieseke A, Nielsen JL, Amann R, Nielsen PH, De Beer D (2005) In situ substrate conversion and assimilation by nitrifying bacteria in a model biofilm. Environ Microbiol 7:1392–1404. doi:10.1111/j.1462-2920.2005.00826.x
43. Tourna M, Freitag TE, Nicol GW, Prosser JI (2008) Growth, activity and temperature responses of ammonia-oxidizing archaea and bacteria in soil microcosms. Environ Microbiol 10:1357–1364. doi:10.1111/j.1462-2920.2007.01563.x

Appendix 3: Publication Chapter 3

RESEARCH LETTER

Differential photoinhibition of bacterial and archaeal ammonia oxidation

Stephanie N. Merbt[1,2], David A. Stahl[3], Emilio O. Casamayor[2], Eugènia Martí[2], Graeme W. Nicol[1] & James I. Prosser[1]

[1]Institute of Biological and Environmental Sciences, University of Aberdeen, Aberdeen, UK; [2]Biogeodynamics and Biodiversity Group, Centre d'Estudis Avançats de Blanes (CEAB-CSIC), Blanes, Spain; and [3]Department of Civil and Environmental Engineering, University of Washington, Seattle, WA, USA

Correspondence: James I. Prosser, Institute of Biological and Environmental Sciences, University of Aberdeen, Cruickshank Building, St Machar Drive, Aberdeen AB24 3UU, UK. Tel.: +441224 273254; fax: +441224 272703; e-mail: j.prosser@abdn.ac.uk

Received 17 September 2011; revised 14 October 2011; accepted 6 November 2011.

DOI: 10.1111/j.1574-6968.2011.02457.x

Editor: J. Murrell

Keywords
nitrification; thaumarchaea; ammonia oxidizers; photoinhibition; primary nitrite maximum; stream.

Abstract

Inhibition by light potentially influences the distribution of ammonia oxidizers in aquatic environments and is one explanation for nitrite maxima near the base of the euphotic zone of oceanic waters. Previous studies of photoinhibition have been restricted to bacterial ammonia oxidizers, rather than archaeal ammonia oxidizers, which dominate in marine environments. To compare the photoinhibition of bacterial and archaeal ammonia oxidizers, specific growth rates of two ammonia-oxidizing archaea (*Nitrosopumilus maritimus* and *Nitrosotalea devanaterra*) and bacteria (*Nitrosomonas europaea* and *Nitrosospira multiformis*) were determined at different light intensities under continuous illumination and light/dark cycles. All strains were inhibited by continuous illumination at the highest intensity (500 μE m^{-2} s^{-1}). At lower light intensities, archaeal growth was much more photosensitive than bacterial growth, with greater inhibition at 60 μE m^{-2} s^{-1} than at 15 μE m^{-2} s^{-1}, where bacteria were unaffected. Archaeal ammonia oxidizers were also more sensitive to cycles of 8-h light/16-h darkness at two light intensities (60 and 15 μE m^{-2} s^{-1}) and, unlike bacterial strains, showed no evidence of recovery during dark phases. The reduces findings provide evidence for niche differentiation in aquatic environments and support for photoinhibition as an explanation of nitrite maxima in the ocean.

Introduction

Nitrification is a key process in the cycling of nitrogen in terrestrial and aquatic ecosystems. The first, rate-limiting step of nitrification, the oxidation of ammonia (NH_3) to nitrite (NO_2^-), is carried out by both ammonia-oxidizing bacteria (AOB, Koops & Pommerening-Röser, 2001) and archaea belonging to the recently described thaumarchaea group (AOA, Spang *et al.*, 2010). The first step in ammonia oxidation is catalysed by ammonia monooxygenase, and the subunit A gene (*amoA*) is the most commonly used marker for tracking ammonia oxidizers in environmental samples. Although sharing a common function, bacterial and archaeal *amo* genes are phylogenetically distinct, suggesting different evolution and phenotypic characteristics between AOB and AOA (Nicol & Schleper 2006). AOB were traditionally considered to be responsible for most ammonia oxidation in natural environments, but AOA *amoA* genes are now known to be ubiquitous and to outnumber those of AOB in many environments, including soils (Leininger *et al.*, 2006), oceans (Wuchter *et al.*, 2006), streams (Merbt *et al.*, 2011) and alpine lakes (Auguet *et al.*, 2011). Although AOA and AOB coexist in many ecosystems, differential sensitivities to pH (Nicol *et al.*, 2008), temperature (Tourna *et al.*, 2008) and ammonium concentration (Martens-Habbena *et al.*, 2009; Verhamme *et al.*, 2011) appear to control their relative abundances and activities, suggesting distinct physiological adaptations for each group.

Photoinhibition of ammonia oxidation has been investigated in laboratory cultures of AOB (e.g. Hooper & Terry, 1974, Guerrero & Jones, 1996a, b). Hyman & Arp

FEMS MICROBIOLOGY LETTERS

(1992) found that light may completely inhibit nitrite production and *de novo* synthesis of ammonia monooxygenase is required after exposure of cultures to light, leading to suggestions that light may be responsible for the inhibition of nitrification in ocean surface waters (Horrigan *et al.*, 1981), coastal areas (Olson, 1981), estuaries (Horrigan & Springer, 1990) and eutrophic rivers (Lipschultz *et al.*, 1985).

The low availability of laboratory cultures has restricted physiological studies of photoinhibition in AOB and, particularly, AOA. This has prevented assessment of the role of light exposure in niche separation and distribution of AOA and AOB in natural environments. Recent observations of the distribution of archaeal *amoA* genes in stream biofilms exposed to light and dark conditions (Merbt *et al.*, 2011) and along a vertical profile in the Atlantic Ocean (Church *et al.*, 2010) suggest, however, that AOA could also be sensitive to light and that sensitivity of AOA and AOB may differ. The aims of this study were to determine the effects of different light intensities on bacterial and archaeal ammonia oxidation using several laboratory cultures of AOA and AOB and to assess their potential to explain AOB and AOA differential distribution and activity in aquatic ecosystems.

Materials and methods

Strains and culture conditions

Photoinhibition of two AOB (*Nitrosomonas europaea* ATCC19718 and *Nitrosospira multiformis* ATCC25196) and two AOA (*Nitrosopumilus maritimus* and *Nitrosotalea devanaterra*) strains was investigated during growth in batch culture. *Nitrosomonas europaea* and *N. multiformis* were obtained from NCIMB (http://www.ncimb.com/). *Nitrosopumilus maritimus* and *N. devanaterra* were obtained from existing laboratory cultures (Könneke *et al.*, 2005; Lehtovirta-Morley *et al.*, 2011). All strains were grown aerobically in 100-ml quartz flasks containing 50 mL inorganic growth medium. AOB were grown in Skinner & Walker (1961) medium containing 1.78 mM ammonia sulphate, adjusted to pH 8.0 with Na_2CO_3 (5% w/v). *Nitrosopumilus maritimus* was grown in HEPES-buffered, synthetic medium (pH 7.6) (Martens-Habbena *et al.*, 2009), and *N. devanaterra* was cultured in acidic (pH 4.5) freshwater medium as described by Lehtovirta-Morley *et al.* (2011). The media for AOA contained ammonium chloride at concentrations of 1 mM for *N. maritimus* and 0.5 mM for *N. devanaterra*. Media were inoculated with 1% or 10% (v/v) of exponential-phase cultures of AOB or AOA, respectively. Bacterial cultures were sampled (1 mL) at intervals of 8 h for 5 days, and archaeal cultures were sampled daily for 10 days.

Experimental design and sample analysis

Photoinhibition was investigated in controlled temperature chambers maintained at 26 °C and illuminated by compact fluorescent lights (55 W) and clear strip lights (30 W) (International Lamps Ltd, Hertford, UK) emitting light with a wavelength spectrum of 400–680 nm with a maximum intensity at approximately 580 nm. Ammonia-oxidizing activity of the different cultures was measured under continuous illumination at an intensity of either 15, 60 or 500 μE m^{-2} s^{-1} and with diurnal cycles of 8-h light (15 or 60 μE m^{-2} s^{-1}) and 16-h dark conditions. Control cultures were incubated in the dark in the same incubator. Triplicate cultures were grown for all light treatments and controls. Light intensities were selected to reflect conditions prevailing in riparian zones of rivers and lakes, with highest light intensity (500 μE m^{-2} s^{-1}) simulating naturally occurring conditions during a clear summer day in open areas and the lower intensities (60 and 15 μE m^{-2} s^{-1}) simulating conditions in shaded areas.

Ammonia-oxidizing activity was determined by measuring increases in nitrite (NO_2^-) concentration over time for each particular culture and light exposure treatment. Specific growth rate was estimated by linear regression during the linear phase of semi-logarithmic plots of nitrite concentration vs. time, as in previous studies (Powell & Prosser, 1992; Könneke *et al.*, 2005; Lehtovirta-Morley *et al.*, 2011). Estimated specific growth rates in control and illuminated cultures were compared using the Student's *t*-test (two-sample assuming unequal variances).

Results

All AOA and AOB strains grew exponentially during incubation in the dark. Initial increases in nitrite concentration were sometimes non-exponential, because of carryover of nitrite with inocula, but subsequent increases in nitrite concentration were exponential. Typical nitrite production kinetics are exemplified in Fig. 1 for cultures of *N. multiformis* and *N. devanaterra* under continuous light at 60 μE m^{-2} s^{-1} and dark controls. Nitrite production kinetics were analysed prior to limitation by reduction in pH (all strains except *N. devanaterra*) or high nitrite concentration (*N. devanaterra*). Continuous illumination at 60 μE m^{-2} s^{-1} reduced the specific growth rate of *N. multiformis* from 1.05 (±0.07) day^{-1} to 0.62 (±0.01) day^{-1} and completely inhibited that of *N. devanaterra*.

Effects of illumination and associated statistical analysis are summarized in Fig. 2 and Table 1, respectively. AOA were more sensitive to illumination than AOB. Continuous illumination at the lowest light intensity examined (15 μE m^{-2} s^{-1}) did not significantly affect the growth of the AOB, *N. europaea* and *N. multiformis*, but inhibited

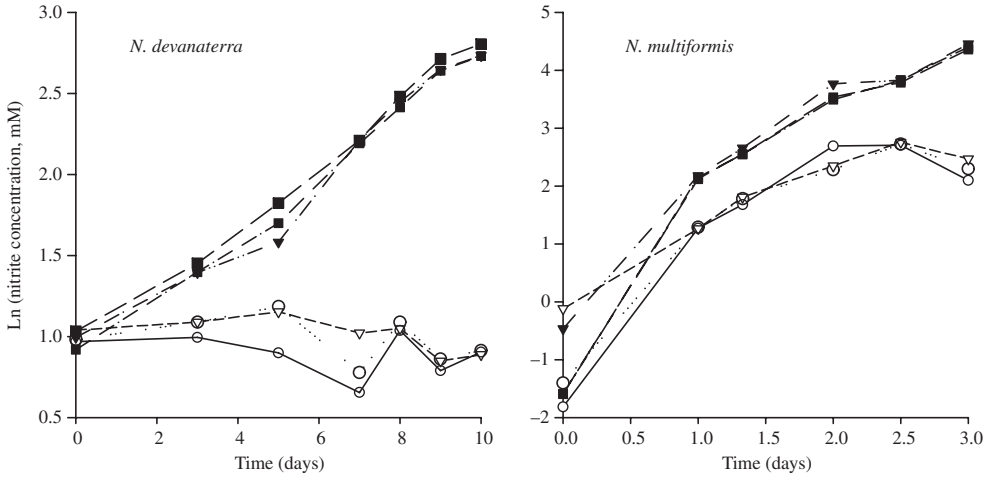

Fig. 1. Semi-logarithmic plots of nitrite concentration vs. time during incubation of triplicate cultures of *Nitrosotalea devanaterra* and *Nitrosospira multiformis* in liquid batch culture in the dark (solid symbols) and under continuous illumination (open symbols) at an intensity of 60 μE m^{-2} s^{-1}.

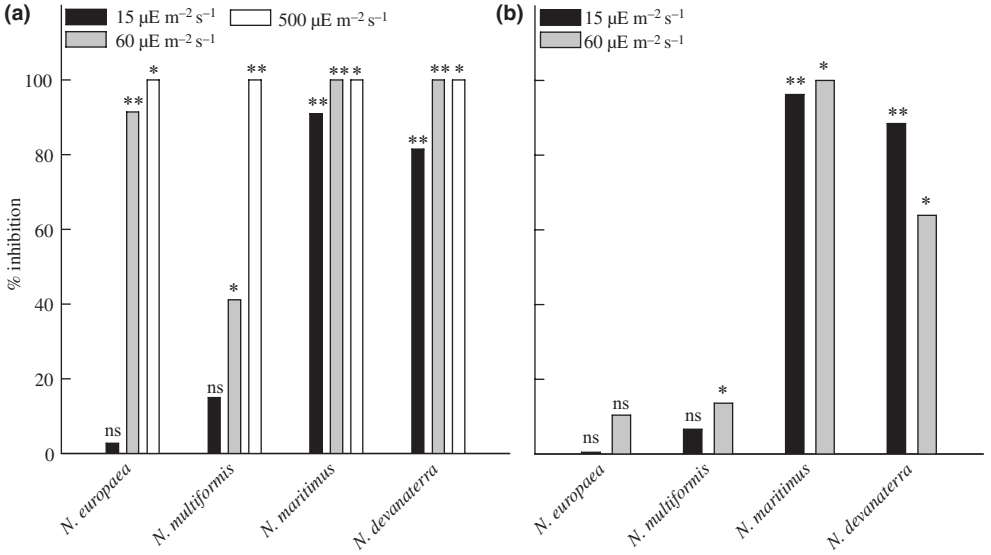

Fig. 2. The reduction in estimated specific growth rate as the percentage of the control, dark-incubated cultures, during incubation of bacterial (*Nitrosomonas europaea* and *Nitrosospira multiformis*) and archaeal (*Nitrosopumilus maritimus* and *Nitrosotalea devanaterra*) ammonia oxidizers under (a) continuous illumination at three intensities (15, 60 and 500 μE m^{-2} s^{-1}) and under (b) 16-h light/8-h dark cycles at 15 and 60 μE m^{-2} s^{-1}. Data are presented as the mean and standard error of triplicate cultures, and significant differences between control and illuminated cultures are represented as ns (no significant difference), $*P < 0.05$ and $**P < 0.001$.

that of the AOA, *N. maritimus* (91% reduced growth rate compared with controls) and *N. devanaterra* (81%) (Fig. 2a, Table 1). Continuous illumination at 60 μE m^{-2} s^{-1} completely inhibited growth of the two studied AOA species, but only partially inhibited growth of AOB strains (Figs 1 and 2, Table 1). The highest light intensity (500 μE m^{-2} s^{-1}) completely inhibited growth of all AOB and AOA strains. Apparent differences in sensitivity to photoinhibition of AOA species were only observed at the lowest light intensity, where *N. devanaterra* was less sensitive than *N. maritimus*. For AOB, *N. europaea* was more sensitive than *N. multiformis*, with respective decreases in specific growth rate of 91% and 41% at 60 μE m^{-2} s^{-1} (Fig. 1, Table 1).

In natural environments, diurnal cycles enable the recovery of ammonia oxidizers from photoinhibition and growth. This was therefore investigated for all strains using 8-h light/16-h dark cycles at the two lowest

Table 1. Mean estimated specific growth rates of triplicate cultures of bacterial (*Nitrosomonas europaea* and *Nitrosospira multiformis*) and archaeal (*Nitrosopumilus maritimus* and *Nitrosotalea devanaterra*) ammonia oxidizers in liquid batch culture. Cultures were incubated in the dark (control), with continuous illumination or with light/dark cycles

	Light intensity ($\mu E\ m^{-2}\ s^{-1}$)	*N. europaea*		*N. multiformis*		*N. maritimus*		*N. devanaterra*	
		Rate	SE	Rate	SE	Rate	SE	Rate	SE
Continuous illumination	15	1.08	0.007	0.71	0.038	0.019	0.004	0.046	0.003
	Control	1.11	0.017	0.83	0.024	0.21	0.005	0.246	0.008
	P-value	ns		ns		**		**	
	60	0.084	0.007	0.62	0.014	−0.008	0.004	−0.028	0.007
	Control	0.99	0.015	1.05	0.071	0.26	0.001	0.206	0.003
	P-value	**		*		**		**	
	500	ng	ng	ng	ng	−0.017	0.005	−0.018	0.002
	Control	0.62	0.023	1.37	0.010	0.16	0.020	0.081	0.008
	P-value	**		**		*		*	
8:16-h light/dark cycling	15	1.61	0.187	1.45	0.041	0.004	0.002	0.022	0.008
	Control	1.54	0.128	1.56	0.080	0.109	0.003	0.190	0.009
	P-value	ns		ns		**		**	
	60	1.01	0.047	0.88	0.010	−0.004	0.025	0.052	0.007
	Control	1.122	0.011	1.016	0.002	0.211	0.002	0.144	0.004
	P-value	ns		*		*		**	

ng, no growth detected; ns, no significant difference between control and treatment.
*$P < 0.05$;
**$P < 0.001$.

light intensities. At 15 $\mu E\ m^{-2}\ s^{-1}$, AOB were not significantly inhibited, as found under continuous illumination. At 60 $\mu E\ m^{-2}\ s^{-1}$, however, photoinhibition was lower than that under continuous illumination. There was no significant reduction in the specific growth rate of *N. europaea*, demonstrating an ability to recover during periods of darkness, while the growth of *N. multiformis* was reduced by only 14%, compared to 41% under continuous illumination (Fig. 1), suggesting partial recovery. Photoinhibition of *N. maritimus* was not influenced by light cycling, with almost complete inhibition at both light intensities. There was evidence of some recovery of growth of *N. devanaterra* at 60 $\mu E\ m^{-2}\ s^{-1}$, where inhibition was only 63% and surprisingly lower than at 15 $\mu E\ m^{-2}\ s^{-1}$ continuous illumination.

Discussion

Light plays a key role in the nitrogen cycle in aquatic ecosystems, stimulating uptake and excretion of inorganic nitrogen and inhibiting nitrification (Nelson & Conway, 1979; Hooper & Terry, 1973). The detrimental effect of light on ammonia-oxidizing bacteria (AOB) has been known for many years. Hooper & Terry (1973, 1974) demonstrated light inhibition of ammonia oxidation by *N. europaea* suspended cells, with maximum inhibition at short, near-UV wavelength (410 nm). Horrigan & Springer (1990) reported variability in the photosensitivity of ammonia oxidizers such as *Nitrosococcus oceanus* and strain SF-2, isolated from sea-surface films, and Guerrero & Jones (1996a) provided further evidence of species-specific and dose- and wavelength-dependent photoinhibition. Results from the present study support these previous findings.

Photoinhibition appears to operate on the initial step of ammonia oxidation, which is catalysed by ammonia monooxygenase. This step is common to both AOB and AOA, although subsequent metabolism of hydroxylamine, the product of initial ammonia oxidation, has not yet been determined for AOA. Broad similarities in AOA *amoA* gene sequences predict potentially similar AMO structure and therefore similar sensitivities to photoinhibition, while phylogenetic separation of AOA and AOB sequences and other physiological distinctions between archaea and bacteria suggest that levels of photoinhibition may differ and may give rise to niche differentiation, which is supported by our results. The effect of light on AOA has not previously been investigated. This study therefore provides the first evidence of photoinhibition in AOA and significantly greater inhibition of AOA than that of AOB. In addition, the study demonstrates differences in photosensitivity within AOB and AOA. Photoinhibition may therefore contribute to niche differentiation between and within AOA and AOB and may determine their distribution and diversity in light-affected ecosystems.

Our findings influence explanations for several phenomena in aquatic environments. Nitrite often accumulates at the base of the euphotic zone, forming the

primary nitrite maximum, which is explained by either nitrate reduction to nitrite, by light-limited phytoplankton or by differential photoinhibition of ammonia oxidizers and nitrite oxidizers (Lomas & Lipschultz, 2006). While other environmental factors may drive the distribution of AOA and AOB, the latter hypothesis assumes a key role for photoinhibition of ammonia oxidizers in surface waters, which is relieved with increasing depth, as light intensity decreases. It further assumes that nitrite oxidizers are more photosensitive than ammonia oxidizers, leading to the accumulation of nitrite through greater inhibition of nitrite production and/or slower recovery following photoinhibition. Cultivation-based studies provide contradictory evidence for this hypothesis, indicating that AOB are more photosensitive than nitrite oxidizers (Guerrero & Jones, 1996a), but that they recover more quickly from photoinhibition when subsequently incubated in the dark (Guerrero & Jones, 1996b). However, this model was developed prior to the discovery of the dominance of AOA in marine ecosystems. Greater photoinhibition and slower recovery of AOA, compared with AOB, observed in our study suggest that the difference between photoinhibition of ammonia and nitrite oxidizers is less than previously thought, reducing confidence in this explanation of the nitrite maximum.

The light intensities investigated are similar to those causing *in situ* inhibition of nitrification in previous studies: 100 μE m^{-2} s^{-1} in the eutrophic Delaware River (Lipschultz *et al.*, 1985) and approximately 40–70 μE m^{-2} s^{-1} in a Californian bight (Olson, 1981). In the mixed layer of natural aquatic systems, however, turbidity may promote nitrification both by protecting nitrifiers from photoinhibition and by limiting substrate competition with phytoplankton. Findings also provide a physiological explanation for the higher accumulation of AOA and AOB in river biofilms on the dark side, rather than on the illuminated side of cobbles (Merbt *et al.*, 2011), and the greater abundance of *amoA* genes with decreasing light intensity in the ocean (Church *et al.*, 2010). Despite this evidence of photoinhibition in natural ecosystems, AOA *amoA* abundance is high in regions of high irradiance, such as surface waters of the Mediterranean Sea (Galand *et al.*, 2010) and high mountain lakes (Auguet & Casamayor, 2008; Auguet *et al.*, 2011). This may reflect differences in photosensitivity within AOA, which may also contribute to consistent phylogenetic changes observed in AOA along vertical gradients in the Gulf of Mexico from upper (0–100 m) to deeper layers (450 m) (Beman *et al.*, 2008) and in a deep alpine lake in the Pyrenees (J.C. Auguet, X. Triado-Margarit, N. Nomokonova, L. Camarero & E.O. Casamayor, unpublished data).

Although our findings provide a rationale for future ecological and physiological diversity studies, they were performed with a limited number of strains, of which only one, *N. maritimus*, was isolated from a marine ecosystem. In addition, photoinhibition was investigated in suspended batch culture and may be influenced in natural systems by growth in biofilms and aggregates. Although AOA appear to be more photosensitive, they outnumber AOB in the upper water column (Beman *et al.*, 2008), with high transcriptional activity (Church *et al.*, 2010), and other environmental factors undoubtedly contribute to their relative distributions. Studies of AOB also suggest that photoinhibition depends on wavelength (Hooper & Terry, 1974; Guerrero & Jones, 1996a), which, like intensity, will vary with water depth. Nevertheless, the findings suggest light as an additional factor determining niche differentiation in ammonia oxidizers that may determine their distribution and relative contributions to nitrogen cycling in aquatic ecosystems.

Acknowledgements

We thank Jenna McWilliam and David Hadwen for laboratory assistance. The project was financed by the GRACCIE project (Spanish Ministry of Science and Education Consolider Program, ref: CSD2007-00067). S.N.M. is supported by a JAE-pre-doctoral fellowship from the Spanish National Research Council (CSIC), and G.W.N. by a NERC Advanced Fellowship (NE/D010195/1). Additional support was from NSF Award MCB-0920741 to D.A.S. and M. Hackett and from NSF Award OCE-1046017 to D.A.S., A. Ingalls, E.V. Armbrust, A.H. Devol and J. Moffett.

References

Auguet J-C & Casamayor EO (2008) A hotspot for cold crenarchaeota in the neuston of high mountain lakes. *Environ Microbiol* **10**: 1080–1086.

Auguet J-C, Nomokonova N, Camarero L & Casamayor EO (2011) Seasonal changes of freshwater ammonia-oxidizing archaeal assemblages and nitrogen species in oligotrophic alpine lakes. *Appl Environ Microbiol* **77**: 1937–1945.

Beman JM, Popp BN & Francis CA (2008) Molecular and biogeochemical evidence for ammonia oxidation by marine Crenarchaeota in the Gulf of California. *ISME J* **2**: 429–441.

Church MJ, Wai B, Karl DM & DeLong EF (2010) Abundances of crenarchaeal *amoA* genes and transcripts in the Pacific Ocean. *Environ Microbiol* **12**: 679–688.

Galand PE, Gutierrez-Provecho C, Massana R, Gasol JM & Casamayor EO (2010) Inter-annual recurrence of archaeal assemblages in the coastal NW Mediterranean Sea (Blanes Bay Microbial Observatory). *Limnol Oceanogr* **55**: 2117–2125.

Guerrero M & Jones R (1996a) Photoinhibition of marine nitrifying bacteria. I. Wavelength dependent response. *Mar Ecol Prog Ser* **141**: 183–192.

Guerrero M & Jones R (1996b) Photoinhibition of marine nitrifying bacteria. II. Dark recovery after monochromatic or polychromatic irradiation. *Mar Ecol Prog Ser* **141**: 193–198.

Hooper AB & Terry KR (1973) Specific inhibitors of ammonia oxidation in *Nitrosomonas*. *J Bacteriol* **115**: 480–485.

Hooper AB & Terry KR (1974) Photoinactivation of ammonia oxidation in *Nitrosomonas*. *J Bacteriol* **119**: 899–906.

Horrigan SG & Springer AL (1990) Oceanic and estuarine ammonium oxidation: effects of light. *Limnol Oceanogr* **35**: 479–482.

Horrigan SG, Carlucci AF & Williams PM (1981) Light inhibition of nitrification in sea-surface films. *J Mar Res* **39**: 557–565.

Hyman MR & Arp DJ (1992) $^{14}C_2H_2$- and $^{14}C0_2$-1abeling studies of the *de novo* synthesis of polypeptides by *Nitrosomonas europaea* during recovery from acetylene and light inactivation of ammonia monooxygenase. *J Biol Chem* **267**: 1534–1545.

Könneke M, Bernhard AE, de la Torre JR, Walker JB, Waterbury CB & Stahl DA (2005) Isolation of an autotrophic ammonia-oxidizing marine archaeon. *Nature* **437**: 543–546.

Koops H-P & Pommerening-Röser A (2001) Distribution and ecophysiology of the nitrifying bacteria emphasizing cultured species. *FEMS Microbiol Ecol* **37**: 1–9.

Lehtovirta-Morley L, Stoecker K, Vilcinskas A, Prosser JI & Nicol GW (2011) Cultivation of an obligate acidophilic ammonia oxidizer from a nitrifying acid soil. *P Natl Acad Sci USA* **108**: 15892–15897.

Leininger S, Urich T, Schloter M, Schwark L, Qi J, Nicol GW, Prosser JI, Schuster SC & Schleper C (2006) Archaea predominate among ammonia-oxidizing prokaryotes in soils. *Nature* **442**: 806–809.

Lipschultz F, Wofsy SC & Fox LE (1985) The effects of light and nutrients on rates of ammonium transformation in a eutrophic river. *Mar Chem* **16**: 329–341.

Lomas MW & Lipschultz F (2006) Forming the primaryn itrite maximum: Nitrifiers or phytoplankton? *Limnology and Oceanography* **51**: 2453–2467.

Martens-Habbena W, Berube PM, Urakawa H, de la Torre JR & Stahl DA (2009) Ammonia oxidation kinetics determine niche separation of nitrifying Archaea and Bacteria. *Nature* **461**: 976–979.

Merbt SN, Auguet J-C, Casamayor EO & Martí E (2011) Biofilm recovery in a wastewater treatment plant-influenced stream and spatial segregation of ammonia-oxidizing microbial populations. *Limnol Oceanogr* **56**: 1054–1064.

Nelson D & Conway HL (1979) Effects of the light regime on nutrient assimilation by phytoplankton in the Baja California and northwest Africa upwelling systems. *J Mar Res* **37**: 301–318.

Nicol GW & Schleper C (2006) Ammonia-oxidising Crenarchaeota: important players in the nitrogen cycle? *Trends Microbiol* **14**: 207–212.

Nicol GW, Leininger S, Schleper C & Prosser JI (2008) The influence of soil pH on the diversity, abundance and transcriptional activity of ammonia oxidizing archaea and bacteria. *Environ Microbiol* **10**: 2966–2978.

Olson RJ (1981) ^{15}N tracer studies of the primary nitrite maximum. *J Mar Res* **39**: 203–225.

Powell SJ & Prosser JI (1992) Inhibition of biofilm populations of *Nitrosomonas europaea*. *Microb Ecol* **24**: 43–50.

Skinner FA & Walker N (1961) Growth of *Nitrosomonas europaea* in batch and continuous culture. *Arch Mikrobiol* **38**: 339–349.

Spang A, Hatzenpichler R, Brochier-Armanet C, Rattei T, Tischler P, Spieck E, Streit W, Stahl DA, Wagner M & Schleper C (2010) Distinct gene set in two different lineages of ammonia-oxidizing archaea supports the phylum Thaumarchaeota. *Trends Microbiol* **18**: 331–340.

Tourna M, Freitag TE, Nicol GW & Prosser JI (2008) Growth, activity and temperature responses of ammonia-oxidizing archaea and bacteria in soil microcosms. *Environ Microbiol* **10**: 1357–1364.

Verhamme DT, Prosser JI & Nicol GW (2011) Ammonia concentration determines differential growth of ammonia-oxidising archaea and bacteria in soil microcosms. *ISME J* **5**: 1067–1071.

Wuchter C, Abbas B, Coolen MJL *et al.* (2006) Archaeal nitrification in the ocean. *P Natl Acad Sci USA* **103**: 12317–12322.